

PHOTOCHEMICAL TRIGGERING OF REACTIVE ENYNE-ALLENES AND ENEDIYNES
FOR THE APPLICATION IN ANTI-CANCER DRUGS

by

ALEXANDER V. KUZMIN

(Under the Direction of Vladimir V. Popik)

ABSTRACT

The extreme cytotoxicity of natural enediyne antibiotics is attributed to the ability of (Z)-3-ene-1,5-diyne and (Z)-1,2,4-heptatrien-6-yne fragments to undergo cycloaromatization producing DNA-damaging diradicals. The goal of this dissertation work was to develop photoactivatable precursors of reactive enediynes and enyne-allenes. To achieve this goal, we have designed compounds, which upon irradiation can efficiently generate enediyne and/or enyne-allene moiety, constrained within ten-membered ring. Thus, it was found that ten-membered ring cyclic enediynes that possess a carbonyl group in a β position with respect to the one of acetylenic termini undergo very facile cycloaromatization at ambient temperatures. Kinetic data and deuterium-labeling experiments indicate that this reaction proceeds via rate-determining tautomerization to the enyne-allene form followed by very rapid Myers—Saito cyclization.

A reactive ten-membered ring enyne-allene was also developed ($\tau_{25\text{ }^{\circ}\text{C}} = 5\text{--}6\text{ min}$). The cyclic enyne-allene is efficiently generated ($\Phi_{300\text{ nm}} = 0.57$) by UV irradiation of a thermally stable precursor in which a triple bond is masked as a cyclopropenone moiety.

Moreover, we found that incorporation of an additional endocyclic *trans* double bond in a ten-membered cyclic enediyne structure increases the activation energy of the cycloaromatization reaction. The rate-limiting step of the thermal cycloaromatization of a dienediyne is apparently the *trans-cis* isomerization and/or 1,3-hydrogen shift, producing the isomer of dienediyne with the *cis* double bond. The latter isomer then undergoes facile cycloaromatization.

The utility of catalyst-free azide–alkyne [3 + 2] cycloaddition for the immobilization of a variety of molecules onto a solid surface and microbeads was investigated. In this process, the surfaces are derivatized with aza-dibenzocyclooctyne (ADIBO) for the immobilization of azide-tagged substrates via a copper-free click reaction.

INDEX WORDS: enediyne, enyne-allene, antitumor agent, Bergman and Myers—Saito cyclization, photo-Bergman, triggering, cyclopropenone, allene, cyclooctyne, azide, dibenzocyclooctyne, copper-free click reaction, click chemistry.

PHOTOCHEMICAL TRIGGERING OF REACTIVE ENYNE-ALLENES AND ENEDIYNES
FOR THE APPLICATION IN ANTI-CANCER DRUGS

by

ALEXANDER V. KUZMIN

B.S., Saint-Petersburg State University, Russia, 2004

A Dissertation Submitted to the Graduate Faculty of The University of Georgia in Partial
Fulfillment of the Requirements for the Degree

DOCTOR OF PHILOSOPHY

ATHENS, GEORGIA

2010

© 2010

Alexander V. Kuzmin

All Rights Reserved

PHOTOCHEMICAL TRIGGERING OF REACTIVE ENYNE-ALLENES AND ENEDIYNES
FOR THE APPLICATION IN ANTI-CANCER DRUGS

by

ALEXANDER V. KUZMIN

Major Professor:	Vladimir V. Popik
Committee:	George F. Majetich
	Robert S. Phillips

Electronic Version Approved:

Maureen Grasso
Dean of the Graduate School
The University of Georgia
December 2010

DEDICATION

I dedicate this work to my beloved grandmother, Zinaida Kuzmina, and my wife, Anastasia Kuzmina, who believed in me and helped me to get where I am now. Their interminable love and inspiration will stay forever in my heart.

ACKNOWLEDGEMENTS

There have been several people who have influenced and encouraged me during my pursuit and understanding in the field of Chemistry. Many thanks go to Ms. Elena Kushnirchuk, my high school Chemistry and Biology teacher, and to Dr. Alexander Blandov, my undergraduate advisor. Also to Dr. Thomas H. Kinstle, Professor of Organic Chemistry at Bowling Green State University, who helped me to get into graduate school.

My sincerest appreciation goes to my research advisor, Professor Vladimir Popik for his mentoring, guidance, and assistance during this work.

I would like to thank the members of my doctoral committee, Drs. George Majetich and Robert Phillips for their constructive review of this manuscript.

Finally, I would like to recognize some current and former members of the Popik group: Dr. Gregori Karpov, Dr. Alexey Kostikov, Dr. Andrei Poloukhine, Dr. Selvanathan Arumugam, Dr. Victor Sorokoumov, Dr. Dinesh Pandithavidana, Natalia Zhegalova, Emmanuel Nekongo, Christopher McNitt, Dewey Sutton, and Kevin Wickware.

TABLE OF CONTENTS

	Page
DEDICATION	iv
ACKNOWLEDGEMENTS	v
LIST OF SCHEMES	ix
LIST OF FIGURES	xii
 CHAPTER	
1 INTRODUCTION	1
1.1 Natural Enediyne Antibiotics.....	2
1.2 Bergman Cyclization	3
1.3 Myers—Saito and Schmittle Cyclization.....	5
1.4 Neocarzinostatin Family	6
1.5 Calicheamicin Family and Related Natural Enediynes	9
1.6 DNA Damaging Mechanism.....	11
1.7 Photo-Bergman Cyclization of Synthetic Enediynes.....	12
1.8 Triggering of the Bergman Cyclization	20
1.9 Triggering of Myers—Saito and Schmittle Cyclization	27
1.10 References	30
2 ENHANCEMENT OF THE REACTIVITY OF ENEDIYNES VIA KETO-ENOL TAUTOMERIZATION	42
2.1 Introduction.....	42

2.2 Results and Discussion	44
2.3 Reactivity of Enediyne 2.9	48
2.3 Conclusions.....	52
2.4 Experimental Section	53
2.5 Synthetic Procedures.....	55
2.6 Cartesian Coordinates of Optimized Structures.....	66
2.7 References	69
3 DUAL REACTIVITY OF A PHOTOCHEMICALLY-GENERATED CYCLIC	
ENYNE-ALLENE	72
3.1 Introduction.....	72
3.2 Results and Discussion	73
3.3 Photochemistry and Kinetics of Enyne-Allene 3.2	78
3.4 DNA Cleavage Experiment	82
3.5 Conclusions.....	84
3.6 Experimental Section	86
3.7 DNA Cleavage Procedure.....	87
3.8 Synthetic Procedures.....	88
3.9 References.....	97
4 SYNTHESIS AND REACTIVITY OF CYCLIC ENEDIYNE CONTAINING	
ADDITIONAL ENEDOCYCLIC TRANS-DOUBLE BOND	101
4.1 Introduction.....	101
4.2 Results and Discussion	103
4.3 Conclusions.....	112

4.4 Experimental Section	113
4.5 References	119
5 SURFACE FUNCTIONALIZATION USING CATALYST-FREE AZIDE-ALKYNE CYCLOADDITION	122
5.1 Abstract	123
5.2 Introduction	123
5.3 Results and Discussion	125
5.4 Kinetics of Metal-Free Click Immobilization	129
5.5 Experimental Section	138
5.6 References	148
APPENDICES	
A ^1H and ^{13}C NMR Spectra of Essential Compounds	154

LIST OF SCHEMES

	Page
Scheme 1.1: The Bergman cyclization mechanism	4
Scheme 1.2: The Myers—Saito and Schmittel cyclization	5
Scheme 1.3: Structures of natural nine-membered enediyne antibiotics	6
Scheme 1.4: Proposed mechanism of thiol-dependant activation of neocarzinostatin	7
Scheme 1.5: Proposed mechanism of thiol-independent activation of neocarzinostatin	8
Scheme 1.6: Structures of natural ten-membered ring enediyne antibiotics	9
Scheme 1.7: Proposed mechanism of activation of Calicheamicin	10
Scheme 1.8: DNA cleavage by C(5') hydrogen atom abstraction	11
Scheme 1.9: Photochemical cyclization of (Z)-1,6-diphenylhexa-3-en-1,5-diyne	12
Scheme 1.10: Direct photocyclization of 3-benzo-1,5-diyne to naphthalene (Turro)	13
Scheme 1.11: Photolysis of 3-benzo-1,5-diyne in 2-propanol-d ₁	14
Scheme 1.12: Photolysis of pyrene-based enediyne (Funk).	15
Scheme 1.13: Photolysis of cyclodeca-1,5-diyne-3-ene (Hirama)	15
Scheme 1.14: Photolysis of enediyne-amino acid conjugates (Jones).....	16
Scheme 1.15: Photoactivated pyrimidine-based enediynes (Russell).....	16
Scheme 1.16: Bergman cyclization of substituted benzannelated enediynes (Alabugin)	17
Scheme 1.17: Photo-excitation of enediynes via MLCT (Zaleski).....	18
Scheme 1.18: Photo-excitation of a copper metalloenediyne (Zaleski)	18
Scheme 1.19: Photolysis of acridinium-based enediynes (Schmittel)	19

Scheme 1.20: Photoactivation of dynamicin model (Nicolaou)	20
Scheme 1.21: Photoactivation of dynamicin analogues (Wender)	21
Scheme 1.22: Triggering of lactam-based enediynes (Banfi).....	22
Scheme 1.23: Photogeneration of reactive enediynes (Popik).....	23
Scheme 1.24: Enediyne prodrug activated via an allylic rearrangement (Dai)	24
Scheme 1.25: Activation of an enediyne precursor by visible light (Branda)	25
Scheme 1.26: Phototriggering through <i>E-Z</i> isomerization of aza enediynes (Basak)	26
Scheme 1.27: Cleavage of nitrobenzyl carbamates	26
Scheme 1.28: Activation of dynamicin model by a nitroreductase enzyme (Hay)	27
Scheme 1.29: Photochemical activation of acyclic enediynes (Suzuki).....	28
Scheme 1.30: Photoactivation of enyne-allenes (Schmittel)	28
Scheme 1.31: Activation of enediynes through a photochemical ring contraction (Popik)	29
Scheme 2.1: Cycloaromatization of regioisomeric enediynes 2.1a and 2.2a	42
Scheme 2.2: Cycloaromatization of regioisomeric enediynes 2.1b and 2.2b	43
Scheme 2.3: Keto-enol equilibrium of enediyne 2.5 and 2.6	44
Scheme 2.4: Comparison of reactivity of enediyne 2.5 , 2.9 , and 2.12	46
Scheme 2.5: Synthesis of the enediyne 2.9	47
Scheme 2.6: Keto-enol tautomerization of enediyne 2.9	51
Scheme 3.1: Photochemical generation of enyne-allene 3.2	73
Scheme 3.2: Formation of difluorocarbene and its addition to double and triple bonds	74
Scheme 3.3: Preparation of trimethylsilyl fluorosulfonyldifluoroacetate (TFDA)	74
Scheme 3.4: Synthesis of 6-(2-bromophenyl)hex-5-ynyl acetate 3.4	75
Scheme 3.5: Preparation of cyclopropenone 3.6	75

Scheme 3.6: Conversion of cyclopropenone 3.6 to acetal 3.7	76
Scheme 3.7: Preparation of cyclopropenone 3.1	77
Scheme 3.8: Dual reactivity of enyne-allene 3.2 in different media	81
Scheme 3.9: Photolysis of cyclopropenone 3.1 and supercoiled DNA	83
Scheme 4.1: Cyclization of benzo-fused enediyne 4.4	101
Scheme 4.2: Cycloaromatization of dimesylate 4.6	102
Scheme 4.3: Comparison of the cyclization rates of 2.1 and 4.8	102
Scheme 4.4: Bergman cyclization of dienediyne 4.1	103
Scheme 4.5: Synthesis of dienedine 4.1	104
Scheme 4.6: Epoxidation of the double bond of the dienediyne 4.1	105
Scheme 4.7: Cycloaromatization of dienediyne 4.1	106
Scheme 4.8: Contribution of the trans double bond to the strain energy of 4.1	107
Scheme 4.9: Contribution of different substituents at (<i>E</i>)-double bond to $\Delta E(\text{TS})$	108
Scheme 4.10: The direct Bergman cyclization of dienediyne 4.1	108
Scheme 4.11: Possible mechanism of cyclization of the dienediyne 4.1	109
Scheme 4.12: <i>Trans-cis</i> isomerization of the double bond of cycloheptene	109
Scheme 4.13: Attempt to thermally isomerize 1,4- to 1,2-dihydroanthracene	110
Scheme 4.14: Possible pathways of the cyclization of dienediyne 4.1	111
Scheme 4.15: Thermal cyclization of dienediyne 4.1 in 2-propanol-d ⁸	111
Scheme 4.16: Photolysis of dienediyne 4.1	112
Scheme 5.1: Synthesis of ADIBO-C6-amine (5.6)	126
Scheme 5.2: Synthesis of ADIBO-biotin (5.8) and ADIBO-PEG ₄ -amine (5.9)	127

LIST OF FIGURES

	Page
Figure 2.1: UV spectra of enediyne 2.9 , 2.10 , and 2.11a	49
Figure 2.2: Rate profile for the cycloaromatization of enediyne 2.9	50
Figure 3.1: UV-spectra of cyclopropanone 3.1 , enyne-allene 3.2 , and 3.17	79
Figure 3.2: Rate of cyclization of photo-generated enyne-allene 3.2	80
Figure 3.3: Temperature rate profile for the Bergman cyclization of the enyne–allene 3.2	81
Figure 3.4: Relaxation and linearization of the ϕ X174 supercoiled DNA	82
Figure 3.5: Light-induced cleavage of DNA by the photogenerated enyne–allene 3.2	84
Figure 4.1: Decomposition of (1 <i>E</i>)-6,7-benzocyclodeca-1-ene-4,9-diyne (4.1)	106
Figure 5.1: ADIBO derivatization of an epoxy-coated slide	128
Figure 5.2: Integral fluorescent intensity of Oregon Green azide (5.13)	129
Figure 5.3: Intensity of Oregon Green azide spots on ADIBO-derivatized slide	130
Figure 5.4: Biotinylation of ADIBO-coated slide	131
Figure 5.5: Azide derivatization of an epoxy-coated slide	132
Figure 5.6: Images of two-color derivatization of azide-slides	134
Figure 5.7: Biotinylation of azide-coated slides	135
Figure 5.8: Derivatization of streptavidin-coated beads with azide and ADIBO	136
Figure 5.9: Fluorescent confocal microscope images of beads	137

CHAPTER 1

INTRODUCTION

People suffering from cancer are generally treated with surgery, radiotherapy, and/or chemotherapy. In chemotherapy, the majority of conventional anti-tumor drugs work either by damaging the DNA molecules or by interfering with the cell replication process. This prevents cell division, eventually leading to the cell death. Ideally, the cytotoxic agent should be delivered directly to the targeted site. Unfortunately, achieving selectivity between cancerous and healthy cells is a major problem of modern chemotherapy.

The goal of this dissertation study was to design and prepare model precursors, which upon irradiation would produce enediynes and enyne-allenes in situ, culminating in a rapid cycloaromatization. The second objective was to study the reactivity and nuclease activity of the prepared compounds.

Development of enediynes and enyne-allenes for use in phototherapy would be of great interest for a number of reasons. First, this approach has the potential to confine drug action to a desired location. Precursors of enediynes and enyne-allenes, which have no cytotoxicity in the dark but can be easily activated upon irradiation with light, allow for temporal and spatial control of the drug release. Thus, photoactivatable enediynes and enyne-allenes have prospective applications in treatment of some cancers. In addition, they can be used in non-oncological applications, for example, generation of polymeric materials, and antimicrobial chemotherapy.

In chapter one of this dissertation, natural enediyne antibiotics, their structures, current applications, and limitations are discussed. The literature describing techniques, which allow triggering of reactive enediynes and enyne-allenes, will also be reviewed. Chapters two, three, and four will describe enediynes and enyne-allenes and discuss their reactivity as well as several new concepts of triggering enyne-allenes and enediynes will be addressed in those chapters. In chapter five “a strain promoted” click chemistry on the glass surface is discussed.

1.1 NATURAL ENEDIYNE ANTIBIOTICS

Natural enediynes are arguably the most potent anticancer agents ever discovered. The challenging structural complexity of the enediyne antibiotics, their mechanism of action, and their biological activity have created enormous scientific interest. These compounds share (Z)-hexa-3-ene-1,5-diyne (enediyne) or (Z)-hexa-1,2,4,-hepta-trien-6-yne (enyne-allene) moieties, constrained within nine- or ten-membered ring. Extensive studies of these potent compounds found that their cytotoxicity is attributed to the ability of an enediyne fragment to undergo the Bergman cyclization (Scheme 1.1) and produce *p*-benzyne diradicals.¹ These 1,4-diradicals act as “a warhead” inducing the DNA cleavage via hydrogen abstraction from the sugar phosphate backbone.² A similar cycloaromatization reaction of the enyne-allenes generating $\alpha,3$ -didehydrotoluene is known as the Myers—Saito cyclization (Scheme 1.2). The ability of natural enediynes to cleave DNA has challenged many scientists to develop these compounds into anticancer drugs. In spite of toxicity issues, neocarzinostatin (NCS),³ the first discovered anti-tumor antibiotic having an enediyne-containing chromophore, was advanced into anticancer clinical trials. Later, neocarzinostatin as a part of a polymer-based conjugate has been approved for the treatment of cancers of the liver and brain, as well as leukemia, in Japan.⁴

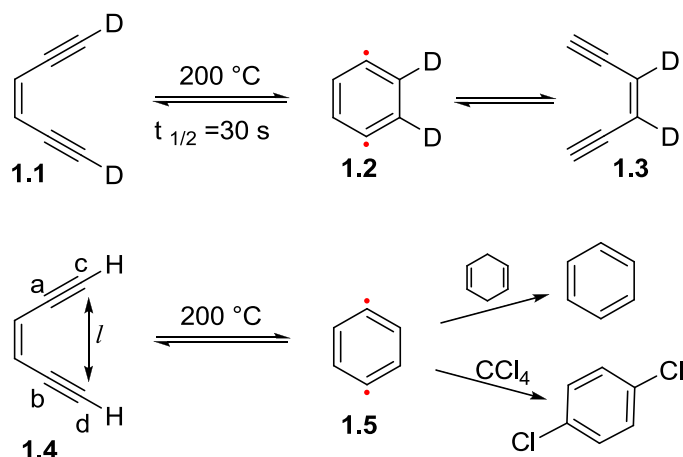
In 2000, the natural enediyne calicheamicin as a monoclonal antibody (anti-CD33) conjugate was approved in the U.S. under the trade name of Mylotarg for the treatment of elderly patients with acute myeloid leukemia.⁵ The monoclonal antibody-CD33 was used to target cancerous cells because a majority of myeloid leukaemia cells and normal committed myeloid precursor cells in the bone marrow express CD33, which is a transmembrane receptor. While overall response rates were only 30%, the drug was relatively well tolerated by most patients. The major drawback of Mylotarg is the high cost of the treatment since utilization of monoclonal antibodies. After ten years on the U.S. market, Mylotarg was withdrawn because studies did not show its efficacy and the treatment was linked to death from liver and lung toxicity.

There are a number of detailed reviews^{1-2, 6} and books covering natural enediynes,⁷ including a book which is devoted to neocarzinostatin.⁸ This literature review is focuses on highlighting important aspects of natural enediynes and covering some of their model derivatives.

1.2 BERGMAN CYCLIZATION

The Bergman cyclization derives its name from the work published in 1972 by Bergman and co-workers, which describes reversible cyclization of compounds containing a (*Z*)-hexa-3-ene-1,5-diyne moiety to form the reactive *p*-benzyne biradical.⁹ In this paper, Jones and Bergman reported that heating (3*Z*)-3-hexene-1,5-diyne-d₂ (**1.1**) to 200 °C in the gas phase led to a rapid deuterium exchange giving only a different isomer **1.3** and the starting material **1.1** in the ratio 1:1 (Scheme 1.1). It should be mentioned that cycloaromatization of enediynes was early observed by Mayer, Sondheimer, and Masamune, but the exact mechanism of cyclization has not been elucidated.

Scheme 1.1 The Bergman cyclization mechanism.



The main conclusion of this work was that 1,4-dehydrobenzene (**1.5**) can be generated by simply heating a fairly stable enediyne **1.4**. Further evidence to support the existence of the diradical **1.5** was obtained when enediyne **1.4** was heated in a solution of 1,4-cyclohexadiene and carbon tetrachloride to give benzene and 1,4-dichlorobenzene, respectively. These reactions are a good indication of free radicals, suggesting the intermediacy of *p*-benzyne diradical **1.5**.¹⁰

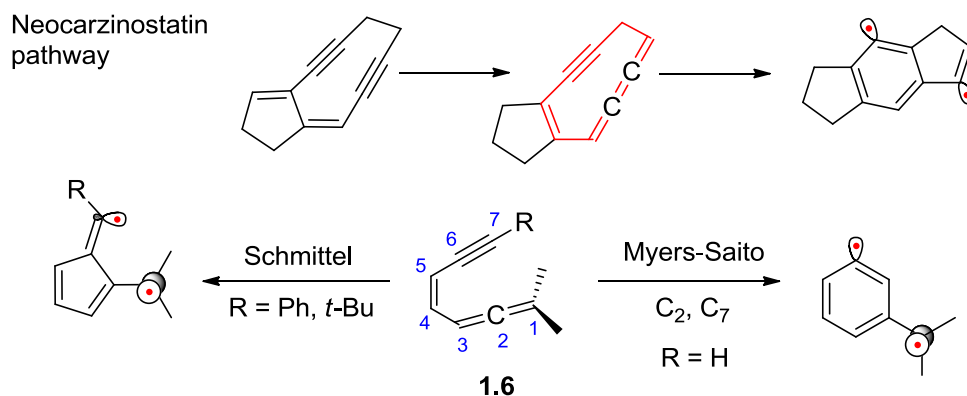
The cycloaromatization of acyclic enediynes has a large energy activation barrier. As a result, acyclic enediynes are stable and undergo cyclization only at high temperatures. On the other hand, natural enediyne antibiotics are stable at ambient temperature, but rapidly undergo cyclization after activation. Nicolaou *et al.* proposed to use the distance between the terminal alkynyl carbons to predict the reactivity of enediynes (*l*, Scheme 1.1).¹¹ Thus, the empirically determined “critical range”, where spontaneous cyclization should occur at room temperature, was found to be of 3.31-3.2 Å.¹² Later, it was extended to 3.4-2.9 Å, based on DFT calculations and experimental data.¹³ In general, addition of a benzene ring to an enediyne moiety decreases the rate of Bergman cyclization of enediyne compounds. For example, Semmelhack *et al.* have

investigated a series of 10-membered fused-enediynes which show the reactivity dependence on the olefinic character of the arene π bond.¹⁴

1.3 MYERS—SAITO AND SCHMITTEL CYCLIZATION

The Myers—Saito cyclization derives its name from independently discovered results published in 1989 by the Myers and Saito groups.¹⁵ The Myers—Saito cyclization is a cycloaromatization reaction of (Z)-1,2,4-hepta-trien-6-yne (enyne-allene), producing $\alpha,3$ -didehydrotoluene analogs (Scheme 1.2).¹⁶ These $\alpha,3$ -didehydrotoluene derivatives produced during cycloaromatization of simple enyne-allens are σ,π -diradicals. Antibiotics of the Neocarzinostatin family also undergo the Myers—Saito cyclization but this is believed to proceed via a σ,σ -diradical. The cycloaromatization of enyne-allenes is usually irreversible.

Scheme 1.2 The Myers—Saito and Schmittel cyclization.



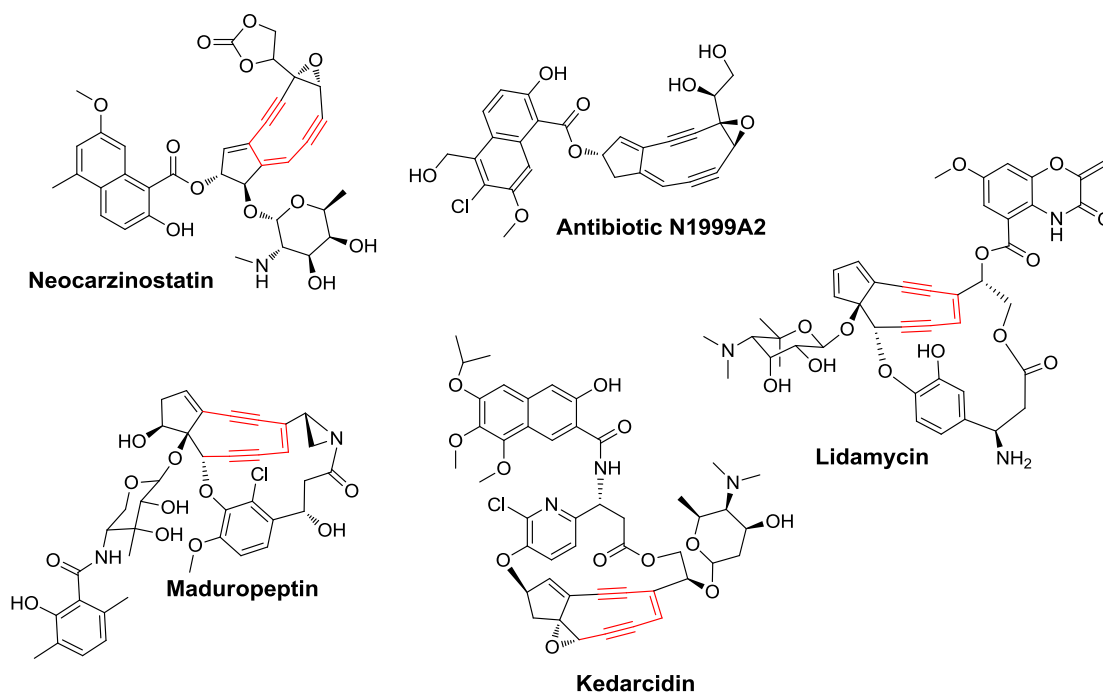
In 1995, Schmittel *et al.* discovered an alternative reaction to the Myers—Saito cyclization for enyne-allenes.¹⁷ The authors demonstrated that enyne-allene **1.6** may also undergo a novel C2-C6 ring closure cyclization when the alkyne terminal hydrogen is replaced by bulky groups such as phenyl or *tert*-butyl (Scheme 1.2). These bulky substituents increase the cyclization barrier of the Myers—Saito reaction due to steric hindrance. In addition, a phenyl

substituent lowers the barrier of the Schmitt cyclization by delocalization of the formed radical, which is also a σ,π -diradical.¹⁸

1.4 NEOCARZINOSTATIN FAMILY

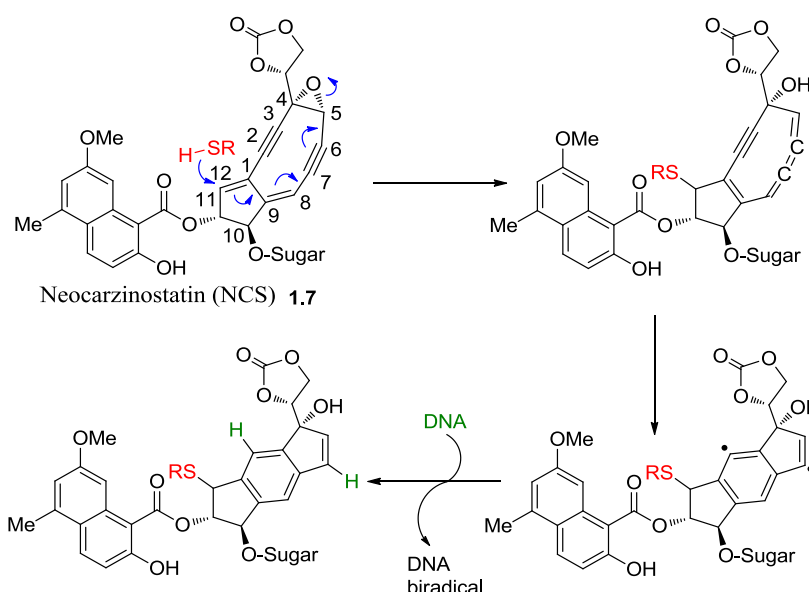
The enediynes have been categorized into two subgroups: nine- and ten-membered ring chromophore cores. The first enediyne antibiotic that contains a nine-membered ring, neocarzinostatin (NCS), was isolated from *Streptomyces carzinostaticus* and reported by Ishida *et al.* in 1965. NCS was found to be a 1:1 complex of chromophore and an apoprotein.³ This apoprotein binds tightly to NCS with $K_D = 1 \times 10^{-10}$ M, which explains the stability of the complex.¹⁹ The nine-membered ring enediynes are usually noncovalently associated with an apoprotein that plays a role of protection and transportation of the chromophore. The structure of the active nine-membered enediyne unit was resolved only in 1985 (Scheme 1.3).²⁰

Scheme 1.3 Structures of natural nine-membered enediyne antibiotics.



While being definitely a member of the enediyne family, NCS contains no (*Z*)-3-hexene-1,5-diyne fragment, as can be seen from Scheme 1.3. At the same time, NCS possesses a unique mechanism of action. A nucleophile can be used to activate NCS-chromophore into a labile, reactive species that induces DNA damage.

Scheme 1.4 Proposed mechanism of thiol-dependant activation of neocarzinostatin.



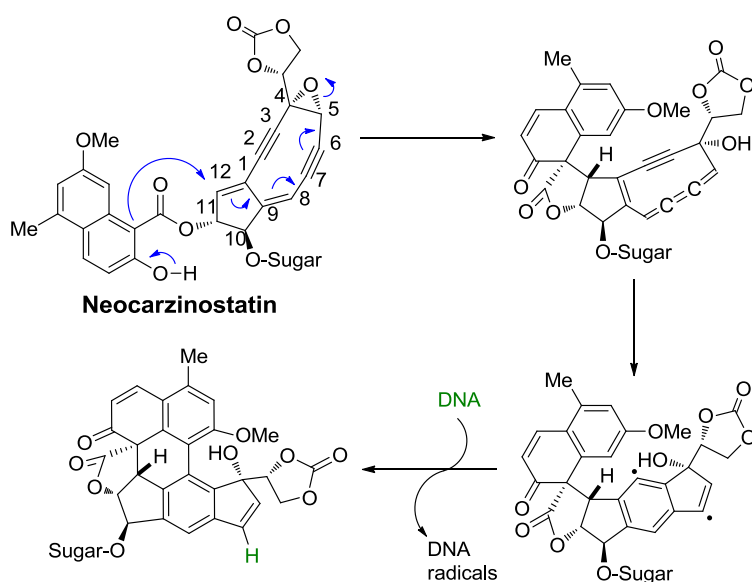
According to the accepted mechanism, an attack of a thiol nucleophile at C12 results in ring opening of the epoxide followed by formation of a highly strained cumulene (Scheme 1.4),²¹ which has been observed by NMR at low temperature.²² The extended cumulene-enyne is believed to undergo Myers—Saito-type cyclization.^{23,22} The produced diradical can abstract one or two hydrogen atoms from DNA, leading to single- and/or double-strand cleavage.²⁴

The type of damage that occurs depends on how the diradical is positioned within the minor groove of a DNA molecule. When the diradical has access to only one strand of the DNA it results in the abstraction of only one hydrogen and leads to single-strand DNA cleavage. In contrast, when a diradical that is positioned between both strands, hydrogen atom transfer

produces double-strand DNA scission. Mass spectrometry has been applied to explain the mechanism of action of neocarzinostatin by observing the corresponding intermediates.²⁵

An alternative mechanism was proposed suggesting that NCS can be activated by a general base-catalyzed intramolecular addition reaction in the absence of a nucleophilic thiol (Scheme 1.5).²⁶

Scheme 1.5 Proposed mechanism of thiol-independent activation of neocarzinostatin.

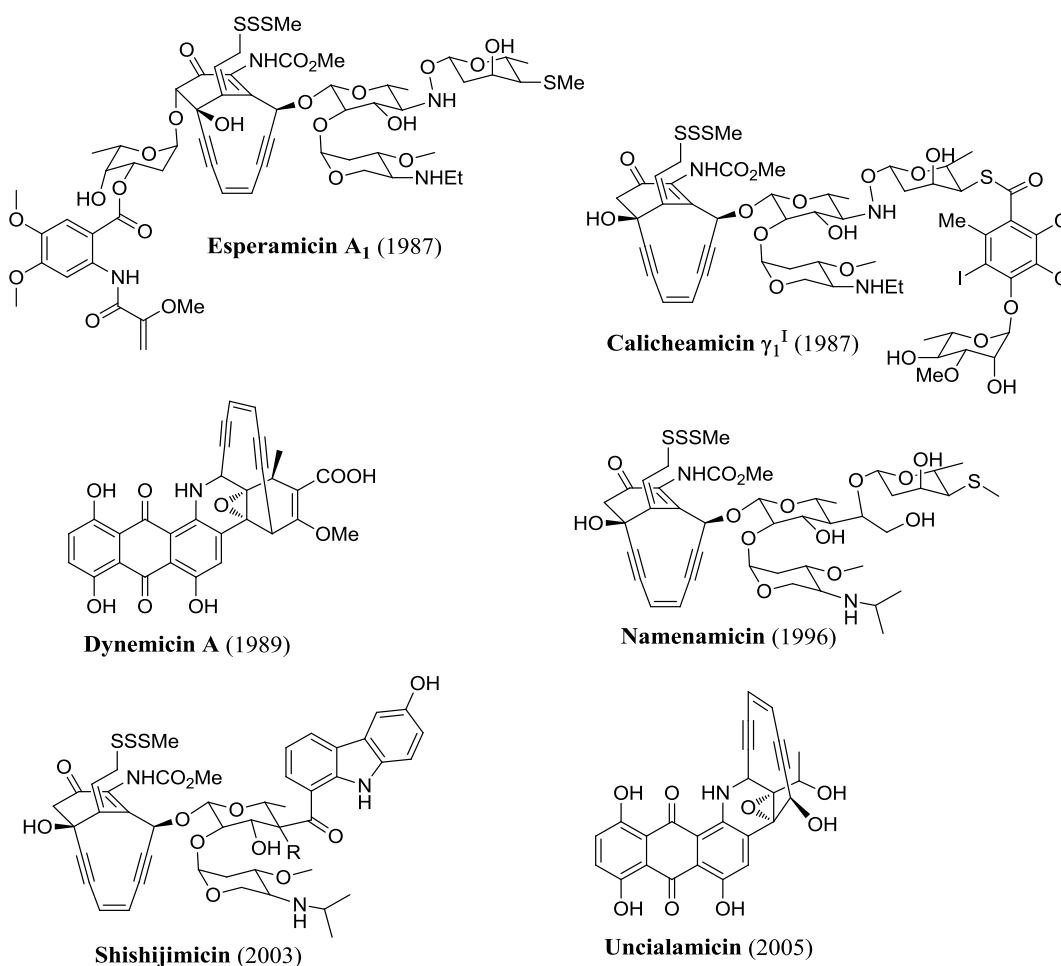


While several groups tried to synthesize neocarzinostatin,²⁷ especially its nine- and 10-membered ring analogs,²⁸ only in 1998 did Myers and co-workers report a total synthesis.²⁹ Due to the instability of precursors of the final product, a special technique was used involving extraction and chromatographic isolation procedures at 4 °C under an inert atmosphere. Such conditions significantly improved yield of several precursors of neocarzinostatin. The synthesis of neocarzinostatin required 20 steps. In nature, most of the natural enediyne antibiotics are produced by microorganisms, classified as actinomycetes, to protect themselves against bacteria and viruses.

1.5 CALICHEAMICIN FAMILY AND RELATED NATURAL ENEDIYNES

The calicheamicins are a family of natural enediynes isolated from *Micromonospora echinospora*. The structures of the calicheamicins and esperamicins were first published in 1987 (Scheme 1.6).³⁰ Two years later, another member of the enediyne family, dynemicin A, was discovered.

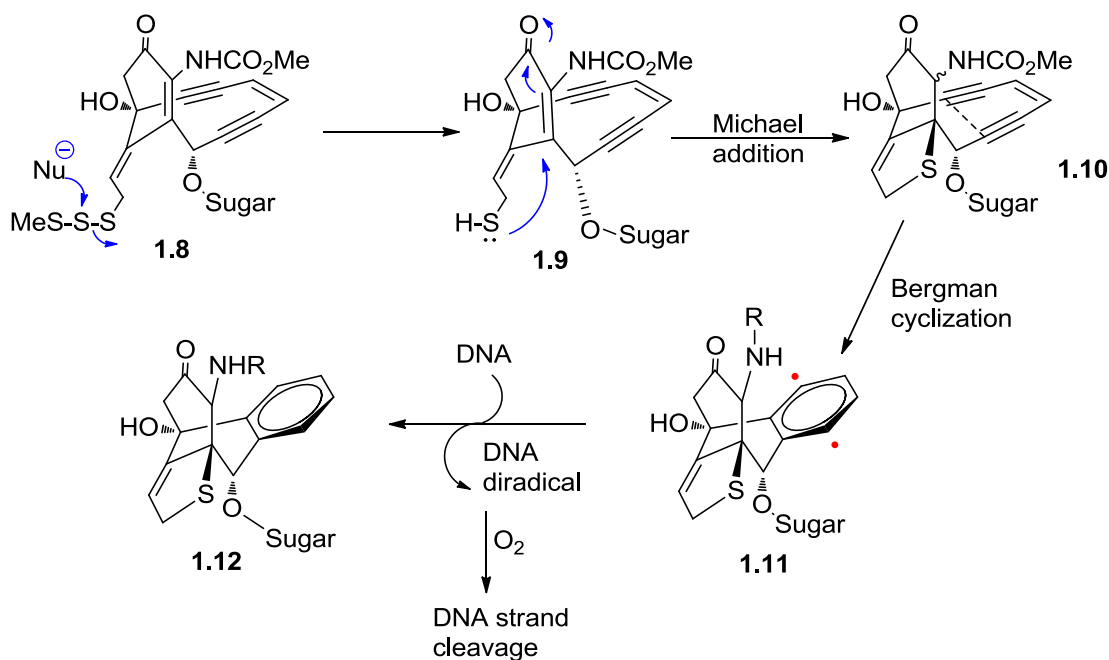
Scheme 1.6 Structures of natural ten-membered ring enediyne antibiotics.



The calicheamicin structure can be divided into three components: an enediyne core, which is responsible for the biological activity; a sugar moiety binds to DNA molecules; and a

trisulfide group that acts as a “triggering device” to activate the enediyne core toward the cyclization (Scheme 1.7).

Scheme 1.7 Proposed mechanism of activation of Calicheamicin.

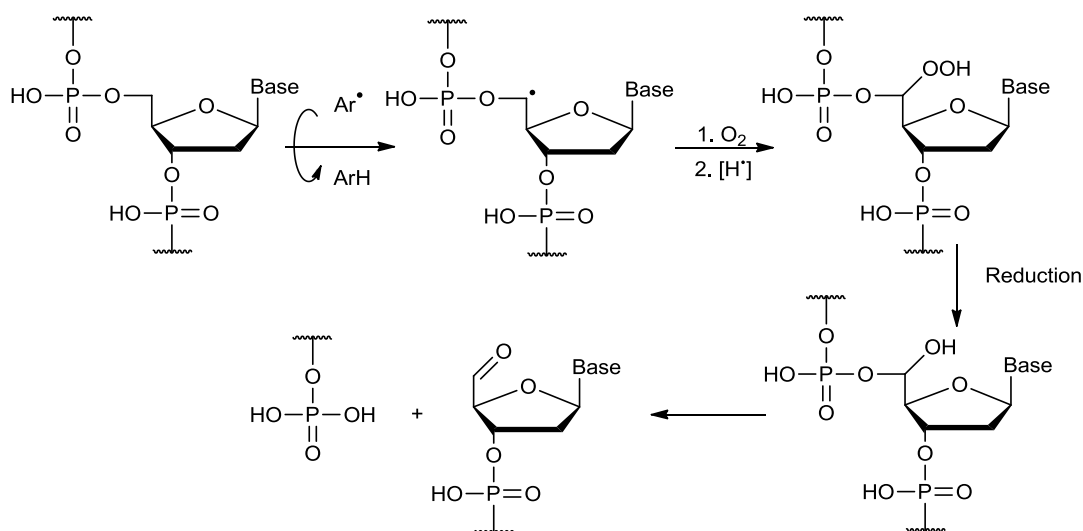


Intensive investigation of natural enediyne antibiotics revealed a very elegant mode of action. The sugar moiety binds the minor groove of DNA prior to a nucleophile (e.g. glutathione) adding to the central sulfur atom of the trisulfide fragment, which causes the formation of a thiol that can add intramolecularly to the α,β -unsaturated ketone. The structural change reduces the barrier for the cyclization reaction. Thus, the enediyne **1.10** undergoes the Bergman cyclization producing a highly reactive *p*-benzyne diradical **1.11**. The latter is positioned in the minor groove of DNA molecules and abstract two hydrogen atoms from sugar phosphate backbone of both strands of the DNA, forming a stable compound **1.12**. The abstraction of hydrogens leads to cleavage of the DNA molecules at both strands, resulting in apoptosis of cells.

1.6 DNA DAMAGING MECHANISM

Considerable effort has been devoted to identifying the details of DNA damage by the Neocarzinostatin chromophore diradical. Goldberg and co-workers demonstrated that at least 80% of the DNA cleavage leads to the 5'-aldehyde of A and T residues selectively (Scheme 1.8).³¹ As can be seen from Scheme 1.8, the presence of O₂ is essential to execute the DNA strand cleavage.

Scheme 1.8 DNA cleavage by C(5') hydrogen atom abstraction.



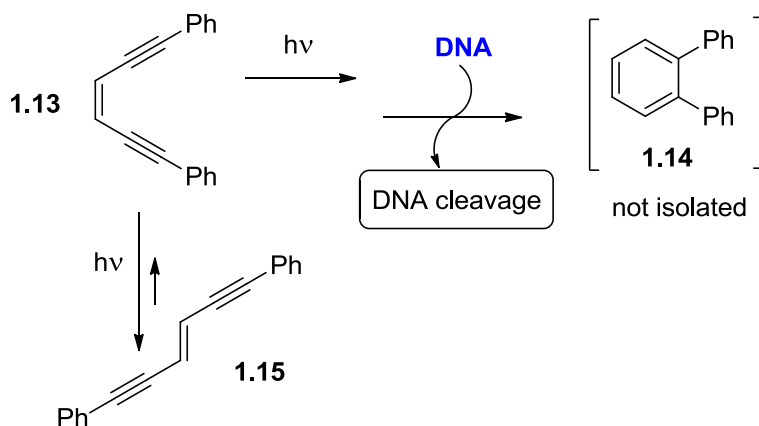
The principal explanation of these breaks is hydrogen abstraction from C(5') of deoxyribose and reaction with molecular oxygen as outlined in Scheme 1.8. Less than 20% of the strand breaks result from hydrogen atom abstraction at C(4')²⁴ and C(1')³² which are not shown here.

1.7 PHOTO-BERGMAN CICLIZATION OF SYNTHETIC ENEDIYNES

A major stumbling block to clinical applications of enediyne antibiotics is their inadequate selectivity in distinguishing between cancerous and normal cells. In the past 20 years, various enediyne model compounds were developed to address the selectivity issue. Artificial enediynes were rationally designed with the intention to boost their reactivity toward the Bergman and/or Myers—Saito cyclization under suitable triggering conditions. For example, the use of light for generation of reactive species allows for temporal and spatial control of produced radicals. Direct irradiation of acyclic and cyclic enediynes, as well as of natural antibiotic Dynemicin A, is known to cause light-induced cycloaromatization. However, quantum and chemical yields of this process are usually very low.

The first intramolecular photochemical cyclization of enediynes was accidentally discovered in 1968.³³ However, no further activity in this field took place for 25 years. In 1993 Kagan and co-workers reported that simple acyclic enediynes **1.13** and **1.14** can be phototoxic (Scheme 1.9).³⁴

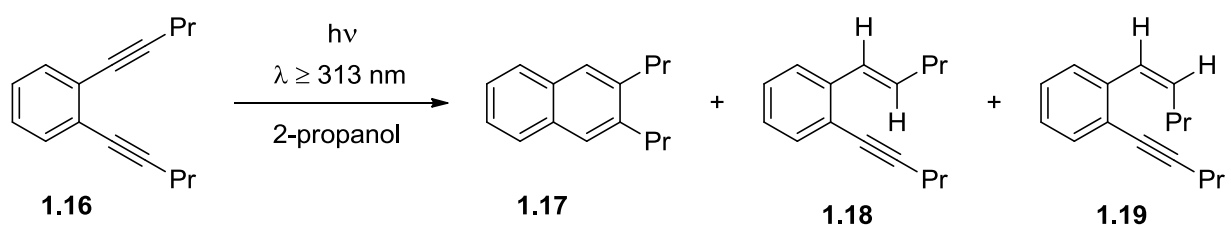
Scheme 1.9 Photochemical cyclization of (Z)-1,6-diphenylhexa-3-en-1,5-diyne.



Enediynes **1.13** and **1.15** were shown to undergo *cis-trans* isomerization around the double bond during photolysis. Compound **1.13** was found to induce DNA strand breaks photochemically. Specifically, enediyne **1.13** photosensitizes the production of strand breaks in double-stranded supercoiled pBR322, and in single-stranded M13 DNA. The DNA cleavage reactions are favored by the presence of oxygen and are inhibited by ethanol. The formation of *o*-terphenyl, the expected product of the Bergman cyclization, **1.14**, was not detected. Thus, the powerful sensitizing properties of **1.13** and **1.15** were possibly caused by the photosensitized formation of $^1\text{O}_2$ and $\text{O}_2^{\cdot -}$, which are known to damage numerous cell components. The mechanism of the DNA cleavage, however, has not been elucidated.

One year later, a paper by Turro and Nicolaou sparked considerable interest in the photochemical Bergman cyclization.³⁵ The authors reported that the photolysis of aromatic enediyne **1.16** gave naphthyl products upon irradiation using a medium pressure Hg lamp, possibly via a 1,4-dehydronaphthalene intermediate (Scheme 1.10).

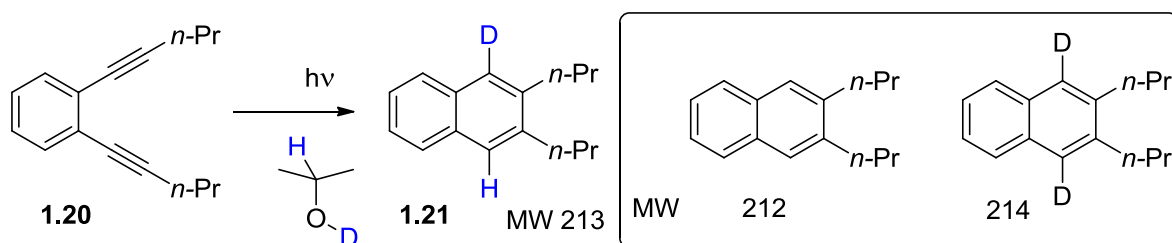
Scheme 1.10 Direct photocyclization of 3-benzo1,5-diyne to naphthalene (Turro).



The choice of solvent played a key role in both the efficiency of the process and the product formation. For example, the highest yield of **1.17** (ca. 40%) was obtained in diphenylmethanol. When the photolysis of dienediyne **1.16** was conducted in 2-propanol- d_1 , a

product of structure **1.21** was eluted. However, no significant production of products of mass 212 or 214 was observed by GC/MS analysis (Scheme 1.11).

Scheme 1.11 Photolysis of 3-benzo1,5-diyne in 2-propanol- d_1 .



The insertion of deuterium in **1.21**, and the formation of **1.18**, and **1.19**, indicate that the photo-Bergman cyclization proceeds through several intermediates, and the mechanism of this reaction is more complex than one of the parent Bergman cyclization. For example, the formation of products **1.18** and **1.19** can be explained by photoreduction of one of the triple bonds of the enediyne functionality. Later, Evenzahav and Turro proposed that the singlet diradical gives the expected aromatic product, while intersystem crossing from the singlet to the triplet state could lead to photoreduction products.³⁶ It was also suggested that the photochemical reaction causes the excitation of an acetylenic unit rather than of the entire enediyne functionality.

In 1996, Funk and co-workers reported the photochemistry of a series of aromatic enediyne molecules, which gave Bergman-type products in the presence of 1,4-cyclohexadiene as a hydrogen donor (Scheme 1.12).³⁷ In addition, water-soluble analogs of the enediynes were effective in binding DNA molecules and in cleaving them upon photolysis.

Scheme 1.12 Photolysis of pyrene-based enediyne (Funk).

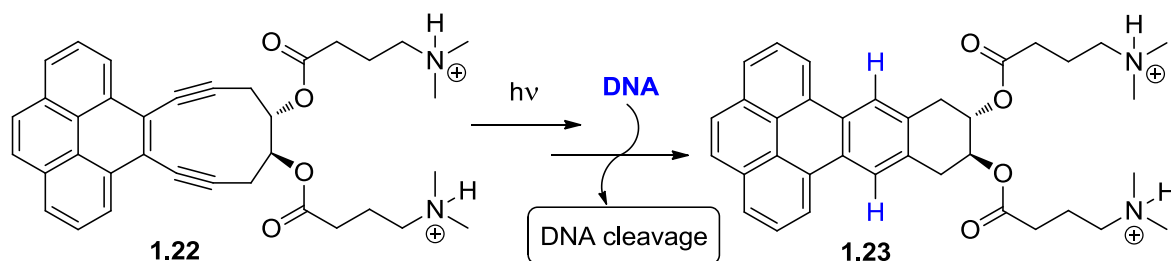
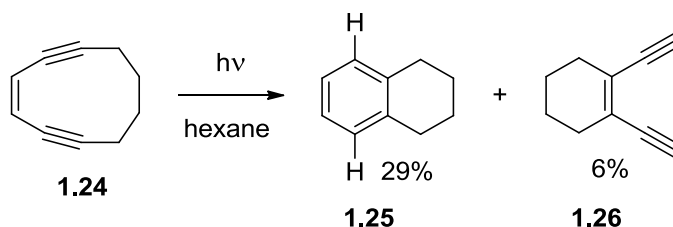


Photo-Bergman reaction of aliphatic enediynes has also been investigated by Hirama and his group.³⁸ Photolysis of cyclodeca-1,5-diyn-3-ene (**1.24**) resulted in the formation of the expected product of Bergman cyclization, tetrahydro naphthalene (**1.25**), and an appreciable amount of 1,2-diethynylcyclohexene (**1.26**, Scheme 1.13). Enediyne **1.26** was isolated and photolysed under the same conditions to give **1.25** in 3% yield.

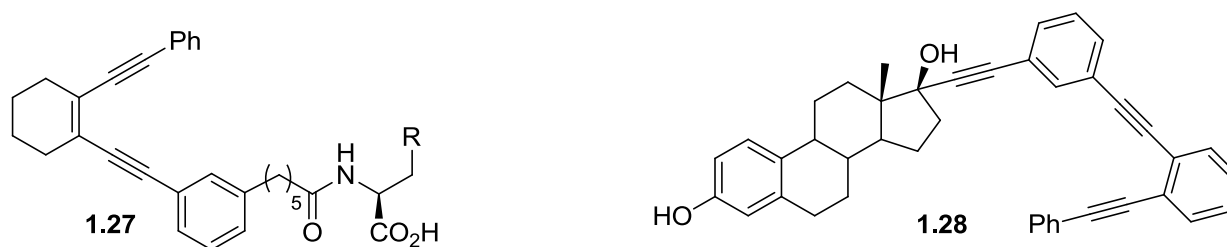
Scheme 1.13 Photolysis of cyclodeca-1,5-diyn-3-ene (Hirama).



In 2000, Jones and co-workers reported the photochemical activation of acyclic enediynes, as a function of ring strain and electronic effects.³⁹ Expanding further the application of the photo-Bergman reaction, protein degradation with photoactivated enediyne-amino acid conjugates was also investigated (Scheme 1.14).⁴⁰ On the basis of molecular architecture, three independent classes of enediynes with defined protein targets have been identified and showed correlation between affinity and protein degrading activity. In order to extend the versatility of

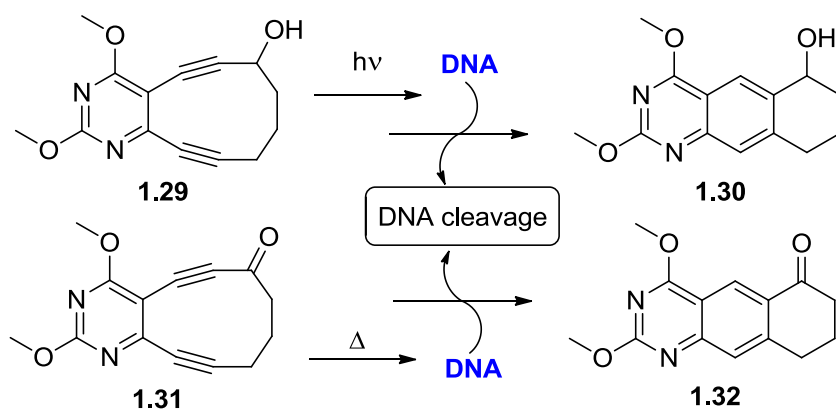
the enediynes as controlled cytotoxins, the preparation of a photo-Bergman precursor as an anti-body conjugate was demonstrated.⁴¹ In addition, a simple acyclic enediyne was also successfully attached to gold nanoparticles.^{41a} Reitz *et al.* also reported preparation of benzo-fused enediynes with attached amino acids.⁴²

Scheme 1.14 Photolysis of enediyne-amino acid conjugates (Jones).



Russell and his group have reported cycloaromatization of pyrimidine-fused enediynes in 2-propanol solution (Scheme 1.15).⁴³ They found that enediyne **1.29** can be forced to undergo thermal- and photo-Bergman cyclization when ketone **1.31** cyclizes only under thermal conditions.

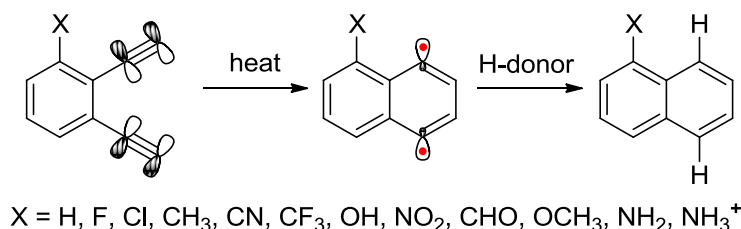
Scheme 1.15 Photoactivated pyrimidine-based enediynes (Russell).



Imidazole-fused enediynes were investigated by Peterson.⁴⁴ Conformationally more rigid enediynes were found to undergo photoinduced Bergman cyclization more efficiently than less rigid analogs. The use of the imidazole-fused enediynes can be potentially beneficial to improve enediynes affinity to DNA molecules, since imidazoles are known to bind to the heterocyclic bases of DNA.⁴⁵ Another way to achieve binding of enediyne compounds to DNA molecules can be accomplished by using effective noncovalent minor groove DNA binding agents,⁴⁶ which was demonstrated by Boger and his group.⁴⁷

The quantum yield of the photochemical Bergman cyclization can be substantially improved by adjusting the electronic properties of substituents, which was shown by Alabugin *et al.* in 2006.⁴⁸ The effect of *ortho*-substituents on the rate of the Bergman cyclization was studied using kinetic experiments, confirming that the cyclization barrier is highly sensitive to the nature of *ortho*-substituents. Thus, it was found that both *ortho*-NO₂ and *ortho*-CHO substituents substantially decrease activation energies of the Bergman cyclization through the inductive effect.

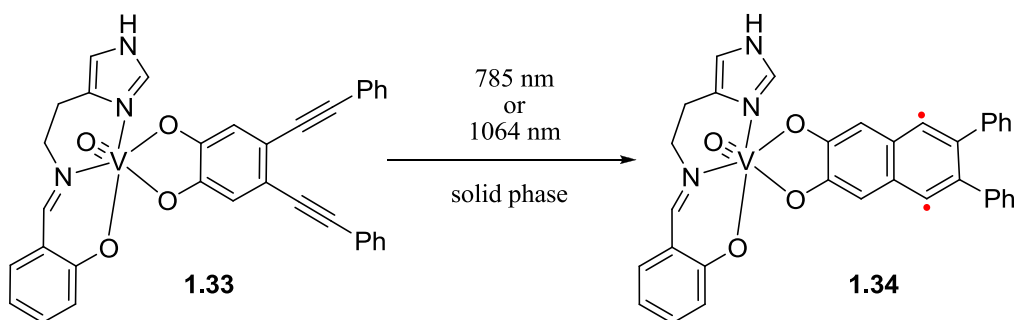
Scheme 1.16 Bergman cyclization of substituted benzannulated enediynes (Alabugin).



The quantum yield can be also increased by using different modes of excitation energy transfer, such as metal-to-ligand charge transfer (MLCT). Thus, an interesting approach to controlling the reactivity of acyclic enediynes and photoinitiating Bergman cyclization with long-wavelength excitation was reported by Zaleski and co-workers.⁴⁹ Long-wavelength

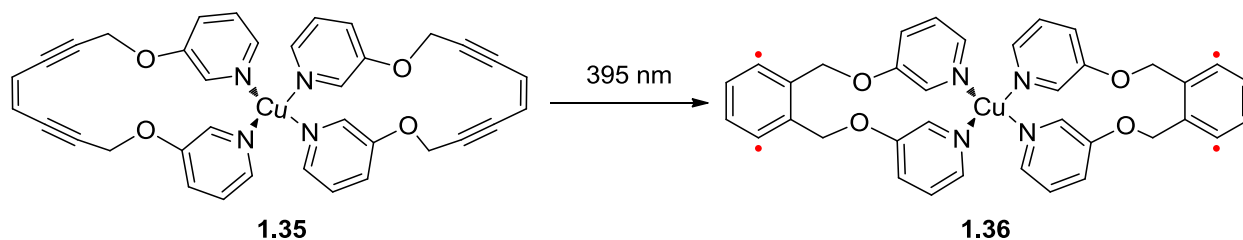
electronic transition was generated via MLCT. A vanadium metalloenediynes compound **1.33** can absorb the visible or near-IR region to produce *p*-benzyne biradicals (Scheme 1.17). The thermal and photothermal reactions of **1.33** led to the formation of high molecular weight species, indicating the formation of polymeric products.

Scheme 1.17 Photo-excitation of enediynes via MLCT (Zaleski).



Zaleski has also described a copper metalloenediynes compound **1.35** that is capable of the DNA cleavage (Scheme 1.18).⁵⁰ The authors suggested a mechanism for photo-Bergman cyclization which is derived from energy transfer to the enediynes unit upon charge-transfer excitation.

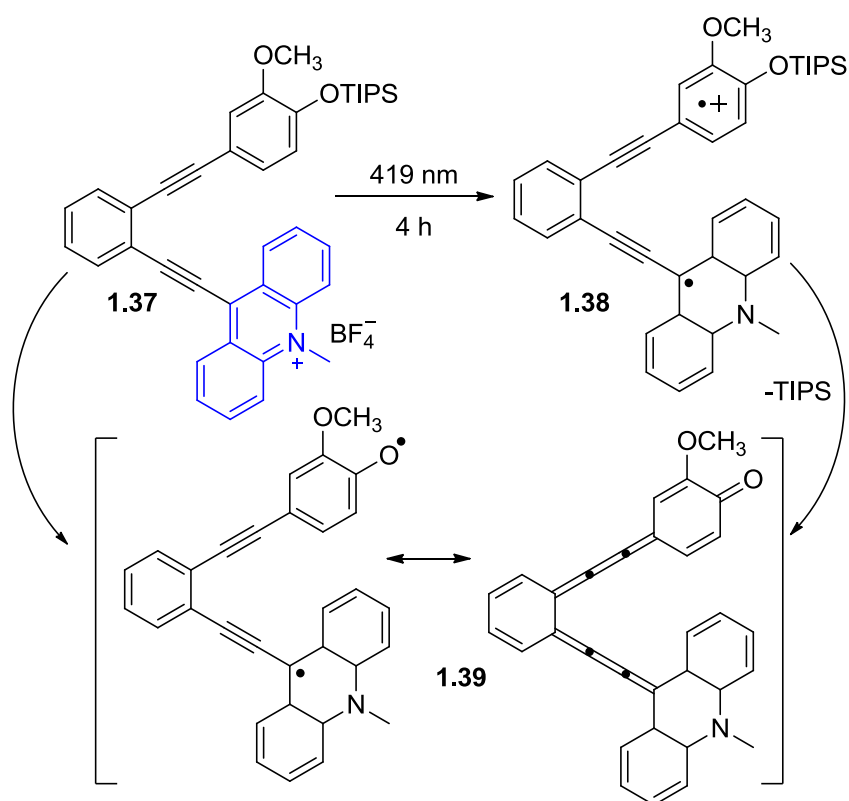
Scheme 1.18 Photo-excitation of a copper metalloenediynes (Zaleski).



A photoinduced electron transfer (PET) strategy can be used to activate enediynes compounds to undergo the cycloaromatization reaction. Enediynes **1.37** was designed by Schmitt and co-workers as a potential precursor to *s-cis* biscumulene **1.39** (Scheme 1.19).⁵¹

Upon photoexcitation of the acridinium component (shown in blue) of the enediyne **1.37**, an intramolecular electron transfer is expected to give an acridine radical, as depicted by the structure **1.38**. According to the authors, the affinity of **1.37** to DNA was determined to be $K = 4.5 \times 10^6 \text{ M}^{-1}$. It was found that only one type of **1.37**-DNA complex was formed. Irradiation of compound **1.37** and DNA with 300 nm, 350 nm, and 419 nm light resulted in the DNA cleavage. Irradiation at 419 nm led to a complete cleavage of the DNA molecules.

Scheme 1.19 Photolysis of acridinium-based enediynes (Schmittel).



Schmittel also pointed out that acridinium salts may induce DNA cleavage upon irradiation though PET from the DNA to the photoexcited acridinium. Thus, the mode of action of **1.37** may be different from a proposed route as shown in the Scheme 1.19. One of the

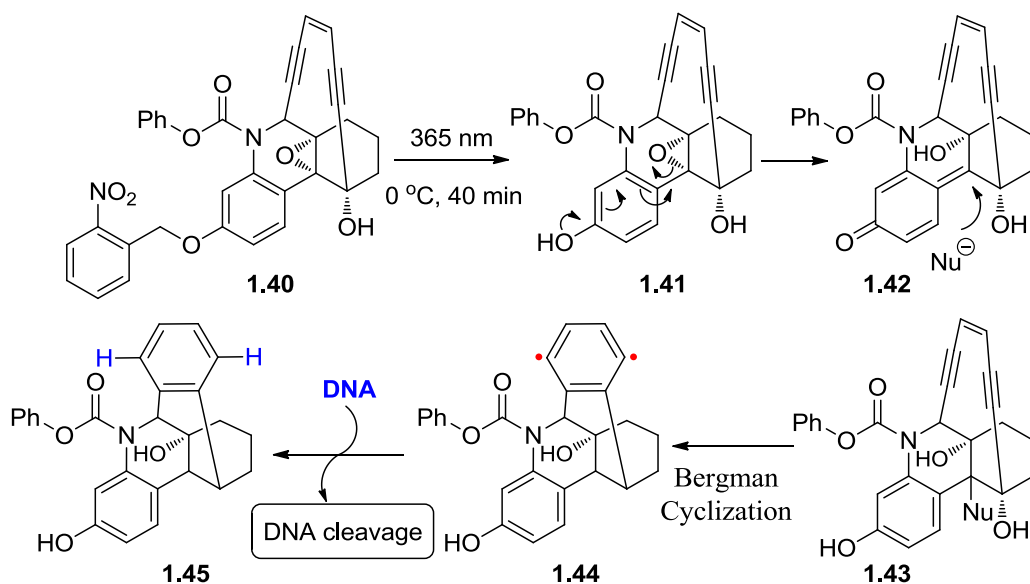
advantages of the designed systems is the possibility to use long wavelength light to activate enediynes for DNA cleavage.

1.8 TRIGGERING OF THE BERGMAN CYCLIZATION

The alternative strategy of photoactivation is the *in situ* generation of the reactive enediyne systems, which then undergo thermal Bergman cyclization. One important requirement for the developed drugs to be used for photodynamic-type therapy is the use of longer excitation wavelengths. Human tissue transmits light most effectively in the red part of the visible spectrum. The use of the longer wavelengths will ensure deeper light penetration.

A dynemicin-based model compound was reported by Nicolaou and his group, which uses photocleavable protecting group.⁵² Irradiation of **1.40** with 365 nm light results in the formation of the free phenol, which is followed by the opening of a ring-like epoxide. The change in flexibility of the ten-membered ring enediyne allows the Bergman cyclization as shown in Scheme 1.20.

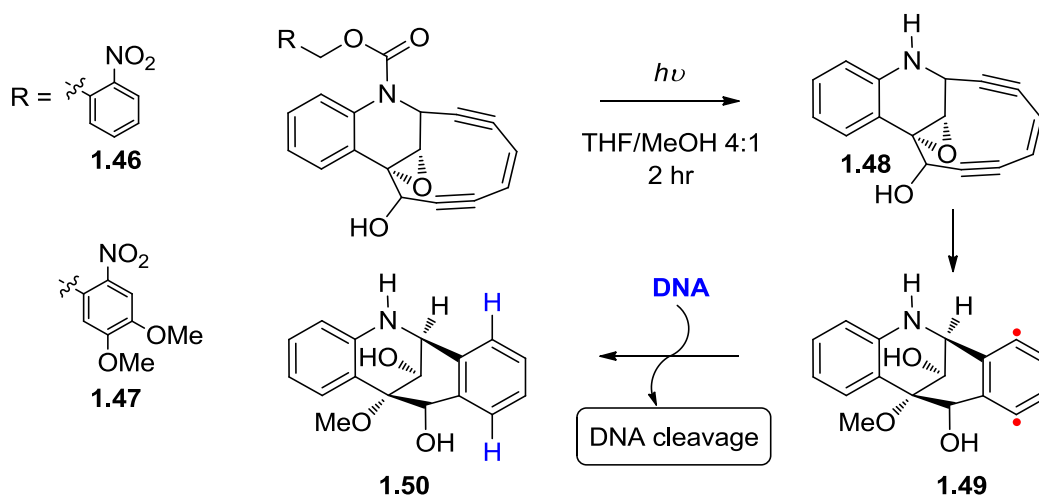
Scheme 1.20 Photoactivation of dynemicin model (Nicolaou).



According to the proposed mechanism, compound **1.40** under irradiation with light is converted into the diol **1.41**. Then, the quinone-methide **1.42** formed by epoxide ring opening is attacked by a nucleophile, which results in the release of strain by enediyne **1.43** undergoing the Bergman cyclization (Scheme 1.20). Although, no quantum yield was reported for the enediyne **1.40**, it should be mentioned that the quantum efficiency of the parent 2-nitrobenzyl is usually 0.1-40%. A relatively long time of irradiation, which is 40 min at 0 °C, was required to deprotect enediyne **1.40**.

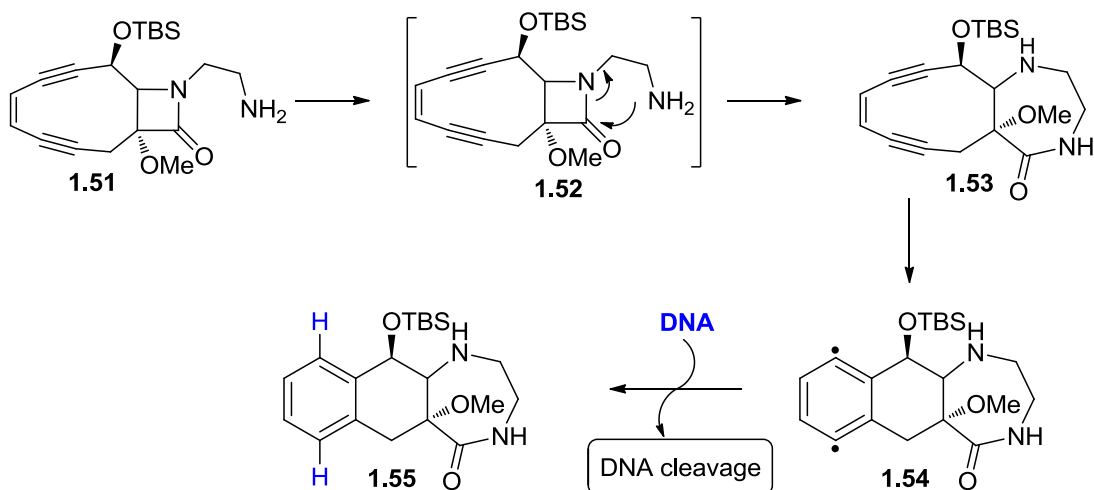
A similar approach to regulate reactivity of dynemicin analogues was used by Wender and his group.⁵³ Compounds **1.46** and **1.47** undergo cycloaromatization upon irradiation with 365 nm light (Scheme 1.21). Irradiation of a dilute solution of **1.46** and **1.47** in THF containing 25% of MeOH gave the cycloaromatized product **1.50**. Photodeprotection of the amine serves to increase electron density close to the oxirane bond, facilitating its hydrolytic opening. Photoactivation of these compounds in the presence of DNA led to the formation of both circular relaxed form II and linear form III cleavage products.

Scheme 1.21 Photoactivation of dynemicin analogues (Wender).



As it has been shown for natural enediynes, opening of the epoxide ring serves to initiate the Bergman cyclization because by an acid-catalyzed process. In comparison, cyclopropyl or cyclobutyl moieties cannot be used for the stabilization of enediynes because of the difficulty in opening them. On the other hand, the β -lactam is an excellent choice to use it as a molecular lock. Its ring can also be opened by nucleophiles such as thiol,⁵⁴ enzymes such as transpeptidase⁵⁵ or β -lactamase,⁵⁶ and under basic conditions.⁵⁷ Thus, Banfi and Guanti reported intramolecular trans-amidation of simple monocyclic β -lactams bearing a tethered amine.⁵⁸ The cyclic lactam serves as a constraint preventing the Bergman cyclization at ambient temperature. The authors also studied the effect of substituents and of reaction media on the rate of transamidation (Scheme 1.22).⁵⁹

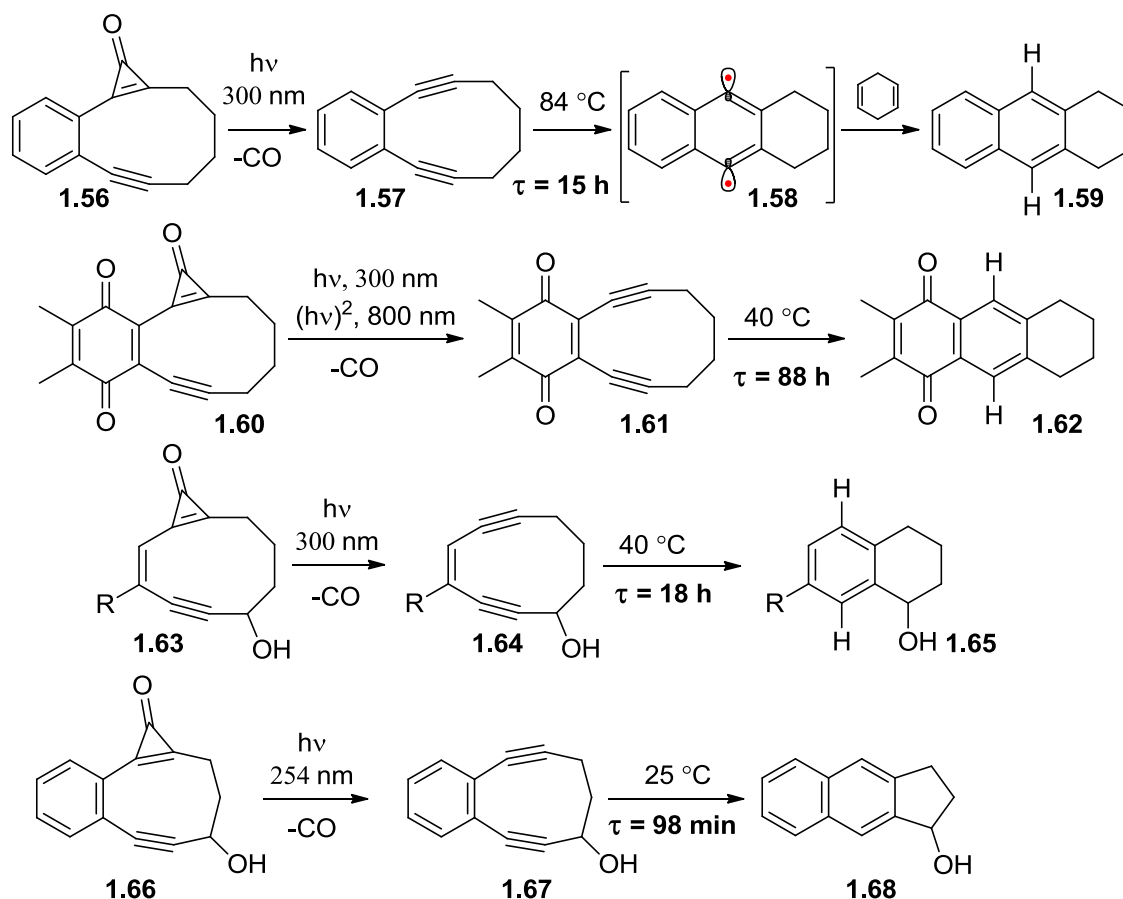
Scheme 1.22 Triggering of lactam-based enediynes (Banfi).



Banfi and Guanti have established that the β -lactam ring can stabilize a reactive ten-membered enediyne. On the other hand, triggering the transamidation can be achieved under mild conditions.

Popik and co-workers have demonstrated the triggering of cycloaromatization by photochemical generation of a triple bond.⁶⁰ This strategy involves the use of cyclopropenone as a protecting group to mask one of the triple bonds of the enediyne moiety. Photodecarbonylation of cyclopropenones is a very efficient reaction producing quantitative yields of corresponding acetylenes.⁶¹ At the same time, cyclopropenones **1.56** and **1.60** are stable and show no signs of decomposition on heating up to 90 °C (Scheme 1.23).

Scheme 1.23 Photogeneration of reactive enediynes (Popik).

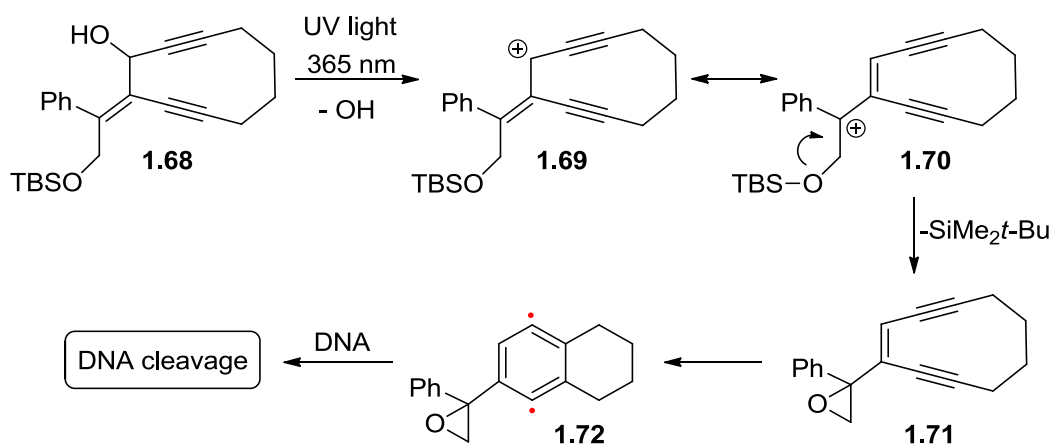


It is important to note that generation of reactive enediynes can also be achieved by a non-resonant two-photon excitation.⁶² Thus, irradiation of **1.60** with ultrashort 800-nm pulses

from a laser generates enediyne **1.61** in good yield (Scheme 1.23). However, it should be noted that fusion of the enediyne moiety with the benzene of the *p*-quinone ring increases the thermal stability of enediynes **1.57** and **1.61**, whereas enediyne **1.64** is more reactive and undergoes spontaneous Bergman cyclization under ambient conditions.

A photochemical triggering to form a double bond between two triple bonds of the enediyne moiety was successfully used to control the reactivity of enediyne compounds. Thus, several enediyne compounds possessing an exocyclic 2-hydroxy-1-phenylethylidene unit were prepared by Dai and co-workers.⁶³ UV irradiation of enediyne **1.68** with a protected hydroxymethyl group on the exocyclic double bond results in a photochemical alkene isomerization followed by an allylic rearrangement to form the epoxy enediyne **1.71**, which was confirmed by MS (Scheme 1.24).

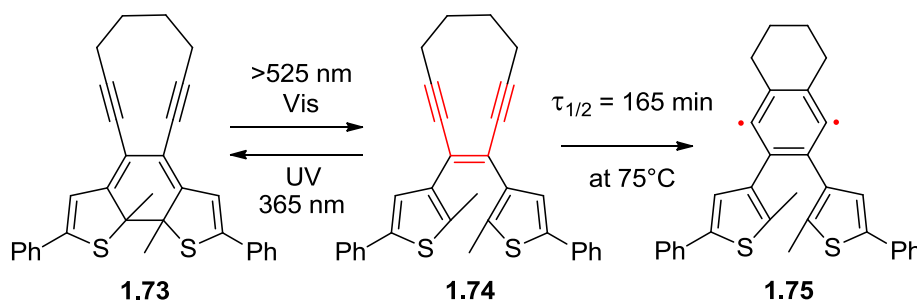
Scheme 1.24 Enediyne prodrug activated via an allylic rearrangement (Dai).



Irradiation of both enediyne **1.68** and the circular supercoiled DNA resulted in efficient single-strand cleavage. Cleavage of DNA can be explained via both Bergman cyclization pathway and alkylation of the DNA base by the formed epoxide **1.71**.

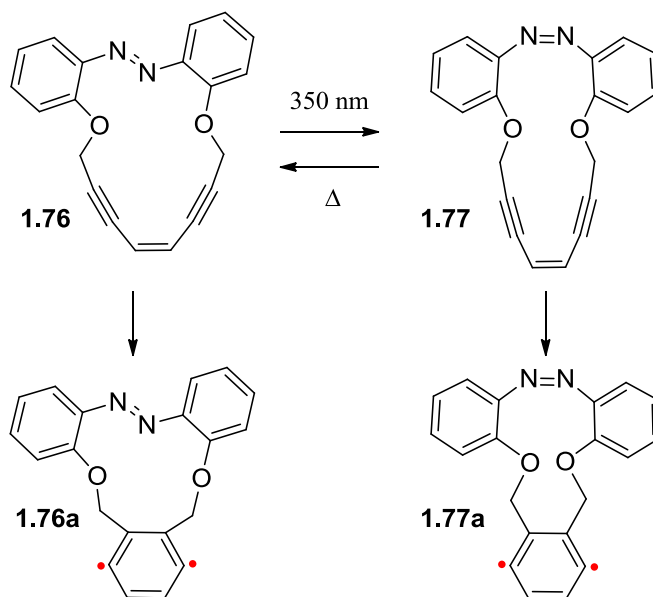
In 2007, Branda and co-workers showed that photochemical rearrangement of dithienylethene⁶⁴ can be used to create the enediyne structure (Scheme 1.25).⁶⁵ Only isomer **1.74** has the conjugated π -system that can undergo the Bergman cyclization and produce the biradical **1.75**, while isomer **1.73** is inactive. UV light triggers the photocyclization of the hexatriene in **1.74** converting it to its ring-closed counterpart **1.73**. Visible light activates the system by triggering the ring-opening reaction, regenerating enediyne **1.74**. In overall, the proposed concept is interesting and use of visible light is an advantage over UV-light. Nevertheless, the rate of cycloaromatization is rather slow ($k = 6.8 \times 10^{-5} \text{ s}^{-1}$, at 75 °C) and needs to be improved in order to use enediyne **1.74** *in vivo*.

Scheme 1.25 Activation of an enediyne precursor by visible light (Branda).



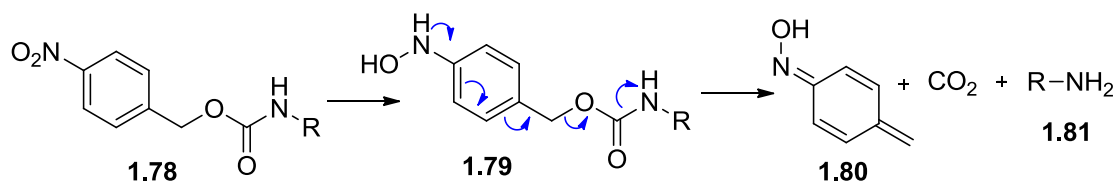
Aza compounds are well known to undergo reversible *E/Z*-isomerization induced by light or heat. In their pioneering work, Basak and co-workers reported the preparation of 16-membered ring enediyne compounds incorporating the azobenzene moiety (Scheme 1.26).⁶⁶ The photochemical *trans-cis* isomerization of the $\text{N}=\text{N}$ bond apparently brings acetylenic termini closer. This change in geometry reduces the offset temperature for the Bergman cyclization by 24 °C. Thus, the compound **1.77** can undergo the Bergman cyclization at 70 °C, when *trans*-isomer **1.76** requires heating up to 94 °C. It should be noted that produced enediyne **1.77** spontaneously isomerizes back to the starting material.

Scheme 1.26 Phototriggering through *E-Z* isomerization of aza enediynes (Basak).



Enzyme activation of enediyne compounds was reported using a nitrobenzyl carbamate to protect an amine moiety.⁶⁷ Nitrobenzyl carbamates can undergo enzymatic reduction to give hydroxylamine **1.79** followed by 1,6-elimination to release the free amine component as shown in Scheme 1.27.

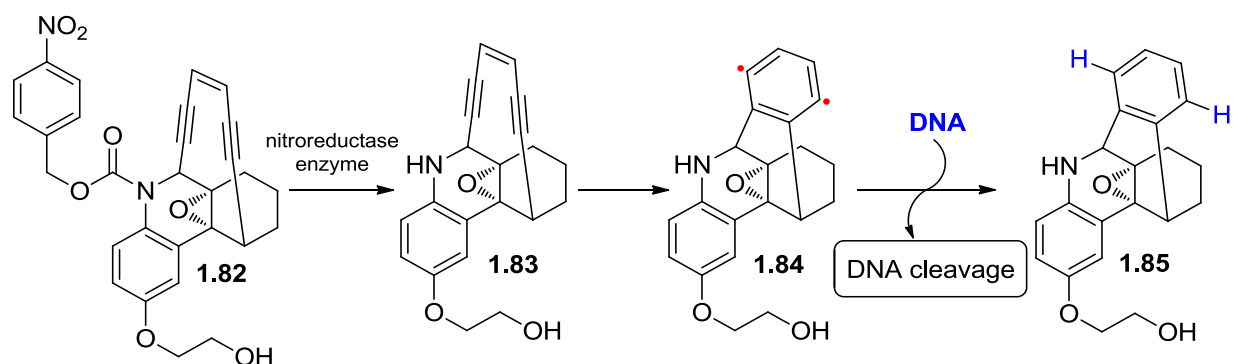
Scheme 1.27 Cleavage of nitrobenzyl carbamates.



Reduction of 4-nitrobenzyl carbamate **1.82** by a nitroreductase enzyme (NTR) from *E. coli* B produces secondary amine **1.83** (Scheme 1.28). The formation of the free amine **1.83** promotes opening of the epoxide followed by Bergman cyclization of the enediyne core. One of

the limitations of this system is that the cytotoxicity of **1.82** was shown to be oxygen-dependent, which may limit activity in hypoxic regions of tumors.

Scheme 1.28 Activation of dynamicin model by a nitroreductase enzyme (Hay).

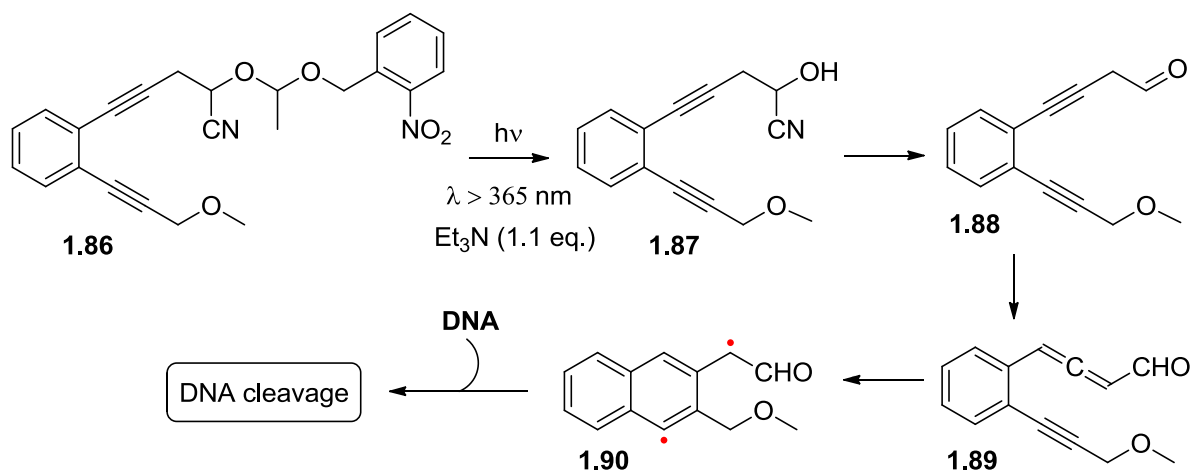


1.9 TRIGGERING OF MYERS—SAITO AND SCHMITTEL CYCLIZATION

In contrast to *p*-benzyne, which exists in equilibrium with the corresponding enediyne, $\alpha,3$ -didehydrotoluene is formed from enyne-allenes irreversibly. Usually, acyclic enyne-allene can undergo spontaneous cyclization under ambient temperature, while cyclic enyne-allenes are virtually unknown because of an even lower activation barrier.

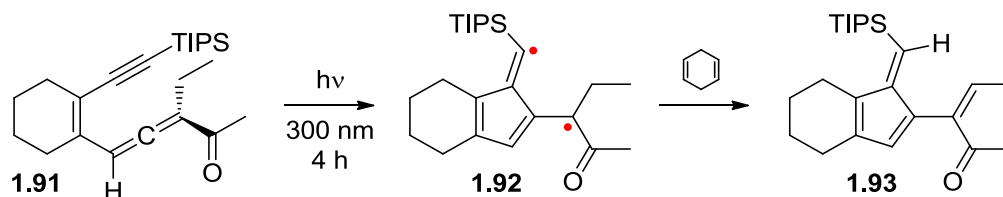
Ichiro Suzuki *et al.* reported the synthesis and DNA damaging ability of enediyne model compounds possessing photo-triggering devices (Scheme 1.29).⁶⁸ The activation method of enediyne **1.86** involves the photochemical deprotection of the cyanohydrin moiety, which results in the formation of the aldehyde **1.88**, which promotes isomerization of one of the triple bonds to the corresponding allene-aldehyde **1.89**. In fact, the rate of this isomerization is so rapid that it is almost impossible to synthetically prepare the parent propargylic aldehyde because of a spontaneous isomerization. The formed enyne-allene **1.89** undergo Myers—Saito cyclization to give $\alpha,3$ -didehydrotoluene-type biradicals.

Scheme 1.29 Photochemical activation of acyclic enediynes (Suzuki).



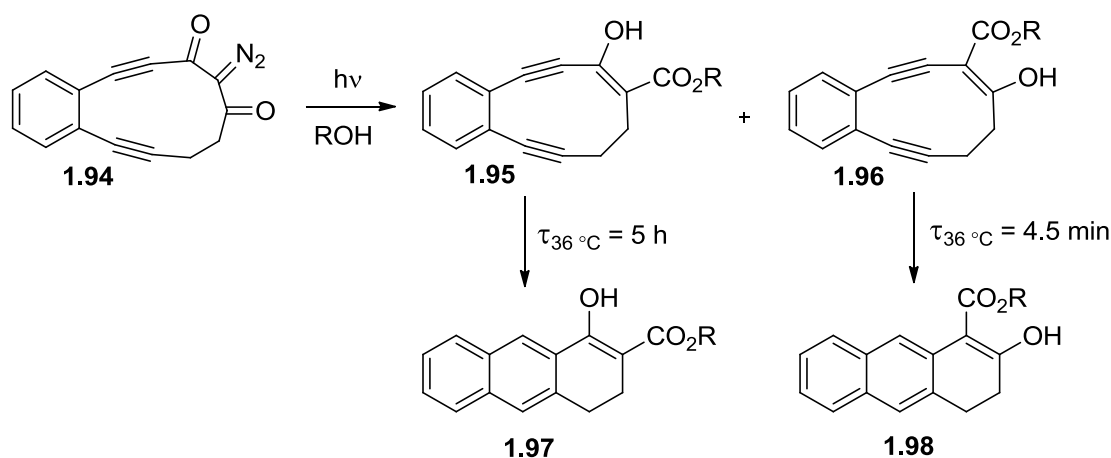
Schmittel *et al.* reported enyne-allene compounds that can be photochemically activated to undergo cycloromatization.⁶⁹ In order to improve the efficiency of the photocyclization, enyne-allenes were specially designed using the strict requirements, such as (i) avoiding benzannulated derivatives due to their high excitation energy;⁷⁰ (ii) using cycloalkenes to prevent cis-trans isomerization of the double bond; (iii) attaching an internal triplet sensitizer moiety; and finally, (iv) introducing a triisopropylsilyl group at the alkyne to increase the cyclization barrier, thus, preventing thermal side reactions during photolysis. Enyne-allene **1.91** was found to be stable at ambient temperature and it undergoes thermal cyclization only at 151 °C. Surprisingly, compound **1.91** can undergo the photochemical reaction providing only C²-C⁶ product **1.93** via the intermediate **1.92** (Scheme 1.30).

Scheme 1.30 Photoactivation of enyne-allenes (Schmittel).



The activation of enediyne compounds by photochemical ring contraction was reported by Popik and co-workers.⁷¹ This strategy is based on the fact that 11-membered ring enediynes are much more stable than their 10-membered analogs. To achieve ring contraction, the photochemical Wolff rearrangement was employed. The photolysis of eleven-membered enediyne **1.94** incorporating the α -diazo- β -diketone moiety results in the formation of two reactive isomers **1.95** and **1.96**, which undergo rapid cycloaromatization (Scheme 1.31).

Scheme 1.31 Activation of enediynes through a photochemical ring contraction (Popik).



As can be seen from the aforementioned examples, many different approaches were undertaken in order to control the reactivity of enediyne compounds by photoirradiation. However, there are a number of requirements which have to be considered before advancing the enediyne compounds to practical drugs. For example, the photoactivatable enediyne prodrugs should be soluble in aqueous solutions, have high affinity to DNA molecules, and undergo efficient photochemical transformation upon irradiation with a long wavelength light.

1.10 REFERENCES

- (1) Nicolaou, K. C.; Dai, W. M. Chemistry and biology of enediyne anticancer antibiotics. *Angew. Chem., Int. Ed.* **1991**, *30*, 1387-1416.
- (2) Smith, A. L.; Nicolaou, K. C. The Enediyne Antibiotics. *J. Med. Chem.* **1996**, *39*, 2103-2117.
- (3) Ishida, N.; Miyazaki, K.; Kumagai, K.; Rikimaru, M. Neocarzinostatin, an antitumor antibiotic of high molecular weight: Isolation, physicochemical properties and biological activities. *J. Antibiot. Ser. A* **1965**, *18*, 68-76.
- (4) Maeda, H.; Ueda, M.; Morinaga, T.; Matsumoto, T. Conjugation of Poly(Styrene-Co-Maleic Acid) Derivatives to the Antitumor Protein Neocarzinostatin - Pronounced Improvements in Pharmacological Properties. *J. Med. Chem.* **1985**, *28*, 455-461.
- (5) Hamann, P. R.; Hinman, L. M.; Beyer, C. F.; Lindh, D.; Upešlaciš, J.; Flowers, D. A.; Bernstein, I. An Anti-CD33 Antibody–Calicheamicin Conjugate for Treatment of Acute Myeloid Leukemia. Choice of Linker. *Bioconjugate Chem.* **2001**, *13*, 40-46.
- (6) (a) Galm, U.; Hager, M. H.; VanLanen, S. G.; Ju, J.; Thorson, J. S.; Shen, B. Antitumor Antibiotics: Bleomycin, Enediynes, and Mitomycin. *Chem. Rev.* **2005**, *105*, 739-758; (b) Kar, M.; Basak, A. Design, Synthesis, and Biological Activity of Unnatural Enediynes and Related Analogues Equipped with pH-Dependent or Phototriggering Devices. *Chem. Rev.* **2007**, *107*, 2861-2890; (c) Basak, A.; Mandal, S.; Bag, S. S. Chelation-Controlled Bergman Cyclization: Synthesis and Reactivity of Enediynyl Ligands. *Chem. Rev.* **2003**, *103*, 4077-4094; (d) Gredičak, M.; Jerić, I. Enediyne compounds - new promises in anticancer therapy. *Acta. Pharm.* **2007**, *57*, 133-150.

- (7) (a) Borders, D. B.; Doyle, T. W.; Dekker, M., *Eneidyne antibiotics as antitumor agents*. 1995: New York; (b) Cragg, G. M., Kingston, D.G. and Newman, D.J., *Anticancer agents from natural products*. 2005: Taylor & Francis Group.
- (8) Maeda, H.; Edo, K.; Ishida, N., *Neocarzinostatin: The Past, Present, and Future of an Anticancer Drug*. 1997, New York: Springer.
- (9) (a) Jones, R. R.; Bergman, R. G. *p*-Benzyne. Generation as an intermediate in a thermal isomerization reaction and trapping evidence for the 1,4-benzenediyl structure. *J. Am. Chem. Soc.* **1972**, *94*, 660-661; (b) Lockhart, T. P.; Comita, P. B.; Bergman, R. G. Kinetic evidence for the formation of discrete 1,4-dehydrobenzene intermediates. Trapping by inter- and intramolecular hydrogen atom transfer and observation of high-temperature CIDNP. *J. Am. Chem. Soc.* **1981**, *103*, 4082-4090.
- (10) Bergman, R. G. Reactive 1,4-Dehydroaromatics. *Acc. Chem. Res.* **1973**, *6*, 25-31.
- (11) Nicolaou, K. C.; Ogawa, Y.; Zuccarello, G.; Schweiger, E. J.; Kumazawa, T. Cyclic conjugated enediynes related to calicheamicins and esperamicins: calculations, synthesis, and properties. *J. Am. Chem. Soc.* **1988**, *110*, 4866-4868.
- (12) Nicolaou, K. C.; Zuccarello, G.; Riemer, C.; Estevez, V. A.; Dai, W. M. Design, synthesis, and study of simple monocyclic conjugated enediynes. The 10-membered ring enediyne moiety of the enediyne anticancer antibiotics. *J. Am. Chem. Soc.* **1992**, *114*, 7360-7371.
- (13) (a) Schreiner, P. R. Monocyclic Eneidyne: Relationships between Ring Sizes, Alkyne Carbon Distances, Cyclization Barriers, and Hydrogen Abstraction Reactions. Singlet-Triplet Separations of Methyl-Substituted *p*-Benzynes. *J. Am. Chem. Soc.* **1998**,

- 120, 4184-4190; (b) Schreiner, P. R.; Navarro-Vazquez, A.; Prall, M. Computational Studies on the Cyclizations of Eneidyne, Enyne-Allenenes, and Related Polyunsaturated Systems. *Acc. Chem. Res.* **2005**, *38*, 29-37.
- (14) Semmelhack, M. F.; Neu, T.; Foubelo, F. Arene 1,4-Diradical Formation from *o*-Dialkynylarenes. *J. Org. Chem.* **1994**, *59*, 5038-5047.
- (15) (a) Myers, A. G.; Kuo, E. Y.; Finney, N. S. Thermal generation of α ,3-dehydrotoluene from (Z)-1,2,4-heptatrien-6-yne. *J. Am. Chem. Soc.* **1989**, *111*, 8057-8059; (b) Nagata, R.; Yamanaka, H.; Okazaki, E.; Saito, I. Biradical formation from acyclic conjugated eneyne-allene system related to neocarzinostatin and esperamicin-calicheamicin. *Tetrahedron Lett.* **1989**, *30*, 4995-4998.
- (16) Wang, K. K. Cascade Radical Cyclizations via Biradicals Generated from Eneidyne, Enyne-Allenenes, and Enyne-Ketenenes. *Chem. Rev.* **1996**, *96*, 207-222.
- (17) Schmittle, M.; Strittmatter, M.; Kiau, S. Switching from the Myers reaction to a new thermal cyclization mode in enyne-allenes. *Tetrahedron Lett.* **1995**, *36*, 4975-4978.
- (18) Schmittle, M.; Kiau, S.; Siebert, T.; Strittmatter, M. Steric effects in enyne-allene thermolyses: Switch from the Myers—Saito reaction to the C2–C6-cyclization and DNA strand cleavage. *Tetrahedron Lett.* **1996**, *37*, 7691-7694.
- (19) Povirk, L. F.; Goldberg, I. H. Binding of the nonprotein chromophore of neocarzinostatin to deoxyribonucleic acid. *Biochemistry* **1980**, *19*, 4773-4780.

- (20) Edo, K.; Mizugaki, M.; Koide, Y.; Seto, H.; Furihata, K.; Otake, N.; Ishida, N. The structure of neocarzinostatin chromophore possessing a novel bicyclo-[7,3,0]dodecadiyne system. *Tetrahedron Lett.* **1985**, 26, 331-334.
- (21) Myers, A. G.; Proteau, P. J.; Handel, T. M. Stereochemical assignment of neocarzinostatin chromophore. Structures of neocarzinostatin chromophore-methyl thioglycolate adducts. *J. Am. Chem. Soc.* **1988**, 110, 7212-7214.
- (22) Myers, A. G.; Proteau, P. J. Evidence for spontaneous, low-temperature biradical formation from a highly reactive neocarzinostatin chromophore-thiol conjugate. *J. Am. Chem. Soc.* **1989**, 111, 1146-1147.
- (23) Myers, A. G.; Dragovich, P. S.; Kuo, E. Y. Studies on the thermal generation and reactivity of a class of (σ,π)-1,4-biradicals. *J. Am. Chem. Soc.* **1992**, 114, 9369-9386.
- (24) Chin, D. H.; Kappen, L. S.; Goldberg, I. H. 3'-Formyl phosphate-ended DNA: high-energy intermediate in antibiotic-induced DNA sugar damage. *Proc. Natl. Acad. Sci. U.S.A.* **1987**, 84, 7070-7074.
- (25) Chin, D. H.; Zeng, C. H.; Costello, C. E.; Goldberg, I. H. Sites in the diyne-ene bicyclic core of neocarzinostatin chromophore responsible for hydrogen abstraction from DNA. *Biochemistry* **1988**, 27, 8106-8114.
- (26) Hensens, O. D.; Helms, G. L.; Zink, D. L.; Chin, D. H.; Kappen, L. S.; Goldberg, I. H. Bifunctional involvement of the hydroxynaphthoate ester moiety in the activation of neocarzinostatin chromophore in DNA-mediated site-specific cleavage. *J. Am. Chem. Soc.* **1993**, 115, 11030-11031.

- (27) Wender, P. A.; Harmata, M.; Jeffrey, D.; Mukai, C.; Suffert, J. Studies on DNA - active agents: The synthesis of the parent carbocyclic subunit of neocarzinostatin chromophore *A. Tetrahedron Lett.* **1988**, 29, 909-912.
- (28) (a) Toshima, K.; Ohta, K.; Yanagawa, K.; Kano, T.; Nakata, M.; Kinoshita, M.; Matsumura, S. Novel Dienediyne Systems Related to the Neocarzinostatin Chromophore: Molecular Design, Chemical Synthesis, and Evaluation. *J. Am. Chem. Soc.* **1995**, 117, 10825-10831; (b) Hirama, M.; Fujiwara, K.; Shigematu, K.; Fukazawa, Y. The 10-membered ring analogs of neocarzinostatin chromophore: design, synthesis and mode of decomposition. *J. Am. Chem. Soc.* **1989**, 111, 4120-4122; (c) Suffert, J. Synthesis of a new 10-membered ring functionalised cyclodiynol related to neocarziostatin chromophore. *Tetrahedron Lett.* **1990**, 31, 7437-7440.
- (29) Myers, A. G.; Liang, J.; Hammond, M.; Harrington, P. M.; Wu, Y.; Kuo, E. Y. Total Synthesis of (+)-Neocarzinostatin Chromophore. *J. Am. Chem. Soc.* **1998**, 120, 5319-5320.
- (30) (a) Lee, M. D.; Dunne, T. S.; Chang, C. C.; Ellestad, G. A.; Siegel, M. M.; Morton, G. O.; McGahren, W. J.; Borders, D. B. Calichemicins, a novel family of antitumor antibiotics. 2. Chemistry and structure of calichemicin γ_1^I . *J. Am. Chem. Soc.* **1987**, 109, 3466-3468; (b) Golik, J.; Dubay, G.; Groenewold, G.; Kawaguchi, H.; Konishi, M.; Krishnan, B.; Ohkuma, H.; Saitoh, K.; Doyle, T. W. Esperamicins, a novel class of potent antitumor antibiotics. 3. Structures of esperamicins A1, A2, and A1b. *J. Am. Chem. Soc.* **1987**, 109, 3462-3464.

- (31) Kappen, L. S.; Goldberg, I. H. Deoxyribonucleic acid damage by neocarzinostatin chromophore: strand breaks generated by selective oxidation of C-5' of deoxyribose. *Biochemistry* **1983**, 22, 4872-4878.
- (32) Kappen, L. S.; Goldberg, I. H.; Wu, S. H.; Stubbe, J.; Worth, L.; Kozarich, J. W. Isotope effects on the sequence-specific cleavage of dC in d(AGC) sequences by neocarzinostatin: elucidation of chemistry of minor lesions. *J. Am. Chem. Soc.* **1990**, 112, 2797-2798.
- (33) Campbell, I. D.; Ellington, G. J. A Novel Photochemical Cyclisation of *o*-Bisiodoethynylbenzene to Substituted Naphthalenes. *J. Chem. Soc. C.* **1968**, 1968, 2120-2121.
- (34) Kagan, J.; Wang, X.; Chen, X.; Lau, K. Y.; Batac, I. V.; Tuveson, R. W.; Hudson, J. B. DNA Cleavage, antiviral and cytotoxic reactions photosensitized by simple enediyne compounds. *J. Photochem. Photobiol. B: Biol.* **1993**, 21, 135-142.
- (35) Turro, N. J.; Evenzahav, A.; Nicolaou, K. C. Photochemical analogue of the Bergman cycloaromatization reaction. *Tetrahedron Lett.* **1994**, 35, 8089-8092.
- (36) Evenzahav, A.; Turro, N. J. Photochemical Rearrangement of Eneidyne: Is a "Photo-Bergman" Cyclization a Possibility? *J. Am. Chem. Soc.* **1998**, 120, 1835-1841.
- (37) Funk, R. L.; Young, E. R. R.; Williams, R. M.; Flanagan, M. F.; Cecil, T. L. Photochemical Cycloaromatization Reactions of *ortho*-Dialkynylarenes: A New Class of DNA Photocleaving Agents. *J. Am. Chem. Soc.* **1996**, 118, 3291-3292.
- (38) Kaneko, T.; Takahashi, M.; Hiram, M. Photochemical Cycloaromatization of Non-Benzenoid Eneidyne. *Angew. Chem., Int. Ed.* **1999**, 38, 1267-1268.

- (39) Jones, G. B.; Wright, J. M.; Plourde, G.; Purohit, A. D.; Wyatt, J. K.; Hynd, G.; Fouad, F. Synthesis and Photochemical Activity of Designed Enediynes. *J. Am. Chem. Soc.* **2000**, *122*, 9872-9873.
- (40) (a) Plourde, I. I. G.; El-Shafey, A.; Fouad, F. S.; Purohit, A. S.; Jones, G. B. Protein degradation with photoactivated enediyne-amino acid conjugates. *Bioorg. Med. Chem. Lett.* **2002**, *12*, 2985-2988; (b) Fouad, F. S.; Wright, J. M.; Plourde, G.; Purohit, A. D.; Wyatt, J. K.; El-Shafey, A.; Hynd, G.; Crasto, C. F.; Lin, Y.; Jones, G. B. Synthesis and Protein Degradation Capacity of Photoactivated Enediynes. *J. Org. Chem.* **2005**, *70*, 9789-9797.
- (41) (a) Falcone, D.; Li, J.; Kale, A.; Jones, G. B. Photoactivated enediynes as targeted antitumoral agents: Efficient routes to antibody and gold nanoparticle conjugates. *Bioorg. Med. Chem. Lett.* **2008**, *18*, 934-937; (b) LaBeaume, P.; Wager, K.; Falcone, D.; Li, J.; Torchilin, V.; Castro, C.; Holewa, C.; Kallmerten, A. E.; Jones, G. B. Synthesis, functionalization and photo-Bergman chemistry of enediyne bioconjugates. *Bioorg. Med. Chem.* **2009**, *17*, 6292-6300.
- (42) Du, Y.; Creighton, C. J.; Yan, Z.; Gauthier, D. A.; Dahl, J. P.; Zhao, B.; Belkowski, S. M.; Reitz, A. B. The synthesis and evaluation of 10- and 12-membered ring benzofused enediyne amino acids. *Bioorg. Med. Chem.* **2005**, *13*, 5936-5948.
- (43) Choy, N.; Blanco, B.; Wen, J.; Krishan, A.; Russell, K. C. Photochemical and Thermal Bergman Cyclization of a Pyrimidine Enediynol and Enediynone. *Org. Lett.* **2000**, *2*, 3761-3764.

- (44) Zhao, Z.; Peacock, J. G.; Gubler, D. A.; Peterson, M. A. Photoinduced Bergman cycloaromatization of imidazole-fused enediynes. *Tetrahedron Lett.* **2005**, *46*, 1373-1375.
- (45) Purwanto, M. G. M.; Weisz, K. Binding of Imidazole-Derived Nucleosides to a CG Base Pair. *J. Org. Chem.* **2003**, *69*, 195-197.
- (46) (a) Dervan, P. B. Molecular recognition of DNA by small molecules. *Bioorg. Med. Chem.* **2001**, *9*, 2215-2235; (b) Hannon, M. J. Supramolecular DNA recognition. *Chem. Soc. Rev.* **2007**, *36*, 280-295.
- (47) Boger, D. L.; Zhou, J. CDPI3-enediyne and CDPI3-EDTA conjugates: a new class of DNA cleaving agents. *J. Org. Chem.* **1993**, *58*, 3018-3024.
- (48) Zeidan, T. A.; Manoharan, M.; Alabugin, I. V. Ortho Effect in the Bergman Cyclization: Interception of *p*-Benzyne Intermediate by Intramolecular Hydrogen Abstraction. *J. Org. Chem.* **2006**, *71*, 954-961.
- (49) Kraft, B. J.; Coalter, N. L.; Nath, M.; Clark, A. E.; Siedle, A. R.; Huffman, J. C.; Zaleski, J. M. Photothermally Induced Bergman Cyclization of Metalloenediynes via Near-Infrared Ligand-to-Metal Charge-Transfer Excitation. *Inorg. Chem.* **2003**, *42*, 1663-1672.
- (50) Benites, P. J.; Holmberg, R. C.; Rawat, D. S.; Kraft, B. J.; Klein, L. J.; Peters, D. G.; Thorp, H. H.; Zaleski, J. M. Metal-Ligand Charge-Transfer-Promoted Photoelectronic Bergman Cyclization of Copper Metalloenediynes: Photochemical DNA Cleavage via C-4' H-Atom Abstraction. *J. Am. Chem. Soc.* **2003**, *125*, 6434-6446.
- (51) Schmittel, M.; Viola, G.; Dall'Acqua, F.; Morbach, G. A novel concept to activate enediynes for DNA cleavage. *Chem. Commun.* **2003**, 646-647.

- (52) Nicolaou, K. C.; Dai, W. M. Molecular design and chemical synthesis of potent enediynes. 2. Dynemicin model systems equipped with C-3 triggering devices and evidence for quinone methide formation in the mechanism of action of dynemicin A. *J. Am. Chem. Soc.* **1992**, *114*, 8908-8921.
- (53) Wender, P. A.; Zercher, C. K.; Beckham, S.; Haubold, E. M. A photochemically triggered DNA cleaving agent: synthesis, mechanistic and DNA cleavage studies on a new analog of the anti-tumor antibiotic dynemicin. *J. Org. Chem.* **1993**, *58*, 5867-5869.
- (54) Garcías, R. C.; Coll, M.; Donoso, J.; Vilanova, B.; Muñoz, F. Theoretical study of thiolysis in penicillins and cephalosporines. *Int. J. Chem. Kinet.* **2005**, *37*, 434-443.
- (55) Waxman, D. J.; Strominger, J. L. Penicillin-Binding Proteins and the Mechanism of Action of β -Lactam Antibiotics¹. *Ann. Rev. Biochem.* **1983**, *52*, 825-869.
- (56) Knowles, J. R. Penicillin resistance: the chemistry of β -lactamase inhibition. *Acc. Chem. Res.* **1985**, *18*, 97-104.
- (57) Basak, A.; Kumar Khamrai, U. Design and synthesis of a locked bis-propargyl sulphone. *Tetrahedron Lett.* **1995**, *36*, 7913-7916.
- (58) Banfi, L.; Guanti, G. Synthesis of N-Fused "Lactendiyne". *Eur. - J. Org. Chem.* **1998**, *1998*, 1543-1548.
- (59) (a) Banfi, L.; Guanti, G. Lactendiyne: A New Class of Triggered Cyclic Enediynes. *Angew. Chem., Int. Ed.* **1995**, *34*, 2393-2395; (b) Banfi, L.; Guanti, G.; Rasparini, M. Intramolecular Opening of β -Lactams with Amines as a Strategy Toward Enzymatically

- or Photochemically Triggered Activation of Lactenediyne Prodrugs. *Eur. - J. Org. Chem.* **2003**, 2003, 1319-1336.
- (60) (a) Poloukhine, A.; Popik, V. V. Highly efficient photochemical generation of a triple bond: synthesis, properties, and photodecarbonylation of cyclopropenones. *J. Org. Chem.* **2003**, 68, 7833-7840; (b) Poloukhine, A.; Popik, V. V. Mechanism of the cyclopropenone decarbonylation reaction. A density functional theory and transient spectroscopy study. *J. Phys. Chem. A* **2006**, 110, 1749-1757; (c) Poloukhine, A.; Popik, V. V. Two-Photon Photochemical Generation of Reactive Eneidyne. *J. Org. Chem.* **2006**, 71, 7417-7421; (d) Poloukhine, A.; Popik, V. V. Application of Photochemical Decarbonylation of Cyclopropenones for the in Situ Generation of Reactive Eneidynes. Construction of a Cyclopropenone-Containing Eneidyne Precursor by Using a Cyclopropenone Acetal Building Block. *J. Org. Chem.* **2005**, 70, 1297-1305; (e) Poloukhine, A.; Popik, V. V. Photoswitchable eneidynes: use of cyclopropenone as photocleavable masking group for the eneidyne triple bond. *Chem. Commun. (Cambridge, U. K.)* **2005**, 5, 617-619.
- (61) Chiang, Y.; Kresge, A. J.; Popik, V. V. Flash Photolytic Generation and Study of Ynolate Ions and the Corresponding Ketenes in Aqueous-Solution. *J. Am. Chem. Soc.* **1995**, 117, 9165-9171.
- (62) Polukhtine, A.; Karpov, G.; Popik, V. V. Towards photoswitchable eneidyne antibiotics: single and two-photon triggering of Bergman cyclization. *Curr. Top. Med. Chem.* **2008**, 8, 460-469.

- (63) (a) Tachi, Y.; Dai, W.-M.; Tanabe, K.; Nishimoto, S.-i. Synthesis and DNA cleavage reaction characteristics of enediyne prodrugs activated via an allylic rearrangement by base or UV irradiation. *Bioorg. Med. Chem.* **2006**, *14*, 3199-3209; (b) Dai, W.-M. Natural Product Inspired Design of Enediyne Prodrugs via Rearrangement of an Allylic Double Bond. *Curr. Med. Chem.* **2003**, *10*, 2265-2283.
- (64) Irie, M. Diarylethenes for Memories and Switches. *Chem. Rev.* **2000**, *100*, 1685-1716.
- (65) Sud, D.; Wigglesworth, T. J.; Branda, N. R. Creating a Reactive Enediyne by Using Visible Light: Photocontrol of the Bergman Cyclization. *Angew. Chem., Int. Ed.* **2007**, *46*, 8017-8019.
- (66) Kar, M.; Basak, A.; Bhattacharjee, M. Photoisomerization as a trigger for Bergman cyclization: Synthesis and reactivity of azoenediynes. *Bioorg. Med. Chem. Lett.* **2005**, *15*, 5392-5396.
- (67) Hay, M. P.; Wilson, W. R.; Denny, W. A. Nitrobenzyl carbamate prodrugs of enediynes for nitroreductase gene-directed enzyme prodrug therapy (GDEPT). *Bioorg. Med. Chem. Lett.* **1999**, *9*, 3417-3422.
- (68) Suzuki, I.; Uno, S.; Tsuchiya, Y.; Shigenaga, A.; Nemoto, H.; Shibuya, M. Synthesis and DNA damaging ability of enediyne model compounds possessing photo-triggering devices. *Bioorg. Med. Chem. Lett.* **2004**, *14*, 2959-2962.
- (69) (a) Schmittel, M.; Mahajan, A. A.; Bucher, G. Photochemical Myers—Saito and C2-C6 cyclizations of enyne-allenes: direct detection of intermediates in solution. *J. Am. Chem. Soc.* **2005**, *127*, 5324-5325; (b) Bucher, G.; Mahajan, A. A.; Schmittel, M. Photochemical

- C2-C6 cyclization of enyne-allenes: detection of a fulvene triplet diradical in the laser flash photolysis. *J. Org. Chem.* **2008**, 73, 8815-8828.
- (70) Spöler, C.; Engels, B. Theoretical Investigation of the Photochemical C2–C6 Cyclisation of Enyne–Heteroallenes. *Chem. - Eur. J.* **2003**, 9, 4670-4677.
- (71) (a) Karpov, G.; Kuzmin, A.; Popik, V. V. Enhancement of the Reactivity of Photochemically Generated Ene-diyne via Keto-Enol Tautomerization. *J. Am. Chem. Soc.* **2008**, 130, 11771-11777; (b) Karpov, G. V.; Popik, V. V. Triggering of the Bergman Cyclization by Photochemical Ring Contraction. Facile Cycloaromatization of Benzannulated Cyclodeca-3,7-diene-1,5-diyne. *J. Am. Chem. Soc.* **2007**, 129, 3792-3793.

CHAPTER 2

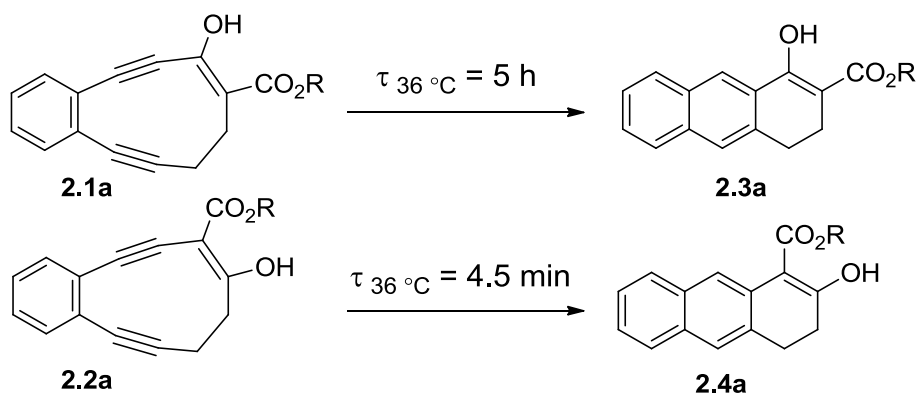
ENHANCEMENT OF THE REACTIVITY OF ENEDIYNES

VIA KETO–ENOL TAUTOMERIZATION

2.1 INTRODUCTION

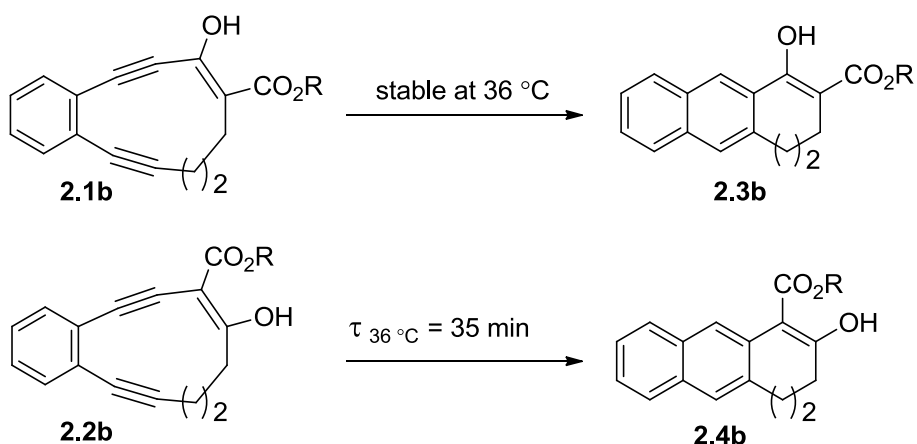
Enediyne **2.2a** was found to undergo a Bergman-type cyclization 70-times faster than its isomer **2.1a** (Scheme 2.1).¹ The remarkable reactivity difference between regioisomeric enediynes **2.1a** and **2.2a** was originally explained by the electronic influence of the substituent at the vinylic terminus of the π -conjugated system. It was suggested that the electron-rich hydroxyl group in **2.2a** can donate electron density to the π -orbitals, therefore increasing the aromatic stabilization of the Bergman cyclization transition state, while presence of the electron-withdrawing ester group in **2.1a** can slow down the cyclization reaction.

Scheme 2.1 Cycloaromatization of regioisomeric enediynes **2.1a** and **2.2a**.



As we know, the fast rate of the Bergman cyclization of enediyne compounds is essential to allow for the spatial and temporal control of generated biradicals. Thus, 11-membered enediyne analogs **2.1b** and **2.2b** were also prepared to experimentally check for a general trend to increase the rate of the Bergman cyclization (Scheme 2.2).

Scheme 2.2 Cycloaromatization of regioisomeric enediynes **2.1b** and **2.2b**.

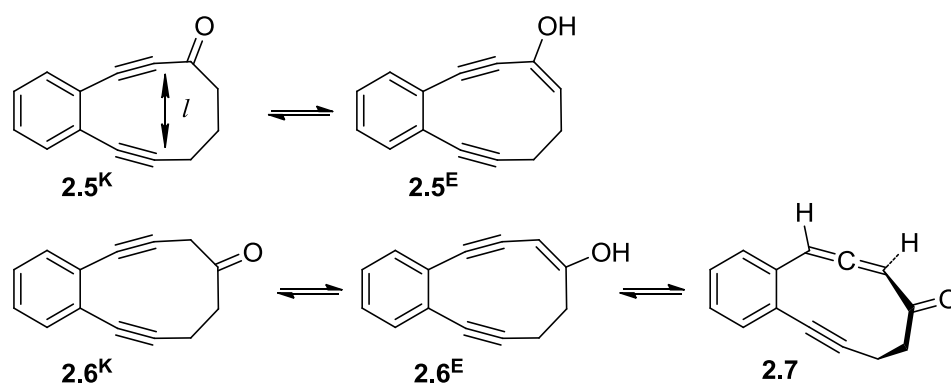


Enediyne **2.1b** was found to be stable at 36 °C and underwent slow decomposition at elevated temperatures ($\tau_{1/2} \sim 40$ h at 150 °C). In contrast, **2.2b** is very reactive for an 11-membered enediyne and cyclizes rapidly. The enhanced reactivity of **2.1a** and **2.2a** can be also explained by the additional ring strain introduced by enolic double bond. However, the distance between acetylenic termini in DFT-optimized structures **2.1b** and **2.2b** is ca. 3.77 Å, which is greater than the Nicolaou “critical distance” for spontaneous cyclization of enediynes.² The separation of acetylenic termini in enediynes by more than 3.31 Å is usually associated with high barrier for the Bergman cyclization, which agrees well with thermal stability of **2.1b** and suggests that the rapid cyclization of **2.2b** proceeds via another mechanism. In other words, such a tremendous difference in reactivity of **2.2b** and **2.1b** suggests that the mechanism of cycloaromatization is different from the Bergman reaction.

2.2 RESULTS AND DISCUSSION

In order to gain a better understanding of the origin of this difference, we carried out a detailed study of the mechanisms of cyclization of ketoesters **2.1a**, **2.2a**, **2.1b** and **2.2b**, and the model ten-membered ring enediynes **2.5** and **2.9**.³ We have analyzed keto-enol equilibrium of two isomeric model enediynes: 4,5-benzocyclodeca-2,6-diyne (**2.5**) and 5,6-benzocyclodeca-3,7-diyne (**2.6**, Scheme 2.3).

Scheme 2.3 Keto-enol equilibrium of enediyne **2.5** and **2.6**.



The cartesian coordinates for the B3LYP/6-31++G(d,p) optimized geometries of structures **2.5^K**, **2.5^E**, **2.6^K**, and **2.6^E**, as well as **2.7** are provided in the Experimental Section 2.11. The relative electronic energies of tautomers and selected transannular distances are shown in the Table 2.1.

Fully enolized tautomers (**2.5^E** and **2.6^E**) of both isomeric keto-enediynes are predicted to be higher in energy than their keto-forms (**2.5^K** and **2.6^K**) by both DFT and MP2 methods. The separation of acetylenic termini (*l*, Scheme 2.2) is smaller in enol (**2.5^E** and **2.6^E**) than in keto-forms (**2.5^K** and **2.6^K**) of these 10-membered ring enediynes.

Table 2.1 Relative electronic energies and transannular distances for keto and enol forms of ten-membered ring keto-enediynes, and enyne-allene tautomer.

	ΔE (kcal/mol) ^a		
	B3LYP/6-311++G(d,p)	MP2/6-31++G(d,p)	d (Å) ^b
2.5^K	8.1	4.8	3.37
2.5^E	19.2	17	3.23
2.6^K	5.2	1.4	3.42
2.6^E	13.7	11.9	3.2
2.7	0	0	

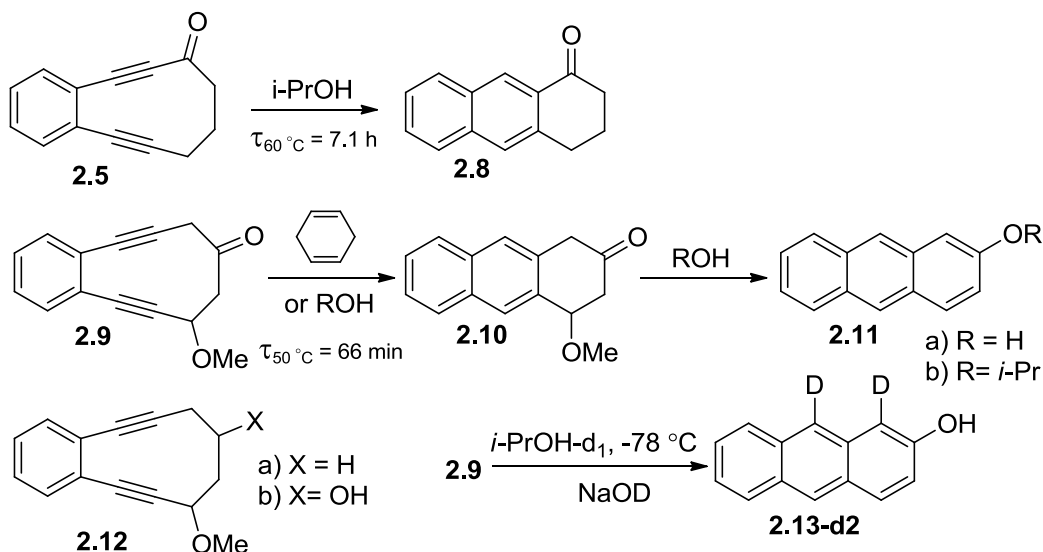
^a ZPVE-corrected energy; the energy of enyne-allene **2.7** was used as the reference.

^b Distance between acetylenic termini (see Scheme 2.2).

The transannular distance in DFT-optimized structure **2.5^K** is in a good agreement with the X-ray data ($l = 3.325$ Å)⁴ for this compound. The enyne-allenone **2.7** is the most stable form among three tautomers of 5,6-benzo-9-cyclodeca-3,7-diynone (**2.6**, Table 2.1). In an established equilibrium, **2.7** should be the predominant component, and the cyclization of enediyne **2.6** should proceed via Myers–Saito pathway (see Ch. 1.2.3), which is not feasible for **2.5**.

To experimentally test these predictions, keto-enediynes **2.5⁵** and **2.9** were prepared. The methoxy substituent in propargylic position of **2.9** was introduced in an attempt to compensate the inductive effect of the carbonyl oxygen in the structure **2.5** on the rate of cycloaromatization. The NMR data shows that enediynes **2.5** and **2.6** exist predominately in their keto-form. Upon mild heating in 2-propanol both **2.5** and **2.6** underwent smooth Bergman cyclization producing 3,4-dihydro-1-(2H)anthracenone (**2.8**) and 3,4-dihydro-4-methoxy-2-(1H)anthracenone (**2.10**). The latter, however, is not stable. Upon heating in protic solvents, on silica gel, and in the presence of trace amounts of acid or base ketone **2.10** loses methanol to give 2-anthracenol derivative **2.11** (Scheme 2.4).

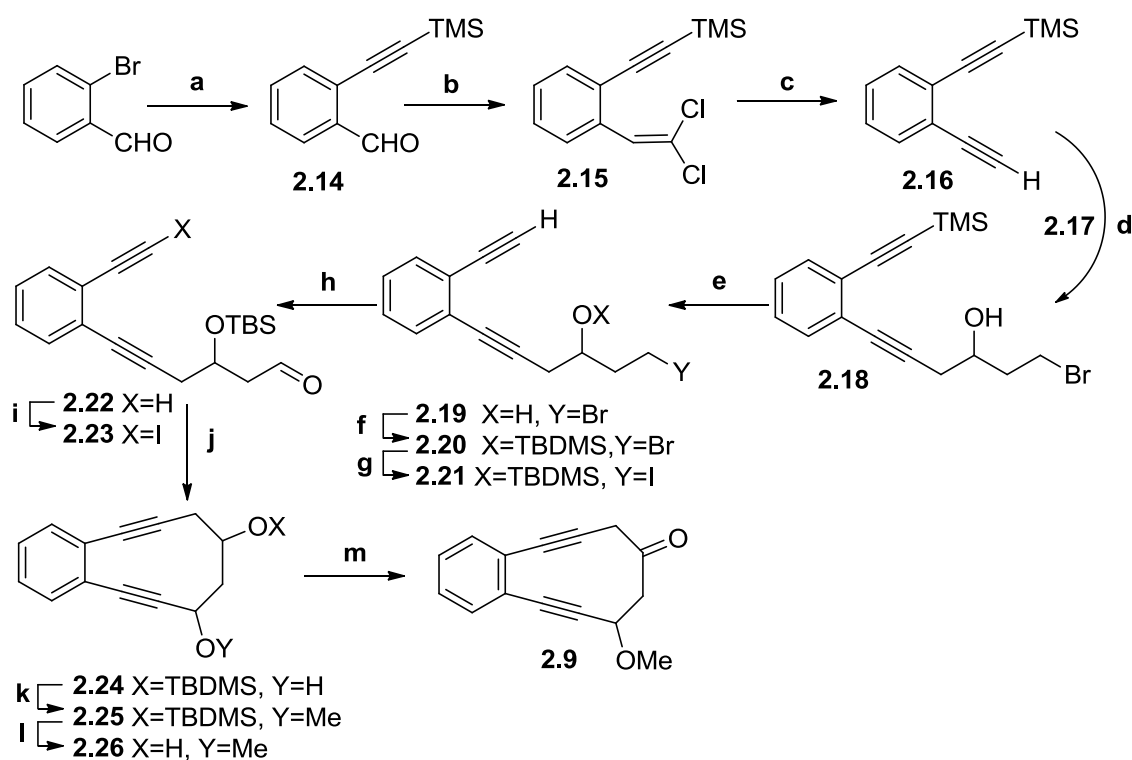
Scheme 2.4 Comparison of reactivity of enediyne **2.5**, **2.9**, and **2.12**.



Enediyne **2.9** was prepared in 13 steps starting from commercially available 2-bromobenzaldehyde (Scheme 2.5). During the synthesis of **2.9**, a convenient approach to produce monoprotected bis-acetylene **2.16** was developed. The first acetylene terminus was introduced by using the *Sonogashira coupling* with ethynyltrimethylsilane to give **2.14**. The second acetylene moiety was furnished in a two step procedure. First, the one-carbon homologation of aldehyde **2.14** to the corresponding terminal alkynes using carbon tetrachloride and triphenylphosphine, which is known as the *Corey–Fuchs alkyne synthesis*, gave compound **2.15**. The latter was treated with 2 equivalents of *n*-butyllithium, followed by simple hydrolysis to afford **2.16** in a high yield. While the intermediate is a lithium acetylide, which could be directly treated with 4-bromo-1-butene oxide (**2.17**) to give **2.18**, the yield was moderate at best. Thus, reaction of the monoanion of **2.16** with $\text{BF}_3 \cdot \text{Et}_2\text{O}$ and then epoxide **2.17** proved to afford the hydroxyl bromide **2.18** in a higher yield. Removal of the silyl group was achieved by treating **2.18** with aqueous potassium carbonate to give **2.19**. The free hydroxyl group was protected as a *tert*-butyldimethylsilyl ether (**2.20**). The Ganem and Boeckman modification of the *Kornblum*

oxidation of bromide **2.20** with silver triflate in DMSO gave aldehyde **2.22** and the starting material as a mixture in a ratio 1:1 by NMR. To improve the yield of preparation of aldehyde **2.22**, bromide **2.20** was converted to iodide **2.21** via the *Finkelstein reaction* using sodium iodide in acetone followed by the *Kornblum oxidation* with silver tetrafluoroborate in DMSO. N-Iodosuccinimide and silver nitrate were utilized to obtain iodide **2.23**.

Scheme 2.5 Synthesis of the enediyne **2.9**



Reagents and conditions: a) ethynyltrimethylsilane, $\text{PdCl}_2(\text{PPh}_3)_2$ / CuI , Et_3N , THF, 94%; b) $\text{PPh}_3/\text{CCl}_4$, 88%; c) $n\text{-BuLi}$ (2 eq.) at -78°C , 90%; d) $n\text{-BuLi}$, $\text{BF}_3\text{Et}_2\text{O}$, 4-bromo-1-butene oxide (2.17), 63%; e) $\text{K}_2\text{CO}_3/\text{MeOH}$, 97%; f) $\text{TBDMS-Cl}/\text{CH}_2\text{Cl}_2$; g) $\text{NaI}/\text{acetone}$, 78%, over 2 steps; h) $\text{AgBF}_4/\text{DMSO}$, 86%; i) NIS , $\text{AgNO}_3/\text{acetone}$, 80%; j) CrCl_2 , NiCl_2/THF , 80%; k) NaH , dimethyl sulfate, 85%; l) HF/MeCN , 98%; m) Dess-Martin periodinane/ CH_2Cl_2 , 97%.

A Nozaki—Hiyama—Kishi reaction was used to promote ring closure. The treatment of aldehyde with two equivalents of chromium(II) chloride in the presence of nickel(II) chloride

gave cyclic alcohol **2.24**. Protection of the alcohol as a methyl ether was followed by desylalation with hydrofluoric acid in acetonitrile, and finally oxidation with Dess-Martin periodinane to give the desired ketone **2.9**. The latter was found to be unstable during purification on silica gel. Thus, enediyne **2.9** was recrystallized from hexanes.

2.3 REACTIVITY OF ENEDIYNE **2.9**

While the distance between acetylenic termini is expected to be somewhat longer in **2.9** (compare to **2.6^K**, Table 2.1), it undergoes cycloaromatization much faster than **2.5**. Life times in 2-propanol are $\tau_{50\text{ }^{\circ}\text{C}} = 66\text{ min}$ and $\tau_{60\text{ }^{\circ}\text{C}} = 7.1\text{ h}$ correspondingly. The reactivity of **2.5** is consistent with previous reports ($\tau = 82\text{ h}$ at $40\text{ }^{\circ}\text{C}$ in $\text{C}_6\text{D}_6/1,4\text{-cyclohexadiene}$).⁶ Cycloaromatization of enediyne **2.9** is also substantially faster than that of the parent compound **2.12a** ($\tau_{60\text{ }^{\circ}\text{C}} = 36.5\text{ h}$ in 1,4-cyclohexadiene)⁵ or alcohol precursor **2.12b** ($\tau_{50\text{ }^{\circ}\text{C}} = 22\text{ h}$ in 2-propanol, Scheme 2.3). The observed high reactivity of **2.9** agrees well with the proposed tautomerization and Myers—Saito cyclization pathway, which is not available to **2.5** (Scheme 2.5). Results of isotope labeling experiments support the proposed mechanism. Treatment of a 2-propanol- d_1 solution of **2.9** with catalytic amounts of NaOD at $-78\text{ }^{\circ}\text{C}$ produces 2-anthracenol with 75% deuteration at the 9-position (**2.13a-d2**, Scheme 2.3). Since the abstraction of deuterium from the solvent by a 1,4-naphthyl diradical is highly unlikely, isotope substitution at the 9-position apparently occurs during ketonization of **2.6^E** to **2.7**. The second deuterium in the 1-position is incorporated via base-catalyzed proton exchange α - to the carbonyl group of **2.10**.

Acid-base catalysis of the cycloaromatization reaction of enediyne **2.9** was studied in aqueous solutions. Preparative experiments using 5% 2-propanol as co-solvent allowed us to isolate 2-anthracenol (**2.13a**) in 75 to 80% yield under both acidic and basic conditions. The formation of **2.10** and subsequent conversion to **2.11a** was followed spectroscopically using

characteristic absorbance of **2.10** at 228 nm (Figure 2.1). Measurements were made at 40 ± 0.10 °C either with a Cary 300 UV spectrometer or, for the faster reactions in basic solutions, with a Cary 50 spectrometer equipped with stopped-flow attachment. The fragment of a typical kinetic curve is shown on an inset in Figure 2.1.

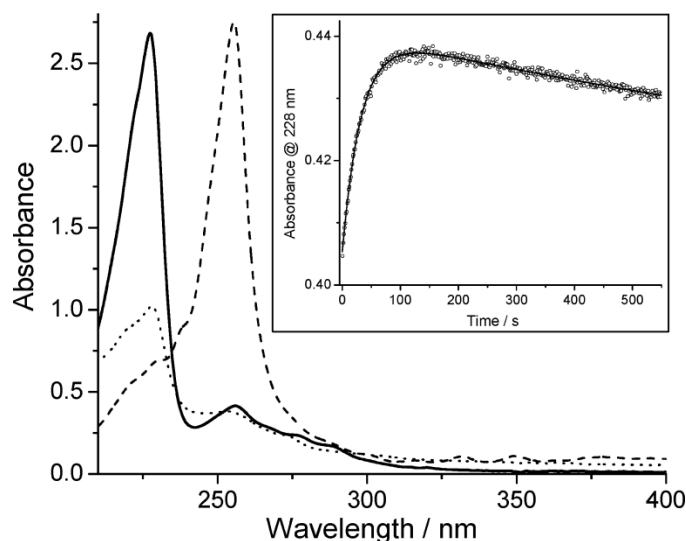


Figure 2.1 UV spectra of $\sim 4 \times 10^{-5}$ M 2-propanol solutions of **2.9** (dotted line), **2.10** (solid line), and **2.11a** (dashed line). The inset shows part of the kinetic curve at 228 nm in biphosphate buffer (BR = 0.74). The line was drawn using parameters obtained by least-squares fitting of a double-exponential equation.

Rates of cyclization of **2.9** were determined in dilute aqueous solutions of perchloric acid and sodium hydroxide, as well as in biphosphate ion, bicarbonate ion, and TRIS buffers. The kinetic data obeyed the first-order rate law well and observed pseudo first order rate constants were determined by least squares fitting to a double exponential function.

The isomerization reaction proved to be strongly catalyzed by all of the buffers examined. Therefore, measurements were consequently performed in series of solutions of varying buffer concentration and the observed rates were extrapolated to zero buffer

concentration. These buffer-independent rate constants together with observed rate constants, determined in perchloric acid and sodium hydroxide solutions, are shown as the rate profile on Figure 2.2.

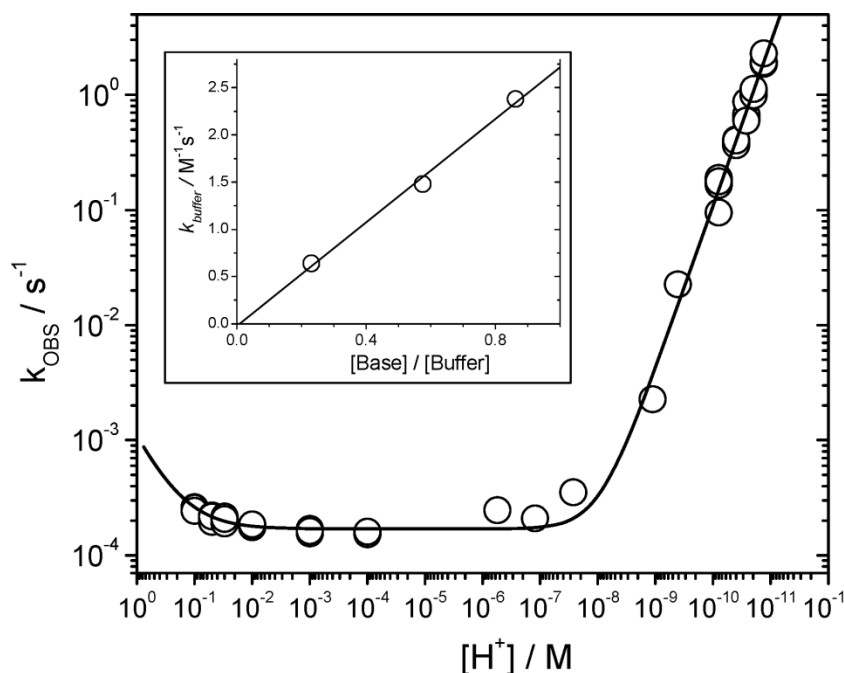
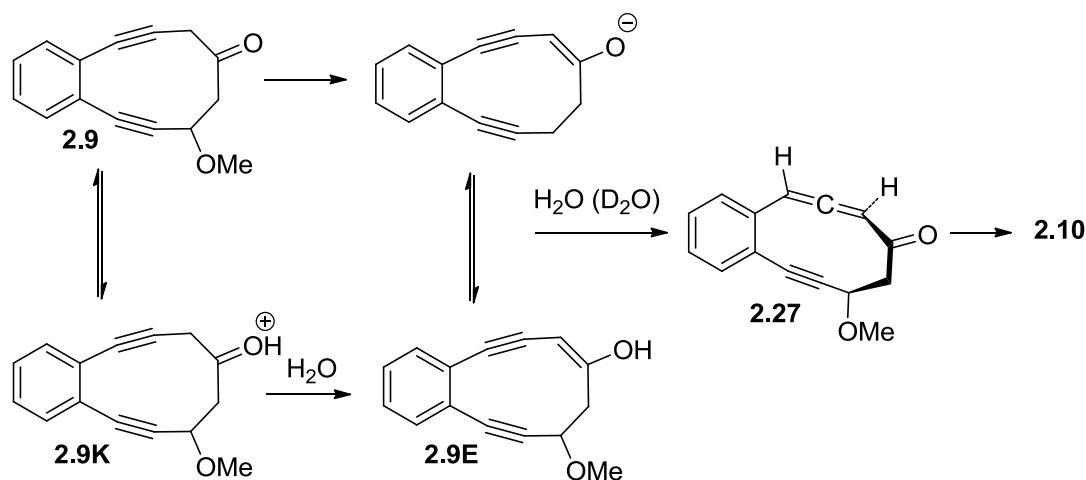


Figure 2.2 Rate profile for the cycloaromatization of enediyne **2.9** in aqueous solution at 40 °C. The inset shows the dependence of the buffer catalysis on the fraction of basic component of the buffer.

This rate profile shows a horizontal region between pH 2 and pH 7, in which the rate constant $k_{\text{H}_2\text{O}}$ has the value $(1.7 \pm 0.5) \times 10^{-4} \text{ s}^{-1}$ and is independent of the acidity of the medium. The reaction is catalyzed better by base, as illustrated by the upward slope of the rate profile above pH 8. The hydroxide ion catalysis measured in NaOH solutions is characterized by the second-order rate constant $k_{\text{OH}^-} = 1509 \pm 88 \text{ M}^{-1} \text{ s}^{-1}$. There is also a region of weak catalysis below pH 3 ($k_{\text{H}^+} = (9.3 \pm 0.7) \times 10^{-4} \text{ M}^{-1} \text{ s}^{-1}$). It is important to note that the rate of conventional Bergman cyclization is independent of the acid concentration.⁷ The slopes of biphosphate buffer-dilution plots ($k_{\text{cat}} = 2.38 \pm 0.06$, 1.48 ± 0.04 , and $0.64 \pm 0.03 \text{ M}^{-1} \text{ s}^{-1}$ for BR

= 1/6, 5/7, and 10/3, respectively) represent pH-independent catalysis by the buffer components, which can be partitioned into contributions from the acidic and basic components of the buffer by plotting k_{cat} against the fraction of base component in the buffer ($f_{\text{B}} = [\text{base}]/[\text{buffer}]$), as illustrated in the inset in Figure 2.2. As k_{cat} extrapolates to zero at $f_{\text{B}} = 0$ and has a value of $2.72 \pm 0.10 \text{ M}^{-1} \text{ s}^{-1}$ at $f_{\text{B}} = 1$, we can conclude that cycloaromatization of **2.9** is catalyzed by general base but shows no general acid catalysis. These features can be accommodated by the reaction mechanism shown in Scheme 2.5, in which cycloaromatization occurs through the rate-limiting enolization of ketone **2.9^K** (or its protonated form at low pH).

Scheme 2.6 Keto-enol tautomerization of enediyne **2.9**.



Below pH 8 water serves as the base, removing a proton from the α position with respect to the carbonyl group of the substrate, while at higher pH, hydroxide ion takes over, as the deprotonating agent. Strong general base catalysis is characteristic for reactions proceeding via the rate-limiting C–H deprotonation step. Specific acid catalysis is another common feature of enolization reactions, because O-protonation of ketones increases their C–H acidity and the rate of tautomerization. The enol or enolate form of **2.9** is reprotonated in the γ position to produce allene **2.27**. The latter then undergoes facile Myers—Saito cyclization to afford ketone **2.10**.

Rates of the cycloaromatization of **2.9** were also measured in dilute DCl solutions in D₂O. The observed solvent isotope effect agrees well with the rate-limiting enolization. The reaction was slower in D₂O at very low DCl concentrations, producing a secondary isotope effect $k_{\text{H}_2\text{O}}/k_{\text{D}_2\text{O}} \approx 1.4$ in the normal direction. At this pH water acts as a base, accepting proton from **2.9^K** (Scheme 2.6) to become a hydronium ion. This is a bond-loosening process that results in a secondary isotope effect in the normal direction ($k_{\text{H}}/k_{\text{D}} > 1$). On the other hand, the slope of DCl catalysis is almost twice as steep as that of HClO₄ ($k_{\text{H}}^+/k_{\text{D}}^+ \approx 0.6$). This inverse isotope effect is due to the fact that acids are weaker in D₂O. Thus, the fraction of the more reactive protonated species **2.9^K** grows faster with D⁺ concentration than with H⁺ concentration. The absence of a primary kinetic isotope effect on the cyclization of **2.9** in D₂O shows that reprotonation in the γ position (i.e., ketonization to allene **2.27**) of **2.9^E** is much faster than enolization. Clean exponential growth of the absorbance at 228 nm indicates that conversion of **2.9** to **2.10** proceeds without significant accumulation of intermediates (e.g., **2.6^E** or **2.27**). This observation allows us to conclude that cyclization of enyne- allene- **2.7** is much faster than the tautomerization step. Since the rate constant of the overall process in basic solutions approaches 10 s⁻¹, we can estimate the upper limit for the lifetime of **2.27** at 40 °C as ~100 ms.

2.3 CONCLUSIONS

In conclusion, the rates of cycloaromatization of enediynes can be substantially enhanced by introducing a carbonyl group in the β position with respect to the acetylenic terminus. Cyclization of such β -keto enediynes proceeds via tautomerization into the more reactive enyne-allene form, which then undergoes facile Myers—Saito cyclization. Cycloaromatization of 8-methoxy-5,6-benzocyclodeca-3,7-diynone (**2.9**) is weakly catalyzed by hydronium ion and shows strong general base catalysis. These observations, along with the values of the solvent

isotope effect, indicate that enolization to **2.9^E** is the rate-limiting step in the cyclization of **2.9**. Unstable α -carbalkoxy- β -keto enediyne **2.2a** already exists in enol form. The rates of their cycloaromatization show significant primary isotope effects, suggesting that enol–keto–allene tautomerization controls the overall rate of the reaction. Enyne-allene undergoes the Myers–Saito cyclization with the lifetime less than 100 ms at 40 °C. The described strategy opens a new approach for controlling enediyne reactivity.

2.4 EXPERIMENTAL SECTION

MATERIALS AND METHODS

All moisture- and oxygen-sensitive reactions were carried out in oven-dried glassware under argon atmosphere. All solvents were purified and dried by distillation immediately before use. Tetrahydrofuran, diethyl ether, hexanes, benzene, and toluene were distilled from sodium metal; dichloromethane was distilled from phosphorus pentoxide; ethyl acetate and acetone were distilled from anhydrous calcium chloride. Ultra-dry inhibitor-free THF from Aldrich was used for palladium-catalysed cross coupling reactions. All other materials were purchased from Aldrich, Alfa Aesar, Acros Organics, Strem Chemicals or GFS Chemicals and used without purification unless otherwise stated. Dess-Martin periodinane was prepared according to the original literature procedure.⁸ Chromatographical purification of reaction products was performed using Sorbtech standard grade flash chromatography silica gel (40-63 μ m particle size, 60Å porosity) or Sorbtech premium grade flash chromatography silica gel (40-75 μ m particle size, 60Å porosity). TLC analyses were performed using polyester-backed silica gel TLC plates from Whatman, Aldrich or Sorbent Technologies.

INSTRUMENTS

GC/MS analyses were performed using Shimadzu QP-2010S GC – mass spectrometer equipped with high-precision quadrupole with pre-rods and mass number range 1.5m/z to 900 m/z. Nuclear magnetic resonance (NMR) spectra were recorded in deuteriochloroform using Varian Mercury Plus 400 MHz or Varian Unity Inova 500 MHz NMR spectrometers with tetramethylsilane (TMS) as an internal standard. ^1H -NMR and ^{13}C -NMR chemical shifts (δ) are reported in ppm versus TMS reference. UV-visible spectra were recorded on Varian Cary 50 UV-visible spectrometer or Varian Cary 300 Bio UV-Vis spectrometer. IR spectra were recorded using Shimadzu IR Prestige FT-IR spectrometer. Melting points were determined using Fisher-Johns melting point apparatus and are reported uncorrected.

KINETICS MEASUREMENTS

Rate measurements were performed using Carry-300 Bio UV-Vis spectrometer equipped with a thermostatable cell holder or, for the faster reactions in basic solutions, with a Cary 50 spectrometer equipped with a stopped-flow attachment. Rates of cyclization of **2.9** were determined in dilute aqueous solutions of perchloric acid and sodium hydroxide, as well as in biphosphate ion, bicarbonate ion, and TRIS buffers. The concentrations of perchloric acid, sodium hydroxide, and the buffers were varied over appropriate ranges, and replicate determinations were made at each concentration. The ionic strength of the reaction solutions was maintained at $\mu = 0.10$ M through the addition of sodium perchlorate, as required. Rate measurements in buffers were performed in series of solutions of varying buffer concentration but constant buffer ratio, which at the constant ionic strength employed, served to hold hydrogen ion concentrations constant along a buffer series. Observed rate constants determined under these conditions proved to be accurately proportional to buffer concentration in a given buffer series, and buffer-independent rate constants, k_u , were obtained by least-squares fitting to equation (1):

$$k_{\text{obs}} = k_{\text{u}} + k_{\text{cat}}[\text{buffer}] \quad (1)$$

Hydrogen ion concentrations of the buffer solutions were obtained by calculation using pKa values of the buffer acids from the literature and activity coefficients recommended by Bates.⁹

BUFFER CATALYSIS

Use of equation (1) to obtain buffer-independent rate constants for the construction of a rate profile also produced buffer catalytic coefficients, k_{cat} . They were partitioned into contributions from the acidic and basic components of the buffers according to equation (2):

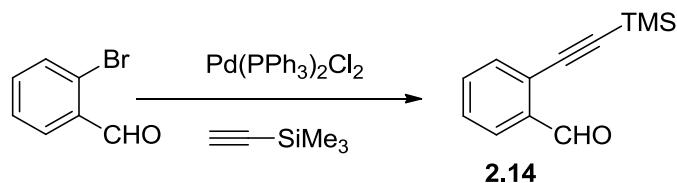
$$k_{\text{cat}} = k_{\text{AH}} + (k_{\text{B}} - k_{\text{AH}})f_{\text{B}} \quad (2)$$

in which k_{B} and k_{AH} are general base and general acid catalytic coefficients, respectively, and f_{B} is the fraction of buffer present in the basic form.

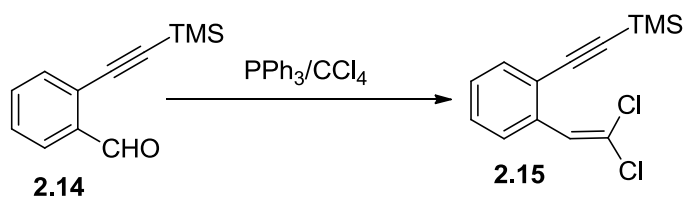
THEORETICAL PROCEDURES

Quantum mechanical calculations were carried out using the Gaussian 03 program.¹⁰ Geometry optimizations were conducted at B3LYP/6-31++G(d,p) level, while single point energies were calculated at the B3LYP/6-311++G(d,p) and MP2(FC)/6-31++G(d,p) levels of theory. Zero-point vibrational energy (ZPVE) corrections, required to correct the raw relative energies to 0 °K, were obtained from B3LYP/6-31+G(d,p) method. Analytical second derivatives were computed to confirm each stationary point to be a minimum by yielding zero imaginary vibrational frequencies for the intermediates and one imaginary vibrational frequency for each transition state. These frequency analyses are known to overestimate the magnitude of the vibrational frequencies. Therefore, we scaled the corresponding ZPVE by 0.9772.¹¹

2.5 SYNTHETIC PROCEDURES

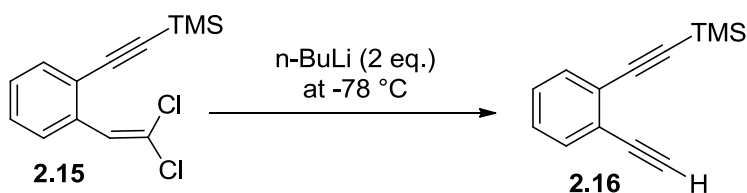


2-[(Trimethylsilyl)ethynyl]benzaldehyde (2.14).¹² A degassed solution of 2-bromobenzaldehyde (41 g, 0.224 mol) in THF (300 mL) was placed into a round-bottom flask (500 mL). Pd(PPh₃)₂Cl₂ (1.5 g, 1.5%), CuI (1.5 g, 3.5%), trimethylsilylacetylene (36 mL, 1.2 eq), Et₃N (50 mL), and PPh₃ (one spatula) were added under argon atmosphere. The reaction mixture was stirred for 12 hours at room temperature, then diluted with hexanes (150 mL) and filtered through a short layer of silica gel. After evaporation of solvent, the crude brown oil was purified by flash chromatography (5% of ether in hexane, R_f = 0.3) to give 42.48 g (94%) of **2.14** as a yellow solid (m.p. = 48-50 °C). ¹H NMR (CDCl₃, 400 MHz): 0.23 (s, 9 H), 7.41-7.46 (m, 1 H), 7.52-7.59 (m, 2 H), 7.91 (d, J=8 Hz, 1 H), 10.56 (s, 1 H).

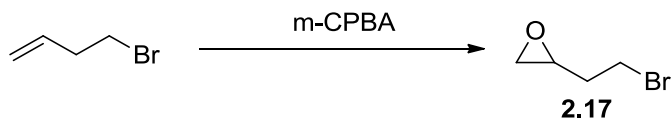


[2-(2,2-Dichlorovinyl)phenylethynyl]-trimethylsilane (2.15).¹³ A solution of CCl₄ (100 mL, 1.0 mol, 5 eq.) was added to a solution of 2-[(Trimethylsilyl)ethynyl]benzaldehyde **2.14** (40.5 g, 0.2 mol) and triphenyl phosphine (158 g, 0.6 mol) in THF (150 mL) via syringe during 4.5 hours at 60 °C. The reaction was monitored by TLC and GCMS. Upon the completion, the reaction mixture was diluted with hexanes (200 mL) and filtered from triphenylphosphine and triphenylphosphine oxide. The content was washed with aqueous saturated solution of sodium carbonate (3x150 mL), brine (2x150 mL) and dried over magnesium sulfate. The solvents were removed in vacuo and residue was purified by column chromatography (R_f = 0.3, 1% ether in

hexanes, technical silica gel) to give 47.5 g (88%) of **2.15** as yellow oil. ^1H NMR (CDCl_3 , 400 MHz): 0.27 (s, 9 H), 7.2-7.28 (m, 1 H), 7.30-7.36 (m, 1 H), 7.46-7.50 (m, 1 H), 7.76-7.8 (m, 1 H); ^{13}C NMR (CDCl_3 , 100 MHz): 0.09, 100.89, 102.91, 122.59, 123.15, 127.37, 128.13, 128.25, 128.55, 132.48, 135.78; EI-MS m/z : 270/268.

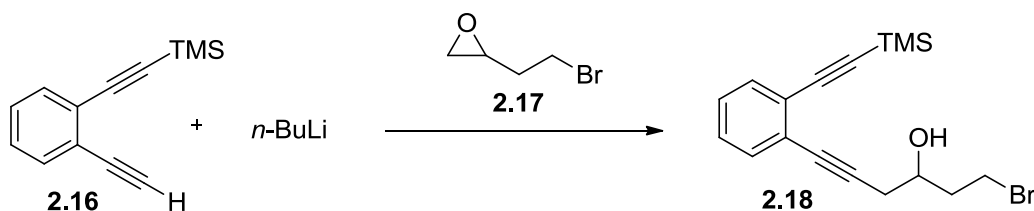


(2-Ethynyl-phenylethynyl)-trimethylsilane (2.16).¹⁴ A solution of $n\text{-BuLi}$ (1.6 mL of 2.56 M in hexane) was added to a stirred solution of [2-(2,2-Dichloro-vinyl)-phenylethynyl]-trimethylsilane **2.15** (0.485g, 18.03 mmol) in THF (10 mL) via syringe at $-78\text{ }^\circ\text{C}$. In 30 minutes, the mixture was quenched with saturated aqueous solution of ammonium chloride (10 mL) and diluted with ether (20 mL). The organic layer was separated, washed with brine (3x25 mL), and dried over MgSO_4 . The solvents were removed under reduced pressure and crude product was purified by column chromatography ($R_f = 0.3$, hexanes) to give 0.32 g (90%) of **2.16** as yellow oil. ^1H NMR (CDCl_3 , 400 MHz): 0.27 (s, 9 H), 3.30 (s, 1 H), 6.98-7.02 (m, 2 H), 7.19-7.24 (m, 2 H).

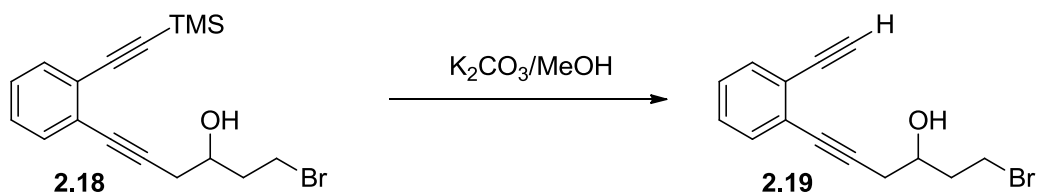


4-bromo-1,2-epoxybutane (2.17).¹⁵ A solution of $m\text{-CPBA}$ (12.88 g of 77%, 57.5 mmol, 1.1 eq) in dichloromethane (100 mL) was added to a solution of 4-bromobutane-1 (7.25 g, 53.7 mmol) in dichloromethane (40 mL) via dropping funnel at $0\text{ }^\circ\text{C}$. The reaction mixture was stirred for 40 hours at room temperature and filtered from $m\text{-CPBA}$. The residue was diluted with ether (100

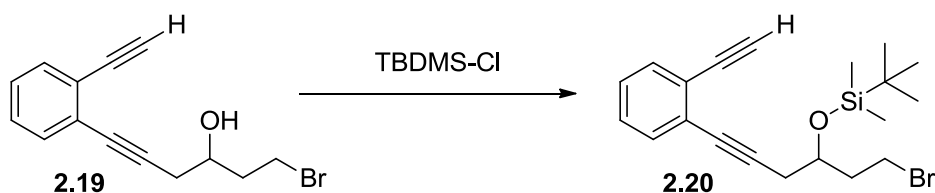
mL), washed with saturated solution of Na₂CO₃ (3x100 mL), brine (2x100 mL), and dried over MgSO₄. The solvent was removed under reduced pressure to give 5.63 g (70%) of epoxide **4** as a colorless liquid. ¹H NMR (CDCl₃, 400 MHz): 1.58 (m, 1 H), 2.00-2.10 (m, 1 H), 2.12-2.21 (m, 1 H), 2.58 (dd, *J*₁=4.8 Hz, *J*₂=2.8 Hz, 1 H), 2.84 (t, 1 H), 3.07-3.12 (m, 1 H), 3.49-3.54 (m, 2 H).



1-Bromo-6-(2-trimethylsilanylethynyl-phenyl)-hex-5-yn-3-ol (2.18).⁶ A solution of *n*-BuLi (29.5 mL, 75.6 mmol, 2.56M in hexane) was added to a stirred solution of mono-protected bis-acetylene **2.16** (13.6 g, 68.7 mmol) in dry THF (250 mL) at -78 °C. The reaction mixture was stirred for 1 h followed by addition of BF₃•Et₂O (10.6 mL, 82.4 mmol). After 15 min, 4-bromo-1,2-epoxybutane (**2.17**) (10.37 g, 68.67 mmol) was added, and the reaction mixture was stirred for 1 hour at -78 °C and then quenched with a saturated aqueous solution of NH₄Cl (100 mL). The mixture was extracted with ether (3x100 mL), washed with brine (3x100 mL), dried over anhydrous magnesium sulfate, filtered, and concentrated under reduced pressure. The residue was purified by column chromatography (*R*_f = 0.15, 15% EtOAc in hexanes) to give 15.1 g (63%) of **2.18** as yellow oil. ¹H NMR (CDCl₃, 400 MHz): 0.27 (s, 9 H), 2.04-2.21 (m, 2 H), 2.48 (broad singlet, 1 H), 2.60 (dd, *J*₁=16.8 Hz, *J*₂=6.8 Hz, 1 H), 2.73 (dd, *J*₁=16.8 Hz, *J*₂=4.4 Hz, 1 H), 3.58 (m, 2 H), 4.05-4.13 (m, 1 H), 7.23-7.36 (m, 2 H), 7.37-7.42 (m, 1 H), 7.45-7.49 (m, 1 H).

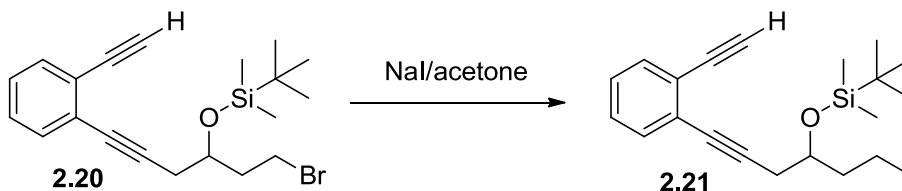


1-Bromo-6-(2-ethynylphenyl)hex-5-yn-3-ol (2.19).⁶ K₂CO₃ (6.2 g, 44.7 mmol) was added to a solution of **2.18** (15 g, 44.7 mmol) in methanol (200 mL). The reaction mixture was stirred at room temperature for 20 minutes, then quenched with brine (100 mL), and extracted with ether (3x100 mL). The organic layer was separated, washed with brine (3x100 mL), dried over MgSO₄, and concentrated under reduced pressure. The residue was purified by column chromatography (R_f = 0.1, 15% EtOAc in hexanes) to give 11.7 g (95%) of **2.19** as light-yellow oil. ¹H NMR (CDCl₃, 400 MHz): 2.09-2.26 (m, 2 H), 2.40 (d, 5.6 Hz, 1 H), 2.63 (dd, *J*₁=16.8 Hz, *J*₂=6.4 Hz, 1 H), 2.76 (dd, *J*₁=16.8 Hz, *J*₂=4.4 Hz, 1 H), 3.34 (s, 1 H), 3.55-3.65 (m, 2 H), 4.05-4.14 (m, 1 H), 7.22-7.32 (m, 2 H), 7.38-7.44 (m, 1 H), 7.48-7.52 (m, 1 H).



1-Bromo-3-[(*tert*-Butyldimethylsilyl)-oxyl]-6-(2'-ethynylphenyl)hex-5-yne (2.20).⁶ TBDMSCl (16.0 g, 0.1 mol), imidazole (14.4 g, 0.18 mol), and DMAP (1.3 g, 9.1 mmol) were added to a stirred solution of **2.19** (14.0 g, 50.5 mmol) in CH₂Cl₂ (200 mL). The reaction mixture was stirred for 3 hours and quenched with water (100 mL). The organic layer was washed with brine (3x100 mL), and dried over magnesium sulfate. The solvent was removed under pressure and the residue was purified by flash chromatography (R_f = 0.2, hexanes) to give 19.1 g (97 %) of **2.20** as yellow oil. ¹H NMR (CDCl₃, 400 MHz): 0.10 (s, 3 H), 0.13 (s, 3 H), 0.91 (d, 3.3 Hz, 9 H),

2.12-2.24 (m, 1 H), 2.32-2.42 (m, 1 H), 2.60 (dd, $J_1=16.8$ Hz, $J_2=7.6$ Hz, 1 H), 2.69 (dd, $J_1=16.8$ Hz, $J_2=4.4$ Hz, 1 H), 3.32 (s, 1 H), 3.48-3.58 (m, 2 H), 4.06-4.12 (m, 1 H), 7.21-7.30 (m, 2 H), 7.39-7.43 (m, 1 H), 7.46-7.50 (m, 1 H).

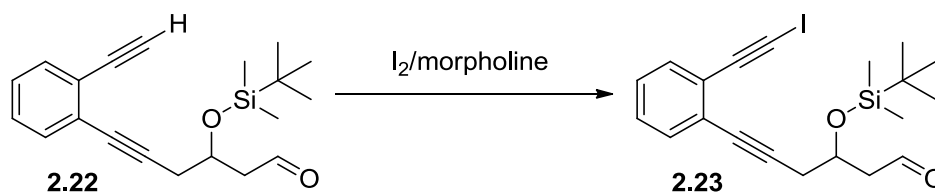


3-[(*tert*-Butyldimethylsilyl)oxyl-6-(2'-ethynyl)-1-iodohex-5-yne (2.21).⁶ Sodium iodide (9.52 g, 63.4 mmol) was added to a solution of **7** (19.1 g, 48.8 mmol) in dry acetone (200 mL). The reaction mixture was stirred for 48 h at 50 °C. The solvent was removed in vacuo, and the reasidue was portioned between ether (100 mL) and water (100 mL). The organic phase was dried over anhydrous MgSO_4 , filtered, concentrated in vacuo, and the residue was purified by column chromatography (5% ether in hexanes) to give 17.96 g (84%) of **2.21** as yellow oil. ^1H NMR (CDCl_3 , 400 MHz): 0.13 (s, 6 H), 0.90 (s, 9 H), 2.11-2.21 (m, 1 H), 2.33-2.43 (m, 1 H), 2.60 (dd, $J_1=16.8$ Hz, $J_2=7.6$ Hz, 1 H), 2.68 (dd, $J_1=16.8$ Hz, $J_2=4.4$ Hz, 1 H), 3.21-3.28 (m, 1 H), 3.3-3.37 (m, 2 H), 3.95-4.02 (m, 1 H), 7.21-7.3 (m, 2 H), 7.38-7.42 (1 H), 7.46-7.50 (m, 1 H).

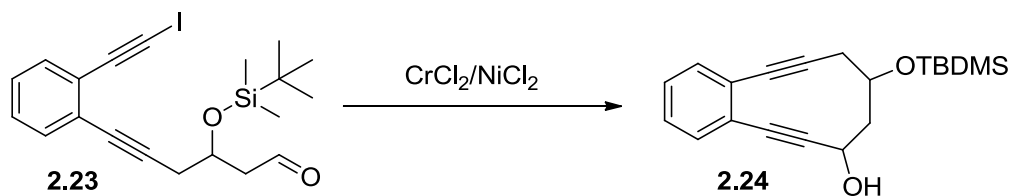


3-[(*tert*-Butyldimethylsilyl)oxyl-6-(2'-ethynyl)-hex-5-ynal (2.22). A solution of 3-[(*tert*-butyldimethylsilyl)oxyl-6-(2'-ethynyl)-1-iodohex-5-yne (**2.21**) (10.72 g, 0.024 mol, 1 eq.) in DMSO (10 mL) was added to a solution of silver tetrafluoroborate (1.3 eq) in DMSO (2ml/0.5

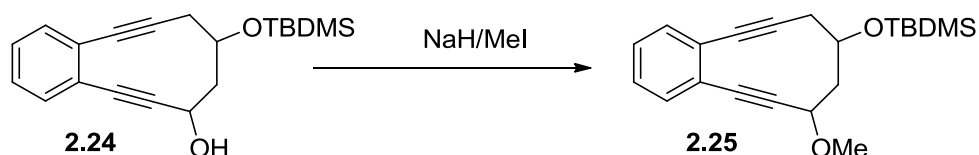
mmol) and stirred for 18 h at room temperature. Reaction was quenched by the addition of brine (50 mL) and extracted with ether (2x100 mL). Organic layer was separated, dried over sodium sulfate, and solvent removed under reduced pressure. The residue was filtered through a layer silica gel to give 6.9 g (86%) of **2.22** as yellow oil. ^1H NMR (CDCl_3 , 400 MHz): 0.09 (s, 3 H), 0.13 (s, 3 H), 0.88 (s, 9 H), 2.64-2.81 (m, 3 H), 2.9-2.97 (m, 1 H), 4.43-4.5 (m, 1 H), 7.22-7.31 (m, 2 H), 7.38-7.42 (m, 1 H), 7.47-7.51 (m, 1 H), 9.85-9.87 (m, 1 H); ^{13}C NMR (CDCl_3 , 100 MHz): -4.64, -4.23, 18.17, 25.91, 20.07, 50.63, 67.37, 80.96, 81.88, 82.64, 90.25, 124.75, 126.53, 127.86, 128.71, 132.06, 132.79, 201.77; HRMS calc. for $\text{C}_{20}\text{H}_{26}\text{O}_2\text{Si}$ - 57 m/z: 269.0998, found: 269.0993.



3-(tert-Butyl-dimethylsilyloxy)-6-(2-iodoethynylphenyl)-hex-5-ynal (2.23). *N*-Iodo-succinimide (3.84 g, 17.07 mmol) and AgNO_3 (276 mg, 1.625 mmol) were added to a solution of **2.22** (5.3 g, 16.25 mmol) in acetone (100 mL). The reaction mixture was stirred for 3 h, diluted with hexanes (100 mL), filtered through a layer of silica gel to give 5.0 g (68%) of **2.23** as an unstable yellow oil. ^1H NMR (CDCl_3 , 400 MHz): 0.10 (s, 3 H), 0.14 (s, 3 H), 0.88 (s, 9 H), 2.67 (dd, $J_1=16.8$ Hz, $J_2=8.4$ Hz, 1 H), 2.74-2.82 (m, 2 H), 2.92-2.99 (m, 1 H), 4.45-4.52 (m, 1 H), 7.22-7.28 (m, 2 H), 7.36-7.4 (m, 1 H), 7.4-7.44 (m, 1 H), 9.89-9.9 (m, 1 H); ^{13}C NMR (CDCl_3 , 100 MHz): -0.01, 0.37, 22.75, 30.51, 33.65, 55.27, 71.96, 86.32, 94.90, 97.87, 130.55, 131.48, 132.36, 133.27, 136.47, 137.48, 206.26; HRMS calc. for $\text{C}_{20}\text{H}_{25}\text{O}_2\text{SiI}$ - 57 m/z: 394.9964, found: 394.9957.

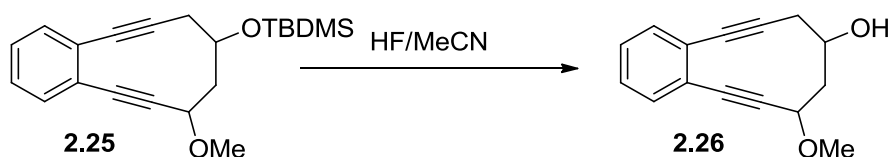


9-methoxy-5,6,11,12-tetradehydro-7,8,9,10-tetrahydrobenzo[10]annulen-7-ol (2.24). A solution of **2.23** (1 g, 2.12 mmol) in THF (20 mL) was added via syringe pump to a suspension of CrCl_2 (680 mg, 5.53 mmol) and NiCl_2 (70 mg, 0.53 mmol) in THF (150 mL) at 0 °C. The reaction mixture was allowed to warm to room temperature, and stirred for 6 h. Brine (100 mL) was added and aqueous phase was extracted with ether (3x100 mL). Combined organic layers were dried over sodium sulfate and solvents removed under reduced pressure. The residue was purified by a column chromatography (gradient mode, from 1% to 5% of ethyl acetate in hexanes) to give 473 mg (65%) of **2.24** as viscous yellow oil. ^1H NMR (CDCl_3 , 400 MHz): 0.11 (s, 3 H), 0.13 (s, 3 H), 0.89 (s, 9 H), 1.83 (d, $J=4$ Hz, 1 H), 2.37-2.42 (m, 1 H), 2.6 (dd, $J_1=16.8$ Hz, $J_2=10$ Hz, 1 H), 2.68 (dd, $J_1=16.8$ Hz, $J_2=3.6$ Hz, 1 H), 4.42-4.48 (m, 1 H), 4.9-4.94 (m, 1 H), 7.22-7.3 (m, 2 H), 7.31-7.38 (m, 2 H); ^{13}C NMR (CDCl_3 , 100 MHz): -4.48, -4.46, 18.1, 25.97, 31.37, 48.67, 61.11, 68.48, 83.79, 86.02, 96.24, 98.85, 127.66, 128.04, 128.34, 128.68, 129.22, 129.92; HRMS calc. for $\text{C}_{20}\text{H}_{26}\text{O}_2\text{Si}$ - 57 m/z: 269.0998, found: 269.0994.



7-methoxy-9-*tert*-Butyldimethylsilyloxy-5,6,11,12-tetradehydro-7,8,9,10-tetrahydrobenzo[10]annulene (2.25). A suspension of sodium hydride (66 mg of 60%, 1.65 mmol) in oil was added to a solution of **2.24** (450 mg, 1.38 mmol) in THF (75 mL) at 0 °C and stirred for 30 min. Dimethyl sulfate (160 μL , 1.38 mmol) was added, the reaction mixture stirred for 45 min, and

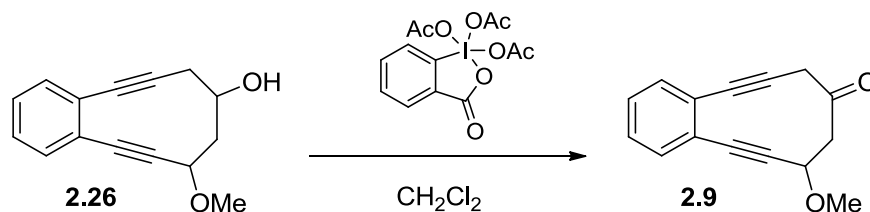
quenched with an aqueous solution of ammonium chloride (100 mL). Aqueous phase was extracted with ether (3x50 mL), combined organic layers washed with brine (3x50 mL), and dried over sodium sulfate. The solvent was removed under reduced pressure and the residue was purified by column chromatography ($R_f = 0.15$, 0.5% EtOAc in hexanes) to give 350 mg (75%) of **2.25** as a yellow oil. ^1H NMR (CDCl_3 , 400 MHz): 0.09 (s, 3 H), 0.1 (s, 3 H), 0.88 (s, 9 H), 2.3-2.37 (m, 1 H), 2.42-2.49 (m, 1 H), 2.56 (dd, $J_1=16.8$ Hz, $J_2=10$ Hz, 1 H), 2.68 (dd, $J_1=16.8$ Hz, $J_2=3.6$ Hz, 1 H), 3.45 (s, 3 H), 4.37-4.4 (m, 1 H), 7.21-7.29 (m, 2 H), 7.3-7.34 (m, 1 H), 7.37-7.4 (m, 1 H); ^{13}C NMR (CDCl_3 , 100 MHz): -4.62, 18.13, 25.99, 31.40, 47.08, 57.03, 69.00, 69.99, 83.75, 86.54, 96.26, 97.44, 127.60, 128.24, 128.35, 128.53, 129.35, 129.88; HRMS calc. for $\text{C}_{21}\text{H}_{28}\text{O}_2\text{Si}$ - 57 m/z: 283.1154, found: 283.1147.



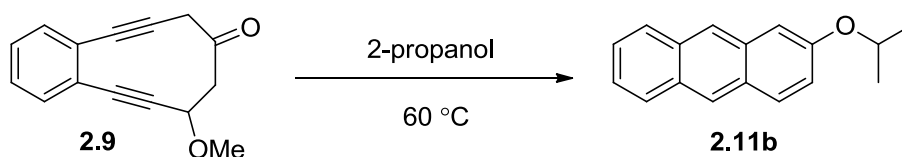
10-methoxy-5,6,11,12-tetradehydro-7,8,9,10-tetrahydrobenzo[10]annulen-8-ol (2.26).

Concentrated solution of hydrogen fluoride (2 mL) was added to a stirred solution of **2.25** (350 mg, 1.02 mmol) in MeCN (100 mL). The reaction mixture was stirred for 3 h, diluted with ether (100 mL), and washed with brine (3x50 mL). Organic layer was separated and dried over sodium sulfate. Solvents were evaporated under reduced pressure and the residue was purified by column chromatography ($R_f = 0.15$, 20% of ethyl acetate in hexanes) to give 230 mg (98%) of **2.26** as light-yellow oil. ^1H NMR (CDCl_3 , 400 MHz): 2.38-2.48 (m, 2 H), 2.56 (dd, $J_1=16.8$ Hz, $J_2=10$ Hz, 1 H), 2.68 (dd, $J_1=16.8$ Hz, $J_2=3.6$ Hz, 1 H), 3.49 (s, 3 H), 4.44 (dd, $J_1=5.6$ Hz, $J_2=2.4$ Hz, 1 H), 7.22-7.28 (m, 2 H), 7.31-7.35 (m, 1 H), 7.37-7.4 (1 H); ^{13}C NMR (CDCl_3 , 100 MHz): 30.46,

46.2, 57.44, 68.81, 70.12, 84.21, 86.97, 95.31, 96.82, 127.76, 127.96, 128.57, 128.66, 129.51, 129.55; HRMS calc. for $C_{15}H_{14}O_2$ m/z: 226.0994, found: 226.0986.

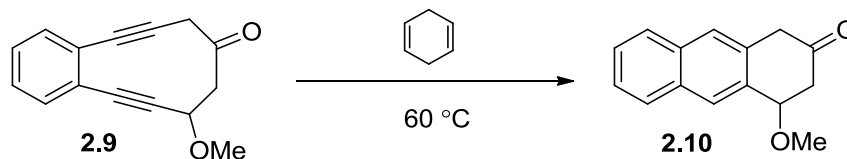


10-methoxy-5,6,11,12-tetradehydro-9,10-dihydrobenzo[10]annulen-8(7H)-one (2.9). Dess-Martin periodinane (650 mg, 1.5 mmol) was added to a solution of **2.26** (230 mg, 1.01 mmol) in dichloromethane (75 mL). The reaction mixture was stirred for 2 h, diluted with ether/hexanes (1:1, 100 mL), and filtered through a thick layer of Celite-545. Solvents were removed under reduced pressure to give 225 mg (97%) of **2.9** as yellow oil. 1H NMR ($CDCl_3$, 400 MHz): 2.88 (dd $J_1=12.8$ Hz, $J_2=3.2$ Hz, 1 H), 3.38 (d, $J=15.6$ Hz, 1 H), 3.48-3.52 (m, 4 H), 3.61 (d, $J=15.6$ Hz, 1 H), 4.6 (dd $J_1=10.8$ Hz, $J_2=3.2$ Hz, 1 H), 7.26-7.3 (m, 2 H), 7.34-7.39 (m, 2 H); ^{13}C NMR ($CDCl_3$, 100 MHz): 38.1, 49.6, 57.0, 69.8, 87.4, 87.9, 88.2, 95.3, 127.5, 127.9, 128.2, 128.5, 128.7, 129.0, 198.1; HRMS calc. for $C_{15}H_{12}O_2$ m/z: 224.0837, found: 224.0829.



2-iso-Propoxyanthracene (2.11b). A degassed solution of **2.9** (50 mg, 0.22 mmol) was heated in isopropanol (35 mL) at 60 °C for 18 h. Solvent was then removed under reduced pressure, and the residue was purified by column chromatography (hexanes) to give 14 mg (27%) of **2.11b** as a white solid. 1H NMR ($CDCl_3$, 400 MHz): 1.44 (d, $J=6$ Hz, 6 H), 4.75 (sep, $J=6$ Hz, 1 H), 4.27 (dd, $J_1=8.8$ Hz, $J_2=2.4$ Hz, 1 H), 7.2 (d, $J=2.4$ Hz, 1 H), 7.36-7.46 (m, 2 H), 7.89 (d, $J=8.8$ Hz, 1 H), 7.91-7.97 (m, 2 H), 8.24 (s, 1 H), 8.33 (s, 1 H); ^{13}C NMR ($CDCl_3$, 100 MHz): 22.2, 69.9,

106.0, 121.7, 124.2, 124.5, 125.6, 126.3, 127.7, 128.3, 128.4, 130.0, 130.5, 132.4, 133.0, 155.4;
HRMS calc. for C₁₇H₁₆O₂ m/z: 236.1201, found: 236.1196.



4-Methoxy-3,4-dihydro-1H-anthracen-2-one (2.10). A degassed solution of **2.9** (50 mg, 0.22 mmol) was heated in cyclohexadiene (5 mL) for 24 hours at 60 °C. The solvent was then removed under reduced pressure, and the residue was purified by column chromatography (R_f = 0.1, 15% EtOAc in hexanes) to give 32 mg (64%) of **2.10** as colorless oil and 4 mg (9%) of 2-anthracenol (**2.11a**).¹⁶ **2.10:** ¹H NMR (acetone-d₆, 400 MHz): 2.68-2.75 (dd, J_1 =17.2 Hz, J_2 =3.2 Hz, 1 H), 2.81-2.88 (dd, J_1 =17.2 Hz, J_2 =3.6 Hz, 1 H), 3.25 (s, 3 H), 3.64 (d, J =19.6 Hz, 1 H), 3.88 (dd, J_1 =19.6 Hz, J_2 =1.6 Hz, 1 H), (t, J =3.2 Hz, 1 H), 7.48-7.54 (m, 2 H), 7.72 (s, 1 H), 7.84-7.87 (m, 1 H), 7.9-7.96 (m, 1 H); ¹³C NMR (acetone-d₆, 100 MHz): 44.1, 44.7, 55.6, 78.2, 126.1, 126.7, 127.3, 127.4, 127.6, 128.1, 132.1, 132.3, 133.7, 133.8, 205.6; HRMS calc. for C₁₅H₁₄O₂ m/z: 226.0994, found: 226.0990.

1,9-dideutero-2-hydroxyanthracene (2.13-d2). NaOD (7 μL, 30%) was added to a solution of **2.9** (10 mg) in *i*-PrOD (100 mL) at -78 °C and stirred for 2 hours, then letting to warm to room temperature very slow for 24 hours. The solvent was distilled and the residue was purified by column chromatography (R_f = 0.15, 10% EtOAc in hexanes) to give 3 mg (32%) of **2.13-d2** as a yellow solid with 75% deuteration at the 9-position. ¹H NMR (acetone-d₆, 400 MHz): 7.21 (d, J =8.8 Hz, 1 H), 7.36-7.46 (m, 2 H), 7.94-8.2 (m, 3H), 8.25 (s, 0.3 H), 8.43 (s, 1 H), 8.78 (br s, 1 H). HRMS calc. for C₁₄H₈D₂O m/z: 196.0855, found: 196.0850 and for C₁₄H₉DO m/z: 195.0793, found: 196.0788.

2.6 CARTESIAN COORDINATES OF OPTIMIZED STRUCTURES

2.5^K

C -4.04368000 0.41746500 0.02272200
C -2.92839000 1.25505000 0.05991600
C -1.63283700 0.71759000 0.03819600
C -1.47469900 -0.70448000 -0.02397700
C -2.61008000 -1.52946900 -0.06790200
C -3.88723400 -0.97177900 -0.04184800
H -5.03938300 0.85031100 0.04191500
H -3.05065100 2.33217200 0.10523000
H -2.47707000 -2.60515200 -0.11837900
H -4.75910300 -1.61769400 -0.07283900
C -0.44918800 1.51426700 0.05544400
C 0.68649600 1.94603100 0.03670300
C -0.14562900 -1.21167500 -0.03100500
C 1.05754300 -1.40054200 0.00106500
C 2.99211600 1.10629500 -0.48190200
H 2.62310000 0.73181800 -1.44285300
H 3.99577300 1.50136200 -0.67088800
C 2.10306400 2.29995800 -0.04127000
H 2.44940400 2.67622600 0.93136900
H 2.23821800 3.12422300 -0.75350800
C 2.50135400 -1.38823000 0.09406000
C 3.10955800 -0.05727500 0.54821100
H 2.62870500 0.23010600 1.49157700
O 3.19499800 -2.36398400 -0.16023000
H 4.16065200 -0.27073200 0.75974200

2.5^E

C 4.05457200 0.33587300 -0.09928600
C 2.96473400 1.19443000 -0.25176500
C 1.65278100 0.71310400 -0.13684800
C 1.44590700 -0.68109700 0.13281500
C 2.55616200 -1.52568100 0.28591300
C 3.85153100 -1.02133700 0.17096700
H 5.06333900 0.72748300 -0.18994800
H 3.12056500 2.24814200 -0.45899500

H 2.39107800 -2.57804700 0.49276700
 H 4.70106800 -1.68660500 0.29136600
 C 0.49260700 1.53550400 -0.26040100
 C -0.65413700 1.93833300 -0.28326100
 C 0.09901900 -1.13857700 0.19998600
 C -1.11271100 -1.23034200 0.12424600
 C -2.52117200 -1.17866500 -0.07029700
 C -3.26651000 -0.06647700 0.13616700
 C -2.82030100 1.23827400 0.75737600
 H -2.17859700 1.04585700 1.62466300
 H -3.71679900 1.74159300 1.13608600
 C -2.07612200 2.25859700 -0.16625200
 H -2.54737900 2.28585300 -1.15780500
 H -2.19243900 3.26183400 0.26338000
 O -3.03991700 -2.35945700 -0.55660300
 H -3.99881200 -2.26973900 -0.64985100
 H -4.32085300 -0.13235200 -0.13500900

2.6^K

C -4.01340100 0.63008900 0.16724000
 C -2.82850700 1.36615000 0.16301500
 C -1.58851800 0.72066500 0.04299000
 C -1.55202500 -0.70384500 -0.07530900
 C -2.75539400 -1.42560600 -0.06937800
 C -3.97724500 -0.76356100 0.05066100
 H -4.96535400 1.14381000 0.26162000
 H -2.85182200 2.44737200 0.25268700
 H -2.72148700 -2.50665200 -0.15809900
 H -4.90068000 -1.33467500 0.05434700
 C -0.33913300 1.41204900 0.02466200
 C 0.82492200 1.75625100 -0.02237200
 C -0.27031400 -1.32522600 -0.18304700
 C 0.89701400 -1.65616100 -0.24425200
 C 2.93195400 0.68429900 -0.78804100
 H 2.40606500 0.40611000 -1.70518000
 H 3.96835300 0.93420100 -1.04796300
 C 2.26839700 1.94406000 -0.16225600
 H 2.73176100 2.14255500 0.81173700

H 2.48154200 2.80988200 -0.80045500
 C 2.34814100 -1.83216500 -0.23060600
 H 2.65658200 -2.59352200 0.49271000
 H 2.71496300 -2.13188400 -1.22263900
 C 3.01198800 -0.49695800 0.17966000
 O 3.59160100 -0.39718100 1.24293000
2.6^E
 C 4.14332900 0.53669800 -0.07035900
 C 2.97675100 1.29761600 -0.16402900
 C 1.71637900 0.68744900 -0.09660200
 C 1.63497100 -0.73669100 0.06777400
 C 2.82238700 -1.47960200 0.16552000
 C 4.06525000 -0.84987800 0.09481400
 H 5.11114600 1.02609500 -0.12418500
 H 3.03236200 2.37418000 -0.28990300
 H 2.75827100 -2.55514800 0.29534800
 H 4.97277100 -1.44146900 0.17033300
 C 0.48486000 1.40704100 -0.17233800
 C -0.68960600 1.71874000 -0.18886300
 C 0.33587900 -1.32022300 0.09962000
 C -0.87034400 -1.47092200 -0.01551600
 C -2.26557000 -1.53888400 -0.22349200
 C -3.11495700 -0.51517900 0.05406900
 C -2.80132800 0.77487000 0.77171800
 H -2.15264300 0.56051400 1.62647600
 H -3.75278700 1.15262400 1.15818400
 C -2.13615800 1.90622800 -0.07459400
 H -2.60197100 1.96288000 -1.06698300
 H -2.34773500 2.86198000 0.42051700
 O -4.44183800 -0.57652300 -0.27780900
 H -4.62924400 -1.39815500 -0.75477200
 H -2.66653700 -2.43490200 -0.69887900

2.7

C 3.91690200 0.78127700 -0.38861900
 C 2.66362400 1.38870500 -0.42318200
 C 1.50030700 0.66467900 -0.10504600
 C 1.60920600 -0.71151700 0.24514700

C 2.88485400 -1.29335900 0.29848900
 C 4.02934500 -0.56247600 -0.01908200
 H 4.80322100 1.35674200 -0.63801300
 H 2.56834300 2.43683700 -0.68761600
 H 2.97439900 -2.33888900 0.58098200
 H 5.00374900 -1.03982100 0.02221200
 C 0.22014500 1.29274400 -0.06396700
 C -0.92731700 1.66805400 0.06464700
 C 0.43301300 -1.54615600 0.58235500
 C -0.76735400 -1.45004300 0.05439600
 C -2.98481200 0.51981900 0.86903800
 H -2.38795000 0.16373500 1.71439400
 H -4.00057600 0.73537700 1.21075700
 C -2.35348400 1.84016900 0.32687800
 H -2.88843900 2.15945900 -0.57598800
 H -2.50684000 2.62617400 1.07654700
 C -1.94588800 -1.43431200 -0.53338200
 C -3.10290700 -0.55263500 -0.20638600
 O -4.13679200 -0.66524000 -0.85441700
 H 0.59429900 -2.33206500 1.32206700
 H -2.11968100 -2.07533000 -1.39771100

2.7 REFERENCES

- (1) Karpov, G. V.; Popik, V. V. Triggering of the Bergman Cyclization by Photochemical Ring Contraction. Facile Cycloaromatization of Benzannulated Cyclodeca-3,7-diene-1,5-diynes. *J. Am. Chem. Soc.* **2007**, *129*, 3792-3793.
- (2) Nicolaou, K. C.; Zuccarello, G.; Riemer, C.; Estevez, V. A.; Dai, W. M. Design, synthesis, and study of simple monocyclic conjugated enediynes. The 10-membered ring enediyne moiety of the enediyne anticancer antibiotics. *J. Am. Chem. Soc.* **1992**, *114*, 7360-7371.

- (3) Karpov, G.; Kuzmin, A.; Popik, V. V. Enhancement of the reactivity of photochemically generated enediynes via keto-enol tautomerization. *J. Am. Chem. Soc.* **2008**, *130*, 11771-11777.
- (4) Cousson, A.; Dancy, I.; Beau, J.-M. (1R)-4,5-Benzocyclodeca-4-ene-2,6-diyn-1-yl 2,3,4,6-Tetra-O-acetyl- β -D-glucopyranoside and 4,5-Benzocyclodeca-4-ene-2,6-diyn-1-one. *Acta Crystallogr. C* **1995**, *51*, 718-721.
- (5) Boger, D. L.; Zhou, J. CDPI3-enediyne and CDPI3-EDTA conjugates: a new class of DNA cleaving agents. *J. Org. Chem.* **1993**, *58*, 3018-3024.
- (6) Semmelhack, M. F.; Neu, T.; Foubelo, F. Arene 1,4-Diradical Formation from *o*-Dialkynylarenes. *J. Org. Chem.* **1994**, *59*, 5038-5047.
- (7) Perrin, C. L.; Rodgers, B. L.; O'Connor, J. M. Nucleophilic Addition to a *p*-Benzyne Derived from an Enediyne: A New Mechanism for Halide Incorporation into Biomolecules. *J. Am. Chem. Soc.* **2007**, *129*, 4795-4799.
- (8) Dess, D. B.; Martin, J. C. Readily accessible 12-I-5 oxidant for the conversion of primary and secondary alcohols to aldehydes and ketones. *J. Org. Chem.* **1983**, *48*, 4155-4156.
- (9) Bates, R. G., *Determination of pH. Theory and practise*. 1973, New York: Wiley. 49.
- (10) Gaussian 03, R. C., Frisch, M. J.; Trucks, G. W.; Schlegel, H. B.; Scuseria, G. E.; Robb, M. A. C., J. R.; Montgomery, Jr., J. A.; Vreven, T.; Kudin, K. N.; Burant, J. C.; Millam, J. M. I., S. S.; Tomasi, J.; Barone, V.; Mennucci, B.; Cossi, M.; Scalmani, G.; Rega, N. P., G. A.; Nakatsuji, H.; Hada, M.; Ehara, M.; Toyota, K.; Fukuda, R.; Hasegawa, J. I., M.; Nakajima, T.; Honda, Y.; Kitao, O.; Nakai, H.; Klene, M.; Li, X.; Knox, J. E.; Hratchian, H. P. C., J. B.; Bakken, V.; Adamo, C.; Jaramillo, J.; Gomperts, R.; Stratmann, R. E. Y., O.; Austin, A. J.; Cammi, R.; Pomelli, C.; Ochterski, J. W.; Ayala,

- P.; Y.; Morokuma, K. V., G. A.; Salvador, P.; Dannenberg, J. J.; Zakrzewski, V. G.; Dapprich, S.; Daniels, A. D. S., M. C.; Farkas, O.; Malick, D. K.; Rabuck, A. D.; Raghavachari, K.; Foresman, J. B. O., J. V.; Cui, Q.; Baboul, A. G.; Clifford, S.; Cioslowski, J.; Stefanov, B. B.; Liu, G. L., A.; Piskorz, P.; Komaromi, I.; Martin, R. L.; Fox, D. J.; Keith, T.; Al-Laham, M. A.; Peng, C. Y.; Nanayakkara, A.; Challacombe, M.; Gill, P. M. W.; Johnson, B.; Chen, W.; Wong, M. W. G., C.; and Pople, J. A.; Gaussian, Inc., Wallingford CT, 2004.
- (11) Scott, A. P.; Radom, L. Harmonic Vibrational Frequencies: An Evaluation of Hartree-Fock, Moller-Plesset, Quadratic Configuration Interaction, Density Functional Theory, and Semiempirical Scale Factors. *J. Phys. Chem.* **1996**, *100*, 16502-16513.
- (12) Bedard, T. C.; Moore, J. S. Design and synthesis of molecular turnstiles. *J. Am. Chem. Soc.* **1995**, *117*, 10662-10671.
- (13) Poloukhine, A.; Popik, V. V. Synthesis and Unusual Reactivity of N-Tosyl-4,5-benzoazacyclodeca-2,6-diyne, Yneamino-Containing Enediyne. *J. Am. Chem. Soc.* **2007**, *129*, 12062-12063.
- (14) Huynh, C.; Linstrumelle, G. A short route to dehydro [12] annulenes. *Tetrahedron* **1988**, *44*, 6337-6344.
- (15) Marson, C. M.; Randall, L.; Winter, M. J. Synthesis of hydroxymethyl lactones and spiroketals via cyclization of epoxy oxacarbene complexes. *Tetrahedron Lett.* **1994**, *35*, 6717-6720.
- (16) Coleman, R. S.; Mortensen, M. A. Stereocontrolled synthesis of anthracene [beta]-C-ribosides: fluorescent probes for photophysical studies of DNA. *Tetrahedron Lett.* **2003**, *44*, 1215-1219.

CHAPTER 3

DUAL REACTIVITY OF A PHOTOCHEMICALLY-GENERATED CYCLIC ENYNE-ALLENE

3.1 INTRODUCTION

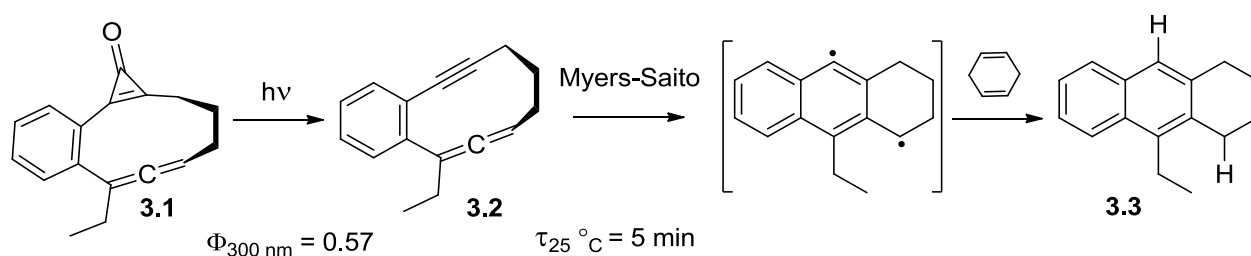
As it was mentioned in the Chapter 1, the lack of anti-tumor selectivity of natural enediynes results in high general toxicity which hampers their clinical applications. To overcome this shortcoming we investigated an alternative strategy for the triggering of the cycloaromatization reaction: the *in situ* photogeneration of reactive enediynes.¹ However, the rate of the Bergman cyclization of even highly strained nine-membered ring enediynes ($\tau_{25\text{ }^{\circ}\text{C}} \sim 2\text{ h}$)^{1a} is not fast enough to allow for the temporal and spatial resolution of *p*-benzyne generation in biological systems. In order to enhance the rate of the formation of cytotoxic 1,4-diradicals, we turned our attention to compounds containing a (*Z*)-1,2,4-heptatrien-6-yne structural fragment, *i.e.*, enyne-allenes. Myers–Saito cyclization (see Ch. 1.2.3) of these substrates produces $\alpha,3$ -didehydrotoluene analogs, which are responsible for the cytotoxicity of natural antibiotics of the neocarzinostatin family.² The Myers–Saito cyclization of enyne-allenes provides a particularly attractive pathway to carbon diradicals because the reaction occurs under mild thermal conditions and various synthetic routes to enyne-allenes are available.

While acyclic enyne-allenes usually undergo spontaneous cyclization under ambient temperature,³ cyclic enyne-allenes are virtually unknown apparently due to their ability to undergo very rapid cycloaromatization.^{1c,4}

3.2 RESULTS AND DISCUSSION

The direct photochemical generation of ten-membered ring cyclic enyne-allene **3.2** is shown in Scheme 3.1. In order to prepare a thermally stable photo-precursor of enyne-allene **3.2**, the triple bond was masked as a cyclopropenone. The π -system of the cyclopropenone moiety in the enyne-allene precursor **3.1** is orthogonal to the plane of the ring, therefore, cyclopropenone **3.1** lacks the crucial in-plane overlap of π -orbitals that is required for cycloaromatization. Photochemical decarbonylation of cyclopropenones is usually an efficient process and has been successfully employed for the generation of reactive enediynes.^{1a,b} Irradiation of cyclopropenone **3.1** results in the loss of carbon monoxide and regeneration of the triple bond, thus, making the substrate susceptible to the Myers–Saito cyclization (Scheme 3.1).

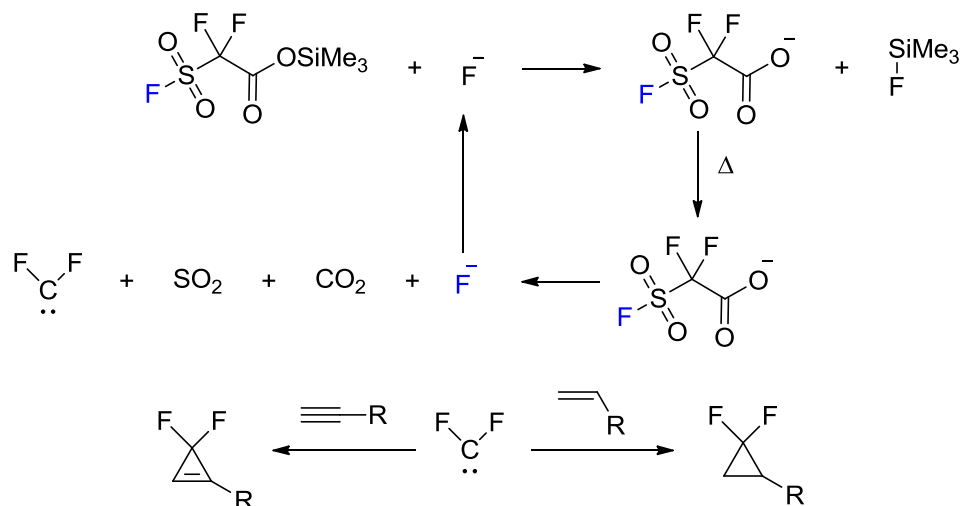
Scheme 3.1 Photochemical generation of enyne-allene **3.2**.



Trimethylsilyl fluorosulfonyldifluoroacetate ($\text{FSO}_2\text{CF}_2\text{CO}_2\text{SiMe}_3$, TFDA)⁵ is a highly versatile source of difluorocarbene,⁶ and can be used for the preparation of gem-difluorocyclopropene through its reaction with alkynes. At elevated temperatures, TFDA undergoes decomposition in the presence of catalytic amounts of fluoride ion forming

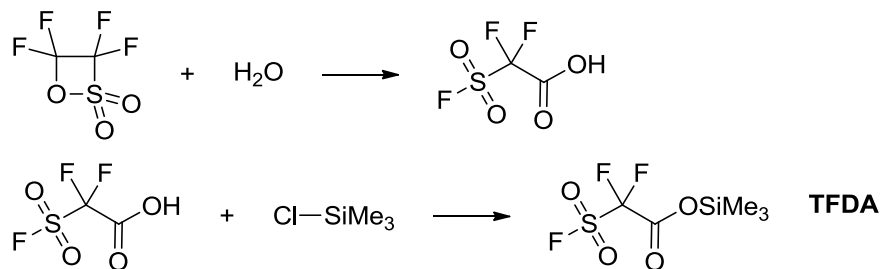
difluorocarbene and fluoride ion. The latter is consumed through the reaction with another molecule of TFDA, repeating the cycle (Scheme 3.2).

Scheme 3.2 Formation of difluorocarbene and its addition to double and triple bonds.



It should be noted that TFDA is an expensive reagent but can be readily synthesized by simply adding an excess of trimethylsilyl chloride to 2,2-difluoro-2-(fluorosulfonyl)acetic acid, and distilling the product (Scheme 3.3). The needed acid can be prepared under mild conditions from commercially available 3,3,4,4-tetrafluoro[1,2]oxathietane 2,2-dioxide, a key monomer in the preparation of Nafion ion membrane resin.⁷

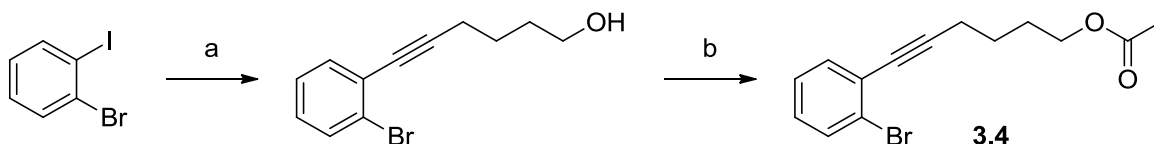
Scheme 3.3 Preparation of trimethylsilyl fluorosulfonyldifluoroacetate (TFDA).



The starting material, 6-(2-bromophenyl)hex-5-ynyl acetate (**3.4**), was synthesized according to the literature procedure⁸ from a commercially available 1-bromo-2-iodobenzene by

reacting it with 5-hexyn-1-ol under the *Sonogashira—Higihara reaction* conditions and treating the resultant alcohol with acetic anhydride (Scheme 3.4). In turn, acetate **3.4** must be carefully purified by a column chromatography to avoid complications during the next step, difluorocarbene addition.

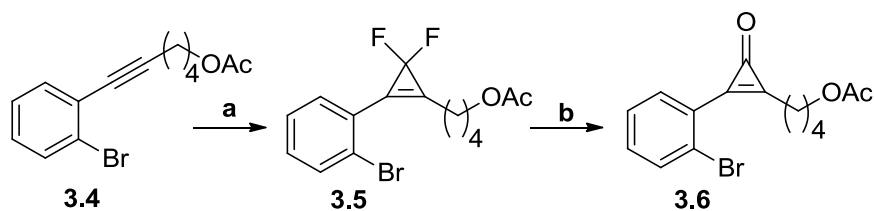
Scheme 3.4 Synthesis of 6-(2-bromophenyl)hex-5-ynyl acetate **3.4**.



Reagents and conditions: (a) 5-hexynol, $\text{PdCl}_2(\text{PPh}_3)_2/\text{CuI}$, THF, 92%; (b) $\text{Ac}_2\text{O}/\text{Et}_3\text{N}$, 90%.

The crucial cyclopropenone moiety was synthesized in a two-step procedure. First, the addition of difluorocarbene, which was generated by the thermolysis of TFDA, to the acetylene **3.4** produced 1,1-difluorocyclopropene **3.5** (Scheme 3.5).

Scheme 3.5 Preparation of cyclopropenone **3.6**.



Reagents and conditions: (a) NaF, TFDA, 120 °C; (b) wet SiO_2 , 85% over two steps.

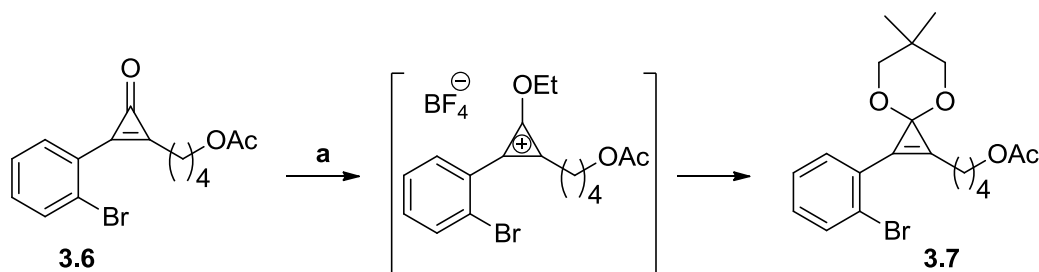
Experiments directed at optimization of this reaction indicated that the rate of addition of the TFDA (1 mL/5 min), concentration of the starting material (1 g/1 mL of diglyme), and additional time of heating can strongly affect the yield of the reaction. Thus, we found that difluorocarbene reacts with our acetylene **3.4** upon the formation and additional heating for two hours, indicated in literature,⁹ only lowers the overall yield. It should be mentioned that

difluorocyclopropene **3.5** decomposes within 2-3 days. However, we managed to isolate and characterize it by NMR spectroscopy.

It is known that *gem*-difluorocyclopropenes are susceptible both to basic¹⁰ and acidic hydrolysis¹¹ affording corresponding cyclopropanones. The hydrolysis of **3.5** was achieved by passing it through wet silica gel to give cyclopropanone **3.6** in high yield.

The presence of the cyclopropanone moiety in the synthetic intermediate **3.6** limits the range of reagents and reaction conditions that can be employed because cyclopropanones readily form salts with Lewis acids and give ring-opening products with various nucleophiles.¹² Conversion of **3.6** into 2,2-dimethyl-1,3-propanediyl acetal **3.7** allows us to circumvent these difficulties (Scheme 3.6).¹³ The 2π -electron cyclopropanone is stable, as is the cyclopropanium cation, which is a 2π -aromatic compound.¹⁴

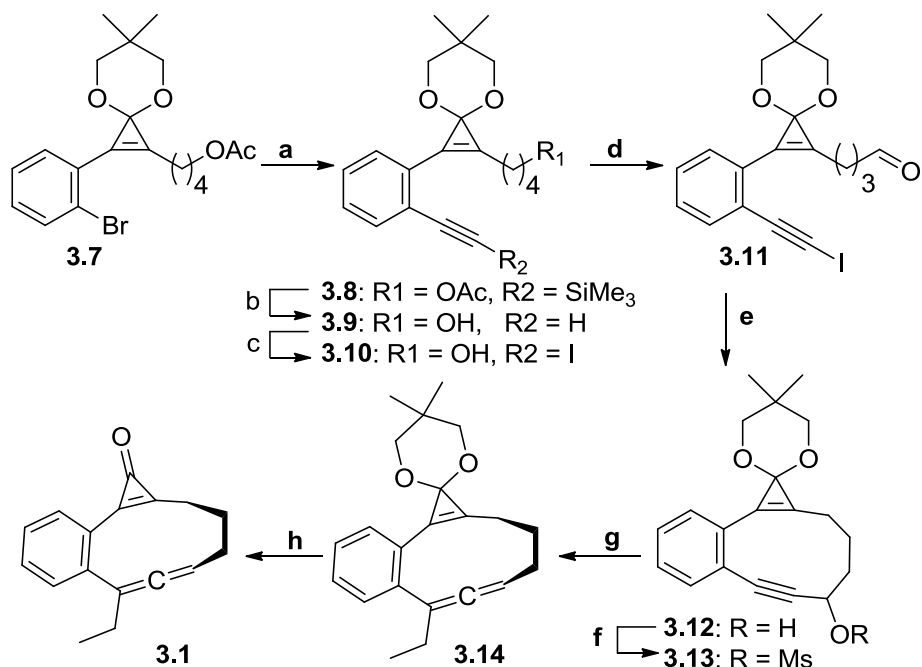
Scheme 3.6 Conversion of cyclopropanone **3.6** to acetal **3.7**.



Reagents and conditions: (a) Et_3OBF_4 , neopentylglycol, Et_3N , 80%.

The acetalization of cyclopropanones requires a strong Lewis acid. Thus, cyclopropanone **3.6** is first converted to cyclopropanium ion by treatment with an excess of triethyloxonium tetrafluoroborate followed by treatment with an alcohol under basic conditions (triethyloxonium tetrafluoroborate is often called Meerwein's reagent after its discoverer Hans Meerwein).

Scheme 3.7 Synthesis of cyclopropenone **3.1**.



Reagents and conditions: (a) Pd(PPh₃)₄/Bu₃SnC≡CSiMe₃, 90 °C, 72%; (b) K₂CO₃/MeOH_{aq}, 84%; (c) I₂/morpholine, 72%; (d) DMP, 73%; (e) CrCl₂, NiCl₂, 95%; (f) MsCl, 90%; (g) CuCN, LiCl, EtMgBr, 83%; (h) Amberlyst® 15, acetone, 75%.

Freshly purified compound **3.7** was immediately used in the next step to ensure good yield of the *Stille coupling reaction* (Scheme 3.7). Tributyl(trimethylsilylethynyl)tin was prepared from trimethylsilylacetylene, which was reacted with *n*-butyl lithium followed by the addition of tributyltin chloride and distillation of the formed product.

Simultaneous saponification of the acetate and removal of the trimethylsilyl protecting group of the compound **3.7** was achieved using potassium carbonate in aqueous methanol to give **3.9**. Iodination of terminal acetylene with an iodine/morpholine system¹⁵ gave iodide **3.10**. Dess–

Martin periodinane¹⁶ was used to oxidize alcohol **3.10** to give iodoaldehyde **3.11**. The *Nozaki–Hiyama–Kishi reaction*¹⁷ was used to close the ten-membered cycle **3.12**.

The key step in the synthesis of enyne-allene precursor **3.1** was the acetylene-allene rearrangement. Several enyne-allenes were prepared by isomerization of propargyl alcohol employing Mitsunobu reaction with 2-nitro-benzenesulfonyl hydrazide.¹⁸ Acetal **3.12**, however, is not stable under Mitsunobu conditions and we had to adopt an alternative procedure.¹⁹ The reaction of freshly prepared propargylic mesylate **3.13** with EtMgBr in the presence of an excess of CuCN and LiCl led to the exclusive formation of the desired allene **3.14**. It should be noted that propargylic mesylates quickly decompose at ambient temperatures. Acetal hydrolysis was achieved using Amberlyst® 15 in aqueous acetone.²⁰ The target 7-ethyl-6-dehydro-2,3,4-trihydro-1*H*-benzo[*a*]cyclopropa[*c*]cyclohept-1-ene (**3.1**, Scheme 3.7) was isolated in 75%.

3.3 PHOTOCHEMISTRY AND KINETICS OF ENYNE-ALLENE **3.2**

The UV spectrum of cyclopropenone **3.1** shows three close lying absorbance bands at 237 nm ($\log \epsilon = 4.3$), 267 nm ($\log \epsilon = 3.8$), and 317 nm ($\log \epsilon = 3.4$). Irradiation of cyclopropenone **3.1** with 300 or 350 nm light results in the efficient decarbonylation ($\Phi_{300 \text{ nm}} = 0.57 \pm 0.03$) and formation of the target ten-membered ring enyne-allene (**3.2**, Scheme 3.1). The cyclic enyne-allene **3.2** undergoes facile spontaneous Myers–Saito cyclization in 2-propanol, producing naphthalene derivative **3.17**. Compound **3.17** was isolated and characterized by NMR spectroscopy. Irradiation of cyclopropenone **3.1** in MeOH and/or MeOH-*d*₄ produced products of insertion of methanol, which were observed by mass spectroscopy.

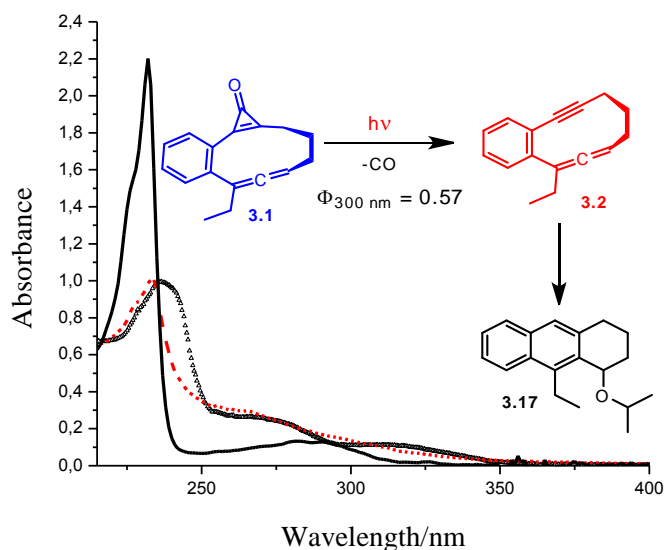


Figure 3.1 UV-spectra of cyclopropanone **3.1** (shown in triangles); enyne-allene **3.2** (dash line); naphthalene derivative **3.17** (solid line).

The accurate rate measurements of cycloaromatization of the enyne-allene **3.2** were conducted by UV spectroscopy following the growth of the characteristic 232 nm band of tetrahydroanthracenes **3.3** and **3.17**.

As can be seen from Figure 3.2, the cyclization reaction follows first order kinetics. The rate of the cycloaromatization of **3.2** at 25 ± 0.1 °C is $k = (2.735 \pm 0.046) \times 10^{-3} \text{ s}^{-1}$ in 2-propanol and $k = (3.41 \pm 1.01) \times 10^{-3} \text{ s}^{-1}$ in THF containing 0.05 M 1,4-cyclohexadiene (1,4-CHD is a good hydrogen donor). The similar rate constants for both reactions and absence of the isotopic effect indicate that the radical and polar pathways share a common rate-limiting step. Also, absence of the kinetic isotopic effect tells us that there is no involvement of hydrogen abstraction in the rate-limiting step.

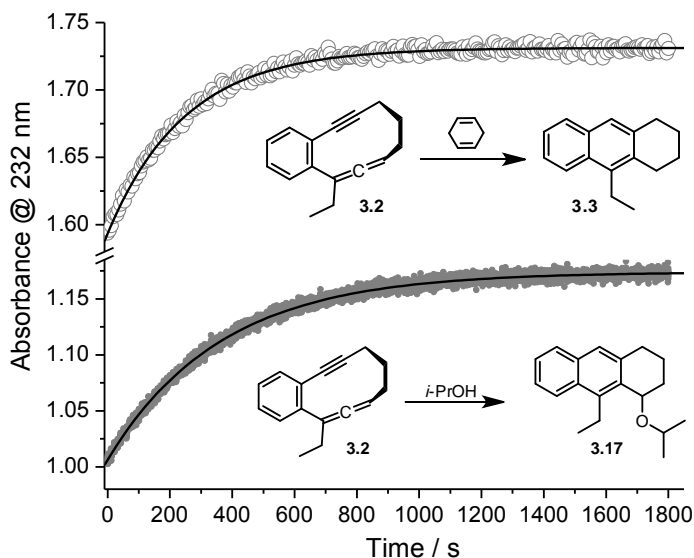


Figure 3.2 Cycloaromatization of the photo-generated enyne-allene **3.2** in THF-1,4-cyclohexa-diene (open circles) and in 2-propanol (filled circles) at 25 °C. Solid lines represent fitting of the experimental data to a single exponential equation.

The cyclization rates of the enyne-allene **3.2** were measured in 2-propanol solutions in the temperature range from 5 to 40 °C with 0.1 °C accuracy. The data so obtained are displayed as the temperature rate profile in Figure 3.3.

The temperature dependence of the cyclization rate of **3.2** follows general trend (Figure 3.2). This observation suggests that the energy barrier (ΔG^\ddagger) for the cyclization reaction grows with the temperature. Least-squares fitting of the obtained data to the Eyring equation provides the following activation parameters: $\Delta H^\ddagger = 16.73 \pm 0.51 \text{ kcal M}^{-1}$ and $\Delta S^\ddagger = -14.6 \pm 1.5 \text{ cal M}^{-1} \text{ K}^{-1}$. In comparison, highly strained 4,5-benzocyclonona-2,6-diynol has $\Delta H^\ddagger = 13.63 \pm 0.22 \text{ kcal M}^{-1}$ and $\Delta S^\ddagger = -30.66 \pm 0.61 \text{ cal M}^{-1} \text{ K}^{-1}$.^{1b}

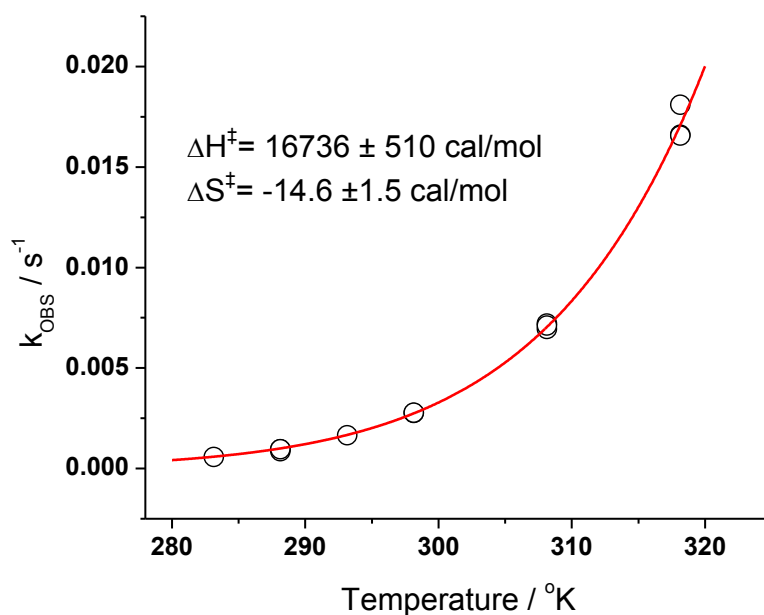
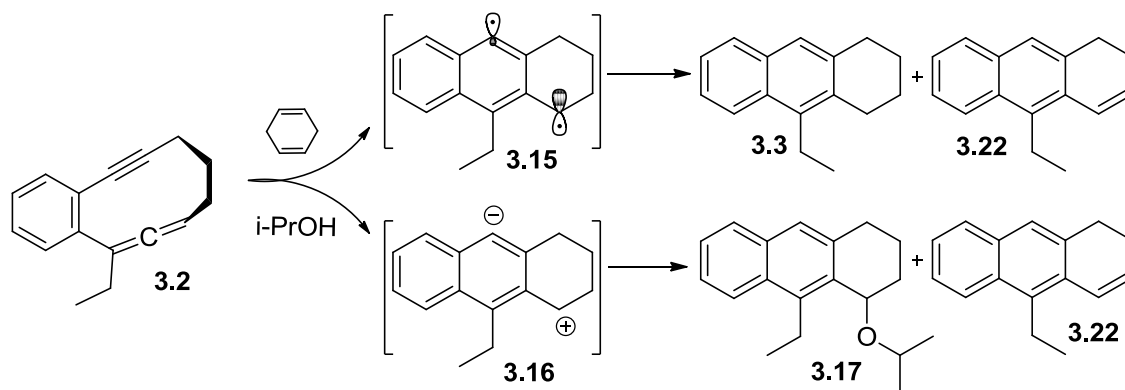


Figure 3.3 Temperature rate profile for the Bergman cyclization of the enyne-allene **3.2** generated in photolysis of **3.1** in 2-propanol. The line shown was drawn using parameters obtained by least-squares fitting of Eyring equation.

Scheme 3.8 Dual reactivity of enyne-allene **3.2** in different media.



The formation of ether **3.17** is inconsistent with the conventional diradical mechanism of the Myers–Saito cyclization. In 2-propanol, the σ,π -diradical **3.15** is expected to abstract hydrogen from the secondary carbon of the alcohol, since this C–H bond is much weaker than

the O–H bond. The O–H insertion observed in 2-propanol suggests a polar, rather than a radical, pathway of the cycloaromatization in that medium (**3.16**, Scheme 3.8).

Similar “dual reactivity” has been reported for acyclic enyne-allenes and was initially explained by the “polar” nature of the $\alpha,3$ -didehydrotoluene, which can be described as a resonance between a zwitterion and a diradical.²¹ This hypothesis was later rejected on the basis of quantum mechanical calculations since frontier orbitals in these two electronic forms of $\alpha,3$ -didehydrotoluene are strictly orthogonal and cannot be mixed.²² Carpenter *et al.* suggested the formation of O–H insertion product happens *via* a non-adiabatic pathway.²³ The author describes this reaction in terms of two crossing diabatic surfaces. Thus, the zwitterionic state (**3.16**) can be considered as an excited state of diradical **3.15**.

3.4 DNA CLEAVAGE EXPERIMENT

Evaluation of the nuclease activity of the photogenerated enyne-allene **3.2** was carried out using supercoiled plasmid DNA cleavage assay. Three forms of this DNA: native (RF I), circular relaxed (RF II, produced by a single-strand cleavage), and linear (RF III, formed by scission of both strands in close proximity) are readily separated by agarose gel electrophoresis (Figure 3.4).

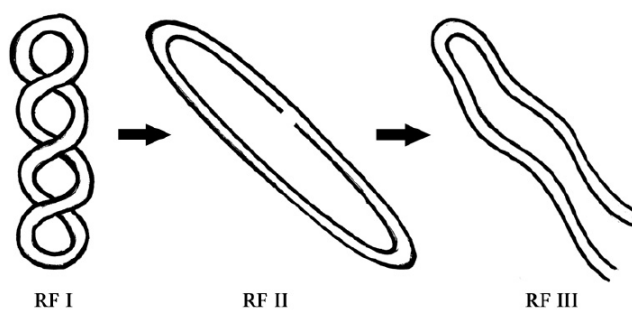
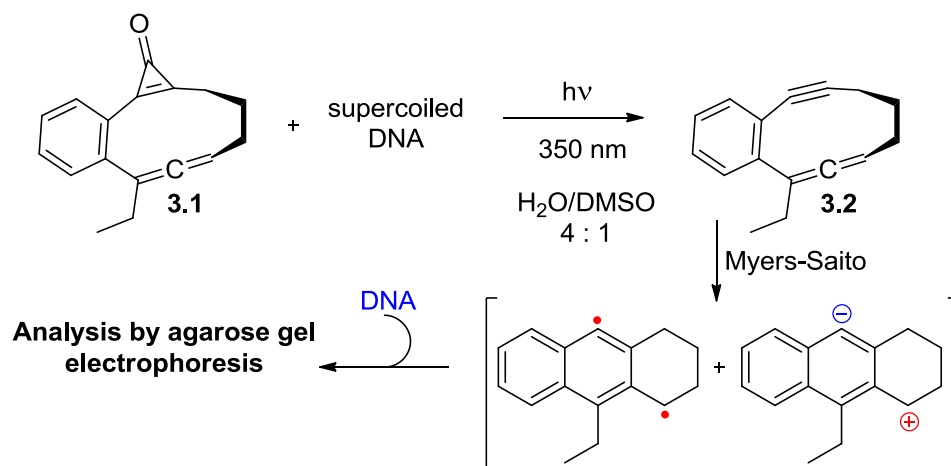


Figure 3.4 Relaxation and linearization of the ϕ X174 supercoiled DNA.

Mobility of large DNA molecules, in general, depends on two factors: the molecular weight and secondary structure. When supercoiled DNA molecules are cleaved, all products have the same molecular weight, thus, their separation is based only on topology. In some cases, cleavage of the DNA backbone at random sites produces a multitude of products, which appear as a single band on the gel due to equal molecular weights and very similar topologies. Conveniently, agarose gel electrophoresis allows us to easily discriminate events of simultaneous double-stranded scission from multiple single strand cleavage events.

Scheme 3.9 Photolysis of cyclopropenone **3.1** and supercoiled DNA.



To produce reactive enyne-allene **3.2** in the presence of DNA, a solution of cyclopropenone **3.1** in water–DMSO (4 : 1) mixtures was added to a solution of ϕX174 supercoiled circular DNA in TE buffer and irradiated for 10 min using 350 nm lamps (Scheme 3.9). The concentration of DNA was kept at $10 \text{ ng } \mu\text{L}^{-1}$ in all experiments, while the initial concentration of cyclopropenone **3.1** varied from 0 to 5 mM. The duration of irradiation was sufficient to achieve at least 95% conversion of **3.1**, as was determined by HPLC. The irradiated and control solutions were incubated for 16 h at 25°C in the dark and analyzed by gel

electrophoresis. At concentrations above 0.1 mM, photo-generated enyne-allene **3.2** was found to induce *ca.* 15% single-strand cleavage of ϕ X174 DNA (RF II), but no observable double-strand cleavage (RF III, Figure 3.5). A further increase in the concentration of precursor **3.1** results in the reduced photo-nuclease efficiency due to aggregation of the substrate. Incubation of the DNA with cyclopropenone precursor **3.1** in the dark does not induce any detectable DNA cleavage.

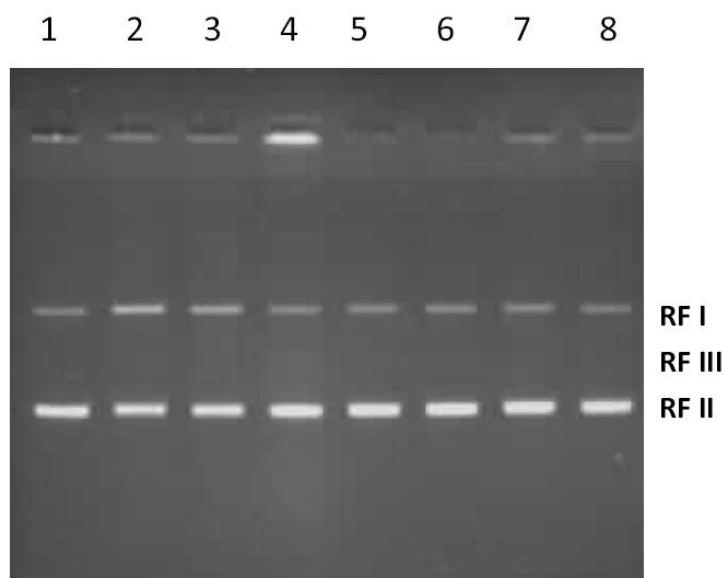


Figure 3.5 Light-induced cleavage of ϕ X174 plasmid DNA by the photogenerated enyne-allene **3.2**. Lanes 1-4: Cyclopropenone **3.1** (0.1, 0.5, 1, and 5 mM) is irradiated in the presence of DNA; lane 5: DNA irradiated without **3.1**; lanes 6-8: DNA incubated in the dark with cyclopropenone **3.1** (0.1, 0.5, and 1 mM).

3.5 CONCLUSIONS

Thus far, our enyne-allene is the most reactive compound among ten-membered ring enediynes. Photoswitchable enyne-allene **3.1** undergoes efficient cyclization reaction producing $\alpha,3$ -didehydrotoluene after irradiation with 300 nm light. It is a first example where cyclic enyne-allene generated photochemically from a thermally stable precursor. In this approach, a

triple bond is masked as a cyclopropanone. Cyclopropanone-containing enyne-allene precursors are unable to undergo cyclization because the enyne-allene fragment is incomplete. On the other hand, photolysis of cyclopropanone **3.1** results in the efficient decarbonylation and the regeneration of a triple bond completing enyne-allene π -system.

The reactivity of benzannulated ten-membered ring enyne-allene **3.2** depends on the reaction media. In solvents of low polarity products of the cycloaromatization reaction are consistent with the intermediate formation of a diradical species. In 2-propanol, the reactions apparently proceed *via* a polar mechanism.

The analysis of the reactivity of acyclic enyne-allenes is complicated by the presence of conformational equilibrium. The position of the equilibrium, which should depend on the solvent polarity, controls the rate and potentially the mechanism of the cycloaromatization reaction. The advantage of cyclic system is that enyne-allene **3.2** is locked in the most reactive conformation and allows us to focus the investigation of enyne-allene reactivity on electronic factors.

The relatively low nuclease efficiency of **3.2** can be explained either by predominant polar cycloaromatization pathway or by the low affinity of **3.1** to a dDNA molecule. In order to address the latter problem, we are currently working on the design and synthesis of cyclopropanone **3.1** analogs containing a dDNA minor-groove binding moiety.

3.6 EXPERIMENTAL SECTION

MATERIALS AND METHODS

All moisture- and oxygen-sensitive reactions were carried out in oven-dried glassware under argon atmosphere. All solvents were purified and dried by distillation immediately before use. Tetrahydrofuran, diethyl ether, hexanes, benzene and toluene were distilled from sodium metal; dichloromethane was distilled from phosphorus pentoxide; ethyl acetate and acetone were distilled from anhydrous calcium chloride. Ultra-dry inhibitor-free THF from Aldrich was used for palladium-catalysed cross coupling reactions. All other materials were purchased from Aldrich, Alfa Aesar, Acros Organics, Strem Chemicals or GFS Chemicals and used without purification unless otherwise stated. Dess-Martin periodinane was prepared according to the original literature procedure.¹⁶ Chromatographical purification of reaction products was performed using Sorbtech standard grade flash chromatography silica gel (40-63µm particle size, 60Å porosity) or Sorbtech premium grade flash chromatography silica gel (40-75µm particle size, 60Å porosity). TLC analyses were performed using polyester-backed silica gel TLC plates from Whatman, Aldrich or Sorbent Technologies.

INSTRUMENTS

GC/MS analyses were performed using Shimadzu QP-2010S GC – mass spectrometer equipped with high-precision quadrupole with pre-rods and mass number range 1.5m/z to 900 m/z. Nuclear magnetic resonance (NMR) spectra were recorded in deuteriochloroform using Varian Mercury Plus 400 MHz or Varian Unity Inova 500 MHz NMR spectrometers with tetramethylsilane (TMS) as an internal standard. ¹H-NMR chemical shifts (δ) are reported in ppm versus TMS reference, ¹³C-NMR chemical shifts (δ) are reported in ppm versus residual

solvent peak reference. UV-visible spectra were recorded on Varian Cary 50 UV-visible spectrometer or Varian Cary 300 Bio UV-Vis spectrometer. IR spectra were recorded using Shimadzu IR Prestige FT-IR spectrometer. Melting points were determined using Fisher-Johns melting point apparatus and are reported uncorrected.

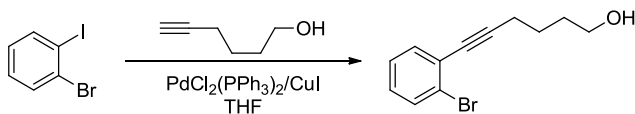
KINETICS

Rate measurements were performed using Carry-300 Bio UV-Vis spectrometer equipped with a thermostatable cell holder. The temperature was controlled with 0.1 °C accuracy. Reactions were monitored by following the growth of the characteristic 232 nm absorbance of 9-ethyl-1-isopropoxy-1,2,3,4-tetrahydroanthracene (**3.17**, in 2-propanol) or 9-ethyl-1,2,3,4-tetrahydroanthracene (**3.3**, in THF with 0.05 M of 1,4-cyclohexadiene). Observed first order rate constants were calculated by least-squares fitting of a single exponential function.

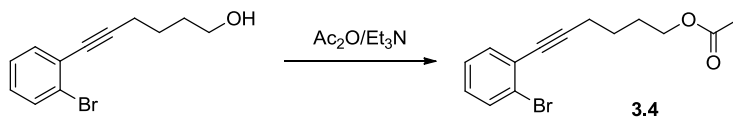
3.7 DNA CLEAVAGE PROCEDURE

In a typical experiment aqueous solutions of cyclopropenone **1** (10 µL) were added to a solution of plasmid DNA (10 ng/µL) in TE buffer (pH 8.0, 27 µL) and irradiated in RMR-600 Rayonet photochemical reactor equipped with 6x4W 350 nm lamps for 10 min. After irradiation solution was incubated in the dark for 16 h at 25 °C. Control samples were incubated with cyclopropenone solution in the dark. Incubated samples and the standard marker solution were mixed with a glycerol based loading buffer (7 µL) containing xylene cyanol loading dye and loaded onto a 1% agarose gel containing 0.5 µg/mL of ethidium bromide. Gel was developed at 80 V (400 mA) for 2 h and photographed on the UV transilluminator. The relative intensities of fluorescent bands on the developed gel were calculated using Alpha Ease FC software package by Alpha Innotech, Inc.

3.8 SYNTHETIC PROCEDURES

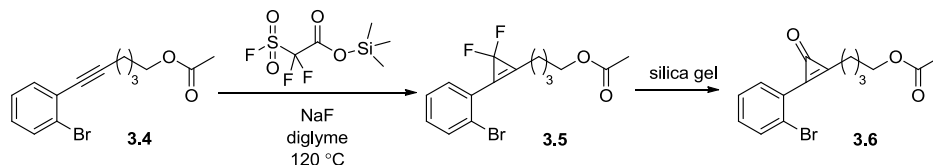


6-(2-Bromophenyl)hex-5-yn-1-ol: $\text{PdCl}_2(\text{PPh}_3)_2$ (0.945 g, 2.149 mmol), CuI (0.819 g, 4.30 mmol), 5-hexyn-1-ol (4.22 g, 43.0 mmol), and PPh_3 (0.564 g, 2.149 mmol) were added to a degassed solution of 2-bromoiodobenzene (12.77 g, 45.1 mmol) in THF (300 ml) and triethylamine (40 ml, 277 mmol) under Ar. The reaction vessel was sealed and heated at 55 °C for 2 days. The mixture was then filtered through small layer of silica gel, solvents were removed in vacuum, and residue purified by chromatography (EtOAc – hexanes 1: 3, R_f = 0.15) to give 10.2 g (40.3 mmol, 92%) of alcohol as yellow oil. ^1H : 1.72-1.8 (m, 4H), 2.52 (t, 2H, J = 6.8 Hz), 3.72 (t, 2H, J = 6 Hz), 7.1-7.3 (m, 2H), 7.4 (d, 1H, J = 7.6 Hz), 7.55 (d, 1H, J = 8 Hz); ^{13}C : 19.58, 25.09, 32.11, 62.66, 80.00, 95.26, 125.70, 126.22, 127.11, 128.93, 132.51, 133.52; FW calc. for $\text{C}_{12}\text{H}_{13}\text{BrO}$: 252.0150, EI-HRMS found: 252.0150.



6-(2-bromophenyl)hex-5-ynyl acetate (3.4). Acetic anhydride (3.63 g, 35.6 mmol) and pyridine (2.81 g, 35.6 mmol) were added to a solution of 6-(2-Bromophenyl)hex-5-yn-1-ol (9 g, 35.6 mmol) in CH_2Cl_2 (20 ml). The reaction mixture was stirred for 3 hours at r.t., solvent was removed in vacuum, and residue was purified by chromatography (EtOAc – Hexanes 1: 9, R_f = 0.1) affording 9.45 g (32.1 mmol, 90%) of acetate **3.4** as yellow oil. ^1H : 1.65-1.75 (m, 2H), 1.8-1.9 (m, 2H), 2.05 (s, 3H), 2.52 (t, 2H, J = 7.2 Hz), 4.13 (t, 2H, J = 6 Hz), 7.05-7.12 (m, 1H), 7.2-7.28 (m, 1H), 7.41 (d, 1H, J = 7.6), 7.55 (d, 1H, J = 8); ^{13}C : 19.46, 21.23, 25.26, 28.00, 64.25,

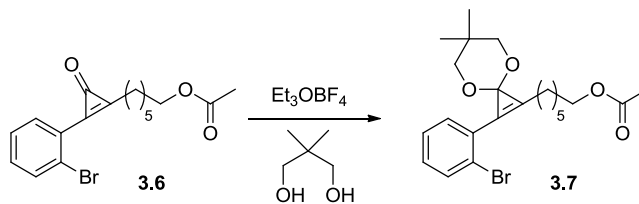
80.10, 94.80, 125.68, 126.06, 127.14, 129.02, 132.51, 133.51, 171.42; FW calc. for C₁₄H₁₅BrO₂: 294.0255, EI-HRMS found: 294.0258.



3-(4-Acetoxybutyl)-2-(2-bromophenyl)cyclopropenone (3.6). A solution of trimethylsilyl fluoro-sulfonyl difluoroacetate (TFDA, 6.3 ml, 32.0 mmol) was added via syringe pump over 15 minutes under argon flow to a pre-heated (120 °C) solution of acetylene **3.4** (3.14 g, 10.64 mmol) and sodium fluoride (0.050 g, 1.191 mmol) in diglyme (6 mL). The reaction mixture was kept at this temperature for 20 min, cooled, and transferred into silica gel column. Flash chromatography with EtOAc – hexanes (1:10, R_f = 0.3) provided 3.3 g, (9.57 mmol, 90%) of 3-(4-acetoxybutyl)-2-(2-bromophenyl)-1,1-difluorocyclopropene (**3.5**) as yellow oil. ¹H: 1.75-1.85 (m, 4H), 2.05 (s, 3H), 2.8-2.88 (m, 2H), 4.1-4.18 (m, 2H), 7.3 (t, 1H, J = 8Hz), 7.39 (t, 1H, J = 8Hz), 7.58 (d, 1H, J = 7.2Hz), 7.66 (d, 1H, J = 7.6Hz); ¹³C: 20.81, 23.69, 28.1, 58.82, 99.9, 102.61, 105.3, 123.46, 124.78, 125.96, 127.66, 128.63, 128.73, 128.84, 131.98, 132.45, 133.38, 170.89, 170.92.

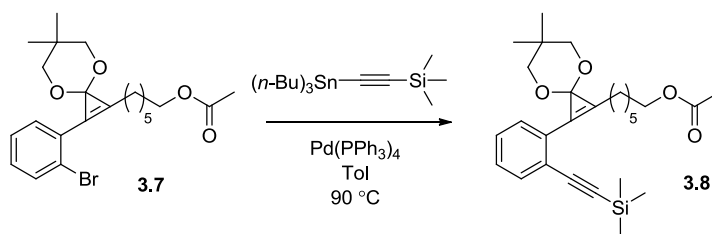
Crude difluorocyclopropene (**3.5**) was transferred into wet silica gel column, washed with 200 mL of an AcOH – hexanes mixture (1:99) and left overnight in the column. Elution with gradient EtOAc – hexanes mixture (1:9 → 1:1) produced, after solvents removal, 2.92 g (9.04 mmol, 85%, 2 steps) of cyclopropenone **3.6** as a dense yellow oil. ¹H: 1.8-1.9 (m, 4H), 2.04 (s, 3H), 2.96 (t, 2H, J = 7.2 Hz), 4.11 (t, 2H, J = 6.4 Hz), 7.36-7.48 (m, 2H), 7.15 (dd, 1H, J = 8 Hz, 1.2 Hz), 7.8 (dd, 1H, J = 7.6 Hz, 1.6); ¹³C: 20.97, 23.26, 27.51, 28.27, 63.65, 123.95, 125.61, 127.9,

133.65, 133.68, 134.07, 153.38, 156.87, 157.21, 171.13; FW calc. for $C_{15}H_{16}BrO_3$ (M+H): 323.0283, ESI-HRMS found: 323.0276.



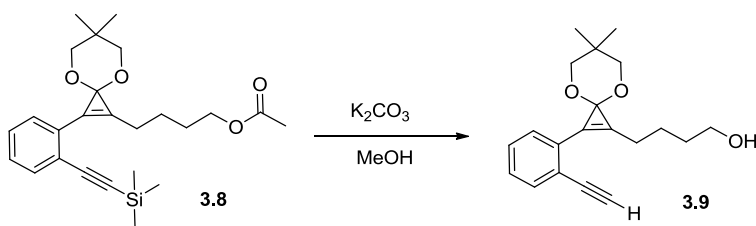
4-[2-(2-bromophenyl)-6,6-dimethyl-4,8-dioxaspiro[2.5]oct-1-en-1-yl]butyl acetate (3.7).

Et_3OBF_4 (3.59 g, 27.3 mmol) was added to solution of cyclopropanone **3.6** (5.87 g, 18.17 mmol) in CH_2Cl_2 (30 mL) under vigorous stirring at r.t. After 30 min, a solution of neopentylglycol (3.78 g, 36.3 mmol) and triethylamine (3.68 g, 36.3 mmol) in CH_2Cl_2 (10 mL) was added dropwise. In 1 hour the reaction mixture was washed with saturated solution of $NaHCO_3$ (2x100 mL), dried with Na_2SO_4 , and solvents removed in vacuum. The crude product was purified by chromatography (ether – hexanes 1:10, 1% of Et_3N , R_f = 0.1) to give 5.95 g (14.53 mmol, 80%) of acetal **3.7** as a yellow solid. M.p. 52 °C; 1H : 0.96 (s, 3H), 1.22 (s, 3H), 1.65-1.75 (m, 4H), 2.04 (s, 3H), 2.91 (t, 2H, J = 7.2), 3.65-3.8 (m, 4H), 4.12 (t, 2H, J = 6 Hz), 7.16-7.22 (m, 1H), 7.32-7.37 (m, 1H), 7.6-7.64 (m, 2H); ^{13}C : 21.20, 22.11, 22.35, 22.70, 25.09, 25.99, 28.57, 30.54, 64.29, 78.27, 83.39, 123.03, 124.42, 127.61, 128.46, 130.57, 132.24, 133.44, 171.39; FW calc. for $C_{20}H_{25}BrO_4+H$: 409.1014, ESI-HRMS found: 409.1012.



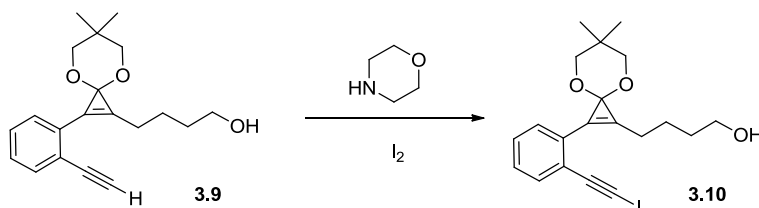
4-(6,6-dimethyl-2-((trimethylsilyl)ethynyl)phenyl)-4,8-dioxaspiro[2.5]oct-1-en-1-yl butyl

acetate (3.8). Pd(PPh₃)₄ (0.555 g, 0.480 mmol) was added to a degassed solution of bromide **3.7** (6.55 g, 16.00 mmol) in toluene (100 mL) and heated to 90 °C under vigorous stirring for 10 min. A solution of trimethyl((tributylstannyl)ethynyl)silane (7.75 g, 20.00 mmol) in toluene (5 mL) was added to the reaction mixture and heated at 90 °C in a sealed vessel for 3 h. Solvent was removed in vacuum and residue was purified by chromatography (ether – hexanes 1:10, 1% of Et₃N) to yield 4.89 g of **3.8** (11.46 mmol, 71.6 %), as yellowish crystals. M.p. 64-65 °C; ¹H: 0.25 (s, 9H), 1.02 (s, 3H), 1.16 (s, 3H), 1.75-1.85 (m, 4H), 2.04 (s, 3H), 2.91 (t, 2H, *J* = 6.8 Hz), 3.73 (m, 4H), 4.11 (t, 2H, *J* = 6 Hz), 7.24-7.37 (m, 2H), 7.54-7.58 (m, 2H); ¹³C: 0.19, 21.18, 22.50, 22.67, 25.00, 26.32, 28.59, 30.54, 64.45, 78.35, 83.90, 98.53, 105.37, 122.96, 124.58, 128.89, 129.73, 130.69, 130.85, 134.49, 171.36; FW calc. for C₂₅H₃₄O₄Si+H: 427.2305, ESI-HRMS found: 427.2299.



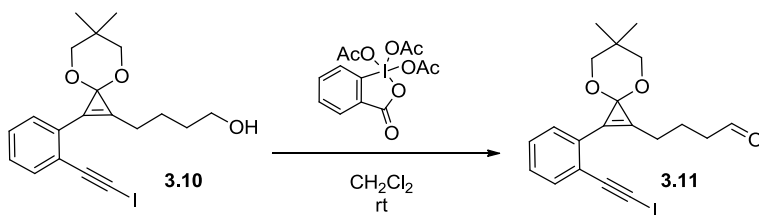
4-(2-(2-ethynylphenyl)-6,6-dimethyl-4,8-dioxaspiro[2.5]oct-1-en-1-yl)butan-1-ol (3.9). Potassium carbonate (0.5 g, 3.62 mmol, 0.3 eq.) was added to a solution of acetate **3.8** (4.89 g, 11.46 mmol) in MeOH (50 ml), the mixture was stirred for 2 h at r.t., diluted with 40 mL of water, and extracted with ether (2x75 mL). Combined organic layers were evaporated in vacuum and the resulting residue was purified by chromatography (ether – hexanes 1:5, 1% of Et₃N) to give 3.01 g (9.6 mmol, 84%) of alcohol **3.9** as yellow oil. ¹H: 1.02 (s, 3H), 1.15 (s, 3H), 1.65-1.74 (m, 2H), 1.75-1.85 (m, 2H), 1.85-1.9 (broad OH), 2.8-2.9 (m, 2H), 3.36 (s, 1H), 3.68-3.8 (m, 6H), 7.25-7.33 (m, 1H), 7.36-7.42 (m, 1H), 7.55-7.61 (m, 1H); ¹³C: 22.49, 22.64, 24.51, 26.31, 30.59, 31.14, 32.65, 62.45, 78.36, 81.57, 83.63, 83.86, 121.97, 124.30, 128.96, 129.18, 130.60, 130.66,

131.64, 134.00; FW calc. for $C_{20}H_{25}O_3+H$: 313.1804, ESI-HRMS found: 313.1801.



4-(2-(2-(iodoethynyl)phenyl)-6,6-dimethyl-4,8-dioxaspiro[2.5]oct-1-en-1-yl)butan-1-ol (3.10**)**

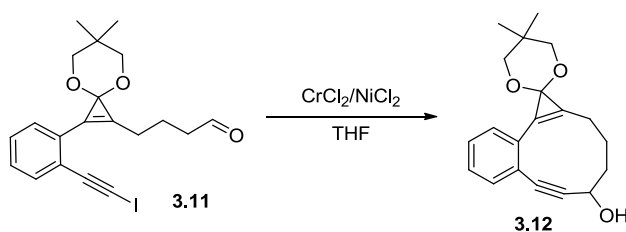
A solution of morpholine (0.742 mL, 8.58 mmol) and iodine (1.089 g, 4.29 mmol) in benzene (20 mL) was vigorously stirred at 45 °C for 15 min to form orange suspension. A solution of acetylene **3.9** (0.670 g, 2.145 mmol) in benzene (3 mL) was added to the reaction mixture. In 30 min the reaction mixture was diluted with 40 mL of ether, filtered, and solvents were removed in vacuum. The residue was purified by chromatography (ether – hexanes 1:4, 1% Et_3N , R_f = 0.1) to give 0.675 g (1.540 mmol, 72 %) of **3.10** as yellow oil. 1H : 1.04 (s, 3H), 1.15 (s, 3H), 1.7-1.9 (m, 5H), 2.85 (t, 2H, J = 6.8 Hz), 3.67-3.79 (m, 6H), 7.26-7.30 (m, 1H), 7.34-7.39 (m, 1H), 7.5-7.58 (m, 2H); ^{13}C : 22.51, 22.7, 24.57, 26.25, 32.75, 62.5, 78.39, 83.83, 93.67, 123.2, 124.08, 128.86, 129.17, 130.29, 130.56, 131.84, 134.41; FW calc. for $C_{20}H_{23}IO_3+H$: 439.0770, ESI-HRMS found: 439.0768.



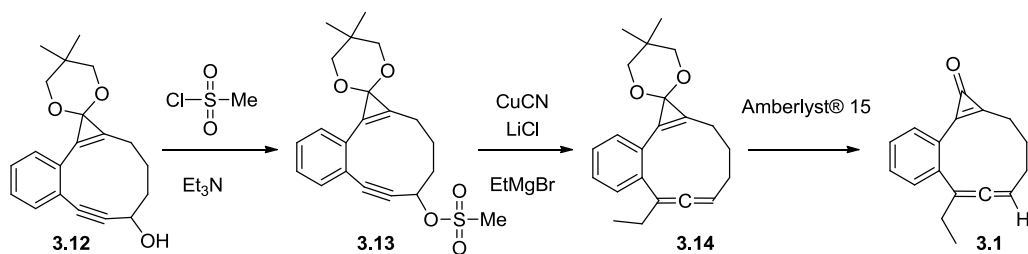
4-(2-(2-(iodoethynyl)phenyl)-6,6-dimethyl-4,8-dioxaspiro[2.5]oct-1-en-1-yl)butanal (3.11**)**

Dess-Martin periodinane (0.755 g, 1.780 mmol) was added to a solution of alcohol **3.10** (0.65 g, 1.483 mmol) in CH_2Cl_2 (50 mL) under vigorous stirring at r.t. In 2 h the reaction mixture was diluted with ether (40 mL), stirred for 15 min, and solvents removed in vacuum.

Chromatographic purification of the residue (ether – hexanes 1:20, 1% of Et₃N) gave 0.469 g (1.075 mmol, 72.5 %) of aldehyde **3.11** as yellow oil. ¹H: 1.03 (s, 3H), 1.16 (s, 3H), 2.03-2.09 (m, 2H), 2.65 (t, 2H, *J* = 7.2 Hz), 2.88 (t, 2H, *J* = 7.2 Hz), 3.68-3.78 (m, 4H), 7.26-7.32 (m, 1H), 7.35-7.4 (m, 1H), 7.5-7.58 (m, 2H), 9.83 (s, 1H); ¹³C: 20.98, 22.51, 22.71, 25.78, 30.57, 43.6, 46.41, 78.39, 83.64, 93.71, 123.23, 124.96, 129.01, 129.24, 130.16, 130.63, 130.95, 134.46, 202.22; FW calc. for C₂₀H₂₃IO₃+H: 437.0614, ESI-HRMS found: 437.0615.



6,7-didehydro-3,4,5-trihydro-5',5'-dimethyl-spiro[benzo[a]cyclopropa[c]cyclodecene-1(2*H*),2'-[1,3]dioxan]-5-ol (3.12). A solution of aldehyde **3.11** (0.215 g, 0.493 mmol) in THF (20 mL) was added dropwise over 5 min to a degassed solution CrCl₂ (0.2 g, 1.627 mmol) and NiCl₂ (6.39 mg, 0.049 mmol) in anhydrous THF (250 mL) at r.t. The reaction mixture was stirred for 2 h, diluted with hexanes (200 mL), and filtered through small layer of silica gel to give the 145 mg (0.467 mmol, 95%) of **3.12** as yellow oil. ¹H: 1.06 (s, 3H), 1.12 (s, 3H), 1.8-1.9 (m, 1H), 2.0-2.2 (m, 1H), 2.32 (s, OH), 2.53 (dd, 2H, *J* = 7.2 Hz), 2.82-2.92 (m, 1H), 2.98-3.06 (m, 1H), 3.68-3.8 (m, 4H), 4.58 (broad signal, 1H), 7.25-7.31 (m, 1H), 7.33-7.39 (m, 1H), 7.4 (d, 1H, *J* = 7.6 Hz), 7.5 (d, 1H, *J* = 7.6 Hz); ¹³C: 11.44, 21.71, 22.34, 22.38, 25.01, 30.46, 36.78, 46.15, 62.26, 78.33, 78.39, 85.16, 86.08, 97.21, 122.3, 126.56, 128.53, 128.58, 129.06, 130.15, 131.62, 132.00; FW calc. for C₂₀H₂₂O₃+H: 311.1646, ESI-HRMS found: 311.1647.



7-Ethyl-6-dehydro-2,3,4-trihydro-1H-benzo[a]cyclo-propa[c]cyclodecen-1-one (3.1).

Methanesulfonyl chloride (0.102 mL, 1.321 mmol) was added to a solution of alcohol **12** (0.41 g, 1.321 mmol) and triethylamine (1.91 mL, 1.321 mmol) in CH₂Cl₂ (4 mL) at 0 °C. The reaction mixture was stirred for 1 h and quenched with biphosphate buffer (1 mL, pH = 8). Organic layer was washed with biphosphate buffer (2x2 mL, pH = 8), separated, and dried over sodium sulfate. Solvent was evaporated to give 0.462 g (90%, 1.189 mmol) of crude mesylate **3.13** as yellowish oil.

A solution of EtMgBr (2.379 mL, 1M in THF) was added to an ice-cold suspension of CuCN (0.213 g, 2.379 mmol) and LiCl (0.202 g, 4.76 mmol) in dry THF (5 mL). Reaction mixture was stirred for 25 min, cooled down to -78 °C, and a solution of crude mesylate **3.13** (0.37 g, 1.650 mmol) in dry THF (2 mL) was added dropwise. After 2 hours at -78 °C, the reaction was quenched by addition of biphosphate buffer (3 mL, pH = 8). The reaction mixture was extracted with ether (3x15 mL), washed with brine (1x20 mL), dried over sodium sulfate, and concentrated under reduced pressure to give 0.32 g (0.992 mmol, 83%) of crude acetal **3.14**.

Amberlyst® 15 (5 mg) was added to a solution of crude acetal **3.14** (0.115 g, 0.357 mmol) in aqueous acetone (ca. 5% H₂O, 5 mL), stirred for 2 h at r.t., and sodium sulfate (100 mg) was added. Solids were removed by filtration, solvents removed in vacuum, and the residue purified by chromatography (EtOAc – hexanes 1:1 → EtOAc) to give 63 mg (0.266 mmol, 75%) of cyclopropenone **3.1** as yellowish oil. ¹H: 1.16 (t, 3H, *J* = 7.6 Hz), 1.85-1.95 (m, 1H), 2.1-2.25

(m, 2H), 2.25-2.37 (m, 1H), 2.4-2.45 (m, 1H), 2.47-2.65 (m, 1H), 2.81-2.85 (m, 1H), 3.0-3.1 (m, H), 5.44-5.48 (m, 1H allenic hydrogen), 7.35 (t, 1H $J = 7.2$ Hz), 7.45-7.52 (m, 2H), 7.87 (d, 1H, $J = 7.2$ Hz); ^{13}C : 12.49, 20.88, 25.09, 26.46, 26.66, 93.73, 106.5, 122.55, 126.69, 127.07, 132.08, 135.03, 139.04, 153.67, 154.91, 160.27, 203.57; FTIR (cm^{-1} in CCl_4) 2950 [aromatic], 1955 [$\text{C}=\text{C}=\text{C}$], 1840 ($\text{C}=\text{O}$), 1720, 1620; FW calc. for $\text{C}_{17}\text{H}_{16}\text{O}$: 236.1201, EI-HRMS found: 236.1208.

Preparative photolysis of cyclopropenone 3.1 in 2-propanol. A degassed solution of cyclopropenone **3.1** (20 mg, 0.085 mmol) in *i*-PrOH (150 mL) was placed in a quartz vessel and irradiated for 15 min in mini-Rayonet® photoreactor equipped with eight 300 nm x 4W lamps. The reaction mixture was left in the dark for 5 h at r.t., then solvents was removed in vacuum, and the residue separated by PTLC (1 mm silica gel on glass plate, 5% of EtOAc in hexanes) to afford 4 mg of 9-ethyl-1-isopropoxy-1,2,3,4-tetrahydroanthracene (**3.17**) (0.015 mmol, 17.3%) and 0.5 mg of 10-ethyl-1,2-dihydroanthracene (2.77 μmol , 3.3%).

9-ethyl-1-isopropoxy-1,2,3,4-tetrahydroanthracene (3.17). ^1H : 1.24 (d, $J = 6.4$ Hz, 3H), 1.28 (d, 3H, $J = 6$ Hz), 1.34 (t, $J = 7.6$ Hz, 3H), 1.55-1.6 (m, 1H), 1.68-1.77 (m, 1H), 2.05-2.18 (m, 1H), 2.4-2.48 (m, 1H), 2.86-2.96 (m, 1H), 3.1-3.18 (m, 1H), 3.2-3.32 (m, 2H), 3.9 (tt, 1H $J_1 = 6$ Hz, $J_2 = 12\text{Hz}$), 5-5.04 (m, 1H), 7.36-7.45 (m, 2H), 7.47 (s, 1H), 7.68-7.74 (m, 1H), 8.02-8.08 (m, 1H); ^{13}C : 16.14, 17.00, 20.85, 21.96, 24.23, 27.25, 30.25, 67.86, 69.09, 124.49, 124.96, 125.53, 126.18, 128.05, 130.84, 133.00, 133.78, 136.11, 139.89; FW calc. for $\text{C}_{19}\text{H}_{24}\text{O}$: 268.1827, EI-HRMS found: 268.1833

9-ethyl-1,2,3,4-tetrahydroanthracene (3.3): Preparative photolysis of cyclopropenone **3.1** in the presence of 1,4-cyclohexadiene was carried out. A degassed solution of cyclopropenone **3.1**

(10 mg, 0.042 mmol) in 1M solution of 1,4-cyclohexadiene in toluene (50 mL) was placed in a quartz vessel and irradiated for 3 min in mini-Rayonet® photoreactor equipped with 8 300 nm x 4W lamps. The reaction mixture was left in the dark overnight at r.t., the solvent was removed in vacuum, and residue separated by PTLC (1 mm silica gel on glass plate, 5% of EtOAc in hexanes) to give 2 mg (23%) of 9-ethyl-1,2,3,4-tetrahydroanthracene (**3.3**) containing minor impurities (<10%) of 10-ethyl-1,2-dihydroanthracene. The latter was identified by GC-MS and HRMS analysis (FW calc. for C₁₆H₁₆: 208.1252, EI-HRMS found: 208.1251). ¹H: 1.33 (t, 3H, *J* = 7.5 Hz), 1.8-1.87 (m, 2H), 1.88-1.95 (m, 2H), 2.9-3.0 (m, 4H), 3.08 (q, 2H, *J* = 7.6), 7.36-7.42 (m, 2H), 7.46 (s, 1H), 7.68-7.72 (m, 1H), 8.02-8.07 (m, 1H); FW calc. for C₁₆H₁₈: 210.1409, EI-HRMS found: 210.1406.

3.9 REFERENCES

- (1) (a) Polukhtine, A.; Karpov, G.; Popik, V. V. Towards photoswitchable enediyne antibiotics: single and two-photon triggering of Bergman cyclization. *Curr. Top. Med. Chem.* **2008**, *8*, 460-469; (b) Pandithavidana, D. R.; Poloukhtine, A.; Popik, V. V. Photochemical Generation and Reversible Cycloaromatization of a Nine-Membered Ring Cyclic Enediyne. *J. Am. Chem. Soc.* **2009**, *131*, 351-356; (c) Karpov, G.; Kuzmin, A.; Popik, V. V. Enhancement of the reactivity of photochemically generated enediynes via keto-enol tautomerization. *J. Am. Chem. Soc.* **2008**, *130*, 11771-11777.
- (2) Wang, K. K. Cascade Radical Cyclizations via Biradicals Generated from Eneidyne, Enyne-Allenenes, and Enyne-Ketenenes. *Chem. Rev.* **1996**, *96*, 207-222.
- (3) Goldberg, I. H. Mechanism of neocarzinostatin action: role of DNA microstructure in determination of chemistry of bistranded oxidative damage. *Acc. Chem. Res.* **1991**, *24*, 191-198.
- (4) (a) Bekele, T.; Brunette, S. R.; Lipton, M. A. Synthesis and cycloaromatization of a cyclic enyne-allene prodrug. *J. Org. Chem.* **2003**, *68*, 8471-8479; (b) Toshima, K.; Ohta, K.; Kano, T.; Nakamura, T.; Nakata, M.; Kinoshita, M.; Matsumura, S. Novel designed enediynes: Molecular design, chemical synthesis, mode of cycloaromatization and guanine-specific DNA cleavage. *Bioorg. Med. Chem.* **1996**, *4*, 105-113.
- (5) Zhan-Ling Cheng, Q.-Y. C. Difluorocarbene Chemistry: A Simple Transformation of 3,3-gem-Difluorocyclopropenes to Cyclopropenones. *Chin. J. Chem.* **2006**, *24*, 1219-1224.

- (6) Tian, F.; Kruger, V.; Bautista, O.; Duan, J.-X.; Li, A.-R.; Dolbier, W. R.; Chen, Q.-Y. A Novel and Highly Efficient Synthesis of *gem*-Difluorocyclopropanes. *Org. Lett.* **2000**, *2*, 563-564.
- (7) Olah, G. A.; Iyer, P. S.; Surya Prakash, G. K. Perfluorinated Resinsulfonic Acid (Nafion-H) Catalysis in Synthesis. *Synthesis* **1986**, *07*, 513-531.
- (8) Boger, D. L.; Zhou, J. CDPI3-enediyne and CDPI3-EDTA conjugates: a new class of DNA cleaving agents. *J. Org. Chem.* **1993**, *58*, 3018-3024.
- (9) Xu, W.; Chen, Q.-Y. 3,3-Difluoro-1-iodocyclopropenes: A Simple Synthesis and Their Reactions. *J. Org. Chem.* **2002**, *67*, 9421-9427.
- (10) Dehmlow, E. V.; Winterfeldt, A. Chlorofluorocarbene Addition to Alkynes - a Novel Path to Cyclopropenones with Uncommon Substituents. *Tetrahedron* **1989**, *45*, 2925-2936.
- (11) Bessard, Y.; Schlosser, M. *gem*-Difluorocyclopropenes by [1+2] cycloaddition reactions between difluorocarbene and acetylenes having terminal or internal triple bonds. *Tetrahedron* **1991**, *47*, 7323-7328.
- (12) Potts, K. T.; Baum, J. S. Chemistry of cyclopropenones. *Chem. Rev.* **1974**, *74*, 189-213.
- (13) Isaka, M.; Ejiri, S.; Nakamura, E. General-Synthesis of Cyclopropenones and Their Acetals. *Tetrahedron* **1992**, *48*, 2045-2057.
- (14) Breslow, R. Quantitative studies on aromaticity and antiaromaticity. *Pure Appl. Chem.* **1971**, *28*, 111-130.
- (15) Crévisy, C.; Beau, J.-M. The esperamicin- calicheamicin aglycones: Ring closure of a simple strained system mediated by chromium(II)-nickel(II) salts. *Tetrahedron Lett.* **1991**, *32*, 3171-3174.

- (16) Dess, D. B.; Martin, J. C. Readily accessible 12-I-5 oxidant for the conversion of primary and secondary alcohols to aldehydes and ketones. *J. Org. Chem.* **1983**, *48*, 4155-4156.
- (17) (a) Takai, K.; Tagashira, M.; Kuroda, T.; Oshima, K.; Utimoto, K.; Nozaki, H. Reactions of alkenylchromium reagents prepared from alkenyl trifluoromethanesulfonates (triflates) with chromium(II) chloride under nickel catalysis. *J. Am. Chem. Soc.* **1986**, *108*, 6048-6050; (b) Aicher, T. D.; Kishi, Y. Synthetic studies towards halichondrins. *Tetrahedron Lett.* **1987**, *28*, 3463-3466; (c) Harwig, C. W.; Py, S.; Fallis, A. G. Taxamycin Studies: CrCl₂/NiCl₂-Mediated Cyclizations and Unusual SeO₂ Oxidations. *J. Org. Chem.* **1997**, *62*, 7902-7903.
- (18) (a) Myers, A. G.; Zheng, B.; Movassaghi, M. Preparation of the Reagent *o*-Nitrobenzenesulfonylhydrazide. *J. Org. Chem.* **1997**, *62*, 7507-7507; (b) Myers, A. G.; Zheng, B. New and Stereospecific Synthesis of Allenes in a Single Step from Propargylic Alcohols. *J. Am. Chem. Soc.* **1996**, *118*, 4492-4493.
- (19) Pacheco, M. C.; Gouverneur, V. Electrophilic Fluorodesilylation of Allenylmethylsilanes: A Novel Entry to 2-Fluoro-1,3-dienes. *Org. Lett.* **2005**, *7*, 1267-1270.
- (20) Kogen, H.; Kiho, T.; Tago, K.; Miyamoto, S.; Fujioka, T.; Otsuka, N.; Suzuki-Konagai, K.; Ogita, T. Alutacenoic acids A and B, rare naturally occurring cyclopropenone derivatives isolated from fungi: Potent non-peptide factor XIIIa inhibitors. *J. Am. Chem. Soc.* **2000**, *122*, 1842-1843.
- (21) (a) Nagata, R.; Yamanaka, H.; Okazaki, E.; Saito, I. Biradical formation from acyclic conjugated eneyne-allene system related to neocarzinostatin and esperamicin-calicheamicin. *Tetrahedron Lett.* **1989**, *30*, 4995-4998; (b) Myers, A. G.; Kuo, E. Y.;

- Finney, N. S. Thermal generation of α ,3-dehydrotoluene from (Z)-1,2,4-heptatrien-6-yne. *J. Am. Chem. Soc.* **1989**, *111*, 8057-8059; (c) Myers, A. G.; Dragovich, P. S.; Kuo, E. Y. Studies on the thermal generation and reactivity of a class of (σ,π)-1,4-biradicals. *J. Am. Chem. Soc.* **1992**, *114*, 9369-9386.
- (22) Cramer, C. J.; Kormos, B. L.; Seierstad, M.; Sherer, E. C.; Winget, P. Biradical and Zwitterionic Cyclizations of Oxy-Substituted Enyne-Allenenes. *Org. Lett.* **2001**, *3*, 1881-1884.
- (23) Cremeens, M. E.; Hughes, T. S.; Carpenter, B. K. Mechanistic Studies on the Cyclization of (Z)-1,2,4-Heptatrien-6-yne in Methanol: A Possible Nonadiabatic Thermal Reaction. *J. Am. Chem. Soc.* **2005**, *127*, 6652-6661.

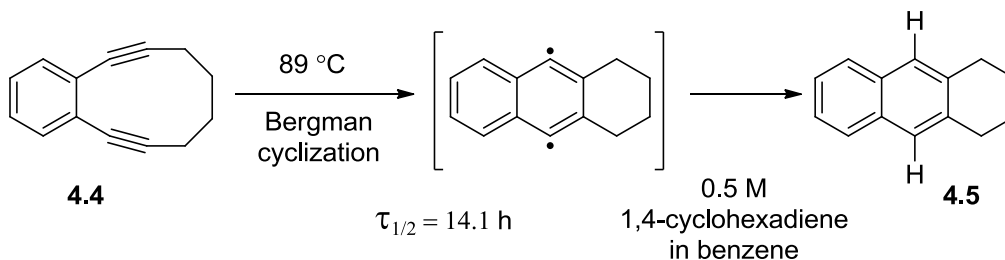
CHAPTER 4

SYNTHESIS AND REACTIVITY OF CYCLIC ENEDIYNE CONTAINING AN ADDITIONAL ENDOCYCLIC TRANS-DOUBLE BOND

4.1 INTRODUCTION

The goal of this project was to enhance the rate of the Bergman cyclization of benzo-fused enediyne **4.4** (Scheme 4.1).¹ The cycloaromatization of enediyne **4.4** is not fast enough to achieve temporal and spatial resolution of *p*-benzyne generation in biological systems.

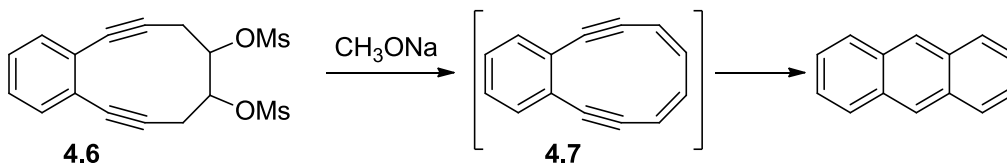
Scheme 4.1 Cyclization of benzo-fused enediyne **4.4**.



In order to achieve this goal, the presence of an additional double bond in a ten-membered enediyne would increase the rate of Bergman cyclization. For example, in attempts to synthesize the [10]annulene **4.7** Musamane *et al.* observed the spontaneous cycloaromatization to form anthracene when dimesylate **4.6** was treated with sodium methoxide (Scheme 4.2).²

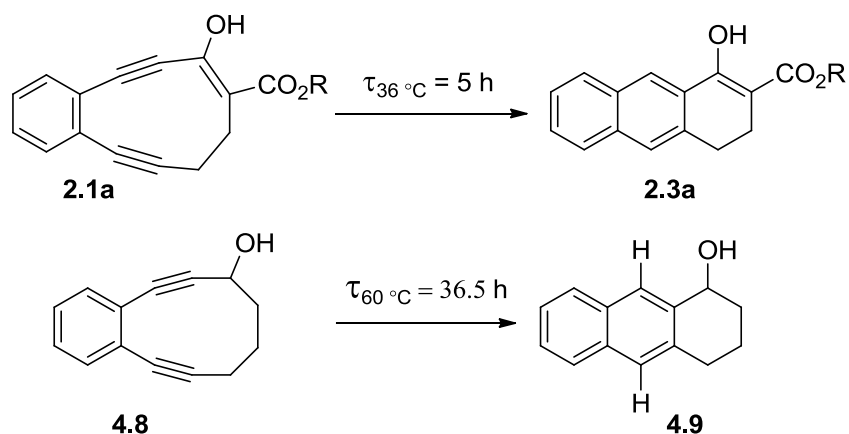
As it was mentioned in Chapter 2, Popik and co-workers recently found that a double bond directly conjugated to one of the triple bonds, in fact, increases the rate of the cycloaromatization of ten-membered enediynes.

Scheme 4.2 Cycloaromatization of dimesylate **4.6**.



Thus, the lifetime of enediyne **2.1a** is 5 hours at 36 °C, while the lifetime of the parent enediyne **4.8** is 36.5 hours at 60 °C (Scheme 4.3).³ This substantial change in reactivity is due to the presence of the double bond, which results in an additional strain of the ten-membered enediyne.

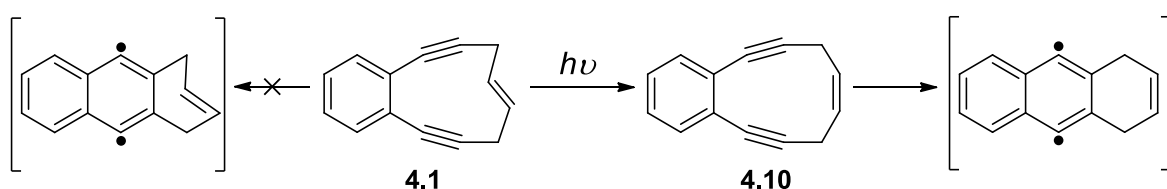
Scheme 4.3 Comparison of the cyclization rates of **2.1** and **4.8**.



In original work, Basak and co-workers reported preparation of 16-membered ring enediyne compounds incorporating azobenzene moiety. The photochemical *trans-cis* isomerization of the $\text{N}=\text{N}$ bond apparently brings acetylenic termini closer. This change in geometry reduces the offset temperature for Bergman cyclization by 24 – 30 °C, from 94 °C to 70 °C (see Chapter 1, Scheme 1.25).

Following the lead of azobenzene isomerization, we have designed a dienediyne macrocycle **4.1**, which incorporates an additional *trans* double bond in a ten-membered benzannulated enediyne cycle. The activation barrier for the cycloaromatization of (1*E*)-6,7-benzocyclodeca-1-ene-4,9-diyne (**4.1**) is expected to be very high, while *cis* isomer **4.10** is expected to undergo spontaneous Bergman cyclization under ambient conditions (Scheme 4.4).

Scheme 4.4 Bergman cyclization of dienediyne **4.1**.



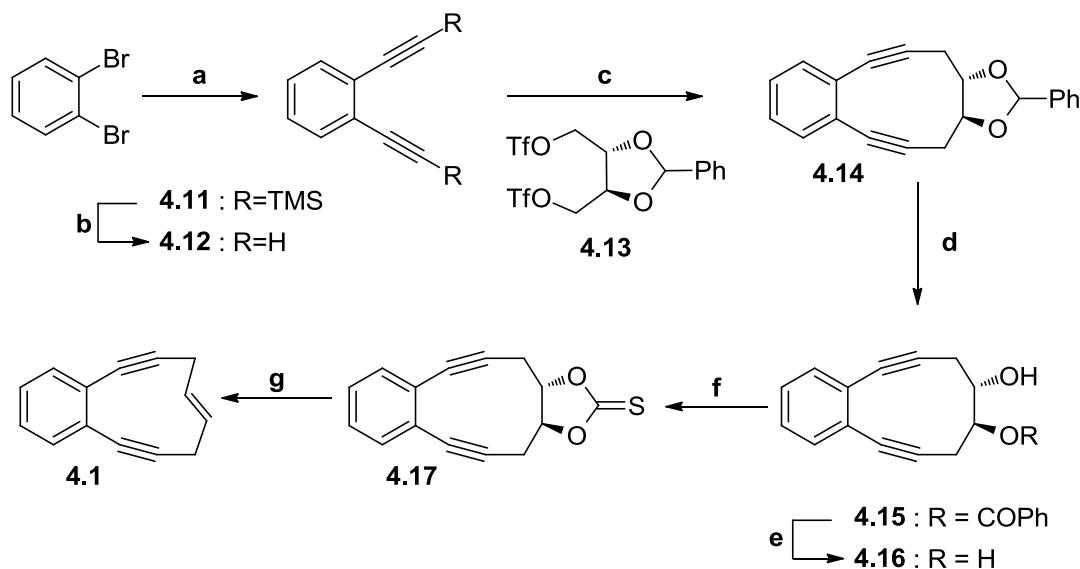
In the next section, we describe the synthesis, as well as thermal and photochemical reactivity of dienediyne (**4.1**).

4.2 RESULTS AND DISCUSSION

Synthesis of dienediyne (1E)-6,7-benzocyclodeca-1-ene-4,9-diyne (4.1)

Dienediyne **4.1** has been prepared in ten steps starting from commercially-available 1,2-dibromobenzene and *L*-tartrate (Scheme 4.5). Enediyne **4.12** was prepared by using the *Sonogashira coupling reaction* followed by the deprotection of the trimethylsilyl groups. *L*-tartrate was refluxed with benzaldehyde in toluene in the presence of catalytic amounts of *p*-Toluene sulfonic acid. The obtained diester was then reduced with sodium borohydride in methanol to produce a corresponding diol, which was treated with triflic anhydride to give ditriflate **4.13**.⁴

Scheme 4.5 Synthesis of dienedine **4.1**.



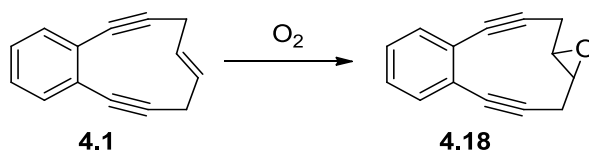
Reagents and Conditions: (a) Pd(PPh₄), CuI, piperidine, HC≡CSi(CH₃)₃, 80 °C, 85%; (b) 0.2 eq. K₂CO₃/ MeOH, 95%; (c) *n*-BuLi (2.1 eq), HMPA/THF, 0 °C to 23 °C 30 min then 6, 43%; (d) Ph₃CBF₄, MeCN, 50 °C, 92%; (e) NaOH/MeOH, rt, 93%; (f) thiophosgene, 4-methylaminopyridine, CH₂Cl₂, 0 °C to 23 °C, 79%; (g) 1,3-Dimethyl-2-phenyl-1,3,2-diazaphospholidine, benzene, 40 °C, 51%.

The key step of the synthesis was the addition of ditriflate **4.13** to the dilithio derivative of **4.12**.⁵ Since the conventional acid-catalyzed hydrolysis of acetal **4.14** results in rapid decomposition of a substrate producing complex reaction mixture, the deprotection of a glycol moiety was conducted using a two step procedure. First, acetal **4.14** was oxidatively hydrolyzed by treatment with trityl fluoroborate to give a racemic hydroxy benzoate **4.15**, which was in turn saponified to produce 1,2-diol **4.16** in 93% yield. Diol **4.16** was then treated with thiophosgene to give thiocarbonate **4.17**. The phosphine-mediated elimination of thiocarbonate group using a modified Corey—Hopkins—Winter procedure⁶ gave the target (*1E*)-6,7-benzocyclodeca-1-ene-4,9-diyne (**4.1**) in 51% yield. The assignment of the *trans* geometry to the double bond in dienediyne **4.1** was based on the fact that Corey—Hopkins—Winter olefination of thiocarbonate

is known to be highly stereospecific.⁷ The configuration of an alkene produced in this reaction match the stereochemistry of the starting glycol. The triflate **4.13** has *trans*-configuration of the diol moiety. No isomerization had been observed on deprotection and thiocarbonylation steps. In addition, dienediyne **4.1** is found to be stable below 100 °C. On the other hand, the parent 3,4-benzocyclodeca-1,5-diyne undergoes cyclization with lifetime of 6 hours at 84 °C in neat 1,4-cyclohexadiene.⁸ Introduction of additional *cis* double bond is expected to make dienediyne **4.10** even more reactive than 3,4-benzocyclodeca-1,5-diyne.

The *trans* double bond in **4.1** is surprisingly reactive; it undergoes slow epoxidation under ambient conditions to produce quantitative yields of oxirane-fused enediyne **4.18** (Scheme 4.6). Even thoroughly degassed solutions of **4.1** eventually show presence of epoxide **4.19**. It is interesting to note that epoxy-enediyne **4.18** is stable at 120 °C and no signs of Bergman cyclization products were detected after prolong heating at this temperature.

Scheme 4.6 Epoxidation of the double bond of the dienediyne **4.1**.

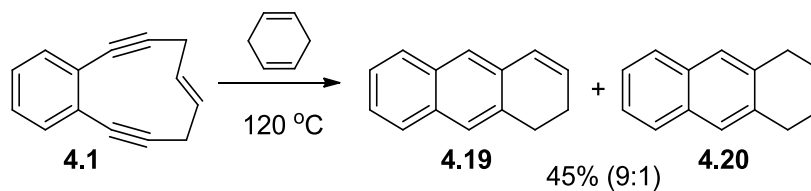


Thermal cycloaromatization of dienediyne 4.1

The deoxygenated solution of dienediyne **4.1** in 1,4-cyclohexadiene was heated at 120 °C in a sealed vessel. The reaction was followed by GC/MS, which showed complete consumption of starting material after three days. The resulting reaction mixture contained 1,2-dihydroanthracene (**4.19**) and 1,4-dihydroanthracene (**4.20**) in 9:1 ratio, as well as substantial amounts of a polymeric material. Dihydroanthracenes **4.19** and **4.20** were isolated chromato-

graphically in 45% yield (Scheme 4.7). Structure of isomeric dihydroanthracenes **4.19** and **4.20** were confirmed by the direct synthesis.

Scheme 4.7 Cycloaromatization of dienediyne **4.1**.



The rate of cycloaromatization of dienediyne **4.1** in neat 1,4-cyclohexadiene at $120 \pm 1\text{ }^{\circ}\text{C}$ was measured by following the decay of the starting material using GC-MS (Figure 4.1).

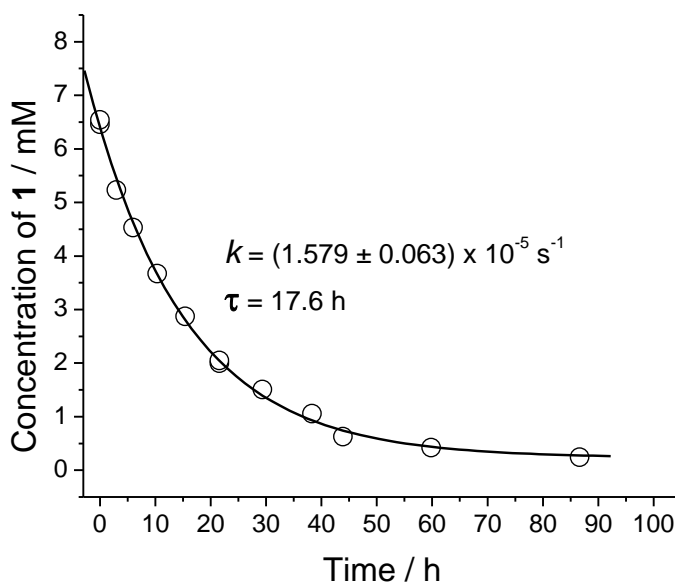


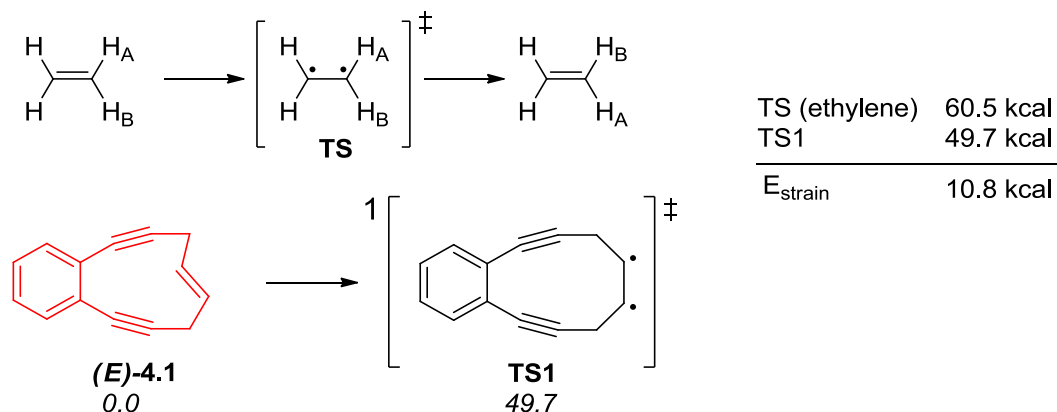
Figure 4.1 Decomposition of 0.0065 M solution of (1*E*)-6,7-benzocyclodeca-1-ene-4,9-diyne (**4.1**) in benzene at $120\text{ }^{\circ}\text{C}$ in the presence of 1.51 M of 1,4-cyclohexadiene.

The half lifetime of dienediyne **4.1** at 120 °C in 1.51 M 1,4-cyclohexadiene in benzene was found to be 10.5±1.5 h. The parent 3,4-benzocyclodeca-1,5-diyne, which lacks the extra *trans*-double bond, is substantially more reactive. It has 10 h lifetime at 84 °C,⁸ while **4.1** is stable at this temperature.

In order to rationalize the product ration found in the thermal cyclization of dienediyne **4.1**, computational methods have been applied to reveal the underlying reaction mechanism. All computations have been carried out using Gaussian 03 Rev. C.02. Structures have been optimized on the BLYP/6-31G** level of theory using the unrestricted broken spin (BS-) Ansatz. Transitions states (TS) and minima have been characterized by frequency calculations.

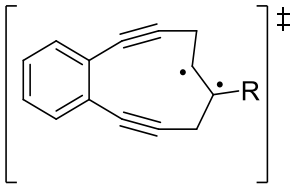
Additional strain energy of the cyclic dienediyne lowers the barrier for double bond isomerization (TS1) in **4.1**. Comparison to the simplest unstrained alkene known, ethylene, leaves 10.7 kcal strain energy for **4.1** (Scheme 4.8).

Scheme 4.8 Contribution of the *trans* double bond to the strain energy of **4.1**.



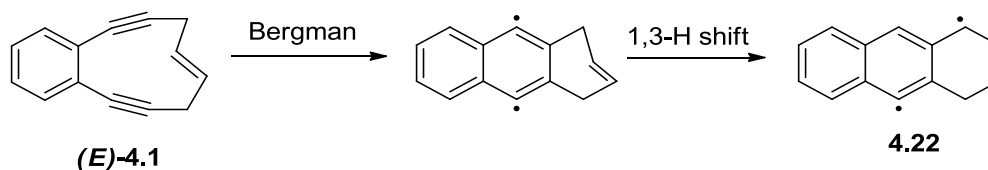
Interestingly, substituents at the (*E*)-double bond stabilizing radical centers in α -position of the transition state, will also lower the barrier for double bond isomerization in **4.1** (Scheme 4.9). Thus, addition of one phenyl substituent will lower the barrier of this reaction for another ca. 9 kcal/mol.

Scheme 4.9 Contribution of different substituents at (*E*)-double bond to $\Delta E(\text{TS})$.

	R	$\Delta E(\text{TS})$
	H	49.7
	CH ₃	48.4
	Cl	45.9
	Ph	41.3

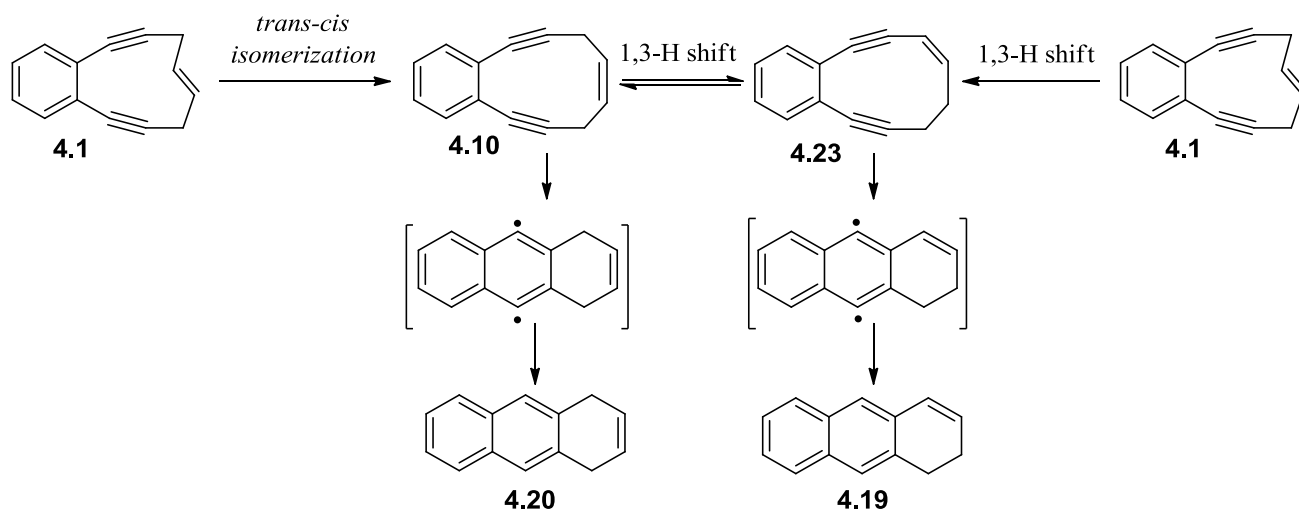
The direct Bergman cyclization of **4.1** is highly endothermic (55.0 kcal) because of the increased strain energy. Although a subsequent 1,3-H shift would give the stabilized allylradical **4.22** as exothermic product (-32.2 kcal), such a pathway has an extremely high activation barrier energy (TS=111.6 kcal, Scheme 4.10).

Scheme 4.10 The direct Bergman cyclization of dienediyne **4.1**.



We expected that the mechanism of cycloaromatization of **4.1** involves the thermal *trans-cis* isomerization of a double bond forming reactive enediyne **4.10** or 1,3-H shift prior to cyclization producing **4.23**. Once formed, dienediynes **4.10** and **4.23** could then undergo facile cycloaromatization and double hydrogen abstraction producing 1,4- and 1,2-dihydroanthracenes (Scheme 4.11).

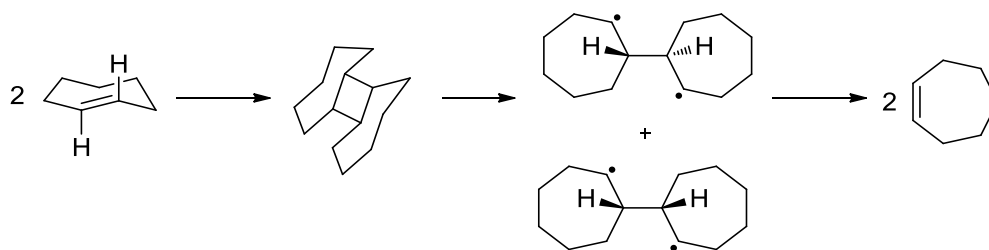
Scheme 4.11 Possible mechanism of cyclization of the dienediynes **4.1**.



However, theoretical analysis of this pathway (*vide infra*) predict ca. 50 kcal/mol barrier for such reaction, which would require temperatures in excess of 300 °C to induce the cyclization. In fact, isomerization of *trans*-cyclooctene proceeds at 292 °C with ~ 48 h life time.⁹ The transition state energy for 1,3-H shift of **4.1** to **4.23** is even higher (68.3 kcal).

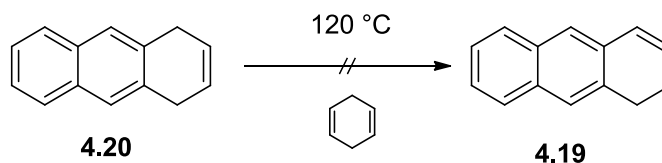
In attempts to understand the mechanism of the cyclization of **4.1**, we turned our attention to some literature examples of cyclic alkenes with *trans* double bonds. The unexpectedly facile isomerization of *trans*-cycloheptene was explained by a bimolecular process.¹⁰ The initial step in this reaction is 2+2 dimerization of the substrate followed by thermal cleavage of the cyclobutane to give *cis*-cycloheptene (Scheme 4.12).

Scheme 4.12 *Trans-cis* isomerization of the double bond of cycloheptene.



Similar mechanism can be used to explain the formation of **4.20**. Some support for this suggestion comes from two experimental observations: first, the formation of 1,4-dihydroanthracene (**4.19**) is observed only at the concentrations of **4.1** above 1×10^{-3} M; second, MS-analysis of reaction mixtures produced at the substrate concentration above this value allowed us to detect trace amounts of dimer of **4.1**.

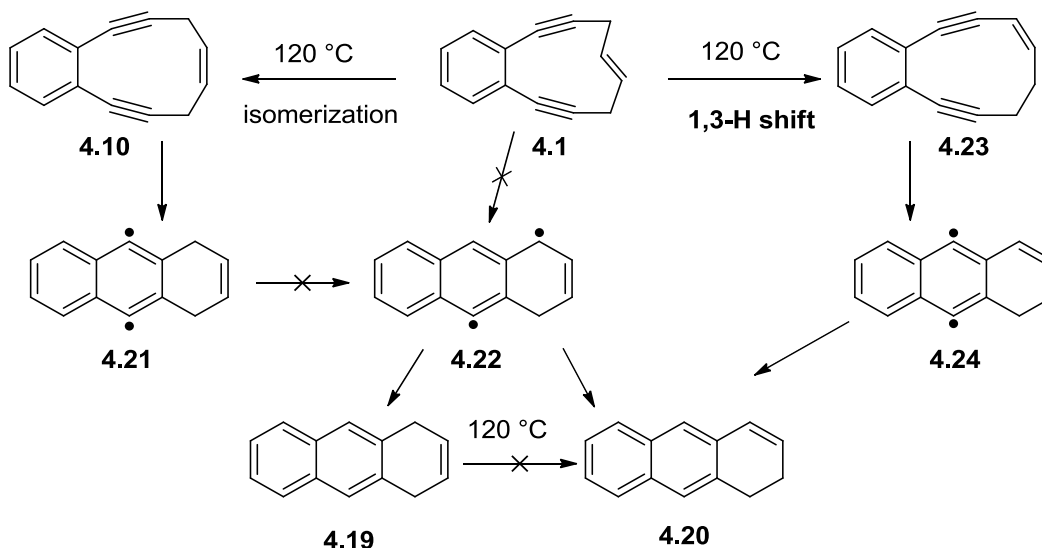
Scheme 4.13 Attempt to thermally isomerize 1,4- to 1,2-dihydroanthracene.



The major product of the thermal cyclization of dienediyne **4.1** is 1,2-dihydroanthracene (**4.19**). The plausible mechanism of its formation is the thermal isomerization of 1,4-dihydroanthracene (**4.20**) to give thermodynamically more stable product. Directly prepared 1,4-dihydroanthracene (**4.20**), however, has proved to be stable at 120 °C and produced no detectable amounts of **4.19** even after prolonged heating (Scheme 4.13).

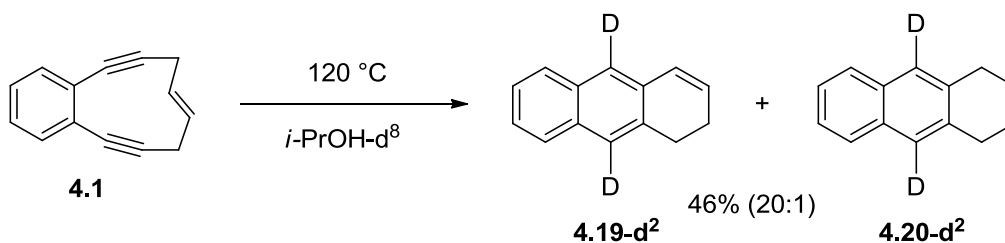
The rate of decomposition of **4.1** is virtually independent from the concentration of the substrate, suggesting that formation of the main product is a unimolecular process. Alternatively, conjugatively stabilized allylic diradical **4.22** might serve as a precursor to both **4.19** and **4.20** (Scheme 4.14). The former can be produced from initial diradical **4.21** via a thermodynamically favorable 1,3-hydrogen shift. Somewhat similar 1,2-phenyl shift was observed in the case of 2-phenyl-1,4-didehydronaphthalenes.¹¹ It is also possible to envision formation of the diradical **4.22** directly from dienediyne **4.1** or in intermolecular hydrogen abstraction.

Scheme 4.14 Possible pathways of the cyclization of dienediyne **4.1**.



Examination of the products of the cycloaromatization of **4.1** in deuterated solvents allows us to rule out participation of **4.22** or other rearranged diradicals. Decomposition of dienediyne **4.1** in isopropanol- d_8 or toluene- d^8 resulted in formation of only two products: **4.19-d²** and **4.20-d²** with no detectable incorporation of deuterium into hydrogenated ring (Scheme 4.15).

Scheme 4.15 Thermal cyclization of dienediyne **4.1** in 2-propanol- d^8 .



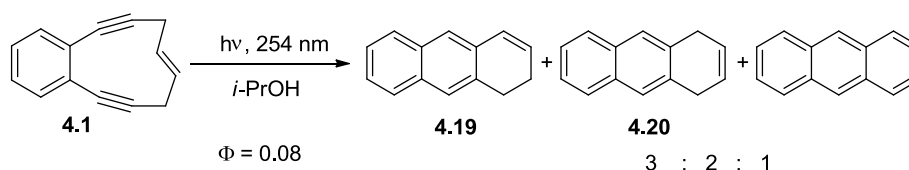
In summary, we ruled out several possible mechanisms because of the high barrier energies, which are required for the dienediyne **4.1** to undergo the cyclization producing 1,2- and 1,4-dihydroanthracenes in the ratio 9:1. While we have little support for a mechanism, which

involves dimerization of **4.1** forming cyclobutane, the feasibility of this pathway remains adequate to be considered for the further experiments.

Photochemical reactivity of dienediyne 4.1.

Low conversion (< 30%) 254 nm photolysis of dienediyne **4.1** in 2-propanol produces a mixture of cycloaromatized products in overall 33% yield (based on conversion, Scheme 4.16). Similarly to the thermally induced cyclization, 1,2-dihydroanthracene (**4.19**) and 1,4-dihydroanthracene (**4.20**) are formed. In addition, fully aromatized anthracene is formed.

Scheme 4.16 Photolysis of dienediyne **4.1**.



We believe that excitation of dienediyne **4.1** results in the isomerization of the double bond to form **4.2** and **4.12**, which then undergo rapid Bergman cyclization to give ultimate products **4.11** and **4.10** correspondingly. Anthracene is apparently formed by the photo-induced oxidation of the latter compounds by traces of oxygen in the irradiated solutions. Further irradiation of dienediyne **4.1** results in the decomposition of the primary products and formation of a complex reaction mixture.

4.3 CONCLUSIONS

Incorporation of an additional endocyclic *trans*-double bond in the structure of ten-membered ring enediynes substantially increases the barrier for the Bergman cyclization. Isomerization of this extra double bond into *cis* geometry produces reactive enediynes, thus opening a new approach to triggering the Bergman cyclization. Conjugation of the double bond in **4.1** with good chromophore should increase the efficiency of photochemical isomerization between *E* and *Z* configurations. For example, stilbene moiety is known to undergo facile

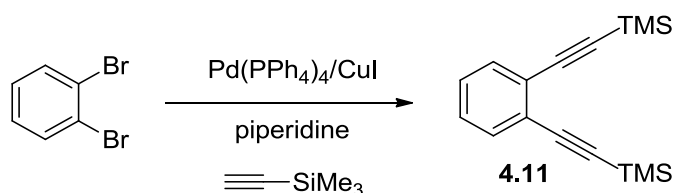
photochemical *trans-cis* isomerization. The preparation of an analog of dienediyne **4.1** containing two aromatic substituents at the *tans* double bond is underway in our laboratory.

4.4 EXPERIMENTAL SECTION

General Procedures

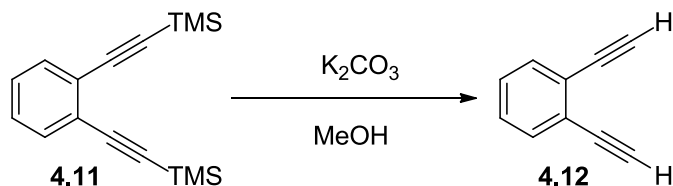
All NMR spectra were recorded in CDCl₃ on a 400 MHz instrument and referenced to TMS unless otherwise noted. Melting points are uncorrected. Purification of products by column chromatography was performed using 40-63 μm silica gel. Tetrahydrofuran was distilled from sodium/benzophenone ketyl; ether and hexanes were distilled from sodium. Other reagents were obtained from Aldrich or VWR and used as received unless otherwise noted. Transition metal compounds were purchased from Strem Chemicals.

Materials: 1,2-ethynylbenzene **4.12**,¹² (2S,3S)-1,4-di-O-trifluoromethanesulfonyl-2,3-O-benzylidene-threitol **4.13**, 1,2-dihydroanthracene (**4.19**),¹³ and 1,4-dihydroanthracene (**4.20**)¹⁴ were prepared according to literature procedures.

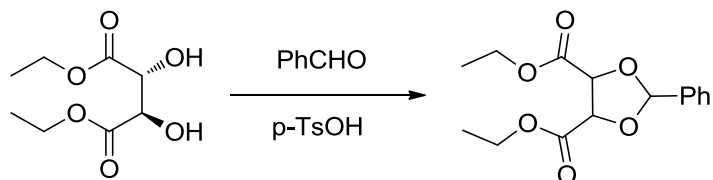


1,2-Bis-trimethylsilanylethynyl-benzene (4.11). Tetrakis(triphenylphosphine)palladium (2 g, 1.7 mmol, 2.3 mol.%) was added to a stirred degassed solution of 1,2-dibromobenzene (17.6 g, 0.074 mol) in piperidine (100 mL) under argon atmosphere. Then, powdered copper (I) iodide (1.4 g, 7.3 mmol, 9.8 mol.%) and trimethylsilyl acetylene (26 mL, 0.26 mol) were added to the mixture. The reaction vessel was purged with argon, sealed, and stirred for two days at 95 °C. The reaction mixture was filtered through small pad of silica gel (EtOAc:hexanes, 5:95) and the

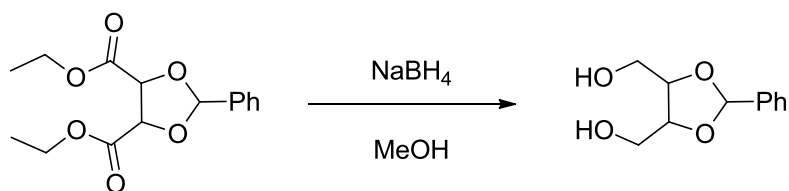
crude product was purified by column chromatography (hexanes, $R_f = 0.35$) to give 11.5 g (57%) of **4.11** as yellow liquid.



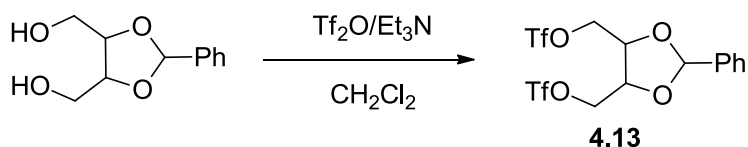
1,2-ethynylbenzene (4.12). K_2CO_3 (2 g, 14.4 mmol) was added to a stirred solution of 1,2-bis-trimethylsilanylethynylbenzene (7 g, 25.9 mmol) in methanol (150 mL) at 0 °C. The reaction mixture was stirred at room temperature for 15 minutes and quenched with water (100 mL). The product was extracted with ether (2x70 mL). Combined extracts were washed with brine (3x50 mL) and dried with anhydrous MgSO_4 . The solvent was evaporated under reduced pressure and the residue was purified by flash chromatography (hexanes, $R_f = 0.3$) to give 3.1 g (96 %) of **4.12** as yellow oil.



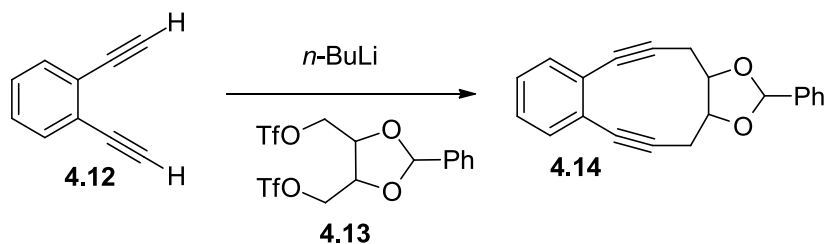
Diethyl (4R,5R)-2-Phenyl-1,3-dioxolane-4,5-dicarboxylate.¹⁵ Diethyl-L-tartrate (34.2 mL, 0.2 mol) in toluene (150 mL), benzaldehyde (40 mL, 0.4 mol), and one spatula of p-toluenesulfonic acid were placed into a round bottom flask. The reaction mixture was refluxed for overnight using Dean-Stark trap to remove water. In 18 hours, the reaction mixture was allowed to warm to room temperature. The solvent was removed under reduced pressure. The residue was purified by column chromatography (EtOAc:Petroleum Ether, 10:90, $R_f = 0.1$) to yield 41.8 g (70 %) of white crystals (m.p. 44-45 °C).



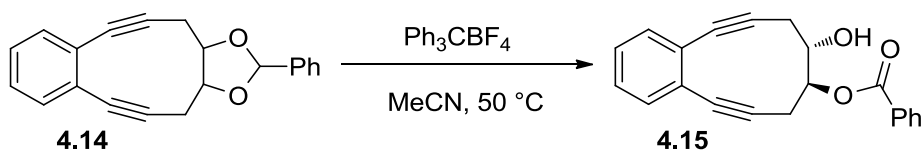
(2S,3S)-2,3-O-benzylidenethreitol.¹⁶ Diethyl 2,3-O-tartrate (20 g, 0.068 mol) was added to a stirred solution of sodium borohydride (6.4 g, 0.17 mol, 2.5 eq) in ethanol (150 mL) at 0 °C. After stirring for 1 h, the mixture was evaporated in vacuo. The residue was taken into ethyl acetate (200 mL). The solution was washed with brine (3 x 50 mL), dried with magnesium sulfate and evaporated in vacuo. The crude product was purified by column chromatography (EtOAc:Petroleum ether, 7:3, R_f = 0.3) to give 12.8 g (90%) of pure (2S,3S)-2,3-O-benzylidenethreitol as viscous oil.



(2S,3S)-1,4-Di-O-trifluoromethanesulfonyl-2,3-O-benzylidenethreitol (4.13). Triflic anhydride (8.5 mL, 0.05 mol) in CHCl_3 (30 mL) was added dropwise to a solution of 2,3-O-benzylidenethreitol (5.047 g, 0.024 mol) and pyridine (5.2 mL) in CHCl_3 (50 mL) at 0 °C. The reaction mixture was stirred for 45 min, diluted with CHCl_3 (50 mL), washed with water, brine and dried with MgSO_4 . Removal of solvent in vacuo provided the ditriflate which was azeotropically dried with benzene (2x50 mL) to yield 10.4 g (95%) of red-orange oil. Crude ditriflate was used in the next step without further purification.



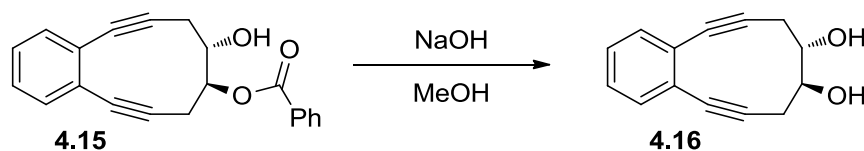
12-phenyl-benzo[5,6]-13,11-dioxo-bicyclo[8,3,0]trideca-5-ene-3,7-diyne (4.14). A solution of *n*-BuLi (6.72 mL, 2.56 M in hexanes) was added dropwise to a solution of 1,2-diethynylbenzene **4.12** (1 g, 7.9 mmol) in THF (400 mL) at 0 °C. HMPA (4 mL) was then added, and the reaction mixture was warmed to r.t., and stirred for 30 min. A solution of **4.13** (3.5 g, 7.4 mmol) in THF (30 mL) was added dropwise in the course of 1 h. The reaction mixture was stirred another 30 min and poured into water/ether (100/200 mL). The organic layer was separated, washed with brine (2x100 mL), dried with magnesium sulfate and concentrated. Column chromatography on silica gel (EtOAc:hexanes, 5:95, R_f = 0.2) of the residue provided 1.02 g (43%) of pure **4.14** as white solid (mp 125-127 °C). ^1H NMR: 2.70 (dd $J_1=17.2$ Hz, $J_2=10.8$ Hz, 1H), 2.83 (dd $J_1=16.8$ Hz, $J_2=10.8$ Hz, 1H), 3.01 (dd $J_1=16.8$ Hz, $J_2=3.2$ Hz, 1H), 3.07 ($J_1=17.2$ Hz, $J_2=3.2$ Hz, 1H), 4.41 (m, 2H), 5.87 (s, 1H), 7.24 (m, 2), 7.33 (m, 2H), 7.4 (m, 3H), 7.5 (m, 1H); ^{13}C NMR: 25.51, 26.16, 81.18, 82.44, 84.92, 85.04, 92.87, 93.76, 102.6, 126.85, 127.95, 127.97, 128.43, 128.55, 128.67, 128.71, 129.91, 136.44; HRMS calc. for $\text{C}_{21}\text{H}_{16}\text{O}_2$ m/z : 300.1150, found: 300.1145.



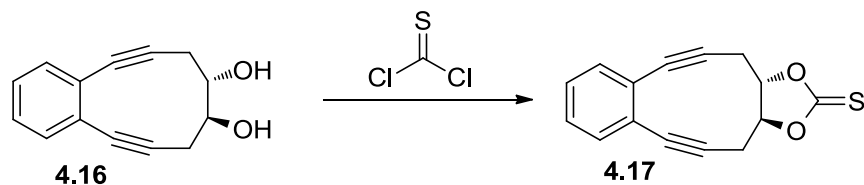
9-hydroxy-5,6,11,12-tetradehydro-7,8,9,10-tetrahydrobenzo[10]annulen-8-yl benzoate 4.15.

Tri-phenylcarbenium tetrafluoroborate (990 mg, 3 mmol) was added to a stirred solution of **4.14** (300 mg, 1 mmol) in MeCN (100 mL) at 55 °C. The mixture was stirred at this temperature for

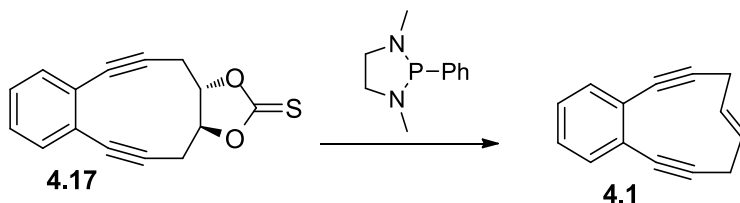
18 h and monitored by TLC. Upon completion, the reaction mixture was poured into 70 mL of phosphate buffer (pH=7) and extracted with dichloromethane (3x50 mL). The organic solution was washed with brine (2x75 mL) and dried over sodium sulfate. The solvent was removed under reduced pressure and residue was purified by column chromatography (R_f = 0.15, 10% EtOAc in Hexane) to give 0.291 g (92%) of pure **4.15** as a yellow solid (mp 126 °C with decomposition). ^1H NMR: 2.65 (d J =8.8 Hz, 1H), 2.84 (dd J_1 =17.2 Hz, J_2 =2.4 Hz, 1H), 2.95 (m, 2H), 3.02 (dd J_1 =17.2 Hz, J_2 =3.2 Hz, 1H), 4.4 (m, 1H), 5.47 (m, 1H), 7.25 (m, 2H), 7.34 (m, 2H), 7.44 (m, 2H), 7.58 (m, 1H), 8.06 (m, 2H); ^{13}C NMR: 24.76, 27.61, 72.3, 74.47, 85.21, 85.29, 93.9, 94.59, 127.87, 128.01, 128.42, 128.44, 128.8, 128.83, 129.09, 129.54, 130.03, 133.72, 166.16. EI-HRMS: calc. for $\text{C}_{21}\text{H}_{16}\text{O}_3$ m/z : 317.1178, found: 317.1173.



Benzo[7,6]cyclodec-7-ene-4,5-diyne-1,2-diol (4.16). Benzoate **4.15** (0.27g, 0.854 mmol) was dissolved in methanol (30mL) containing sodium hydroxide (1%, w/w) and stirred at r.t. for 3 h. The reaction mixture was neutralized with saturated solution of ammonium chloride (30 mL), and extracted with dichloromethane (3x20 mL). The combined organic extracts were washed with brine (2x30 mL), dried over sodium sulfate, and concentrated. Column chromatography of the residue on silica gel (50% EtOAc in hexanes) provided 168 mg (93%) of pure diol **4.16** as yellowish solid (mp 94-96 °C). ^1H NMR: 2.6 (dd J_1 =16.8 Hz, J_2 =10.4 Hz, 2H), 2.83 (dd J_1 =16.8 Hz, J_2 =2.8 Hz, 2H), 3.01 (d J =6 Hz, 2H), 4.13 (m, 2H), 7.23 (m, 2H), 7.31 (m, 2H); ^{13}C NMR: 28.89, 73.06, 85.28, 94.30, 127.94, 128.58, 128.79. EI-HRMS: calc. for $\text{C}_{14}\text{H}_{12}\text{O}_2$ m/z : 212.0837, found: 212.0829.



5,6,11,12-tetradehydro-3a,4,13,13a-tetrahydrobenzo[6,7]cyclodeca[1,2-*d*][1,3]dioxole-2-thione (4.17). Thiophosgene (92 μ L, 1.2 mmol) was added to a stirred solution of diol **7** (212 mg, 1 mmol) and DMAP (293 mg, 2.4 mmol) in 40 mL of distilled CHCl_3 at 0 $^\circ\text{C}$ under argon atmosphere. After 2 h, the reaction mixture was allowed to warm to room temperature and stirred overnight. Silica gel (20 g) was added and the solvent was removed in vacuo. The residue was loaded onto a silica gel column and eluted with 20% ethyl acetate in hexanes. Concentration of collected fractions in vacuo afforded 200 mg (79%) of thiocarbonate **4.17** in 200 mg (79%) as white solid (mp 186-188 $^\circ\text{C}$). ^1H NMR: 2.87 (dd $J_1=16.8$ Hz, $J_2=10.8$ Hz, 2H), 3.21 (dd $J_1=16.8$ Hz, $J_2=3.2$ Hz, 2H), 4.95 (m, 2H), 7.28 (m, 2H), 7.35 (m, 2H); ^{13}C NMR: 26.03, 85.3, 86.61, 89.32, 127.76, 128.56, 128.72, 189.56. EI-HRMS: calc. for $\text{C}_{15}\text{H}_{10}\text{O}_2\text{S}$ m/z : 254.0402, found: 254.0396.



(1*E*)-6,7-benzocyclodeca-1-ene-4,9-diyne (4.1). A solution of **8** (650 mg, 2.56 mmol) in benzene (30 mL) and 1,3-dimethyl-2-phenyl-1,3,2-diazaphospholidine (1.7 mL, 8.19 mmol) were stirred at 40 $^\circ\text{C}$ for 18 h. After cooling to 25 $^\circ\text{C}$, silica gel (10 g) was added to the reaction mixture, and solvent was removed under reduced pressure. The residue was purified by column chromatography (Hexanes, $R_f = 0.2$) to give 235 mg (51%) of **4.1** as white solid (mp 73-75 $^\circ\text{C}$).

^1H NMR: 2.98 (m, 2H), 3.22 (2H), 5.57 (m, 2H), 7.19 (s, 4H); ^{13}C NMR: 24.89, 89.27, 95.62, 126.4, 126.84, 127.49, 130.05. EI-HRMS: calc. for $\text{C}_{14}\text{H}_{10}$ m/z : 178.0782, found: 178.0778.

Preparative thermolysis of dienediynes 4.1. A solution of **4.1** (17.8 mg, 0.1 mmol) in 1,4-cyclohexadiene (5 mL) was degassed with argon and sealed. The reaction mixture was stirred and heated at 120 °C for 3 days. The reaction progress was monitored by GC/MS. After the reaction was completed, 1,4-cyclohexadiene was removed under reduced pressure and the residue was purified by column chromatography on silica gel (hexanes, $R_f = 0.3$) to give 8 mg (45%) of 9 : 1 mixture of **4.10** and **4.11**.

4.10: ^{13}H NMR: 2.40 (m, 2H), 2.98 (t, $J=7.6$ Hz), 6.13 (m, 1H), 6.65 (d, 1H), 7.38 (m, 2H), 7.44 (s, 1H), 7.52 (s, 1H), 7.73 (m, 2H). MS (EI, 70eV) [m/z (relative intensity)] 180 (M^+ , 100).

4.11: ^{14}H NMR: 3.50 (s, 4 H), 5.90 (br s, 2 H), 7.30 (m, 6 H). MS (EI, 70eV) [m/z (relative intensity)] 180 (M^+ , 100).

4.5 REFERENCES

- (1) Kaneko, T.; Takahashi, M.; Hirama, M. Benzannulation alters the rate limiting step in enediynes cycloaromatization. *Tetrahedron Lett.* **1999**, *40*, 2015-2018.
- (2) Darby, N.; Kim, C. U.; Salaun, J. A.; Shelton, K. W.; Takada, S.; Masamune, S. The 1,5-didehydro[10]annulene system. *J. Chem. Soc., Chem. Commun.* **1971**, 1516-1517.
- (3) (a) Henry, N.C.; Sondheimer, F. 5,12-dihydro-6,11-didehydronaphthacene, A derivative of 1,4-didehydronaphthalene. *Tetrahedron Lett.* **1980**, *21*, 217-220; (b) Schottelius, M. J.; Chen, P. 9,10-Dehydroanthracene: *p*-Benzyne-Type Biradicals Abstract Hydrogen

- Unusually Slowly. *J. Am. Chem. Soc.* **1996**, *118*, 4896-4903; (c) Karpov, G.; Popik, V.V. Triggering of the Bergman Cyclization by Photochemical Ring Contraction. Facile Cycloaromatization of Benzannulated Cyclodeca-3,7-diene-1,5-diynes. *J. Am. Chem. Soc.* **2007**, *129*, 3792-3793.
- (4) Funk, R. L.; Young, E. R. R.; Williams, R. M.; Flanagan, M. F.; Cecil, T. L. Photochemical Cycloaromatization Reactions of *ortho*-Dialkynylarenes: A New Class of DNA Photocleaving Agents. *J. Am. Chem. Soc.* **1996**, *118*, 3291-3292.
- (5) Huynh, C.; Linstumelle, G. A short route to dehydro[12]annulenes. *Tetrahedron* **1988**, *44*, 6337-6344.
- (6) Corey, E. J.; Hopkins, B. A mild procedure for the conversion of 1,2-diols to olefins. *Tetrahedron Lett.* **1982**, *23*, 1979-1982.
- (7) (a) Corey, E. J., Winter, A. E. New stereospecific olefin synthesis from 1,2-diols. *J. Am. Chem. Soc.* **1963**, *85*, 2677-2678; (b) Corey, E. J., Carey, F. A., Winter, R. A. E. Stereospecific syntheses of olefins from 1,2-thionocarbonates and 1,2-trithiocarbonates. *trans*-Cycloheptene. *J. Am. Chem. Soc.* **1965**, *87*, 934-935.
- (8) Semmelhack, M. F.; Neu, T.; Foubelo, F. Arene 1,4-Diradical Formation from *o*-Dialkynylarenes. *J. Org. Chem.* **1994**, *59*, 5038-5047.
- (9) Andrews, U. H.; Baldwin, J. E.; Grayston, M. W. On the thermal isomerization of *trans*-cyclooctene to *cis*-cyclooctene. *J. Org. Chem.* **1982**, *47*, 287-292.
- (10) Squillacote, M. E.; DeFellipis, J.; Shu, Q. How Stable Is *trans*-Cycloheptene? *J. Am. Chem. Soc.* **2005**, *127*, 15983-15988.

- (11) Lewis, K. D.; Matzger, A. Bergman Cyclization of Sterically Hindered Substrates and Observation of Phenyl-Shifted Products. *J. Am. Chem. Soc.* **2005**, *127*, 9968-9969.
- (12) Huynh, C.; Linstumelle, G. A short route to dehydro [12] annulenes. *Tetrahedron* **1988**, *44*, 6337-6344.
- (13) RajanBabu, T. V.; Eaton, D. F.; Fukunaga, T. Chemistry of bridged aromatics. A study of the substituent effect on the course of bond cleavage of 9,10-dihydro-9,10-ethanoanthracenes and an oxyanion-assisted retro-Diels-Alder reaction. *J. Org. Chem.* **1983**, *48*, 652-657.
- (14) Muller, P.; Rey, M. Synthesis and Properties of 1, 1-Dihalogeno-cycloprop[*b*]Anthracenes. *Helv. Chim. Acta* **1982**, *64*, 1157-1166.
- (15) Wenger, R.M. Synthesis of Cyclosporine. I. Synthesis of enantiomerically pure (2*S*,3*R*,4*R*,6*E*)-3-hydroxy-4-methyl-2-methylamino-6-octenoic acid starting from tartaric acid. *Helv. Chim. Acta.* **1983**, *66*, 2308-2321.
- (16) Barriere, F.; Barriere, J.; Barton, D.; Cleophax, J.; Gateau-Olesker, A.; Gero, S.; Tadj, F. Novel (4 + 1) fragment combination approach to chiral cyclopentanoids from tartaric acid. *Tetrahedron Lett.* **1985**, *26*, 3121-3124.

CHAPTER 5

SURFACE FUNCTIONALIZATION USING CATALYST-FREE

AZIDE-ALKYNE CYCLOADDITION¹

¹ Kuzmin, A.; Poloukhine, A.; Wolfert, M; Popik, V. V. *Bioconjugate Chem.*, **2010**, *21*, 2076.

Reprinted here with permission of publisher

5.1 ABSTRACT

The utility of catalyst-free azide-alkyne [3 + 2] cycloaddition for the immobilization a variety of molecules onto a solid surface and microbeads was demonstrated. In this process, the surfaces were derivatized with aza-dibenzocyclooctyne (ADIBO) for the immobilization of azide-tagged substrates via a copper-free click reaction. Alternatively, ADIBO-conjugated molecules are anchored to the azide-derivatized surface. Both immobilization techniques work well in aqueous solutions and show excellent kinetics under ambient conditions. We have developed an efficient synthesis of aza-dibenzocyclooctyne (ADIBO), thus far the most reactive cyclooctyne in cycloaddition azides. We also describe convenient methods for the conjugation of ADIBO with a variety of molecules directly or via a PEG linker.

5.2 INTRODUCTION

Surface immobilization of biomolecules is a very important step in the manufacturing of biosensors, microbeads, biochips, probe arrays, medical implants, and other devices.¹ The key requirements for this process are the preservation of biochemical properties of immobilized substrates and robustness of the linkage. Copper (I) – catalyzed Huisgen 1,3-dipolar cycloaddition of azides to terminal acetylenes has emerged as one of the most convenient methods for the functionalization of various surfaces.^{1c, 1e, 2} The triazol linker formed in the azide “click” reaction has excellent chemical stability due to the aromatic character of the heterocycle. Azide tags can be incorporated into biomolecules using a variety of different strategies, such as post-synthetic modification,³ in vitro enzymatic transfer,⁴ the use of covalent inhibitors,⁵ and metabolic labeling by feeding cells a biosynthetic precursor modified with azido functionality.⁶ While conventional copper (I) - catalyzed click chemistry has become commonplace in surface derivatization, as well as polymer and materials synthesis,^{2, 7} the use of metal catalyst often limits

the utility of the method. Copper ions are cytotoxic,⁸ can cause degradation of DNA molecules,⁹ and induce protein denaturation.¹⁰ In addition, the use of catalysts complicates kinetics of the immobilization process, requires polar solvents, and can alter surface properties.¹¹

Conventional azide click coupling methods employ terminal acetylenes, since internal alkynes react with azides only at elevated temperatures. Cyclooctynes, on the other hand, are known to form triazoles without a catalyst under ambient conditions, albeit at rather slow rate.¹² The triple bond incorporated into an eight-membered ring is apparently already bent into a geometry resembling the transition state of the cycloaddition reaction, thus reducing its activation barrier.¹³ Recently-developed cyclooctyne derivatives are substantially more reactive towards azides and offer a convenient metal-free alternative to the copper-catalyzed click reaction.¹⁴ Metal-free click chemistry has been successfully employed for the modification of luminescent quantum dots,¹¹ proteins labeling and purification,¹⁵ as well as for the introduction of fluorescent tags into live cells^{11, 16} and organisms.¹⁷

Among reactive cyclooctyne derivatives, dibenzocyclooctynes are synthetically more accessible.¹⁸ The major limitation of these click reactants is the relatively low rate of azide cycloaddition (ca. $0.05 \text{ M}^{-1} \text{ s}^{-1}$).¹⁵ Substitution of one of the saturated carbons in the cyclooctyne ring for a nitrogen atom not only improves its reactivity, but also simplifies the synthesis.¹⁴ To extend arsenal of bioorthogonal copper-free click reagents, we have developed an efficient synthesis of aza-dibenzocyclooctyne (ADIBO)-containing compounds for azide-coupling reactions.

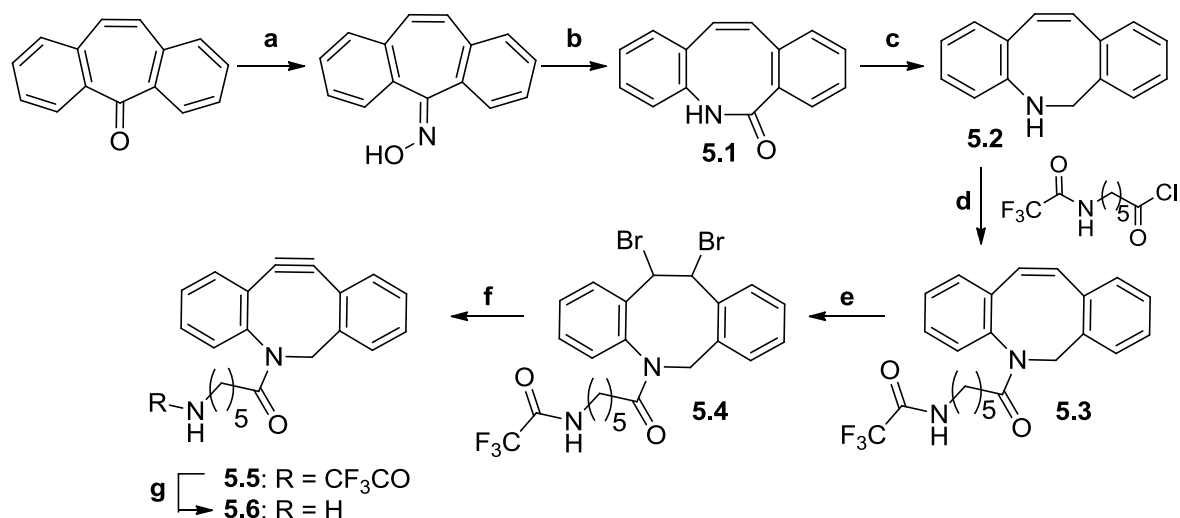
Herein, we describe a novel approach to efficient surface-functionalization using a catalyst-free azide click reaction. This method allows for site-specificity and the covalent anchoring of proteins and other substrates to various surfaces. The same metal-free click reaction

is employed for the PEGylation of unfunctionalized areas of the surface. Such treatment allows for a dramatic reduction or complete elimination of non-specific binding. The copper-free click immobilization strategy discussed in the present report can be applied to the preparation of various types of arrays, as well as to the derivatization of microbeads and nanoparticles.

5.3 RESULTS AND DISCUSSION

The rapid and scalable synthesis of aza-dibenzocyclooctyne-amine conjugate (ADIBO-amine, **5.6**) was developed. The efficient preparation of ADIBO-amine developed in our lab is outlined in Scheme 5.1. It starts with the polyphosphoric acid-catalyzed Beckman rearrangement of dibenzosuberone oxime, which is readily prepared by treating commercially-available dibenzosuberone with hydroxylamine. The lactam **5.1** produced in this reaction is then reduced with lithium aluminum hydride to give dihydrodibenzo[b,f]azocine (**5.2**). The secondary amino group in **5.2** is converted to amide **5.3** by reacting with 1.25 eq. of 6-(trifluoroacetamido)-hexanoyl chloride in the presence of pyridine. The olefin in **5.3** is smoothly converted into an acetylene moiety via a bromination–dehydrobromination sequence to give aza-dibenzocyclooctyne **5.5** in excellent yield (88%). Saponification of the trifluoroacetamide moiety with potassium carbonate in aqueous methanol gives target ADIBO-C6-amine (**5.6**). ADIBO-amine with a shorter aminoalkyl side chain, ADIBO-C3-amine (**5.7**), was prepared following the same synthetic sequence by replacing 6-(trifluoroacetamido)hexanoyl chloride in step “d” with 3-(trifluoroacetamido)propionyl chloride.

Scheme 5.1 Synthesis of ADIBO-C6-amine (**5.6**).^a

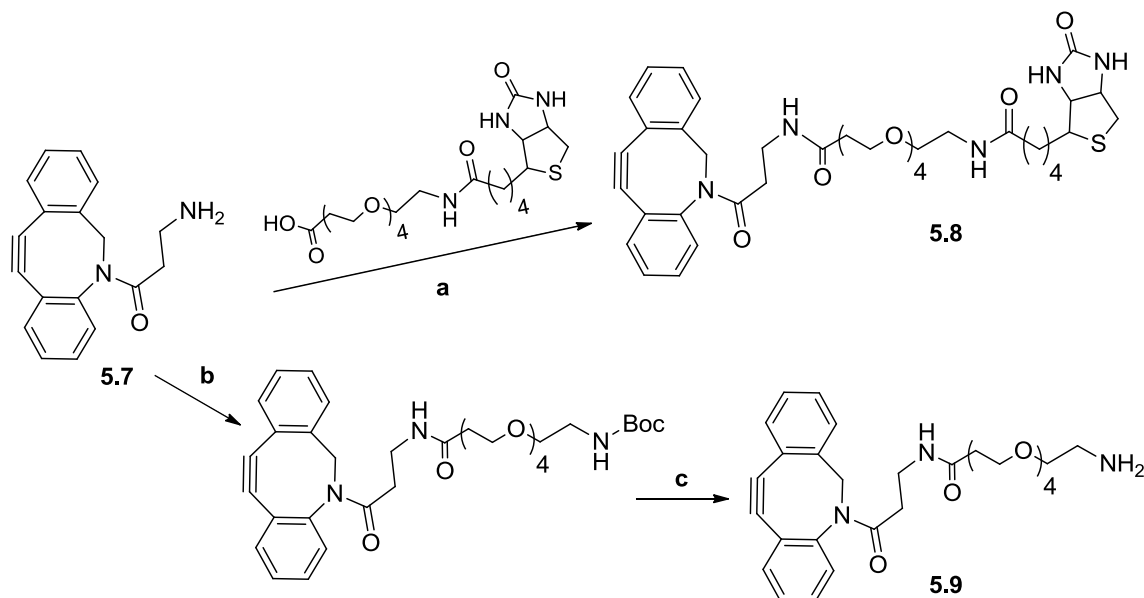


^aReagents and conditions: (a) $\text{NH}_2\text{OH}\cdot\text{HCl}$, pyridine, 60%; (b) PPA, 125 °C, 73%; (c) LiAlH_4 , ether, 58%; (d) pyridine, CH_2Cl_2 , 71%; (e) pyridinium tribromide, 78%; (f) *t*-BuOK, THF, 88%; (g) K_2CO_3 , aq. MeOH, 58%.

Aza-dibenzocyclooctyne-biotin conjugate (ADIBO-biotin, **5.8**) was prepared by HBTU (1-[bis(dimethylamino)methylene]-1*H*-benzotriazolium-3-oxide hexafluorophosphate)-promoted coupling of ADIBO-C3-amine (**5.7**) with biotin-PEG4-acid (Scheme 5.2). EDC-induced coupling of compound **5.7** with *N*-Boc-15-amino-4,7,10,13-tetraoxapentadecanoic acid, followed by trifluoroacetic acid – catalyzed removal of *N*-Boc protection gave Aza-dibenzocyclooctyne-PEG₄-amine (ADIBO-PEG₄-amine, **5.9**, Scheme 5.2).

ADIBO and azide functionalization of glass slides. Derivatization experiments were performed on a glass surfaces due to the ready availability, low cost, high mechanical stability, low intrinsic fluorescence, and easy surface modification techniques of the glass substrate.

Scheme 5.2 Synthesis of ADIBO-biotin (**5.8**) and ADIBO-PEG₄-amine (**5.9**).^a



^aReagents and conditions: (a) HBTU, DIEA, CH₂Cl₂, 89%; (b) Boc-NH-(CH₂CH₂O)₄-CH₂CH₂CO₂H, EDC, DIEA, CH₂Cl₂, 80%; (c) TFA, THF, 79%.

Freshly-prepared epoxide-coated slides were incubated in a DMF solution of ADIBO-amine **5.6** or 6-azidohexylamine in the presence of Hünig's base (*N*-ethyl-*N,N*-diisopropylamine) overnight, and washed with acetone, then methanol (Figure 5.1 and 5.5).

Oregon Green - azide (**5.13**) was used as a model compound to assess the efficiency and kinetics of the metal-free azide click immobilization on ADIBO-coated slides. To ensure that a fluorescent dye is immobilized on the slides only by the click reaction and not due to physical absorption or other chemical reactions, we spotted the epoxy-coated plate with ADIBO-amine **5.6**. After overnight incubation and washing, these plates were immersed in a PBS solution of Oregon Green azide (**5.13**, 0.01 mM) for 100 min and washed using standard procedure. The fluorescence image of the resulting slide demonstrates that dye **5.13** specifically binds to the ADIBO-derivatized surface and not to the rest of the slide (Figure 5.1, insert A).

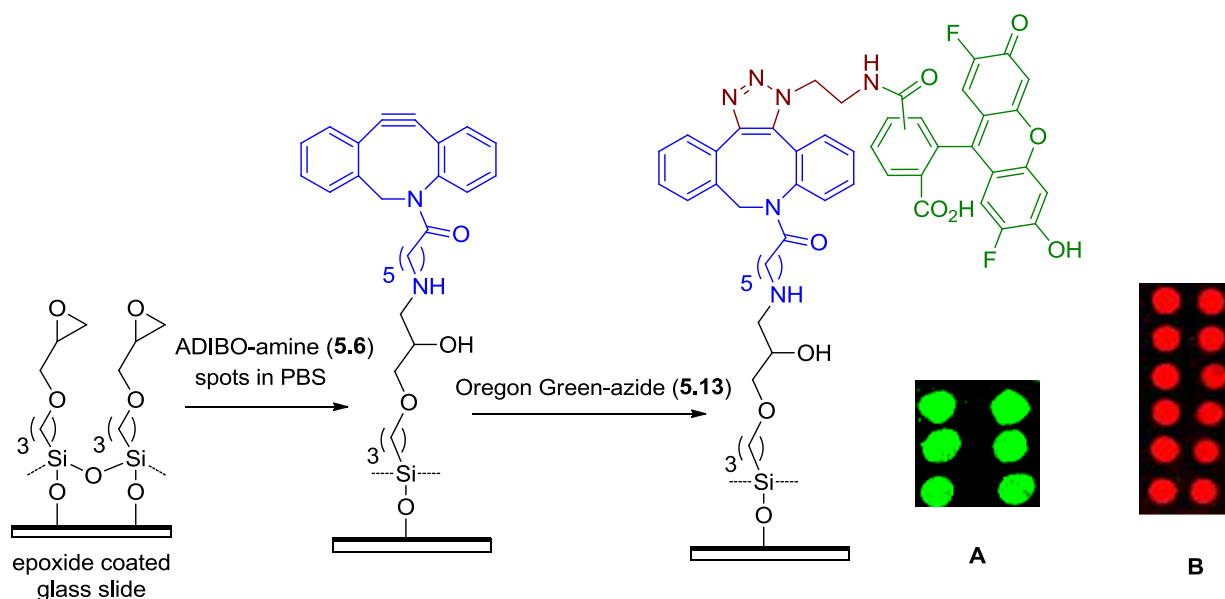


Figure 5.1 Schematic representation of ADIBO derivatization of an epoxy-coated slide followed by copper-free click immobilization of Oregon Green dye. Inserts show fluorescent images ADIBO-slides patterned with (A) Oregon Green azide (**5.13**) and (B) LissamineTM rhodamine B azide (**5.14**).

While the value of relative fluorescence intensity (spot versus background) depends on the starting epoxy plate Oregon Green spots always showed bright fluorescence with 2000-6000 contrast ratios. In addition to epoxy slide prepared in our lab, we have also tested VWR Microarray Epoxy 2 Slides and Corning Epoxide Slides resulting in usually lower intensity. In the following fluorescent dye patterning experiments, 2 μL drops of 0.1 mM or 0.01 mM PBS solutions of azide-dye conjugate were applied onto ADIBO-derivatized slides. Thus, 0.1 mM solution of Lissamine rhodamine B azide (**5.14**) was spotted on the ADIBO-slide, incubated for 1 h and thoroughly washed. The fluorescence image also has a good contrast ratio (Figure 5.1, insert B).

5.4 KINETICS OF METAL-FREE CLICK IMMOBILIZATION

To evaluate the kinetics of the ADIBO – azide reaction on the surface, we spotted 2 μL drops of a 0.1 mM Oregon Green azide (**5.13**) PBS solution onto ADIBO-derivatized slides. The first spot was allowed to react for 284 min; subsequent drops were applied at different times, with the last drop applied just 5 min before washing. The slides were stored in a humidity chamber during this procedure. The immobilization reaction shows excellent kinetics. Within 5 min the relative fluorescent intensity reaches 44–80 % of the maximum value and saturation of fluorescence is achieved at ca. 100 min at 0.1 mM of azide (Figure 5.2).

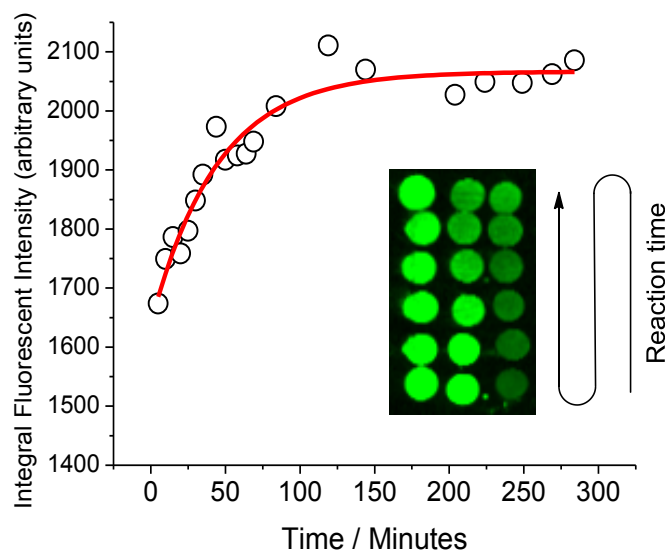


Figure 5.2 Integral fluorescent intensity of Oregon Green azide (**5.13**) spots on ADIBO-derivatized slide versus reaction time.

As a result, incubation with the coupling reagent for 100 min was selected as a standard procedure for subsequent experiments. To optimize the concentration of the substrate for the metal-free click immobilization, we spotted an ADIBO-slide with PBS solutions of various concentration of Oregon Green azide (**5.13**): 10 μM , 50 μM , 0.1 mM, 1 mM, and 5 mM. After incubation for 100 min and washing, the image of the slide was recorded and the integral

fluorescent intensity analyzed (Figure 5.3). The saturation of Oregon Green fluorescence is achieved around 0.1 mM concentration of the azide **5.13**.

Biotinylation of ADIBO-slides and immobilization of Avidin is described below. The exceptional selectivity and high binding constant between avidin and biotin (dissoc. constant = 10^{-15} M)¹⁹ is widely used in bioconjugation and surface immobilization applications.^{1, 2e, 20}

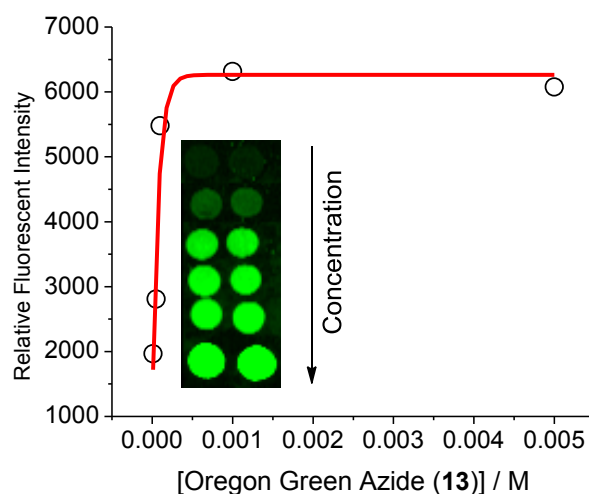


Figure 5.3 Integral fluorescent intensity of Oregon Green azide spots on ADIBO-derivatized slide versus concentration (10 μ M, 50 μ M, 0.1 mM, 1 mM, and 5 mM).

Therefore, we decided to test the efficiency of surface biotinylation using a copper-free azide click reaction. As shown in Figure 5.4, 1 μ L drops of three different concentrations (10 mM, 1 mM, and 0.1 mM) of biotin-dPEG@3+4-azide solutions in PBS were applied onto an ADIBO-functionalized glass slide. For a comparison, 1 μ L drops of a 0.1 mM PBS solution of Oregon Green azide (**5.13**) were also spotted on the slide. To test for the possibility of non-specific absorption of biotin conjugates on the ADIBO-slides, a 1 mM PBS solution of biotin-PEG₄-C \equiv CH was also spotted on the slide. After an hour-long incubation and washing, slides were immersed in a 1% DMF solution of aminoPEG₄azide and incubated overnight. Our initial

experiment showed that dibenzocyclooctynes have significant affinity towards proteins.¹⁹ Exposure to the aminoPEG₄azide solution converts unreacted aza-dibenzocyclooctyne fragments into triazole-PEG conjugates. Patterned biotinylated slides were developed with an avidin-FITC PBS solution for 15 min at 2 °C and washed thoroughly. The fluorescent image of this slide shows selective immobilization of the protein in the biotinylated areas, while non-specific binding of avidin was not observed (Figure 5.4).

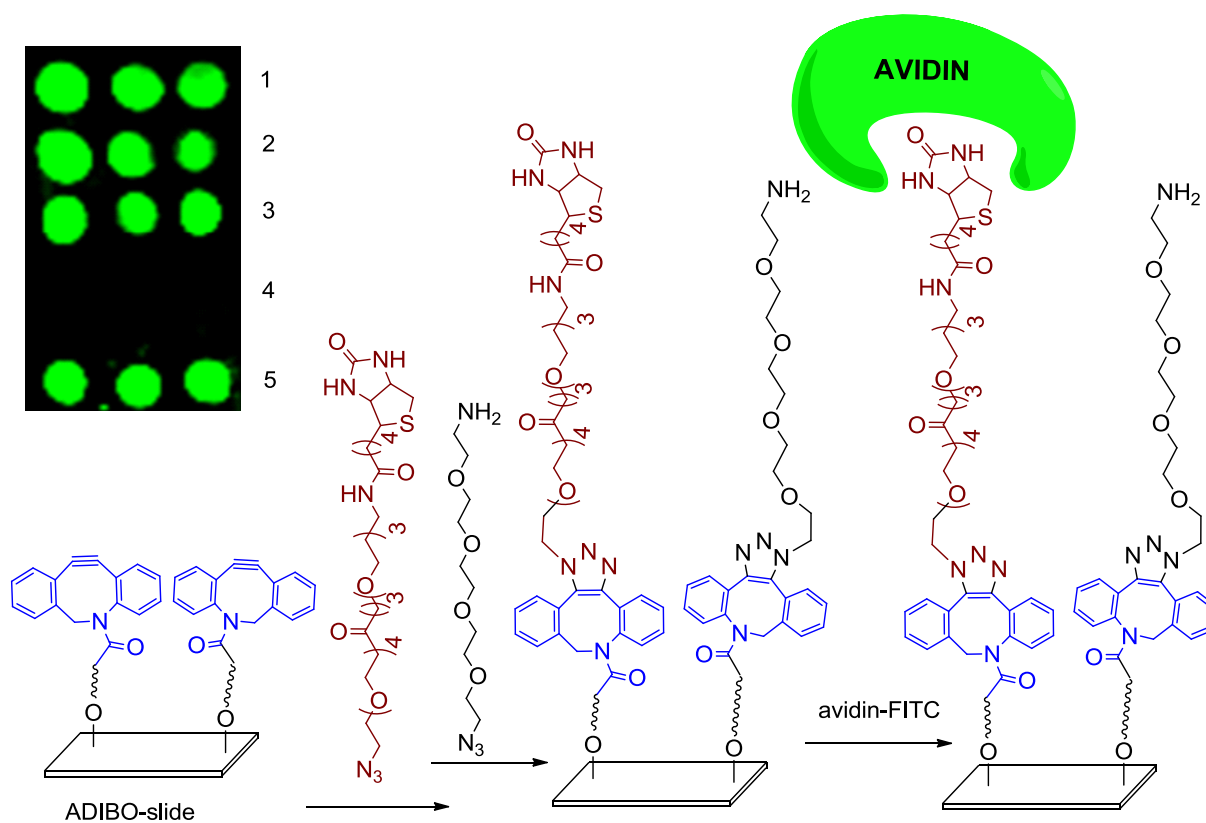


Figure 5.4 Schematic representation of patterned biotinylation of ADIBO-coated slide followed by selective immobilization of avidin-FITC. The insert shows the fluorescent image of ADIBO-slide spotted with 1 μ L of the following solutions: Lane 1 – 3, 10 mM, 1 mM, and 0.1 mM PBS solutions of Biotin-dPEG3+4-azide; Lane 4, 1 mM biotin-PEG₄-C \equiv CH; Lane 5, 0.1 mM of Oregon Green azide (**5.13**). Slide was then treated with aminoPEG₄azide and developed with avidin-FITC solution.

Incubation of the avidin-FITC-patterned slides in a PBS solution containing BSA (*Bovine Serum Albumin*) does not reduce the fluorescence, confirming the immobilization of avidin via

specific biotin-avidin interactions. Globular BSA molecules are usually used as a blocking agent to reduce hydrophobic pockets on the patterned surface. Once blocking of hydrophobic areas has occurred, the areas become more hydrophilic.

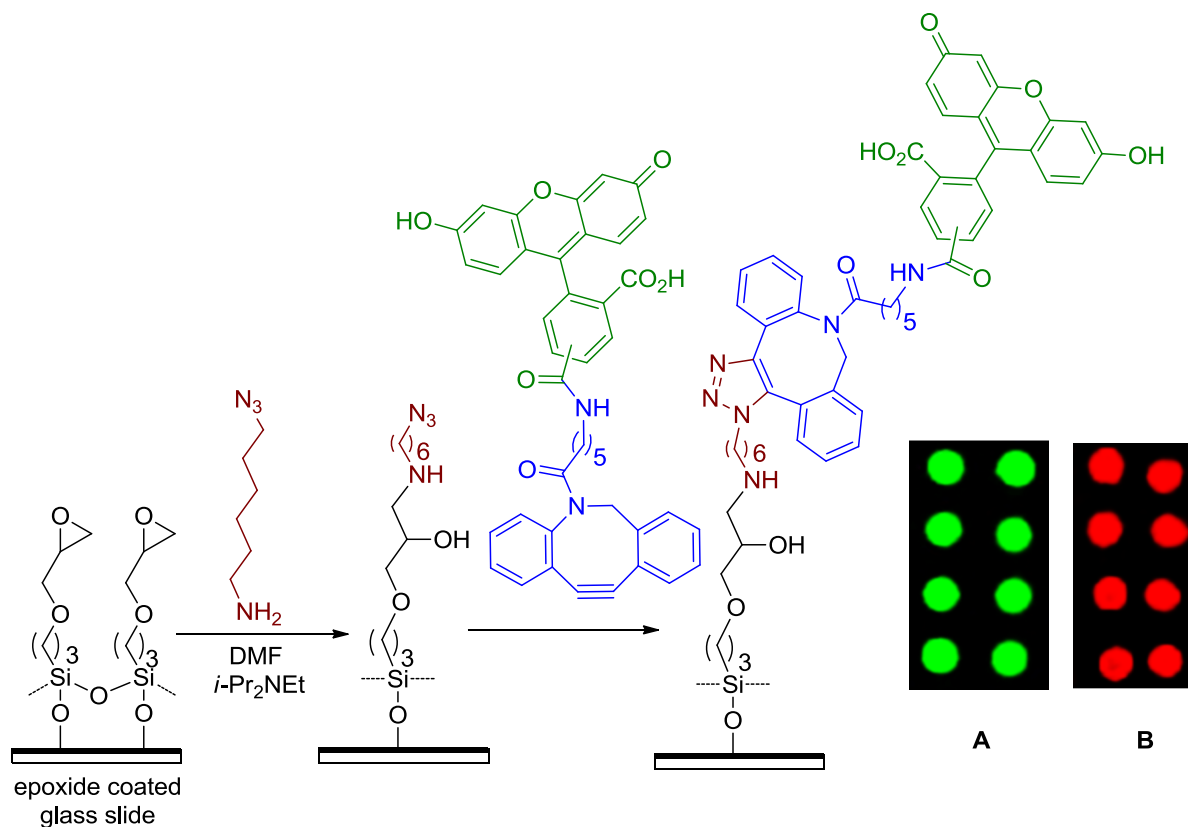


Figure 5.5 Schematic representation of azide derivatization of an epoxy-coated slide followed by copper-free click immobilization of ADIBO-OG (**5.11**). Inserts show fluorescent images of azide-slides patterned with (A) ADIBO-OG (**5.11**); (B) ADIBO-Rhodamine (**5.12**).

Patterning of fluorescent dyes on azide-coated slides was also investigated. To assess the efficiency of a reverse copper-free click surface derivatization, we prepared azide-coated glass slides (*vide supra*). Such a surface provides a convenient platform for immobilization using both conventional copper-catalyzed and catalyst-free azide click reactions. 1 μ L drops of a 1 mM PBS

solutions of aza-dibenzocyclooctyne **6** conjugates with fluorescein (ADIBO-flour, **5.10**) or with Lissamine rhodamine B (ADIBO-Rhodamine, **5.12**), were allowed to react for 12 h, and then washed thoroughly. Fluorescent images of the resulting slides with fluorescein (Figure 5.5, insert A) and Lissamine rhodamine B (Figure 5.5, insert B) illustrate the efficiency of substrate immobilization on the azide-derivatized surface using metal-free click chemistry.

Slides after immobilization are often subjected to vigorous washing procedures, including the use of detergents and sonication in aqueous solutions and organic solvents. To test the stability of the azide surface to the washing procedures and to explore the feasibility of multi-substrate surface derivatization using copper-free click chemistry, we studied the sequential immobilization of two fluorescent dyes. The azide-coated glass slide was initially spotted with 1 μ L drops of a 1 mM PBS solution of ADIBO-flour (**5.10**) and incubated in a humidity chamber for 12 h at rt. The slide was rinsed with acetone, sonicated in DMF for 30 min, and rinsed with distilled water, then immersed in a 0.1 mM solution of ADIBO-Rhodamine (**5.12**) for another 12 h, then thoroughly washed. The fluorescent image recorded with a green (495 - 520 nm) filter clearly shows a pattern of fluorescein – immobilized spots (Figure 5.6, A). The bright background of Lissamine rhodamine B fluorescence and dark spots, where azide groups were consumed in the first step, are visible on the image recorded with a red (532 - 580 nm) filter (Figure 5.6, B). Figure 5.6, insert C, shows merged images A and B, which demonstrates the possibility to put several dyes on the same slide.

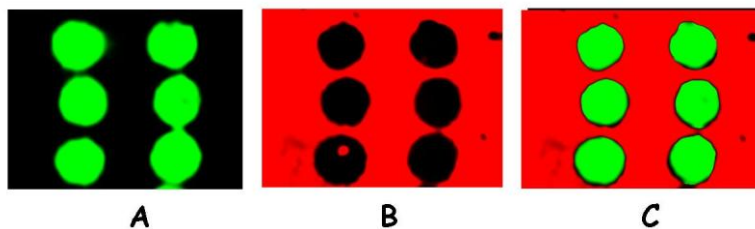


Figure 5.6 Images of two-color derivatization of azide-slides. The slide was spotted with ADIBO-flour (**5.10**), washed and immersed in a solution of ADIBO-Rhodamine (**5.12**). (A) Fluorescent image recorded using 495/520 nm filter; (B) image recorded using 532/580 nm filter; (C) images A and B merged.

Patterned biotinylation of azide-slides and selective immobilization of avidin is described below. To further demonstrate the versatility of the copper-free click reaction for protein immobilization, we have conducted patterned biotinylation of azide-derivatized slides, followed by the immobilization of avidin. Azide-functionalized glass slides was spotted with 1 μ L drops of four different concentrations (10 mM, 1 mM, 0.1 mM, and 0.01 mM) of a PBS solution of ADIBO-biotin (**5.8**). Slides were incubated in a humidity chamber for 30 min, 2.5 h, and 3.5 h and washed with copious amounts of acetone, then water, and sonicated in DMF. To reduce nonspecific binding of the protein, slides were immersed in a blocking solution containing 0.1% ADIBO-PEG₄-amine (**5.9**) in DMF and kept overnight. The slides were then washed, incubated in a solution of avidin-FITC at 2 °C for 15 min, and washed again. As in the case of patterned biotinylation of ADIBO-slides, fluorescent images show selective immobilization of the fluorescently labeled protein in biotinylated areas. No significant non-specific binding of avidin to the slides was observed (Figure 5.7).

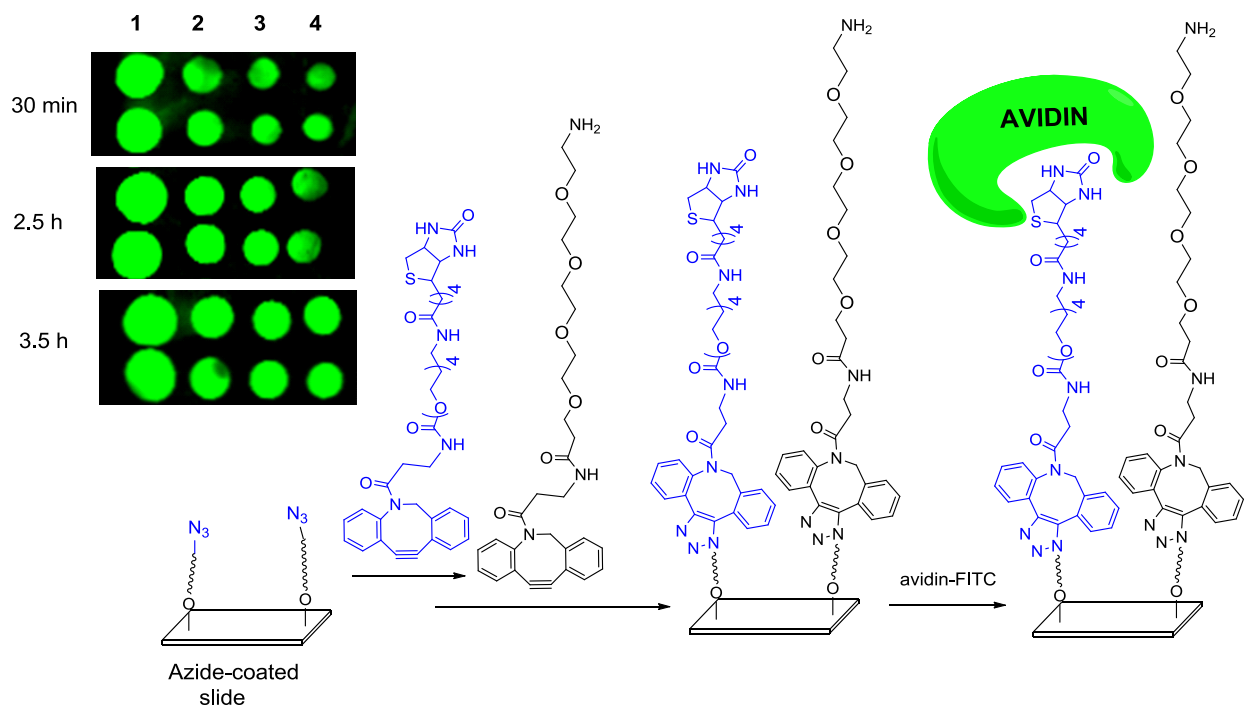


Figure 5.7 Schematic representation of patterned biotinylation of azide-coated slides followed by selective immobilization of avidin-FITC. The insert shows the fluorescent image of azide-derivatized slide spotted with 1 μ L of ADIBO-biotin (**5.8**) solutions of the following concentration: 1) 10 mM; 2) 1 mM; 3) 0.1 mM 4) 0.01 mM. First slide was incubated for 30 min, second – for 2.5 h, and the third – for 3.5 h. Slides were then immersed in a solution of ADIBO-PEG₄-amine, and developed with a solution of avidin-FITC.

Fluorescent intensity of the spots produced at various concentrations of ADIBO-biotin and incubation time illustrate the efficiency of the reaction. Even at 10 μ M concentration of ADIBO-biotin (**5.8**), a 30 min incubation produces a brightly fluorescent spot after avidin-FITC development.

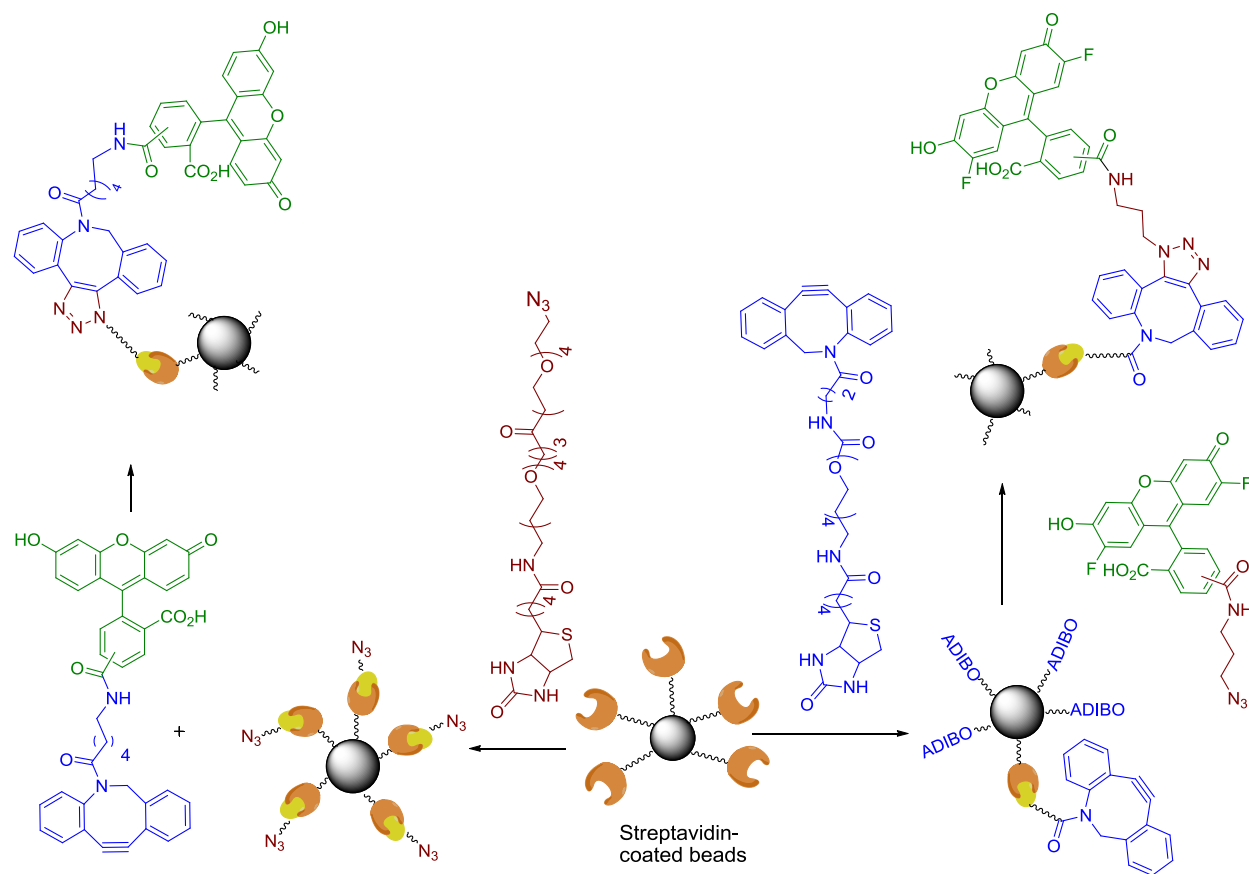


Figure 5.8 Schematic representation of derivatization of streptavidin-coated magnetic beads with azide and aza-dibenzocyclooctyne moieties, followed by the metal-free azide click coupling to fluorescent dyes.

To demonstrate the utility of the copper-free azide click reaction for the modification of microparticle surfaces, we have explored the application of this reaction to the fluorescent labeling of streptavidin-coated magnetic beads. The surface of the beads was derivatized with azide groups by treating a suspension of the beads with biotin-dPEG[®]3+4-azide (Figure 5.8). The aza-dibenzocyclooctyne functionalization of streptavidin beads was achieved by reacting the former with ADIBO-biotin (5.8, Figure 5.8).

The ADIBO-functionalized streptavidin beads were suspended in a PBS solution of Oregon Green azide (**5.13**) and incubated for 3 h at room temperature. Beads were washed and resuspended in PBS for imaging via fluorescent confocal microscopy.

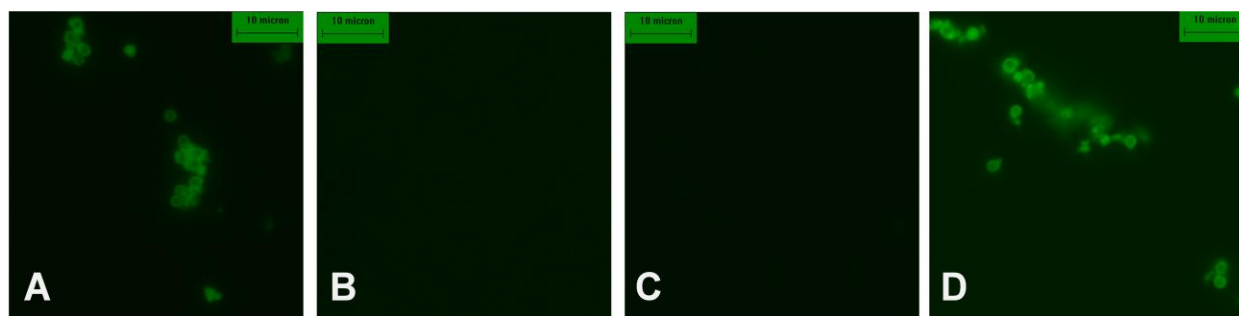


Figure 5.9 Fluorescent confocal microscope images of PBS suspensions of streptavidin-coated magnetic beads: (A) treated with ADIBO-biotin (**5.8**) followed by reaction with Oregon Green azide (**5.13**); (B) treated with biotin-PEG₄-C≡CH and then with Oregon Green azide (**5.13**); (C) incubated with ADIBO-fluor only (**5.10**); (D) treated with biotin-dPEG@3+4-azide and then with incubated ADIBO-fluor (**5.10**).

Figure 5.9A shows the bright fluorescence of these Oregon Green-labeled beads. The starting (unmodified) streptavidin magnetic beads treated with **5.13** under the same conditions show no detectable emission. As an additional control experiment, we have derivatized the beads with terminal acetylene groups by treating streptavidin beads with biotin-PEG₄-C≡CH. Incubation of the resulting particles in an Oregon Green azide (**5.13**) solution, followed by thorough washing, did not induce detectable fluorescence in the beads (Figure 5.9 B). Azide-derivatized microbeads were labeled with fluorescein by reacting them with an ADIBO-fluorescein conjugate (**5.10**, Figure 5.9 C). Magnetic streptavidin beads directly treated with ADIBO-fluor (**5.10**) showed no fluorescence (Figure 5.9 D).

5.5 EXPERIMENTAL SECTION

Materials and Methods:

Preparative reactions were conducted under an air atmosphere. Purification of products by column chromatography was performed using 40-63 μm silica gel. All NMR spectra were recorded on 400 MHz instrument in CDCl_3 and referenced to TMS unless otherwise noted. Images of fluorophore-patterned slides were recorded and fluorescence intensity was quantified using Typhoon 9400 Variable Mode Imager (GE Healthcare) at an excitation / emission setting appropriate for fluorescein (488/520 nm) or LissamineTM rhodamine B (532/580 nm) fluorophores in PBS solution; images of fluorescent microbeads were obtained using Zeiss Observer AX10 inverted microscope with a X-cite Series 120 fluorescent light source and Chroma Technology filters. The relative fluorescent intensity (spot / background) was quantified using ImageJ (NIH) program.

Tetrahydrofuran was distilled from a sodium/benzophenone ketyl; ether and hexanes were distilled from sodium; N,N-Dimethylformamide (DMF) was dried by passing through an alumina column. Biotin-dPEG®3+4-azide and Biotin-PEG4-acid were purchased from Quanta BioDesign; fluorescein SE, Oregon Green® SE, LissamineTM rhodamine B sulfonyl chloride, and FITC-Avidin were obtained from Invitrogen; (3-glycidyloxypropyl)dimethoxymethylsilane was purchased from TCI America; 0.0067 M phosphate buffered saline (PBS) with pH 7.4 was obtained from Thermo Scientific. Bovine Serum Albumin (BSA) was obtained from Fishe BioReagents®. Other reagents were purchased from Aldrich or VWR and used as received unless otherwise noted. Polished glass slides were obtained from VWR and NanoLinkTM streptavidin magnetic microspheres (1% aqueous suspension) were purchased from SoluLink Biosciences. Aza-dibenzocyclooctyne **5.6** conjugates with fluorescein (ADIBO-flour, **5.10**),

Oregon Green® (ADIBO-OG, **5.11**), and Lissamine™ rhodamine B (ADIBO-Rhodamine, **5.12**) were prepared by treating **5.6** with equimolar amounts of fluorescein SE, Oregon Green® SE, Lissamine™ rhodamine B sulfonyl chloride respectively in DMF in the presence of DIEA (diisopropylethylamine). Oregon Green® azide (**5.13**) and Lissamine™ rhodamine B azide (**5.14**) were prepared by reacting equimolar amounts of Oregon Green® SE or Lissamine™ rhodamine B sulfonyl chloride with 3-azidopropyl amine in DMF in the presence of DIEA. Conjugates **5.10** – **5.14** were purified by chromatography (CHCl₃:MeOH:AcOH 100:5:0.5) and their purity was confirmed by HPLC analysis. 1-Amino-11-azido-3,6,9-trioxaundecane (AminoPEG₄azide)²¹ and 6-azidohexylamine²² were prepared according to literature procedures.

5,6-Dihydrodibenzo[b,f]azocine (**5.2**). A solution of dibenzosuberone (25 g, 121 mmol) and hydroxylamine hydrochloride (6.81 mL, 164 mmol) in pyridine (70 mL) was refluxed for 20 h. The reaction mixture was concentrated and poured into 5% aqueous hydrochloric acid (with crushed ice), stirred for 20 min, filtered, and dried in the air to provide 28.1 g of crude dibenzosuberone oxime, as a white precipitate. Dibenzosuberone oxime (16 g, 72.3 mmol) was added to 250 mL polyphosphoric acid at 125 °C, the reaction mixture was stirred for 60 min at this temperature, poured onto crushed ice (~700 mL), stirred for another 30 min, and filtered. The filter cake was washed with water, and dried under vacuum to provide crude dibenzo[b,f]azocin-6(5H)-one **5.1** (11.6 g, 52.4 mmol, 73%) as a grey powder.

A suspension of **5.1** (7.4 g, 33.4 mmol) and lithium aluminum hydride (2.494 mL, 66.9 mmol) in anhydrous ether (200 mL) was refluxed for 15 h. The reaction mixture was quenched by water, filtered, and the filter cake was washed with ether. The filter cake was dispersed in ether (100 mL), stirred for 10 min, and filtered. The combined organic layers were dried over MgSO₄, solvent was removed under vacuum, and the product purified by chromatography

(solvents) to provide 4.04 g (19.49 mmol, 58%) of 5,6-dihydrodibenzo[b,f]azocine (**2**). ^1H : 7.27-7.23 (m, 1 H), 7.2-7.1 (m, 3 H), 6.96-6.9 (m, 1 H), 6.9-6.8 (m, 1 H), 6.65-6.55 (m, 1 H), 6.54-6.48 (m, 1 H), 6.40 (d, $J = 8$ Hz, 1 H), 6.38-6.29 (m, 1 H), 4.51 (d, $J = 6.8$ Hz, 2 H), 4.2 (br s, 1 H); ^{13}C : 147.3, 139.3, 138.3, 134.9, 132.7, 130.3, 129.0, 128.1, 127.8, 127.6, 127.5, 121.8, 118.1, 117.9, 49.6. HRMS (ESI+) calcd for $\text{C}_{15}\text{H}_{14}\text{N}$ $[\text{M}+\text{H}]^+$ 208.1126, found 208.1120.

N-(6-(dibenzo[b,f]azocin-5(6*H*)-yl)-6-oxohexyl)trifluoroacetamide (**5.3**).

6-(trifluoroacetamido)hexa-noyl chloride 23 (0.984 g, 4.52 mmol) was added to a solution of **5.2** (0.75 g, 3.62 mmol) and pyridine (0.859 g (g or mL), 10.86 mmol) in CH_2Cl_2 (ca. 10 mL) at rt, and stirred for 30 min. The reaction mixture was diluted with CH_2Cl_2 (ca. 20 mL), washed with water (2x30 mL), dried over anhydrous MgSO_4 and the solvent was removed under reduced pressure. The residue was purified by chromatography (hexanes:ethyl acetate 2:3) to provide 1.064 g (2.56 mmol, 71%) of **5.3** as yellowish oil. ^1H : δ 7.32-7.22 (m, 4 H), 7.19-7.11 (m, 4 H), 6.77 (d, $J = 13.2$ Hz, 1 H), 6.58 (d, $J = 13.2$ Hz, 1 H), 5.46 (d, $J = 14.8$ Hz, 1 H), 4.20 (d, $J = 14.8$ Hz, 1 H), 3.29-3.15 (m, 2 H), 2.09-2.02 (m, 1 H), 1.93-1.85 (m, 1 H), 1.51-1.32 (m, 4 H), 1.25-1.04 (m, 2 H); ^{13}C : 172.7, 157.5, 141.1, 136.1, 135.8, 134.8, 132.4, 131.8, 130.5, 128.5, 128.2, 128.1, 128.0, 127.3, 127.2, 117.5, 114.6, 54.8, 39.6, 34.3, 28.2, 25.9, 24.3; HRMS (ESI+) m/z calcd for $\text{C}_{23}\text{H}_{24}\text{F}_3\text{N}_2\text{O}_2$ $[\text{M}+\text{H}]^+$ 417.1790, found 417.1783.

N-(6-Trifluoroacetamidohexanoyl)-5,6-dihydro-11,12-didehydrodibenzo[b,f]azocine (**5.5**).

Pyridine hydrobromide perbromide (0.948 g, 2.97 mmol) was added to a solution of **5.3** (1.05 g, 2.70 mmol) in CH_2Cl_2 (4 mL) at rt, and the reaction mixture was stirred overnight. The reaction mixture was diluted with CH_2Cl_2 (20 mL), washed with 5% aqueous hydrochloric acid (mL), dried over MgSO_4 , and solvent removed under vacuum. The residue was passed through a short pad of silica gel (CH_2Cl_2) to give 1.2 g of crude *N*-(trifluoroacetamidohexanoyl)-5,6,11,12-

tetrahydro-11,12-dibromodibenzo[*b,f*]azocine (**5.4**) as waxy semi-solid. To a solution of crude **5.4** (1.2 g, 2.082 mmol) in THF (5 mL) was added to a solution of potassium *t*-butoxide (0.584 g, 5.21 mmol) in THF (10 mL) at rt, the reaction mixture was stirred for 1 h, diluted with ethyl acetate (20 mL), washed with 5% aqueous hydrochloric acid, brine, dried over MgSO₄, and the solvent was removed under reduced pressure. The crude product was purified by chromatography (hexanes:ethyl acetate, 2:1 to 1:1) to afford 0.76 g (1.834 mmol, 88%) of **5.5** as brown oil. ¹H NMR: δ 7.68 (d, *J* = 7.6 Hz, 1 H), 7.45-7.21 (m, 7 H), 6.79 (br s, 1 H), 5.16 (d, *J* = 14.4 Hz, 1 H), 3.67 (d, *J* = 13.6 Hz, 1 H), 3.22-3.14 (m, 1 H), 3.11-3.02 (m, 1 H), 2.24-2.16 (m, 1 H), 1.41-1.22 (m, 4 H), 1.11-0.9 (m, 2 H); MS: *m/z* 414 [*M*⁺]. Calcd for C₂₃H₂₁F₃N₂O₂ 414.

N-(6-Aminohexanoyl)-5,6-dihydro-11,12-didehydrodibenzo[*b,f*]azocine (ADIBO-C6-NH₂, **5.6**).

Solution of K₂CO₃ (2 g, 14.47 mmol) in 15 mL of water was added to a solution of *N*-(6-Trifluoroacetamido hexanoyl)-5,6-dihydro-11,12-didehydrodibenzo[*b,f*]azocine (**5.5**, 2.95 g, 7.12 mmol) in MeOH (30 mL) at rt and stirred overnight. Solvents were removed under reduced pressure, the residue was redissolved in CH₂Cl₂:ethyl acetate (1:4), washed with brine and water. The organic layer was dried over anhydrous Na₂SO₄, and concentrated in vacuum. The crude product was purified by chromatography (CH₂Cl₂:MeOH 10:1 to 10:4) to provide 1.31 g (4.11 mmol, 58%) of **5.6** as slightly yellow oil. ¹H NMR: δ 7.71 (d, *J* = 7.6 Hz, 1 H), 7.45-7.21 (m, 7 H), 5.18 (d, *J* = 14.4 Hz, 1 H), 3.63 (d, *J* = 13.6 Hz, 1 H), 3.55 (m, 4 H), 2.74 (m, 2 H), 2.57 (t, *J* = 6.0 Hz, 2 H), 2.19 (m, 1 H), 1.95 (m, 1 H), 1.41-1.05 (m, 6 H), 1.11-0.9 (m, 2 H); ¹³C: 173.3, 151.8, 147.8, 132.3, 132.1, 128.9, 128.2, 128.0, 127.8, 127.5, 126.5, 122.1, 123.0, 114.8, 107.9, 55.8, 41.4, 34.7, 31.9, 26.0, 24.8; HRMS (ESI+) *m/z* calcd for C₂₁H₂₃N₂O [*M*+H]⁺ 319.1810, found 319.1799.

N-(3-Aminopropionyl)-5,6-dihydro-11,12-didehydrodibenzo[*b,f*]azocine (ADIBO-C3-amine, **5.7**) was prepared following the same protocol as for the preparation of **5.6**. ¹H NMR: (500 MHz): 7.68 (d, *J* = 7.5 Hz, 1 H), 7.45-7.33 (m, 5 H), 7.29 (t, *J* = 7.5 Hz, 1 H), 7.25 (t, *J* = 7 Hz, 1 H), 5.15 (d, *J* = 14 Hz, 1 H), 3.16 (d, *J* = 14 Hz, 1 H), 2.82-2.67 (m, 2H), 2.45-2.35 (m, 1 H), 2.01-1.92 (m, 1 H), 1.6-1.4 (br s, 2 H); ¹³C: 172.14, 151.48, 148.01, 132.12, 129.08, 128.29, 128.21, 127.99, 127.63, 127.01, 125.43, 122.85, 122.57, 114.97, 107.66, 55.25, 38.25, 38.15; HRMS (ESI+) calcd for C₁₈H₁₇N₂O [M+H]⁺ 277.1341, found 277.1339.

Aza-dibenzocyclooctyne-biotin conjugate (ADIBO-biotin, **5.8**).

HBTU (1.916 g, 5.05 mmol) was added to a solution of biotin-PEG4-acid (1.9 g, 3.74 mmol) and DIEA (0.647 g, 5.61 mmol) in CH₂Cl₂ (15 mL) at rt and stirred for 15 min. A solution of **7** (1.238 g, 4.12 mmol) in CH₂Cl₂ (2 mL) was added dropwise, the reaction mixture was stirred for 3 h, and concentrated under reduced pressure (just keep your terminology the same, however you do it). The product was purified by chromatography (CH₂Cl₂ to CH₂Cl₂:MeOH 20:1 to 100:15) to provide 2.44 g (3.32 mmol, 89%) of **5.8** as colorless semi-solid. ¹H NMR (500 MHz, CDCl₃): δ 7.66 (d, *J* = 7 Hz, 1 H), 7.42-7.3 (m, 7 H), 7.28-7.25 (m, 1 H), 7.05-6.99 (m, 1 H), 6.79-6.75 (m, 1 H), 6.61 (br s, 1 H), 5.13 (d, *J* = 14 Hz, 1 H), 4.5-4.45 (m, 1 H), 4.32-4.25 (m, 1 H), 3.68 (d, *J* = 14 Hz, 1 H), 3.65-3.45 (m, 17 H), 3.44-3.36 (m, 2 H), 3.32-3.22 (m, 2 H), 3.15-3.07 (m, 2 H), 2.9-2.82 (m, 1 H), 2.75-2.65 (m, 1 H), 2.55-2.46 (m, 1 H), 2.33 (q, *J* = 6 Hz, 2 H), 2.2 (t, *J* = 7.5 Hz, 2 H), 2.0-1.92 (m, 1 H), 1.75-1.6 (m, 4 H), 1.45-1.35 (m, 5 H); ¹³C: 173.51, 171.99, 171.13, 164.01, 151.1, 148.09, 132.13, 129.14, 128.68, 128.21, 127.83, 127.19, 125.58, 123.07, 122.45, 114.72, 107.86, 70.45, 70.43, 70.39, 70.3, 70.17, 70.03, 69.98, 97.17, 61.83, 60.26, 55.69, 55.52, 53.67, 42.0, 40.52, 39.14, 36.79, 35.89, 35.26,

34.71, 28.29, 28.11, 25.63, 18.59, 17.44, 11.88; HRMS (ESI+) m/z calcd for $C_{39}H_{53}N_5O_8S$ $[M+H]^+$ 750.3537, found 750.3542.

*Aza-dibenzocyclooctyne-PEG₄-amine (ADIBO-PEG₄-amine, **5.9**).*

EDC (0.75 g, 4.68 mmol) was added to a solution of Boc-NH-(CH₂CH₂O)₄-CH₂CH₂CO₂H²⁴ (1.57 g, 4.32 mmol) in CH₂Cl₂ (15 mL) and DIEA (0.7 g, 5.4 mmol) at rt and stirred for 15 min. A solution of ADIBO-amine **7** (1 g, 3.6 mmol) in CH₂Cl₂ (1 mL) was added to the reaction mixture and stirred for 4 h, at which time the solvent was removed under reduced pressure and the crude product purified by chromatography (ethyl acetate:hexanes 1:1 to 9:1) to provide 1.8 g (2.8 mmol, 80%) of crude *N*-Boc-protected ADIBO-PEG₄-amine (**5.9-Boc**) as yellow oil.

A solution of TFA (in what solvent) (0.48 g, 4.2 mmol) was added to a solution of **5.9-Boc** (1.8 g, 2.8 mmol) in THF (30 mL) at rt. The reaction mixture was stirred overnight and the solvent was removed under reduced pressure. The residue was purified by chromatography (CH₂Cl₂:MeOH 10:1 to 10:4) to provide 1.15 g (2.2 mmol, 79%) of ADIBO-PEG₄-amine (**5.9**) as slightly yellow oil. ¹H-NMR (500 MHz): 7.67 (d, J = 7.5 Hz, 1 H), 7.43-7.34 (m, 5 H), 7.31 (t, J = 7.5 Hz, 1 H), 7.29-7.24 (m, 1 H), 6.95-6.88 (m, 1 H), 5.13 (d, J = 14 Hz, 1 H), 4.45-4.2 (br s, 2 H), 3.7-3.5 (m, 22 H), 3.37-3.2 (m, 3 H), 2.68 (t, J = 5 Hz, 2 H), 2.57-2.42 (m, 1 H), 2.4-2.32 (m, 2 H), 2.02-1.92 (1 H); ¹³C-NMR (100 MHz, CDCl₃): 172.13, 171.21, 151.20, 148.16, 129.3, 129.2, 128.78, 128.44, 128.31, 127.9, 127.29, 127.25, 125.68, 123.16, 122.55, 114.81, 107.92, 70.46, 70.39, 70.35, 70.32, 70.30, 70.26, 70.1, 55.62, 48.86, 36.69, 35.41, 34.67; HRMS (ESI+) m/z calcd for $C_{29}H_{38}N_3O_6$ $[M+H]$ 524.2761, found 524.2756.

Cleaning and activation of glass slides surface.

All glass slides were sonicated for 30 min in methanol, rinsed with acetone, and dried in an oven at 145 °C for 1 h. Piranha solution² (90 mL) was prepared by the addition of H₂O₂ (25 mL of 35% v/v) in one portion to 65 mL of conc. H₂SO₄ in a 100 mL Pyrex beaker, which was kept in a water bath. The solution was carefully stirred with a glass rod, followed by inserting glass slides into the solution. After 1 h, slides were removed from the solution and rinsed with copious amounts of distilled water, then acetone, and dried in an oven for 20 min at 145 °C. Glass slides prepared in this fashion were submitted to derivatization procedures immediately.

Preparation of epoxy-derivatized glass slides.

Freshly-activated glass slides were immersed in a solution of freshly-distilled (3-glycidyloxypropyl)dimethoxy-methylsilane (1% v/v) and DIEA (1% v/v) in dry toluene (100 mL) at 25 °C for 16 h. Slides were sonicated two times in methanol for 15 min, thoroughly rinsed with acetone, and dried under a stream of nitrogen.

Preparation of aza-dibenzocyclooctyne (ADIBO, 5.6) - coated glass slides.

Freshly-prepared epoxy-coated glass slides were placed in a solution of aza-dibenzocyclooctyne amine **5.6** (75 mg) and DIEA (1 mL) in DMF (100 mL) and incubated overnight at rt. Slides were then (since you used it below) rinsed with acetone, sonicated for 15 min in methanol, rinsed with acetone, and dried under a stream of nitrogen.

Preparation of azide - coated glass slides. Freshly-prepared epoxy-coated glass slides were immersed in a solution of 6-azidohexylamine (1 mL) and DIEA (1 mL) in DMF (100 mL)

² **Caution:** Piranha solution reacts violently with organic compounds and should be handled with extreme care. Wear thick plastic gloves, lab coat and safety glasses. Any piranha solutions should be handled in a fume hood at all times.

overnight at rt. The slides were then sonicated for 15 min in methanol, rinsed with acetone, and dried under a stream of nitrogen.

Patterned derivatization of glass slides with aza-dibenzocyclooctyne 5.6.

1 μ L drops of 10 mM PBS solution of dibenzocyclooctyne **5.6** were spotted using a micropipette on a freshly-prepared epoxy-coated slide followed by incubation in a humidity chamber containing PBS buffer for 12 h at rt. The slide was washed with copious amounts of acetone, then water, and sonicated in DMF for 30 min.

Patterned immobilization of fluorescent dyes on ADIBO-coated slides.

Solutions of Oregon Green azide (**5.13**, 0.1 mM and 1 mM in PBS) or LissamineTM rhodamine B azide (**5.14**, 0.1 mM) were spotted using a pipette (2 μ L) on a freshly prepared dibenzocyclooctyne plate and incubated in a humidity chamber for various periods of time (*vide infra*). Slides were rinsed with acetone, then sonicated for 15 min in methanol, rinsed with acetone, and dried under a stream of nitrogen.

Patterned immobilization of avidin on ADIBO-coated slides.

1 μ L drops of biotin-dPEG®3+4-azide PBS solutions of different concentrations (10 mM, 1mM, and 0.1 mM) were spotted on a ADIBO-coated glass slide. Slides were incubated in a humidity chamber for 1 h at rt, rinsed with copious amounts of acetone, the water, and sonicated in DMF for 30 min. Slides were then immersed in a blocking solution containing 1% aminoPEG₄azide in DMF and incubated overnight at rt. The slides were then rinsed with acetone, sonicated in DMF for 30 min, and rinsed with distilled water, followed by immersion into a solution of avidin-FITC (50 μ L of 2 mg/mL in 10 mL of PBS) at 2 °C for 15 min. The slides were sonicated in PBS containing 0.1% Tween 20 for 30 min, washed with distilled water,

incubated in PBS containing 0.1% BSA for 12 h at 2 °C, sonicated again in PBS (1% Tween 20) for 30 min, and rinsed with distilled water.

Patterned immobilization of fluorescent probes on azide-coated slides.

1 μ L drops of aza-dibenzocyclooctyne **5.6** conjugates with fluorescein (ADIBO-fluor, **5.10**) solution (1 mM, PBS) (strange sentence- unclear) were spotted on an azide plate followed by incubation in a humidity chamber for 12 h at rt. Slides were rinsed with acetone, then sonicated for 15 min in methanol, rinsed with acetone, and dried under a stream of nitrogen.

For two-color derivatization, azide-coated slides patterned with ADIBO-fluor spots as described above were immersed in a solution of ADIBO-Rhodamine (**5.12**, 1 mM in PBS) and incubated for 3 h at rt. Slides were rinsed with acetone, then sonicated for 15 min in methanol, rinsed with acetone, and dried under a stream of nitrogen.

Patterned immobilization of avidin on azide-coated slides.

1 μ L drops of ADIBO-biotin (**5.8**) solutions of different concentrations (10 mM, 1mM, 0.1 mM, and 0.01 mM in PBS) were spotted on an azide-coated glass slide. Slides were incubated in a humidity chamber for 1 h at rt, rinsed with copious amounts of acetone, then water, and sonicated in DMF for 30 min. Slides were then immersed in a blocking solution containing 0.1% ADIBO-PEG4-amine (**5.9**) in DMF and incubated overnight at rt. The slides were rinsed with acetone, sonicated in DMF for 30 min, and rinsed with distilled water, followed by immersion into a solution of avidin-FITC (50 μ L of 2 mg/mL in 10 mL PBS) at 2 °C for 15 min. The slides were sonicated in a PBS solution containing 0.1% Tween 20 for 30 min, washed with distilled water, incubated in PBS containing 0.1% BSA for 12 h at 2 °C, sonicated again in PBS (1% Tween 20) for 30 min, and rinsed with distilled water.

Preparation of ADIBO-coated magnetic beads.

A solution of ADIBO-biotin conjugate (**5.8**) (25 μ L, 10 mM in PBS) was added to a suspension of streptavidin-coated magnetic beads (25 μ L of 10 mg/mL) in 450 μ L PBS. The resulting mixture was stirred by shaking for 2 h at rt. The reaction mixture was centrifuged at 11,000 rpm for 2 min, the supernatant liquid was decanted, and the pellet resuspended in PBS (450 μ L). The washing step was repeated two times.

Preparation of azide-coated magnetic beads.

A solution of Biotin-dPEG®3+4-azide (25 μ L, 10 mM in PBS) was added to a suspension of streptavidin-coated magnetic beads (25 μ L of 10 mg/mL) in 450 μ L PBS. The resulting mixture was stirred by shaking for 2 h at rt. The reaction mixture was centrifuged at 11,000 rpm for 2 min, the supernatant liquid was decanted, and the pellet resuspended in PBS (450 μ L, pH 7.4). The washing step was repeated two times.

Fluorescent labelling of ADIBO-coated magnetic beads.

A solution of Oregon Green-azide (**5.13**) (10 mM in PBS) was added to a suspension of ADIBO-coated magnetic beads (amounts? solvents?) and incubated for 3 h at rt. Beads were centrifuged at 11,000 rpm for 1 min, the supernatant liquid was decanted, and the pellet resuspended in 450 μ L PBS containing 0.1% Tween 20, centrifuged, washed with PBS, centrifuged and resuspended in 450 μ L PBS for fluorescent microscopy imaging.

Fluorescent labelling of azide-coated magnetic beads.

A solution of ADIBO-fluor (**5.10**, 10 mM in PBS) was added to a suspension of azide-coated magnetic beads and incubated for 3 h at rt. Beads were centrifuged at 11,000 rpm for 1 min, the supernatant liquid was decanted, and the pellet resuspended in 450 μ L PBS containing

0.1% of Tween 20, centrifuged, washed with PBS, centrifuged, and resuspended in 450 μ L PBS for fluorescent microscopy imaging.

5.6 REFERENCES

- (1) (a) Nebhani, L.; Barner-Kowollik, C. Orthogonal Transformations on Solid Substrates: Efficient Avenues to Surface Modification. *Adv. Mat.* **2009**, *21*, 3442-3468; (b) Wong, L. S.; Khan, F.; Micklefield, J. Selective Covalent Protein Immobilization: Strategies and Applications. *Chem. Rev.* **2009**, *109*, 4025-4053; (c) Iha, R. K.; Wooley, K. L.; Nyström, A. M.; Burke, D. J.; Kade, M. J.; Hawker, C. J. Applications of Orthogonal “Click” Chemistries in the Synthesis of Functional Soft Materials. *Chem. Rev.* **2009**, *109*, 5620-5686; (d) Ratner, B. D.; Hoffman, A. S.; Schoen, F. J.; Lemons, J. E., *Biomaterials science: an introduction to materials in medicine*. 2004: Academic Press, San Diego, CA; (e) Im, S. G.; Bong, K. W.; Kim, B.-S.; Baxamusa, S. H.; Hammond, P. T.; Doyle, P. S.; Gleason, K. K. Patterning Nanodomains with Orthogonal Functionalities: Solventless Synthesis of Self-Sorting Surfaces. *J. Am. Chem. Soc.* **2008**, *130*, 14424-14425.
- (2) (a) Fleischmann, S.; Hinrichs, K.; Oertel, U.; Reichelt, S.; Eichhorn, K.-J.; Voit, B. Modification of Polymer Surfaces by Click Chemistry. *Macromol. Rapid. Commun.* **2008**, *29*, 1177-1185; (b) Fournier, D.; Hoogenboom, R.; Schubert, U. S. Clicking polymers: a straightforward approach to novel macromolecular architectures. *Chem. Rev. Soc.* **2007**, *36*, 1369-1380; (c) Michel, O.; Ravoo, B. J. Carbohydrate Microarrays by Microcontact “Click” Chemistry. *Langmuir* **2008**, *24*, 12116-12118; (d) Ku, S.-Y.; Wong, K.-T.; Bard, A. J. Surface Patterning with Fluorescent Molecules Using Click Chemistry Directed by Scanning Electrochemical Microscopy. *J. Am. Chem. Soc.* **2008**, *130*, 2392-2393; (e) Sun, X.-L.; Stabler, C. L.; Cazalis, C. S.; Chaikof, E. L.

Carbohydrate and Protein Immobilization onto Solid Surfaces by Sequential Diels–Alder and Azide–Alkyne Cycloadditions. *Bioconjugate Chem.* **2006**, *17*, 52-57.

- (3) (a) Gramlich, P. M. E.; Wirges, C. T.; Manetto, A.; Carell, T. Postsynthetic DNA Modification through the Copper-Catalyzed Azide-Alkyne Cycloaddition Reaction. *Angew. Chem., Int. Ed.* **2008**, *47*, 8350-8358; (b) Weisbrod, S. H.; Marx, A. Novel strategies for the site-specific covalent labelling of nucleic acids. *Chem. Commun.* **2008**, 5675-5685.
- (4) (a) Fernandez-Suarez, M.; Baruah, H.; Martinez-Hernandez, L.; Xie, K. T.; Baskin, J. M.; Bertozzi, C. R.; Ting, A. Y. Redirecting lipoic acid ligase for cell surface protein labeling with small-molecule probes. *Nat. Biotechnol.* **2007**, *25*, 1483-1487; (b) Ochiai, H.; Huang, W.; Wang, L.-X. Expeditious Chemoenzymatic Synthesis of Homogeneous N-Glycoproteins Carrying Defined Oligosaccharide Ligands. *J. Am. Chem. Soc.* **2008**, *130*, 13790-13803.
- (5) Speers, A. E.; Adam, G. C.; Cravatt, B. F. Activity-Based Protein Profiling in Vivo Using a Copper(I)-Catalyzed Azide-Alkyne [3 + 2] Cycloaddition. *J. Am. Chem. Soc.* **2003**, *125*, 4686-4687.
- (6) Baskin, J. M.; Bertozzi, C. R. Bioorthogonal Click Chemistry: Covalent Labeling in Living Systems. *QSAR Comb. Sci.* **2007**, *26*, 1211-1219.
- (7) (a) Rostovtsev, V. V.; Green, L. G.; Fokin, V. V.; Sharpless, K. B. A Stepwise Huisgen Cycloaddition Process: Copper(I)-Catalyzed Regioselective "Ligation" of Azides and Terminal Alkynes. *Angew. Chem., Int. Ed.* **2002**, *41*, 2596-2599; (b) Hein, J. E.; Fokin, V. V. Copper-catalyzed azide-alkyne cycloaddition (CuAAC) and beyond: new reactivity

- of copper(I) acetylides. *Chem. Soc. Rev.* **2010**, 39, 1302-1315; (c) Mamidyala, S. K.; Finn, M. G. In situ click chemistry: probing the binding landscapes of biological molecules. *Chem. Soc. Rev.* **2010**, 39, 1252-1261.
- (8) Gaetke, L. M.; Chow, C. K. Copper toxicity, oxidative stress, and antioxidant nutrients. *Toxicology* **2003**, 189, 147-163.
- (9) (a) Gierlich, J.; Burley, G. A.; Gramlich, P. M. E.; Hammond, D. M.; Carell, T. Click Chemistry as a Reliable Method for the High-Density Postsynthetic Functionalization of Alkyne-Modified DNA. *Org. Lett.* **2006**, 8, 3639-3642; (b) Burrows, C. J.; Muller, J. G. Oxidative Nucleobase Modifications Leading to Strand Scission. *Chem. Rev.* **1998**, 98, 1109-1152.
- (10) Wang, Q.; Chan, T. R.; Hilgraf, R.; Fokin, V. V.; Sharpless, K. B.; Finn, M. G. Bioconjugation by Copper(I)-Catalyzed Azide-Alkyne [3 + 2] Cycloaddition. *J. Am. Chem. Soc.* **2003**, 125, 3192-3193.
- (11) Bernardin, A.; Cazet, A. I.; Guyon, L.; Delannoy, P.; Vinet, F. o.; Bonnaffé, D.; Texier, I. Copper-Free Click Chemistry for Highly Luminescent Quantum Dot Conjugates: Application to in Vivo Metabolic Imaging. *Bioconjugate Chem.* **2010**, 21, 583-588.
- (12) Wittig, G.; Krebs, A. On the existence of low-membered cycloalkynes. *Chem. Ber.* **1961**, 94, 3260-3275.
- (13) Ess, D. H.; Jones, G. O.; Houk, K. N. Transition States of Strain-Promoted Metal-Free Click Chemistry: 1,3-Dipolar Cycloadditions of Phenyl Azide and Cyclooctynes. *Org. Lett.* **2008**, 10, 1633-1636.

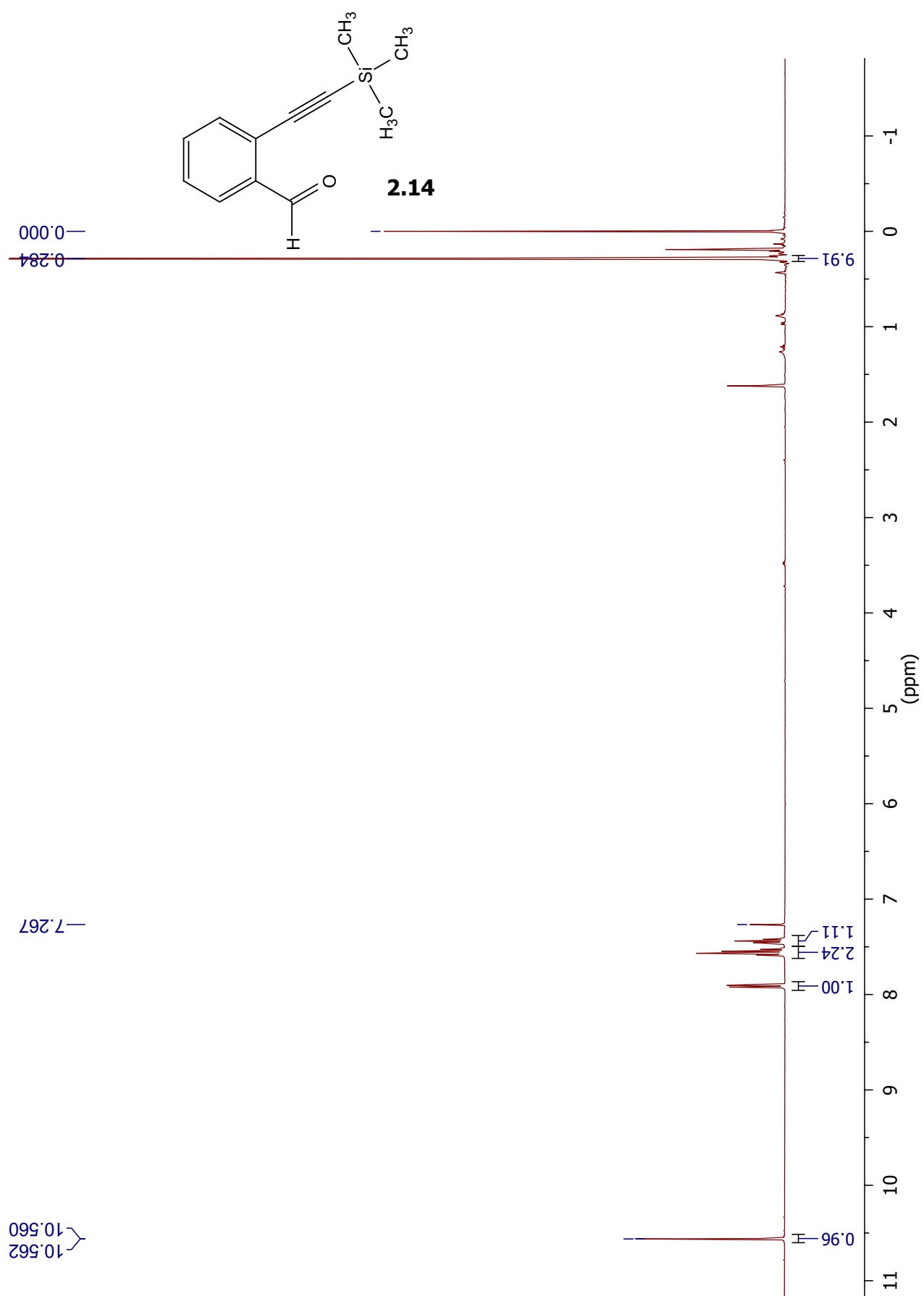
- (14) (a) Baskin, J. M.; Prescher, J. A.; Laughlin, S. T.; Agard, N. J.; Chang, P. V.; Miller, I. A.; Lo, A.; Codelli, J. A.; Bertozzi, C. R. Copper-free click chemistry for dynamic in vivo imaging. *Proc. Natl. Acad. Sci. U.S.A.* **2007**, *104*, 16793-16797; (b) Sletten, E. M.; Bertozzi, C. R. A Hydrophilic Azacyclooctyne for Cu-Free Click Chemistry. *Org. Lett.* **2008**, *10*, 3097-3099; (c) Codelli, J. A.; Baskin, J. M.; Agard, N. J.; Bertozzi, C. R. Second-Generation Difluorinated Cyclooctynes for Copper-Free Click Chemistry. *J. Am. Chem. Soc.* **2008**, *130*, 11486-11493; (d) Jewett, J. C.; Sletten, E. M.; Bertozzi, C. R. Rapid Cu-Free Click Chemistry with Readily Synthesized Biarylazacyclooctynones. *J. Am. Chem. Soc.* **2010**, *132*, 3688-3690; (e) Ning, X.; Guo, J.; Wolfert, Margreet A.; Boons, G.-J. Visualizing Metabolically Labeled Glycoconjugates of Living Cells by Copper-Free and Fast Huisgen Cycloadditions. *Angew. Chem., Int. Ed.* **2008**, *47*, 2253-2255; (f) Debets, M. F.; Berkel, S. S. V.; Schoffelen, S.; Rutjes, F. P. J. T.; Hest, J. C. M. v.; Delft, F. L. v. Aza-dibenzocyclooctynes for fast and efficient enzyme PEGylation via copper-free (3+2) cycloaddition. *Chem. Commun.* **2010**, *46*, 97-99.
- (15) (a) Link, A. J.; Vink, M. K. S.; Agard, N. J.; Prescher, J. A.; Bertozzi, C. R.; Tirrell, D. A. Discovery of aminoacyl-tRNA synthetase activity through cell-surface display of noncanonical amino acids. *Proc. Natl. Acad. Sci. U. S. A.* **2006**, *103*, 10180-10185; (b) Fernandez-Suarez, M.; Baruah, H.; Martinez-Hernandez, L.; Xie, K. T.; Baskin, J. M.; Bertozzi, C. R.; Ting, A. Y. Redirecting lipoic acid ligase for cell surface protein labeling with small-molecule probes. *Nat. Biotechnol.* **2007**, *25*, 1483-1487; (c) Zou, Y.; Yin, J. Cu-free cycloaddition for identifying catalytic active adenylation domains of nonribosomal peptide synthetases by phage display. *Bioorg. Med. Chem. Lett.* **2008**, *18*, 5664-5667; (d) Nessen, M. A.; Kramer, G.; Back, J.; Baskin, J. M.; Smeenk, L. E. J.; de

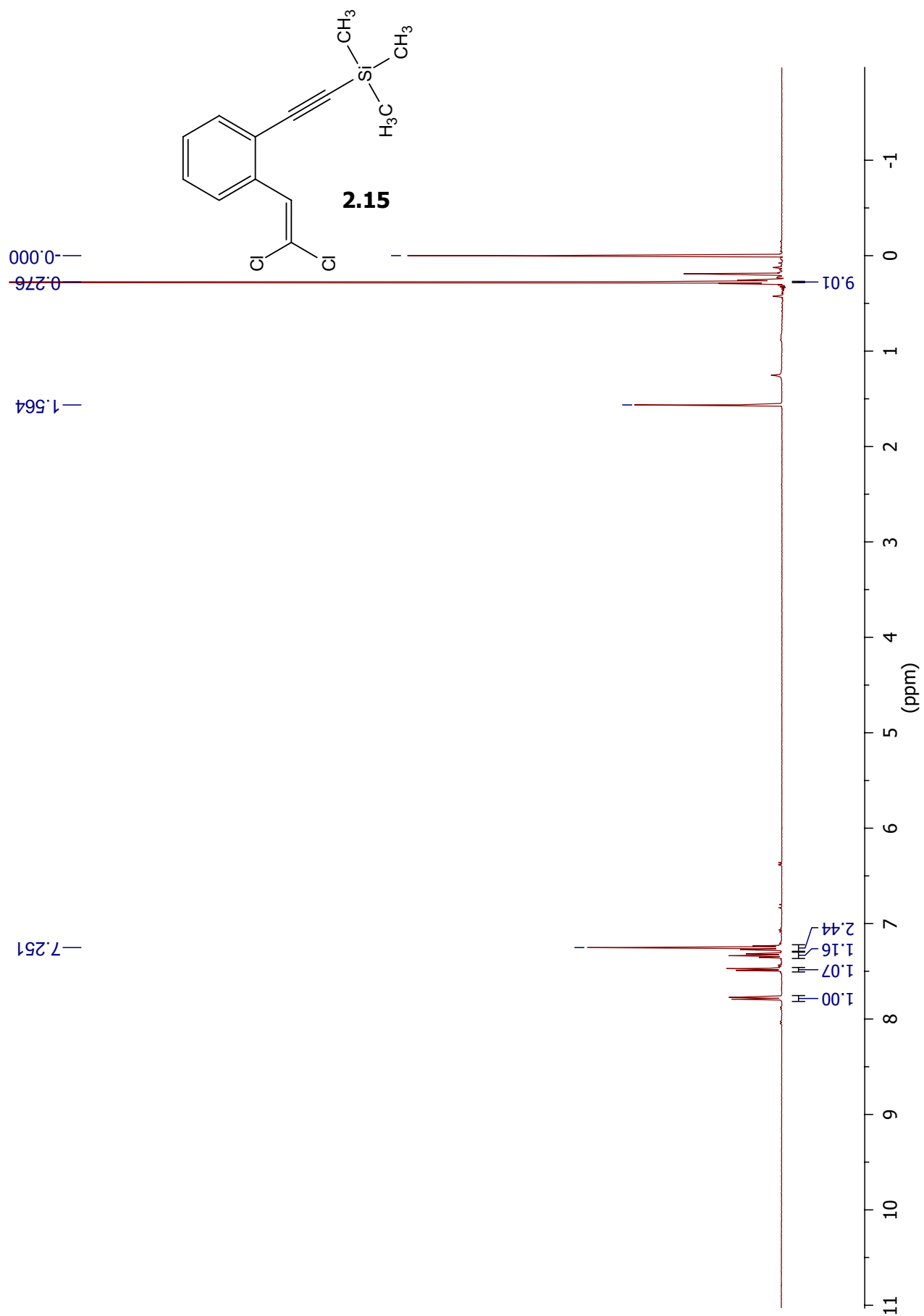
- Koning, L. J.; van Maarseveen, J. H.; de Jong, L.; Bertozzi, C. R.; Hiemstra, H.; de Koster, C. G. Selective Enrichment of Azide-Containing Peptides from Complex Mixtures. *J. Proteome Res.* **2009**, *8*, 3702-3711.
- (16) (a) Wilson, J. T.; Krishnamurthy, V. R.; Cui, W.; Qu, Z.; Chaikof, E. L. Noncovalent Cell Surface Engineering with Cationic Graft Copolymers. *J. Am. Chem. Soc.* **2010**, *132*, 2845-2845; (b) Poloukhine, A. A.; Mbua, N. E.; Wolfert, M. A.; Boons, G.-J.; Popik, V. V. Selective Labeling of Living Cells by a Photo-Triggered Click Reaction. *J. Am. Chem. Soc.* **2009**, *131*, 15769-15776.
- (17) (a) Laughlin, S. T.; Baskin, J. M.; Amacher, S. L.; Bertozzi, C. R. In Vivo Imaging of Membrane-Associated Glycans in Developing Zebrafish. *Science* **2008**, *320*, 664-667; (b) Chang, P. V.; Prescher, J. A.; Sletten, E. M.; Baskin, J. M.; Miller, I. A.; Agard, N. J.; Lo, A.; Bertozzi, C. R. Copper-free click chemistry in living animals. *Proc. Nat. Acad. Sci.* **2010**, *107*, 1821-1826.
- (18) Seitz, G.; Pohl, L.; Pohlke, R. 5,6-Didehydro-11,12-dihydrodibenzo[a,e]-cyclooctene. *Angew. Chem., Int. Ed.* **1969**, *8*, 447-448.
- (19) Green, N. M. Avidin and streptavidin. *Methods Enzymol.* **1990**, *184*, 51-67.
- (20) (a) Jacobs, A. T.; Marnett, L. J. Systems Analysis of Protein Modification and Cellular Responses Induced by Electrophile Stress. *Acc. Chem. Res.* **2010**, *43*, 673-683; (b) Wilchek, M.; Bayer, E. A. Introduction to avidin-biotin technology. *Methods Enzymol.* **1990**, *184*, 5-13; (c) Mader, H. S.; Link, M.; Achatz, D. E.; Uhlmann, K.; Li, X.; Wolfbeis, O. S. Surface-Modified Upconverting Microparticles and Nanoparticles for Use in Click Chemistries. *Chem. Eur. J.* **2010**, *16*, 5416-5424; (d) Böttcher, T.; Sieber, S.

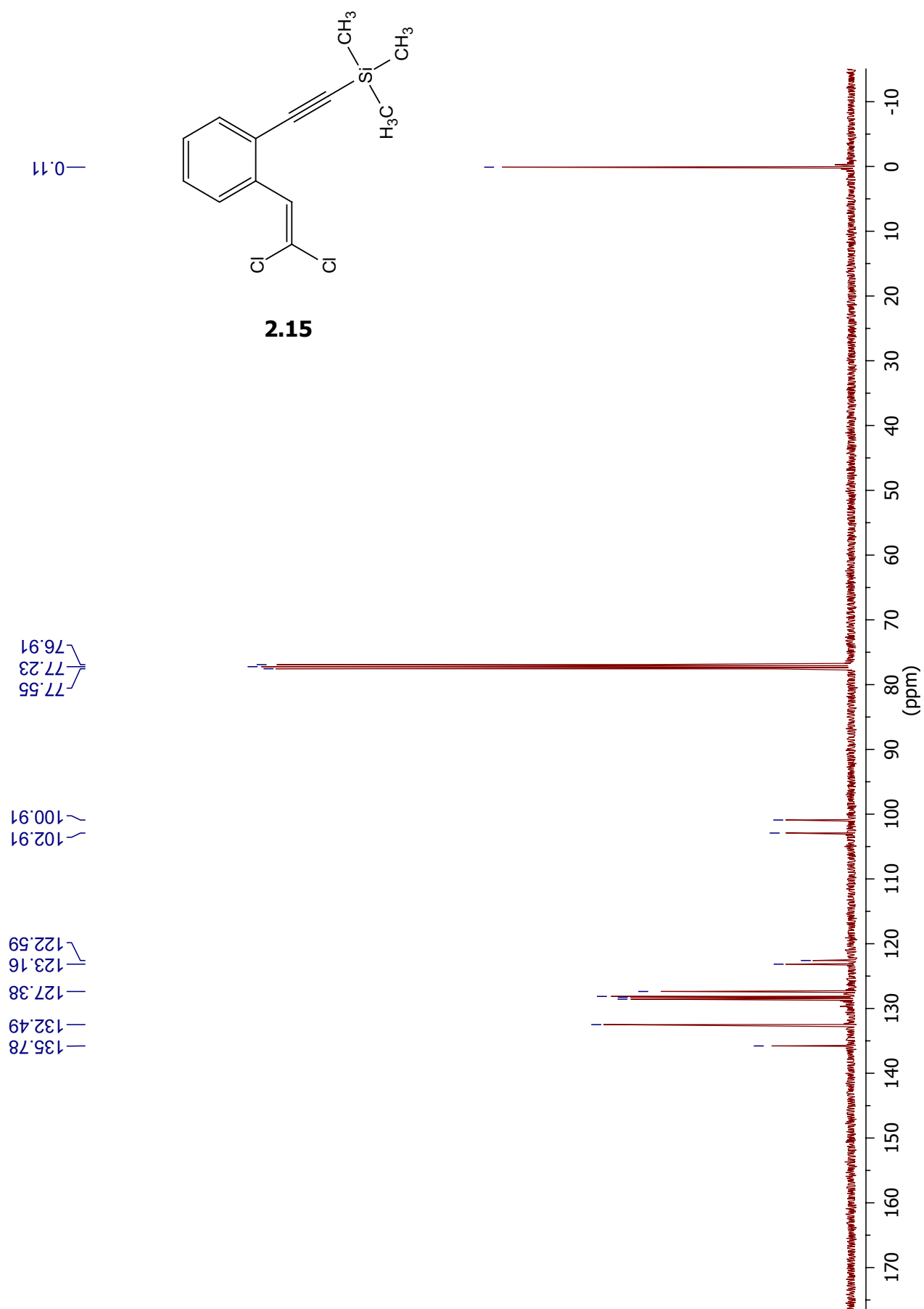
- A. Showdomycin as a Versatile Chemical Tool for the Detection of Pathogenesis-Associated Enzymes in Bacteria. *J. Am. Chem. Soc.* **2010**, *132*, 6964-6972; (e) Landi, F.; Johansson, C. M.; Campopiano, D. J.; Hulme, A. N. Synthesis and application of a new cleavable linker for "click"-based affinity chromatography. *Org. Biomol. Chem.* **2010**, *8*, 56-59; (f) Zhang, J.; Wang, X.; Wu, D.; Liu, L.; Zhao, H. Bioconjugated Janus Particles Prepared by in Situ Click Chemistry. *Chem. Mater.* **2009**, *21*, 4012-4018.
- (21) Schwabacher, A. W.; Lane, J. W.; Schiesher, M. W.; Leigh, K. M.; Johnson, C. W. Desymmetrization Reactions: Efficient Preparation of Unsymmetrically Substituted Linker Molecules. *J. Org. Chem.* **1998**, *63*, 1727-1729.
- (22) Lee, J. W.; Jun, S. I.; Kim, K. An efficient and practical method for the synthesis of mono-N-protected α,ω -diaminoalkanes. *Tetrahedron Lett.* **2001**, *42*, 2709-2711.
- (23) Clark, J. S.; Hodgson, P. B.; Goldsmith, M. D.; Street, L. J. Rearrangement of ammonium ylides produced by intramolecular reaction of catalytically generated metal carbenoids. Part 1. Synthesis of cyclic amines. *Chem. Soc. Perkin Trans. 1* **2001**, 3312-3324.
- (24) Pessi, A.; Bianchi, E.; Ingallinella, P., *Preparation of cholesterol derivatives of peptidyl inhibitors of viral fusion*, in *PCT Int. Appl.* 2009. p. 39.

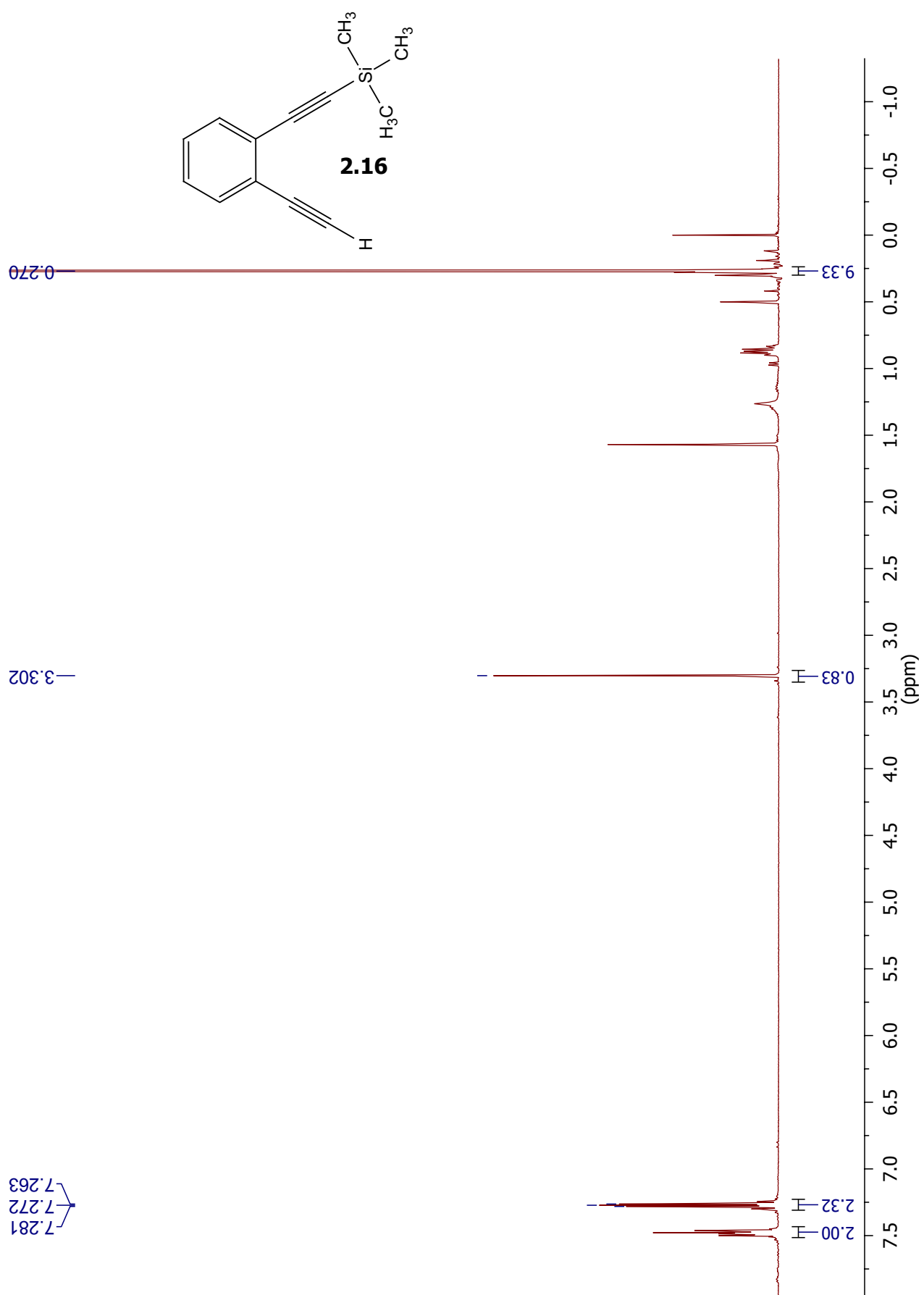
APPENDIX A

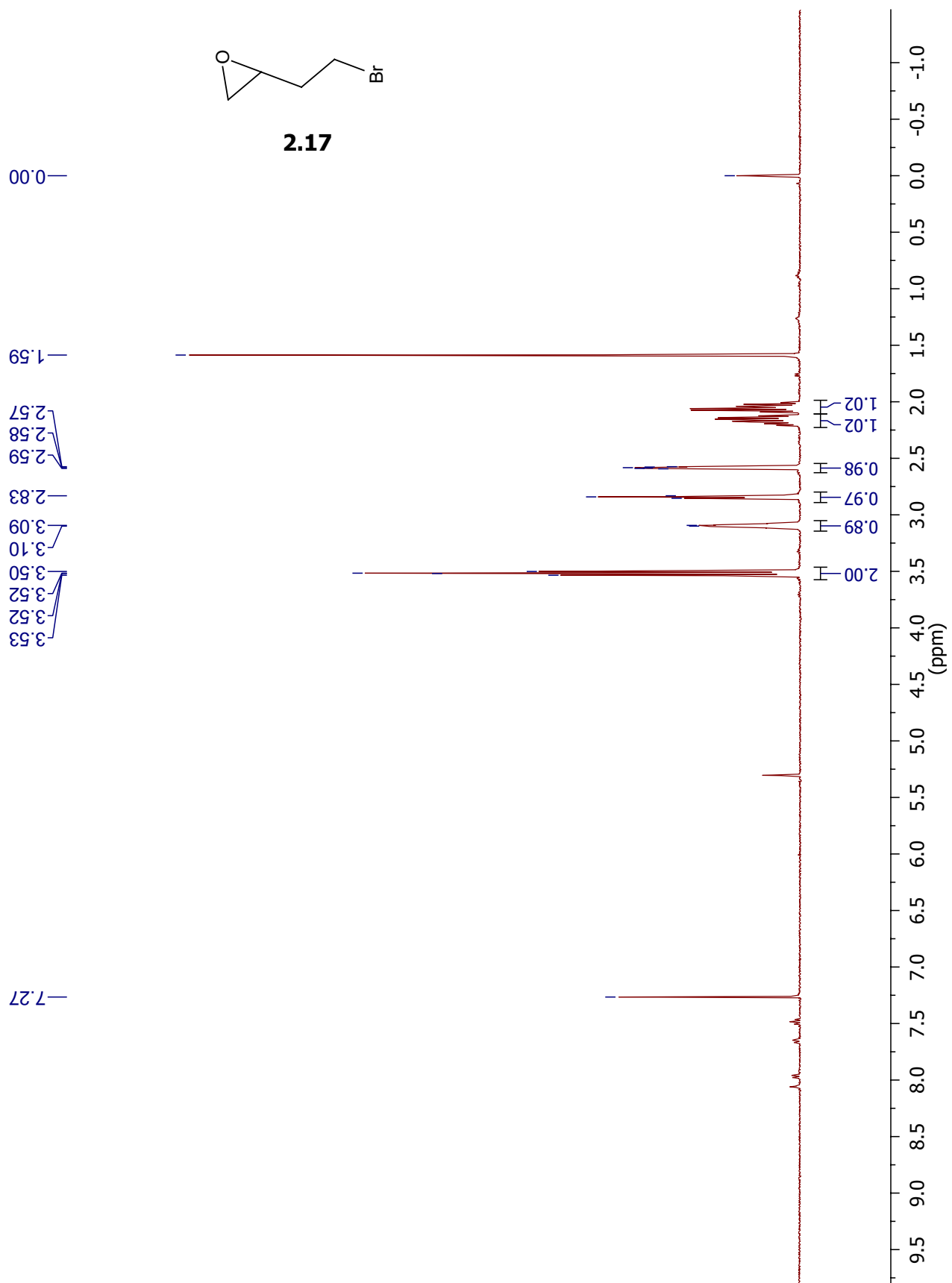
^1H -NMR (1D/2D), ^{13}C -NMR (1D/2D)

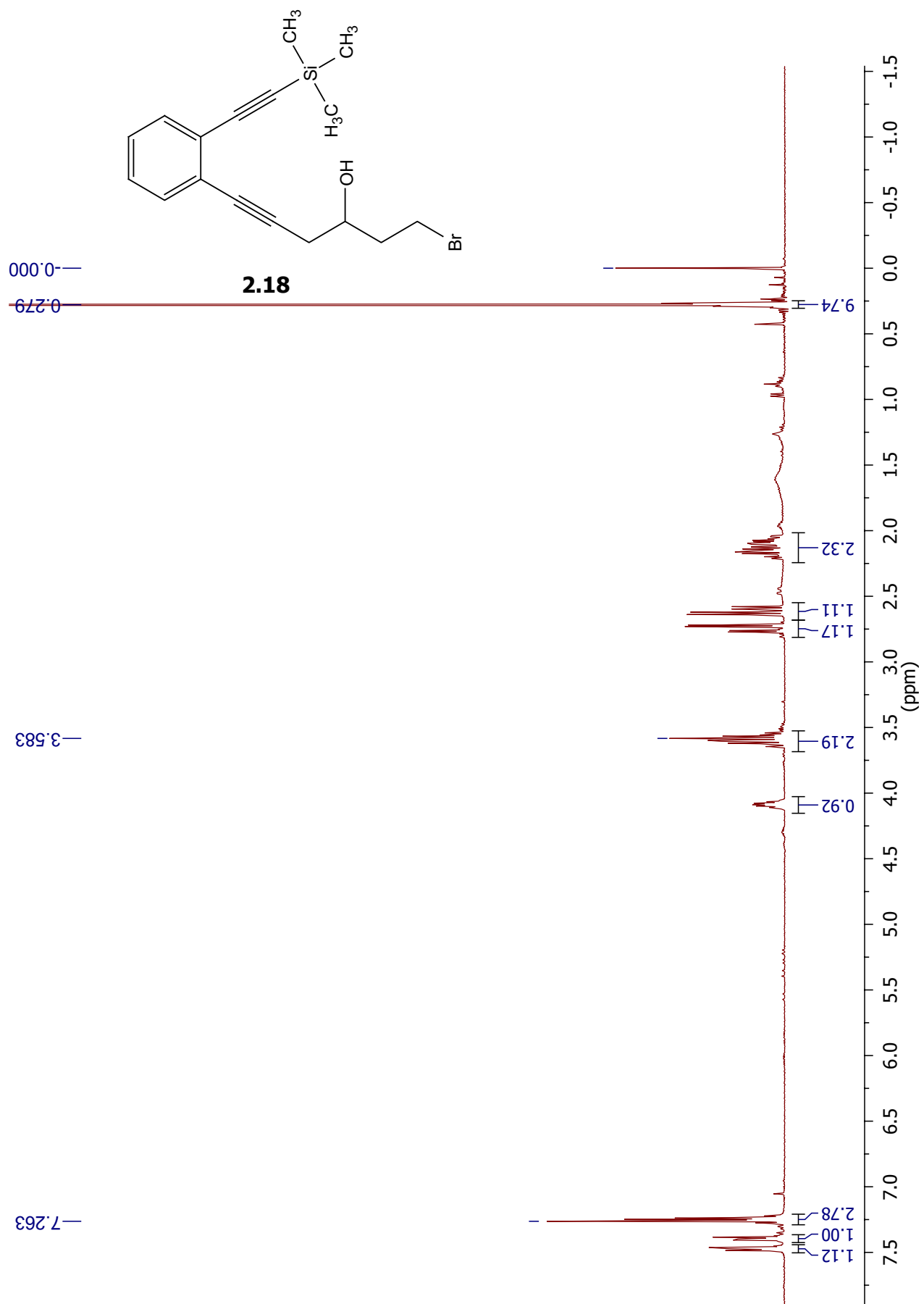


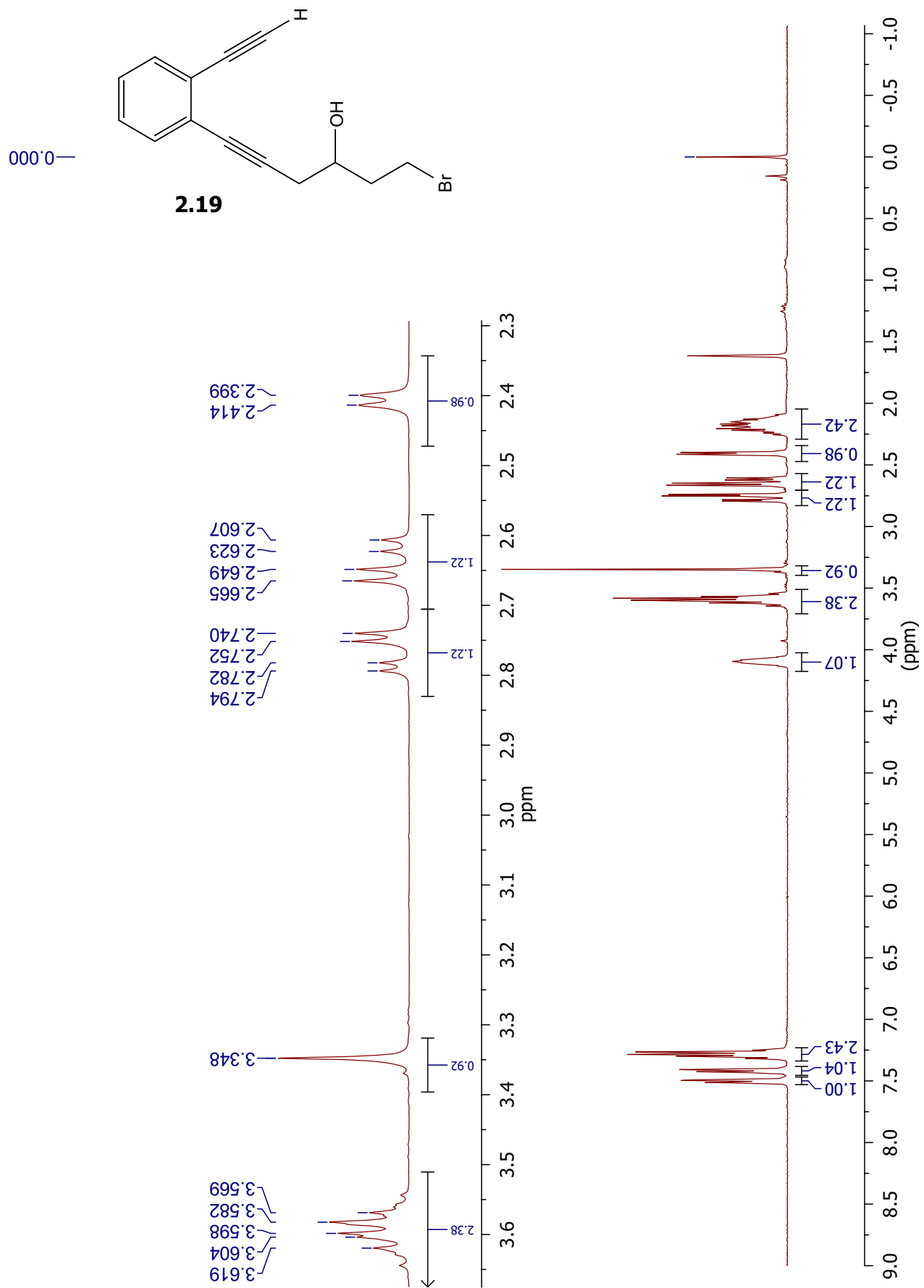


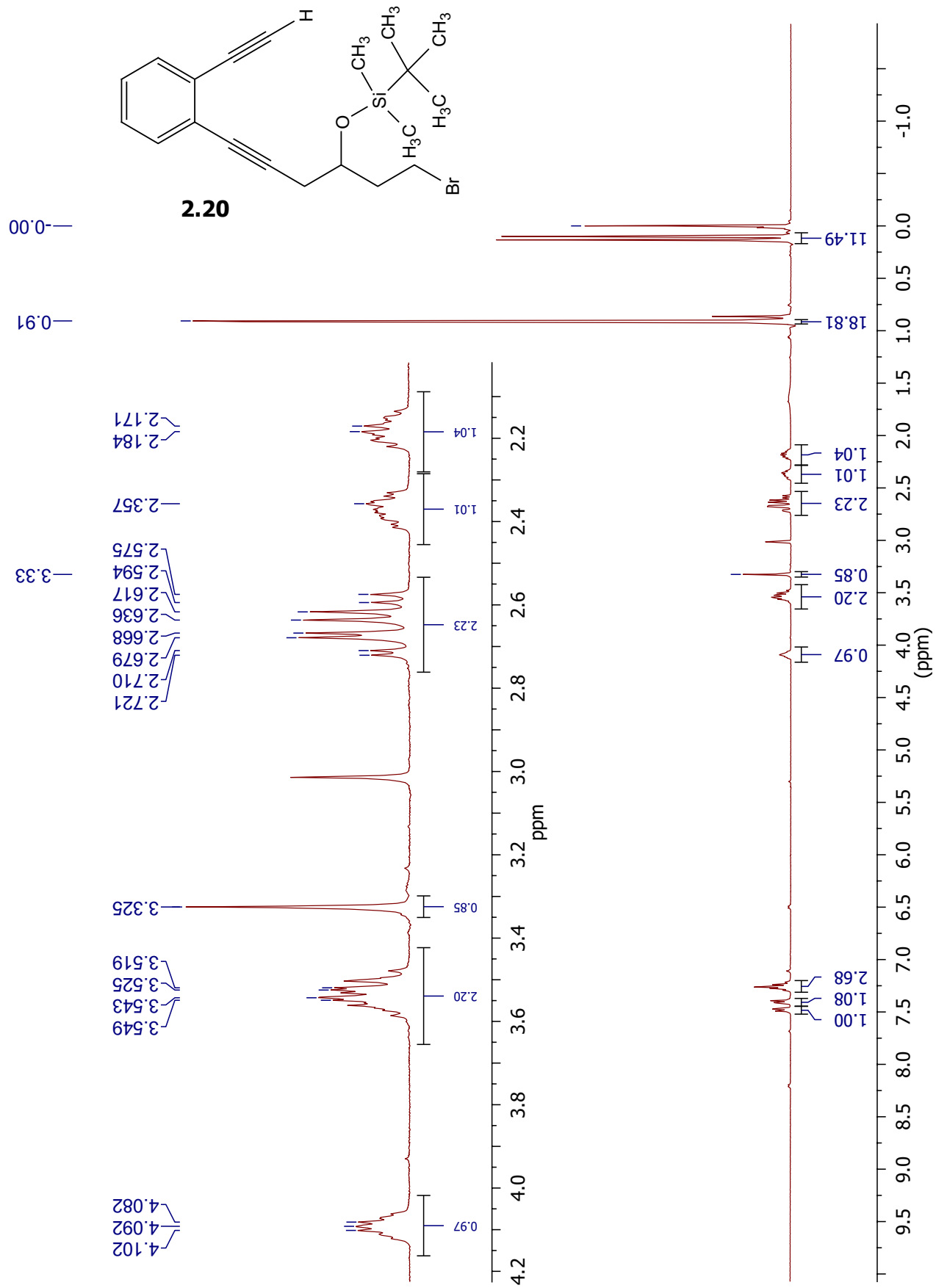


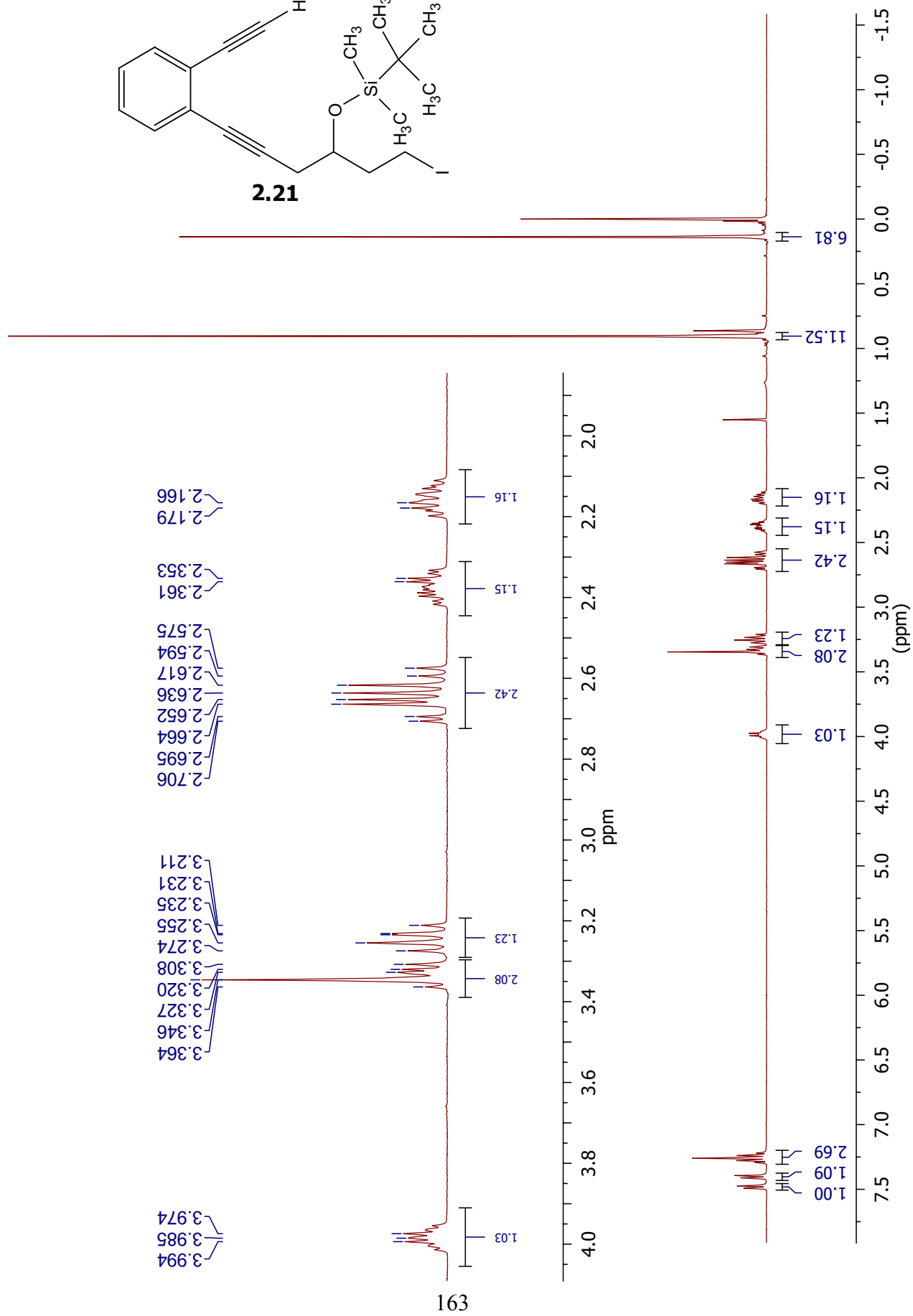
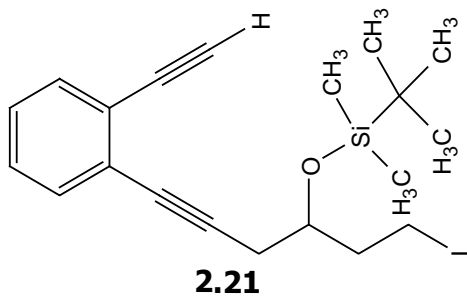


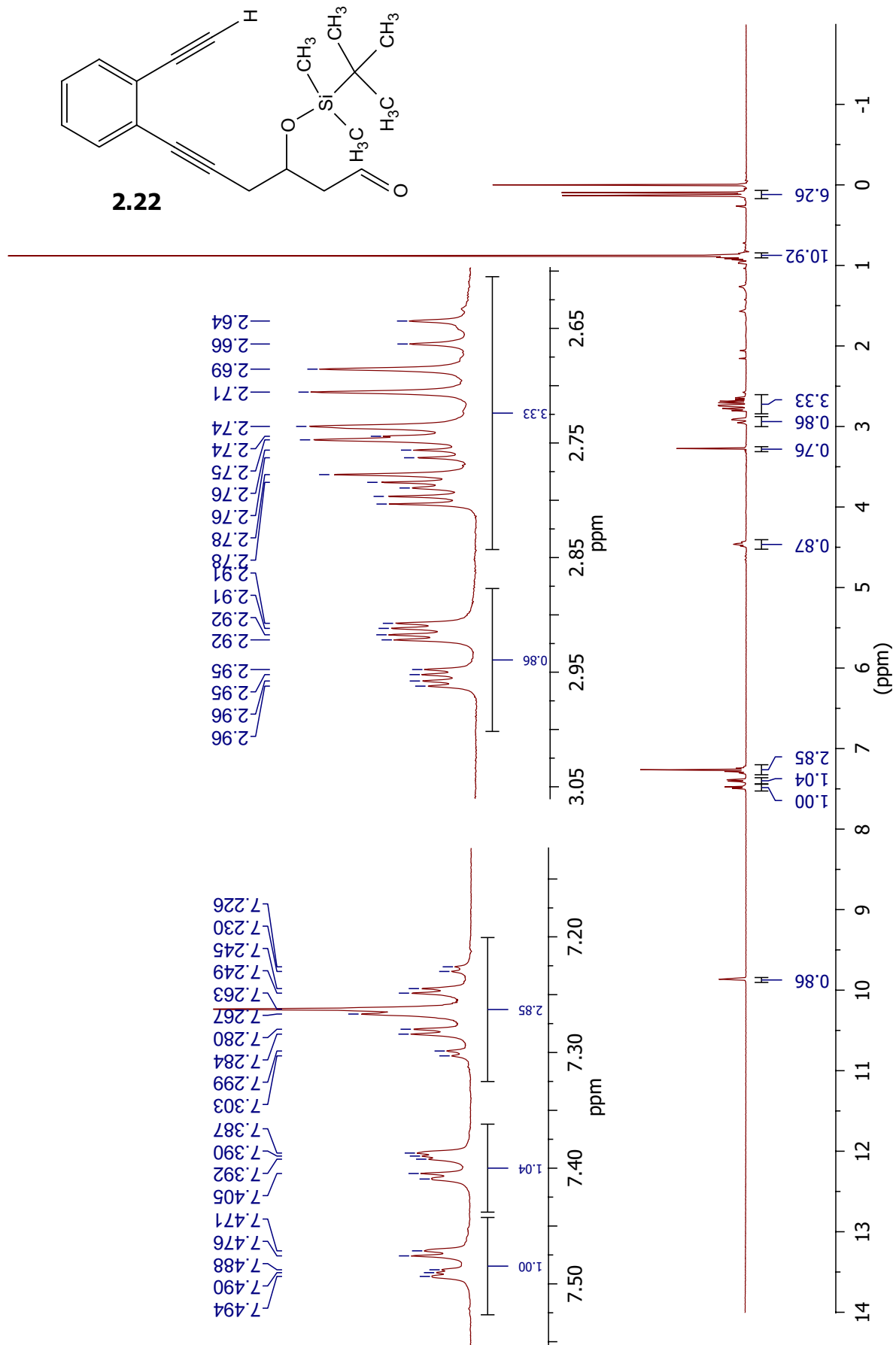


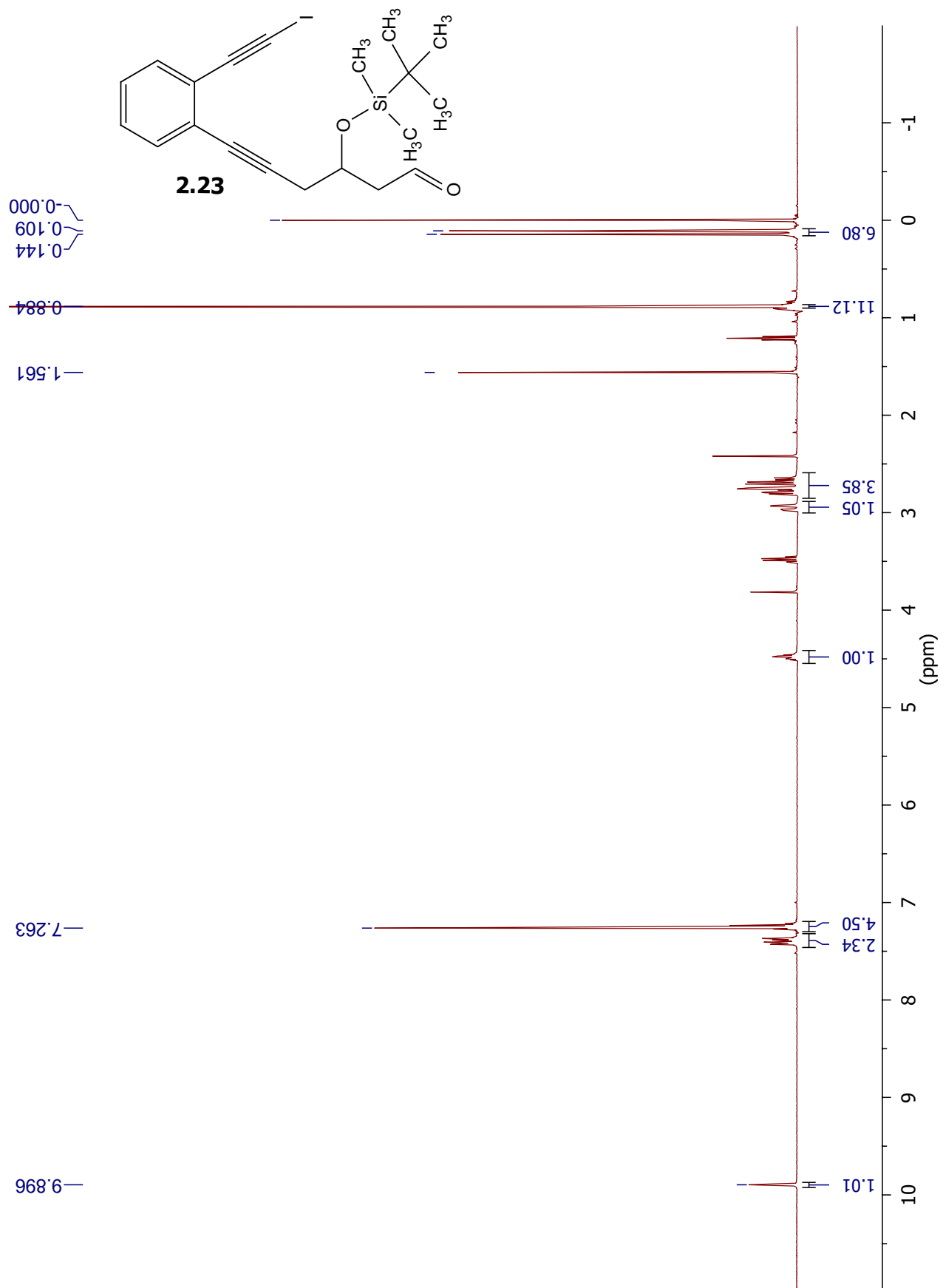


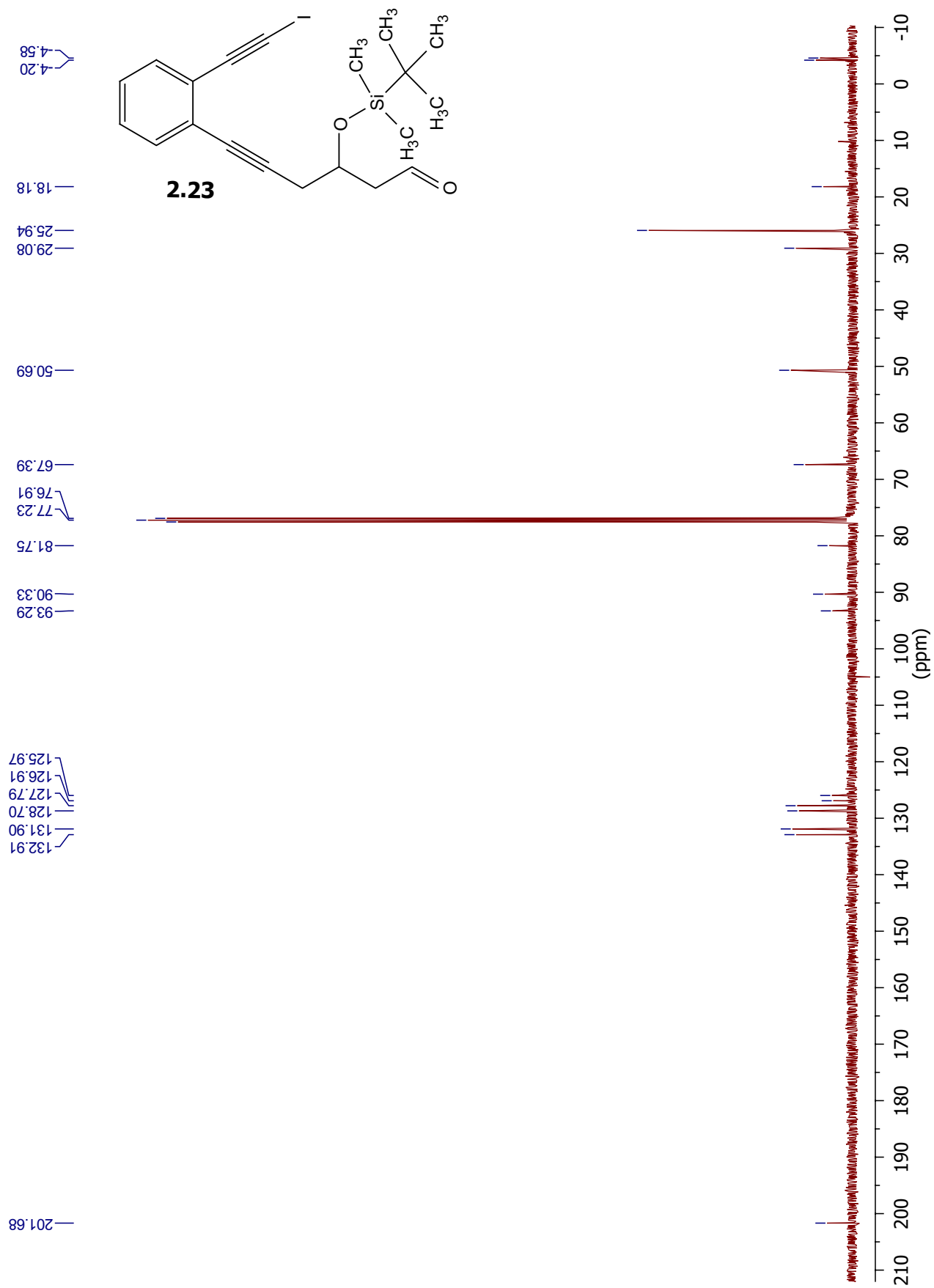


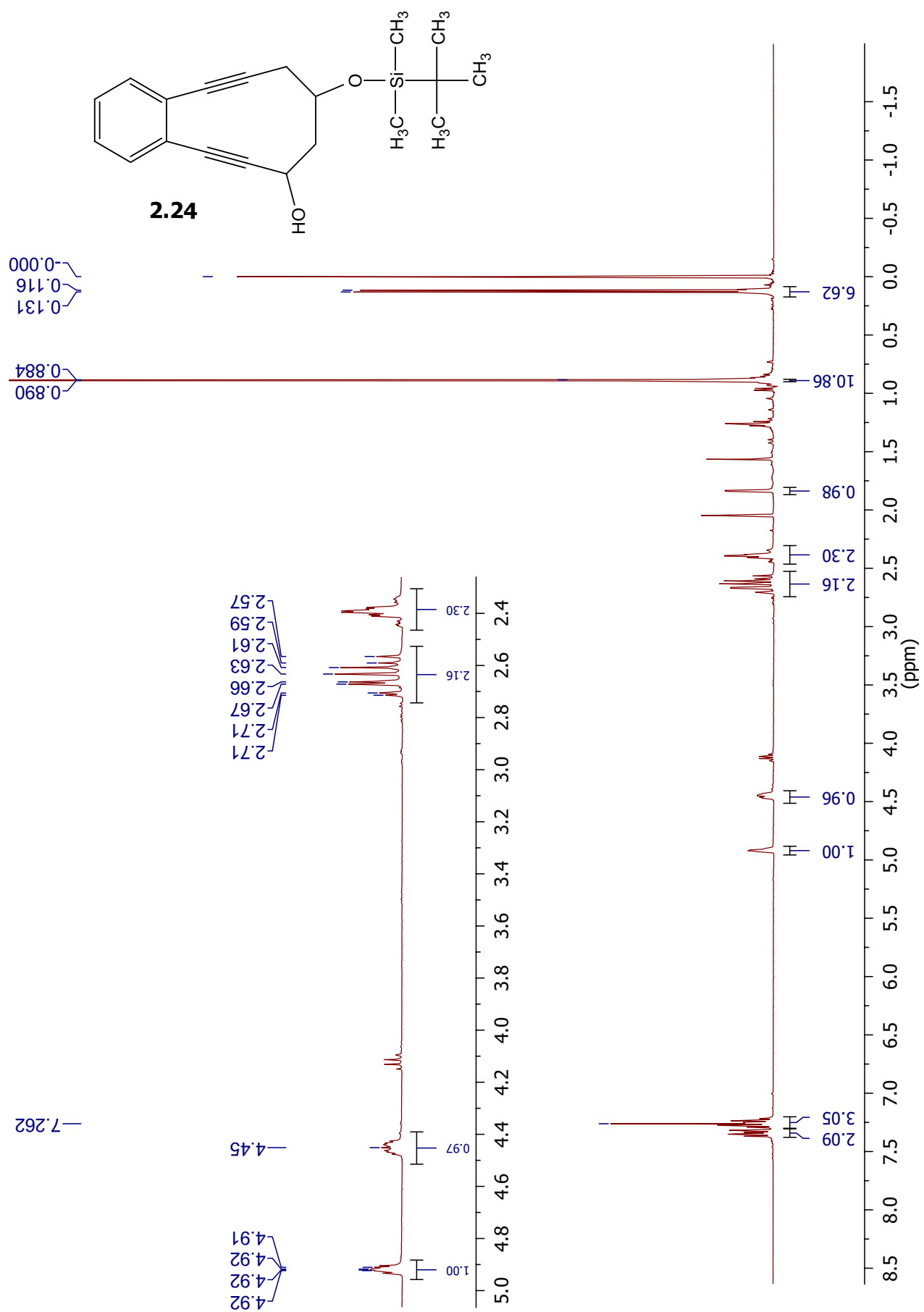


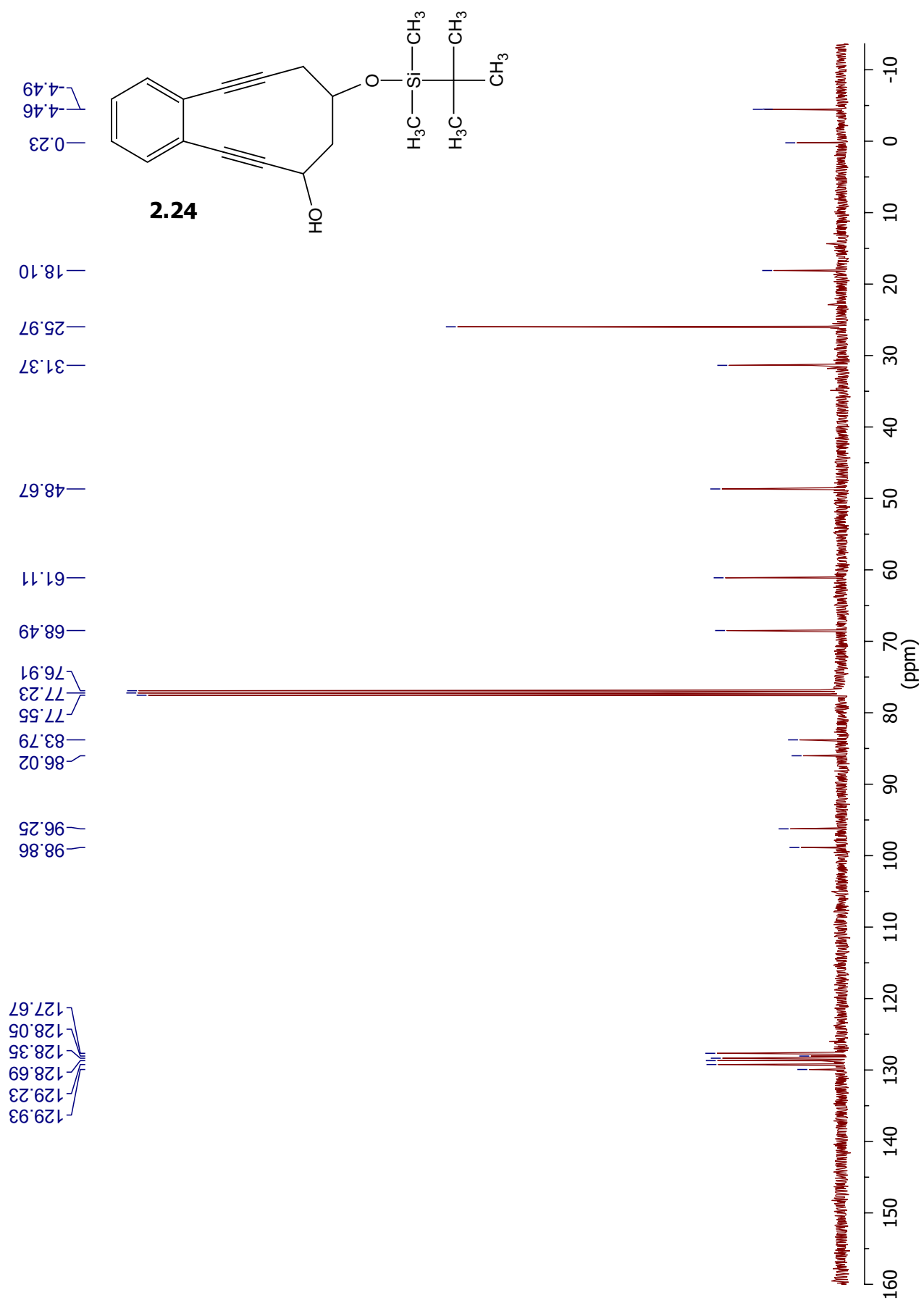


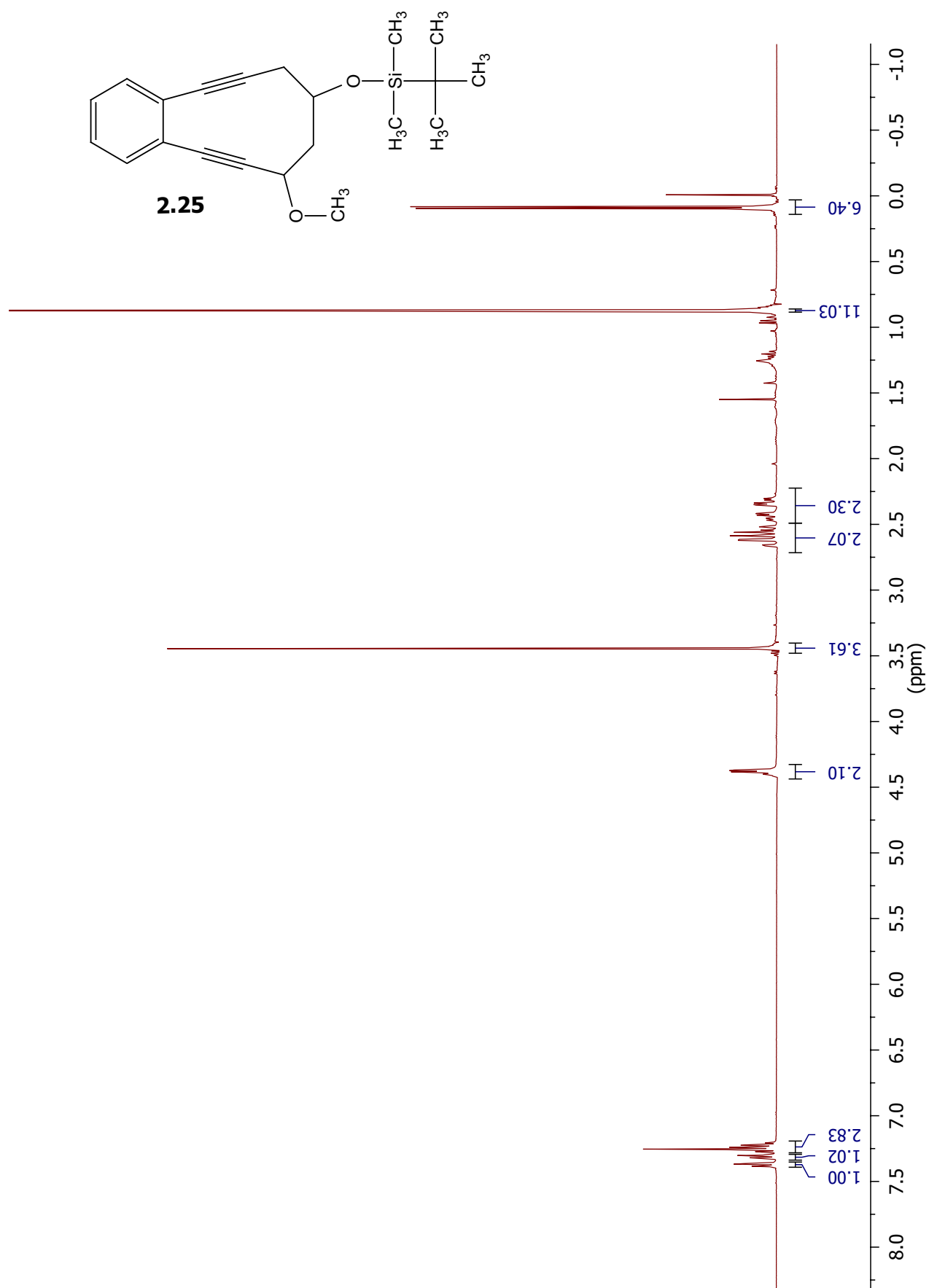


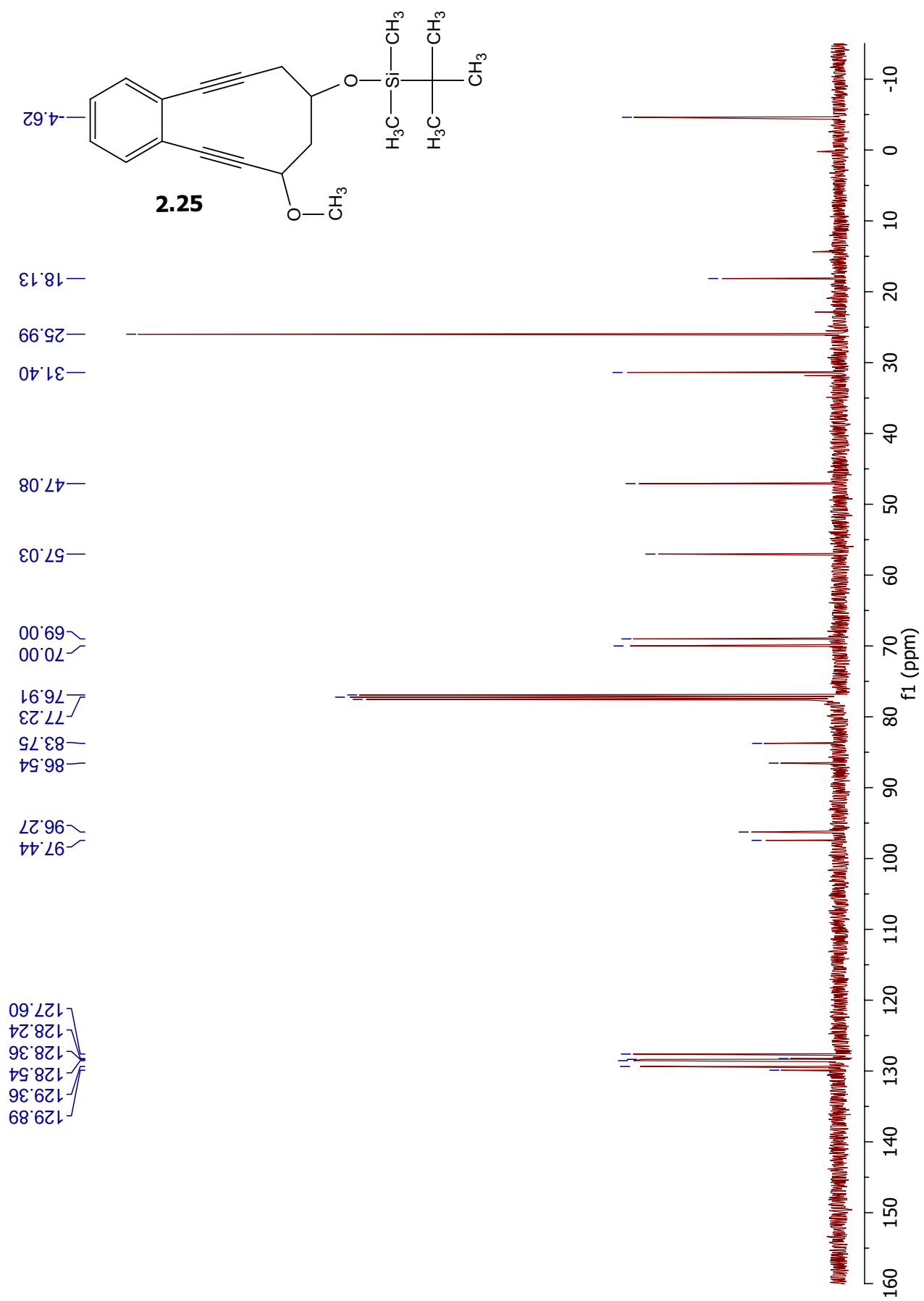


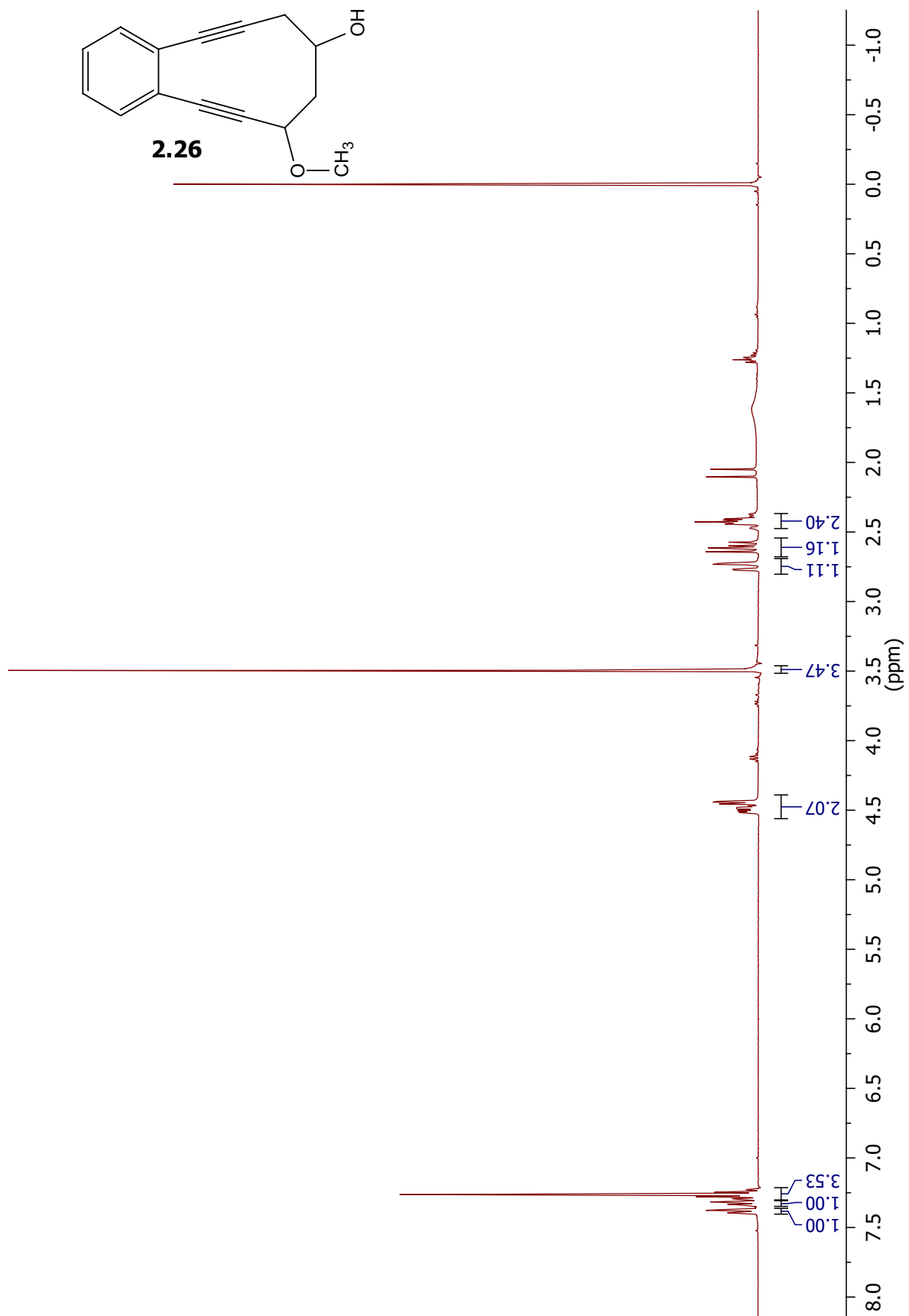


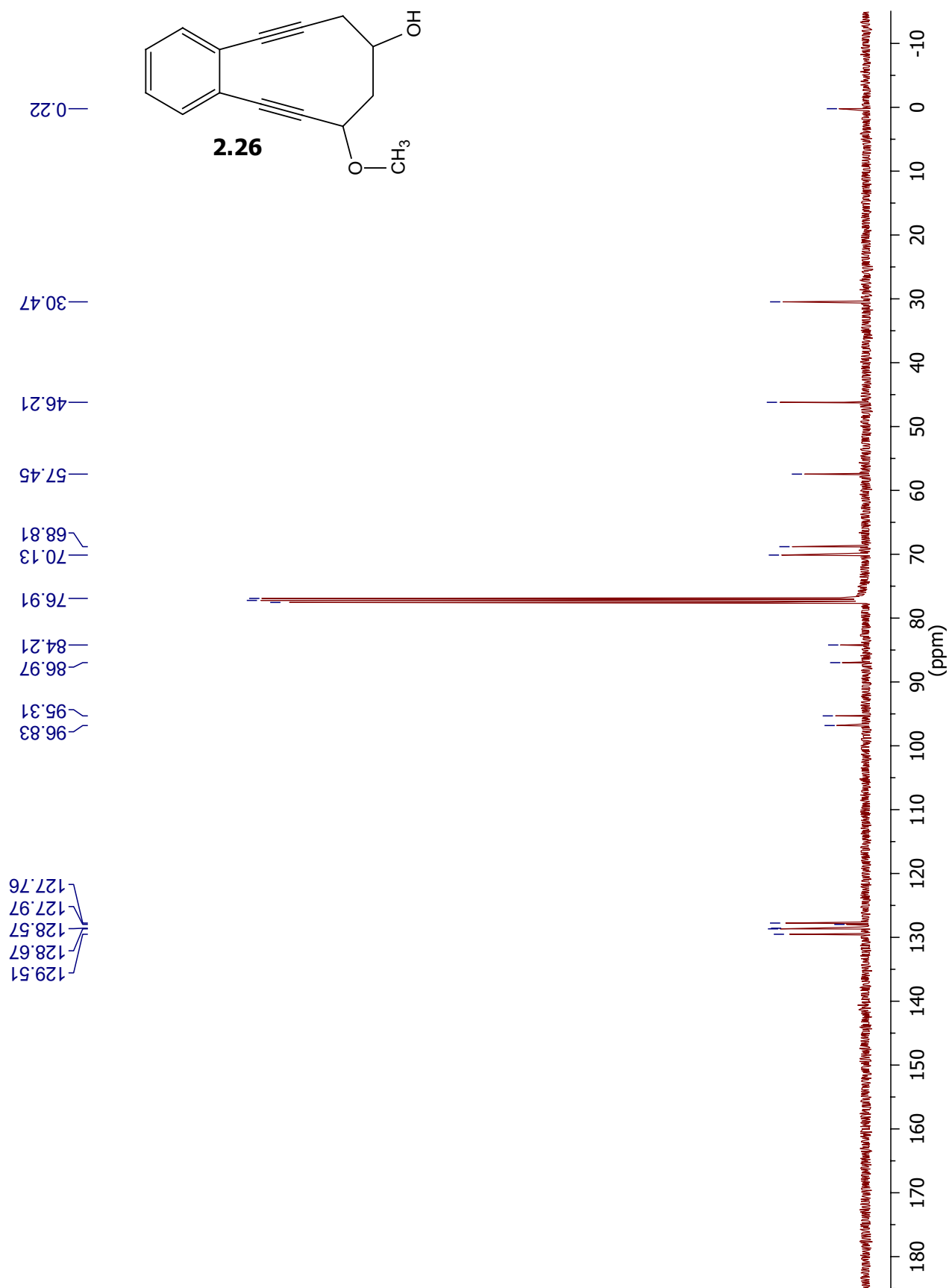


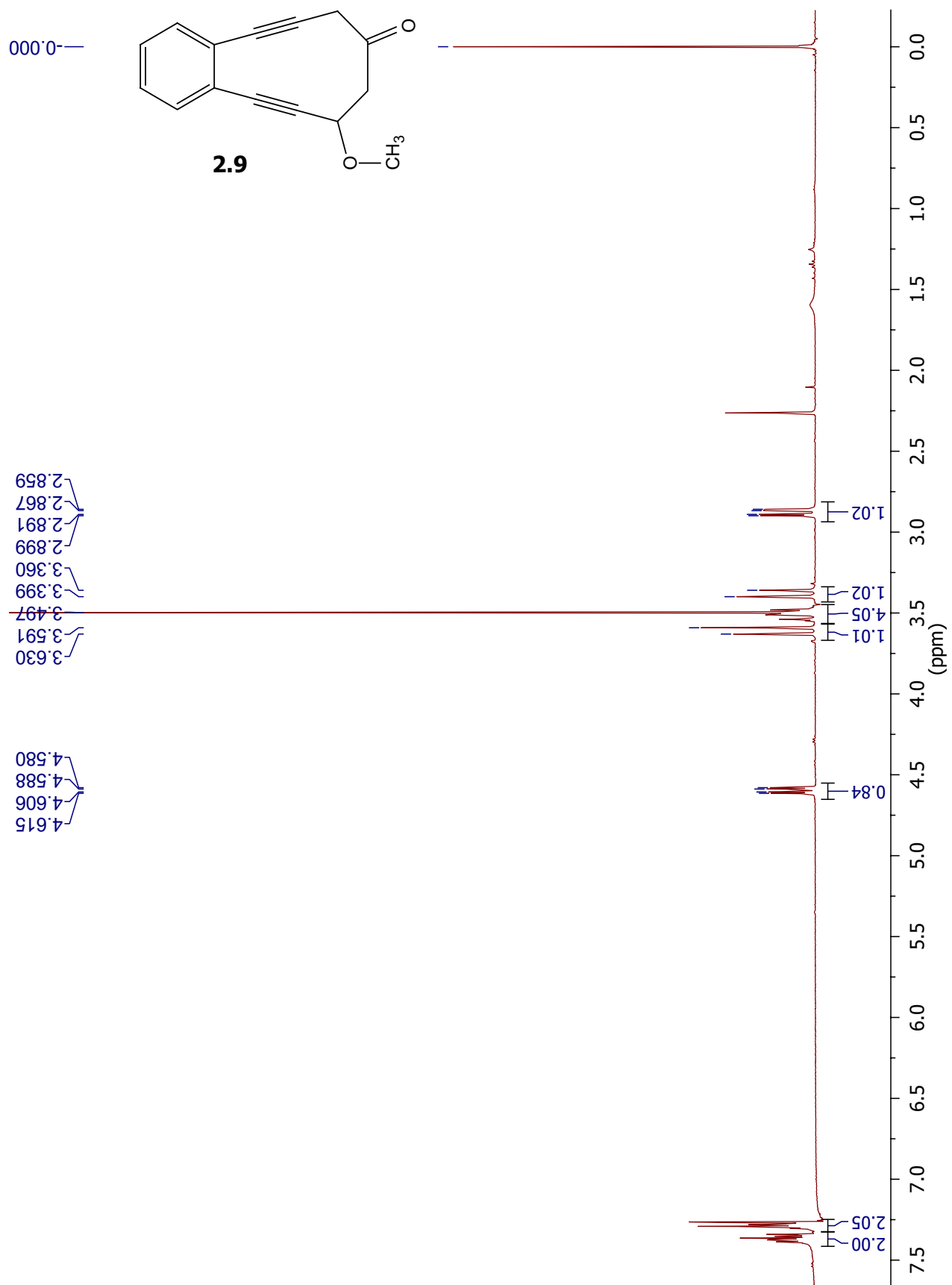


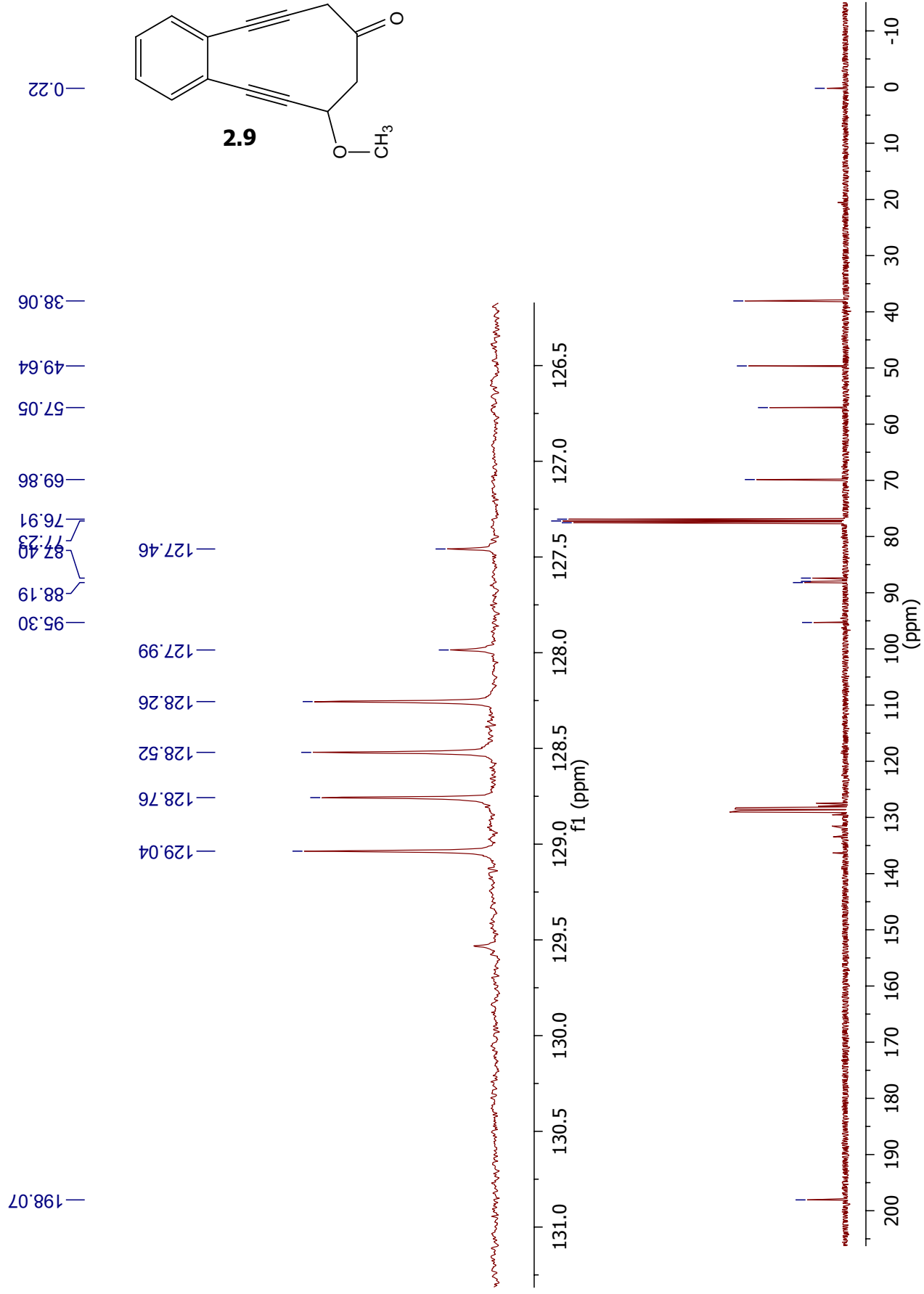


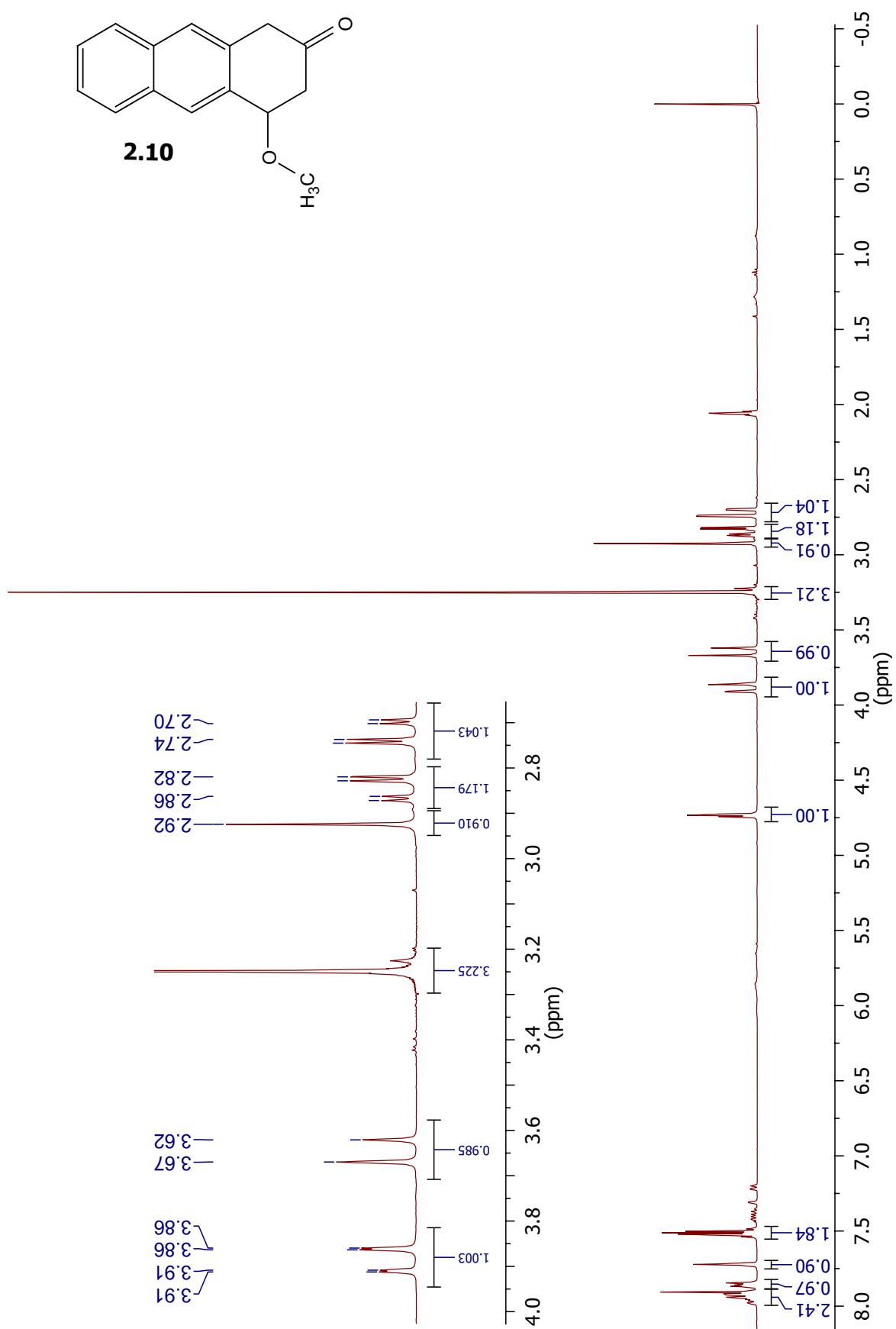
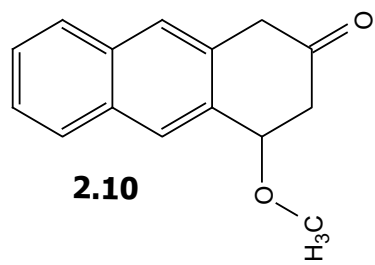


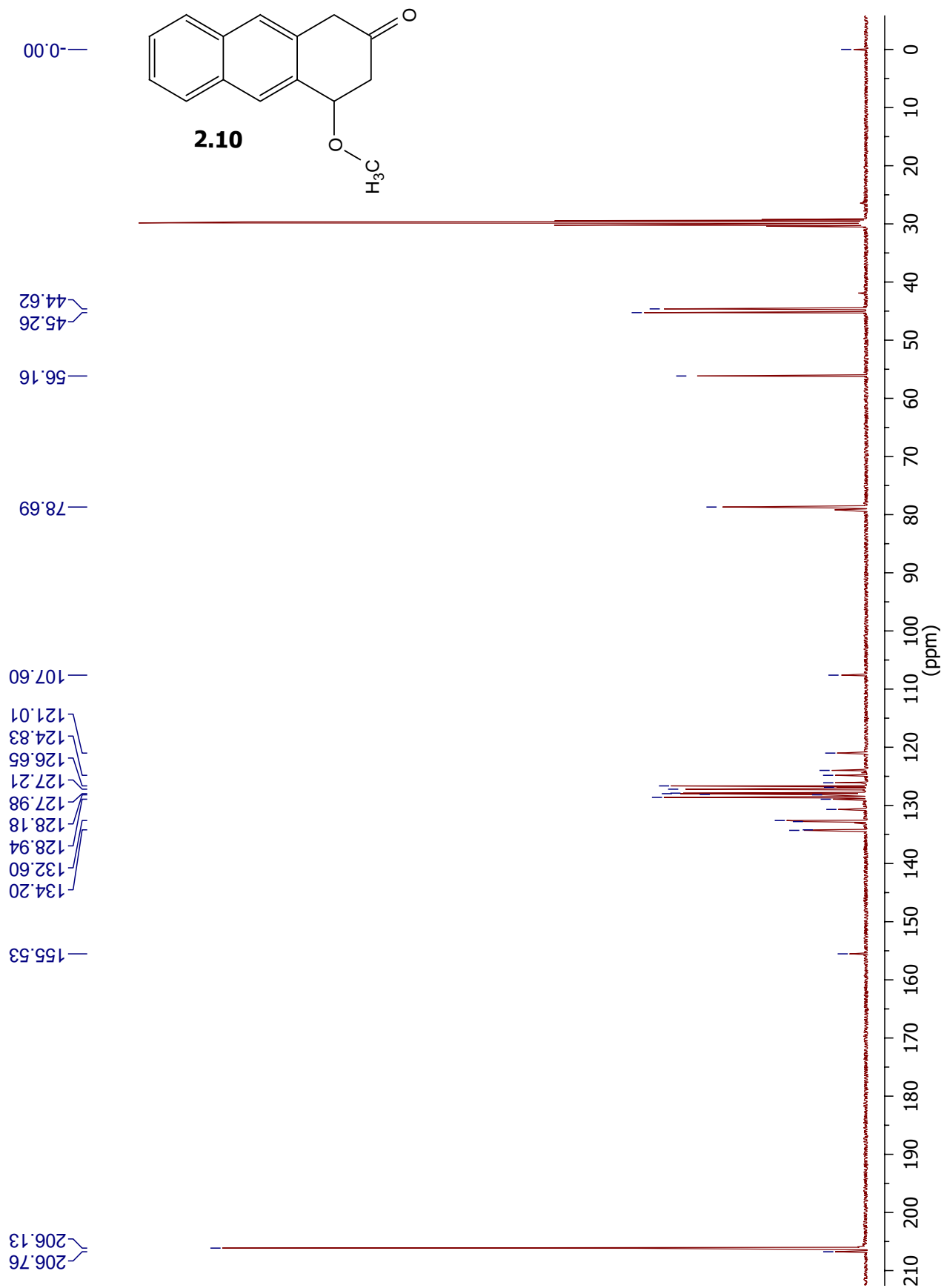


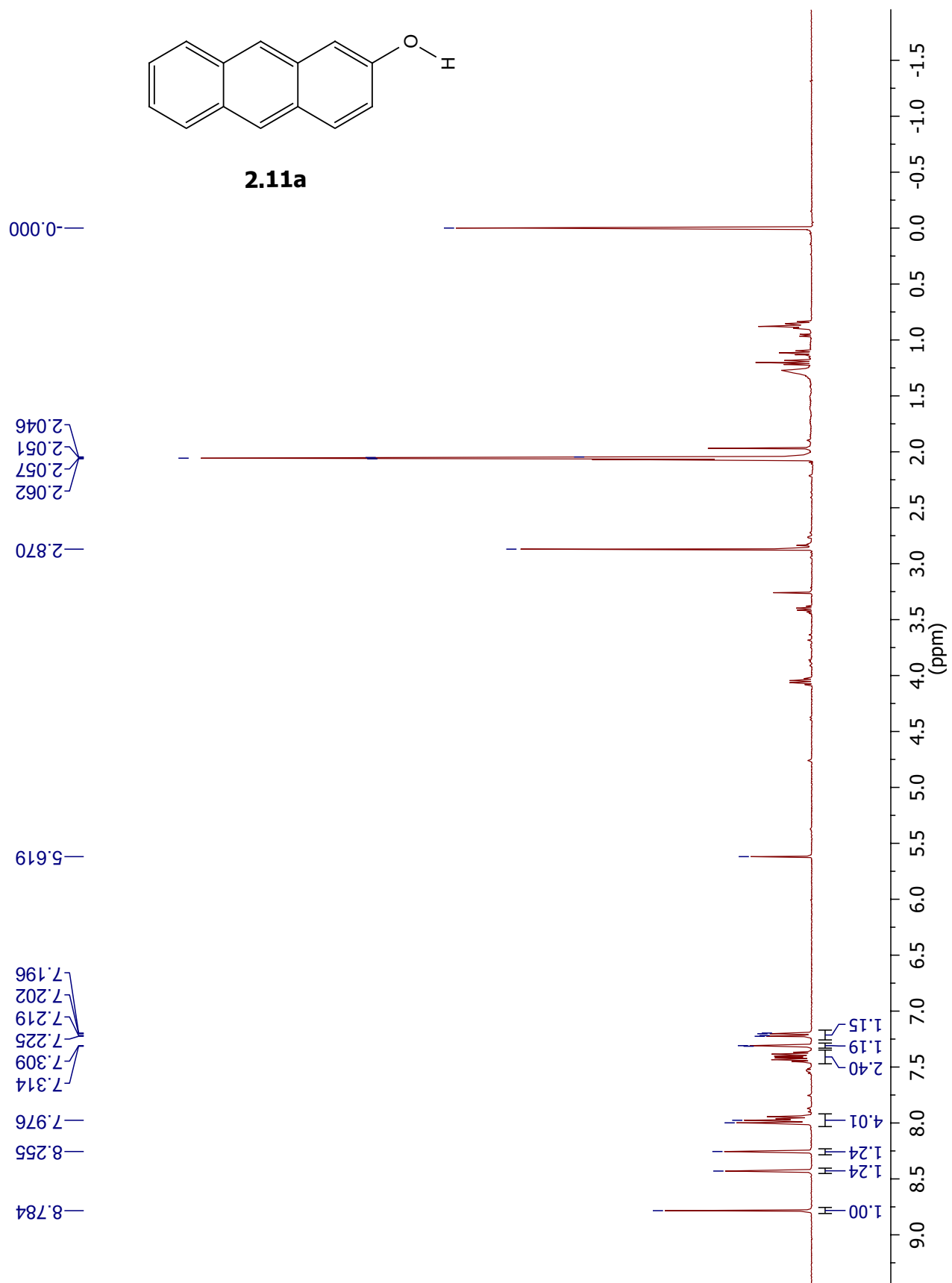


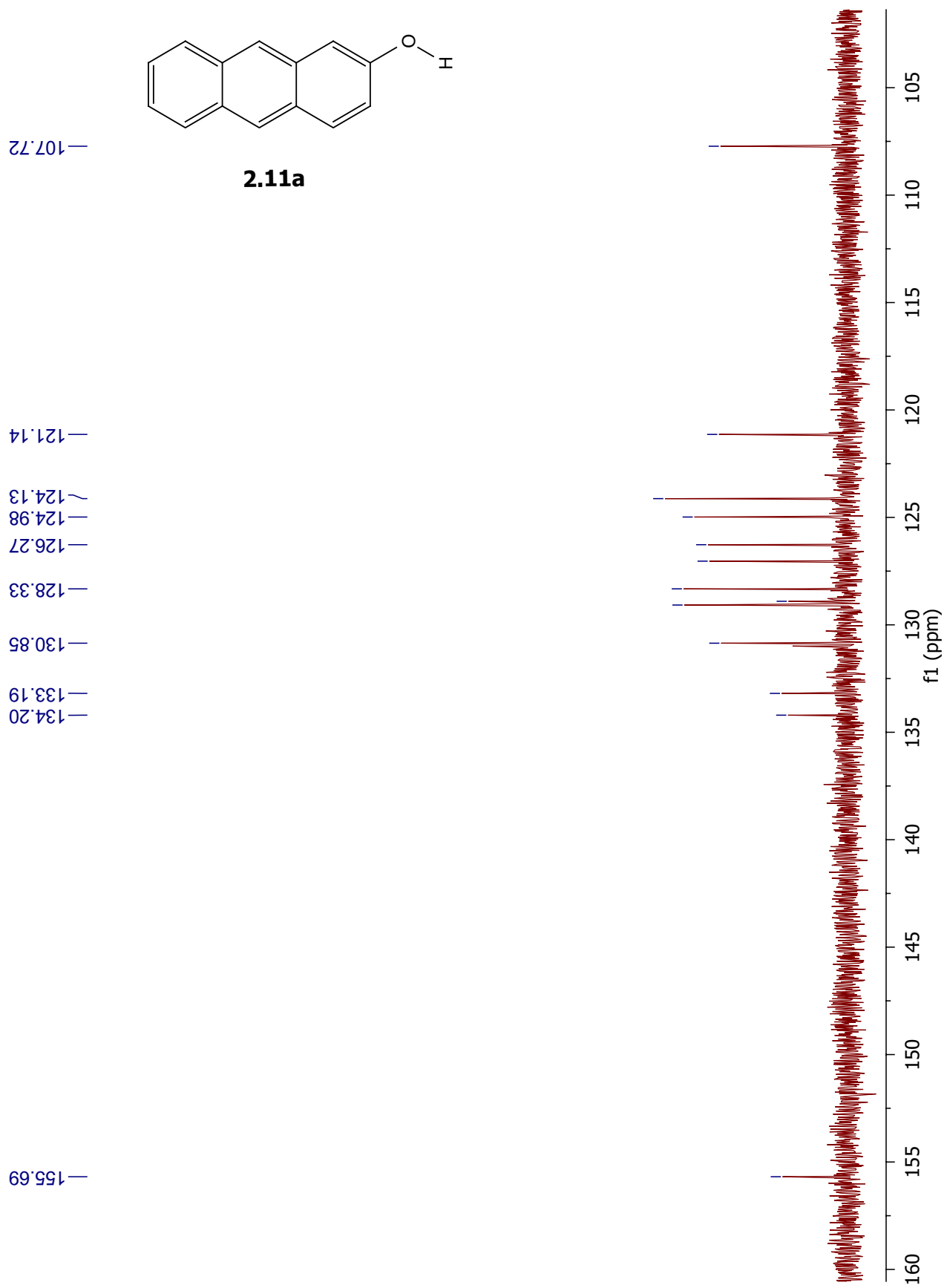


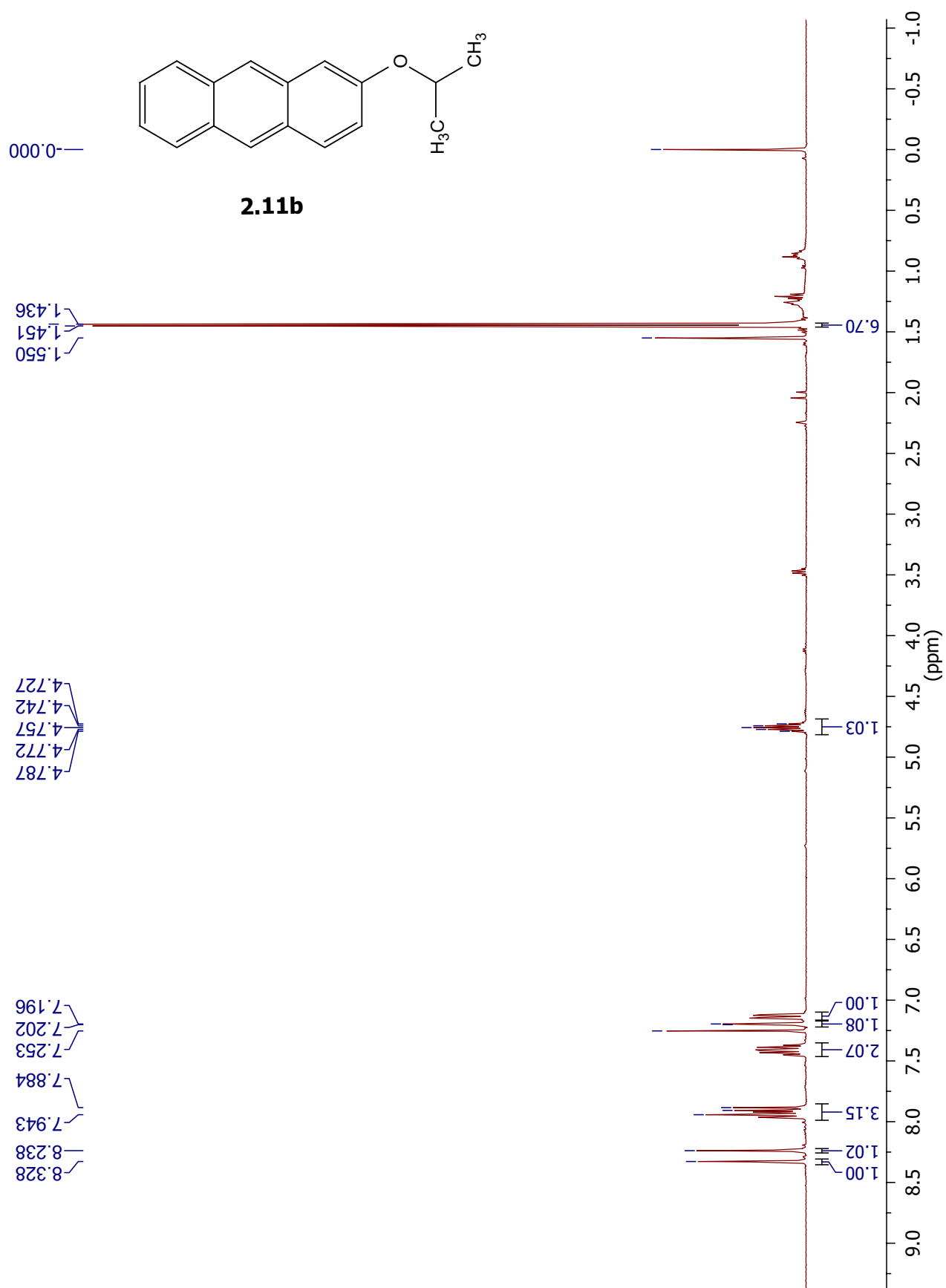


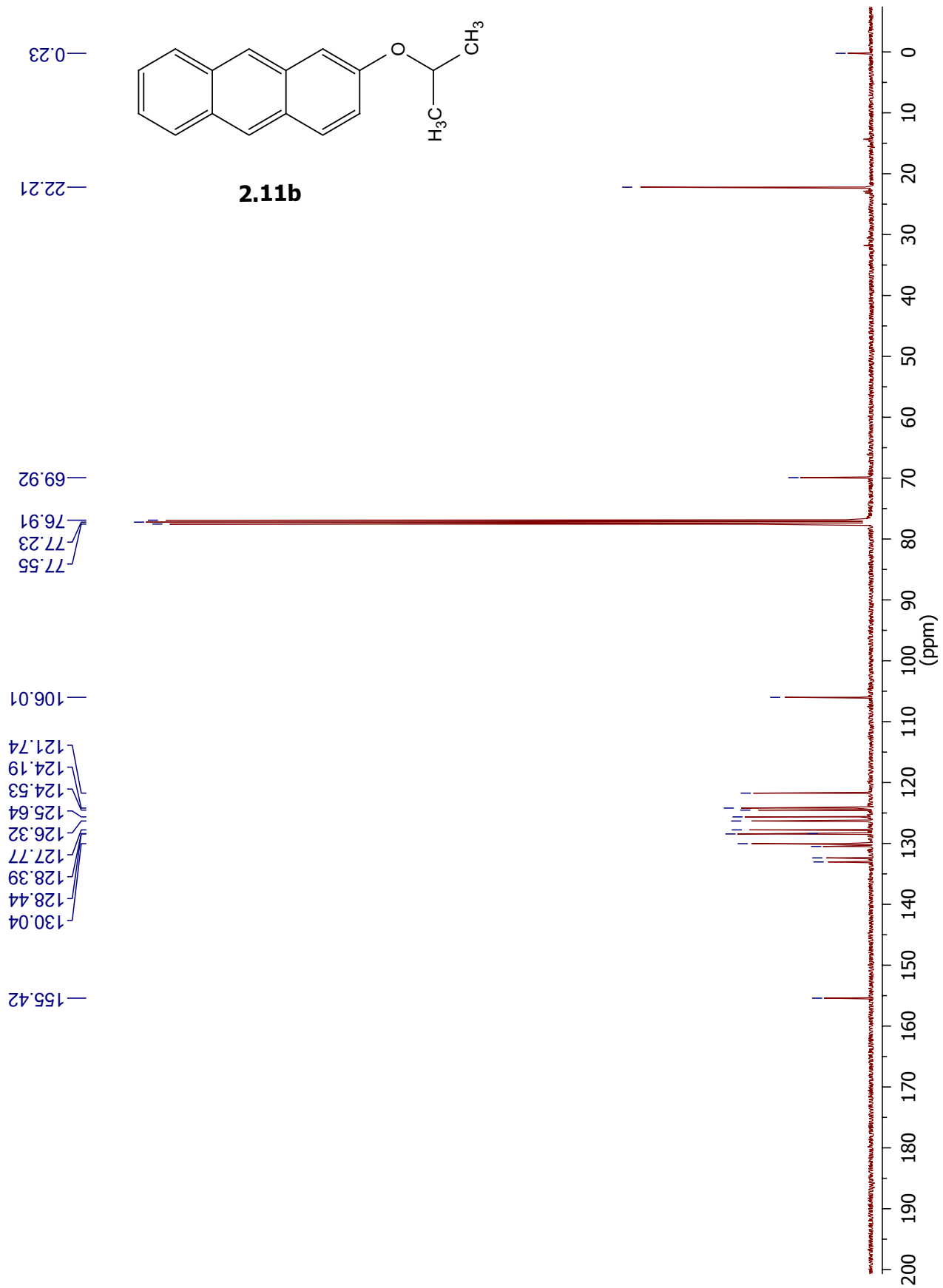


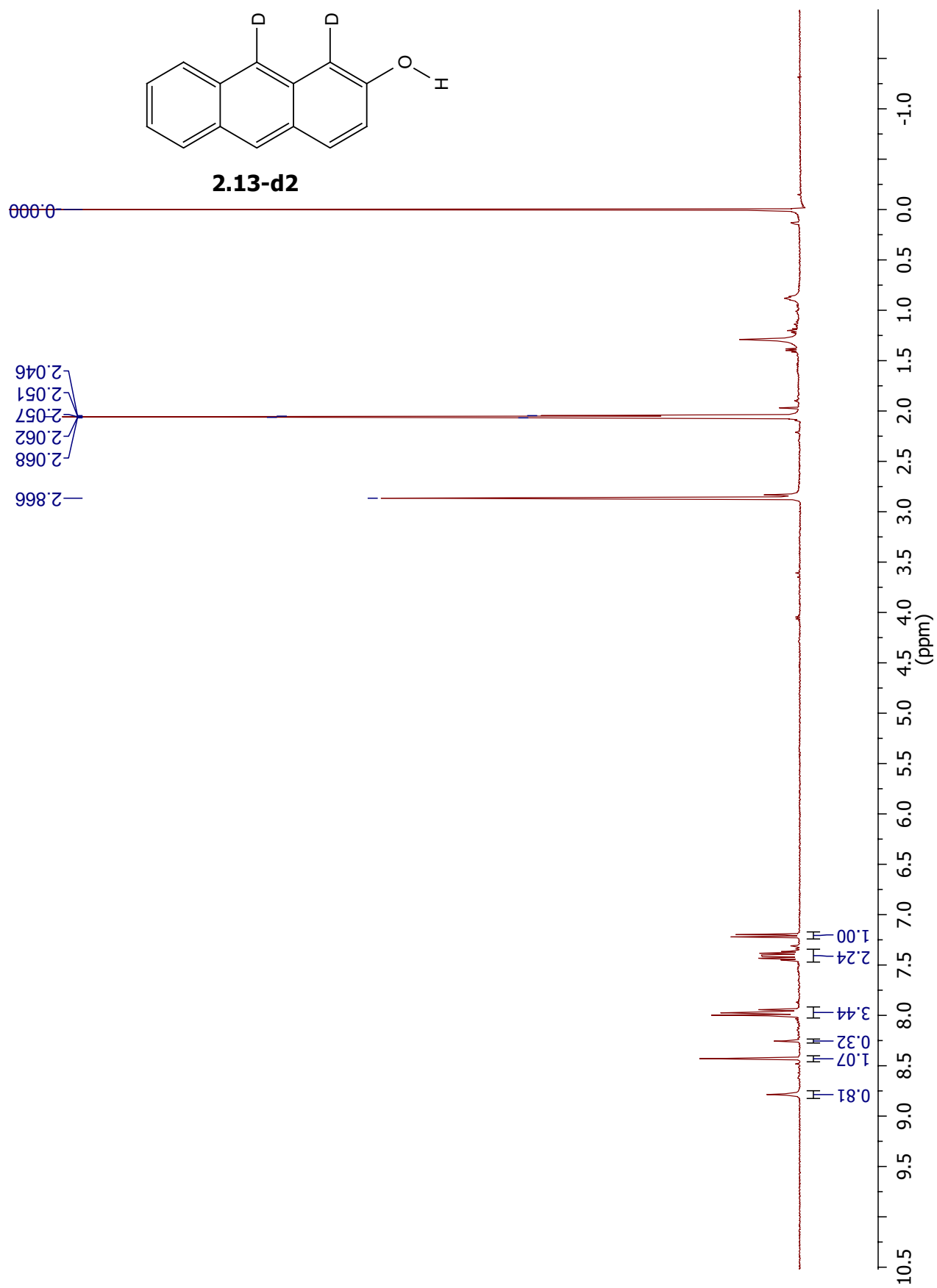


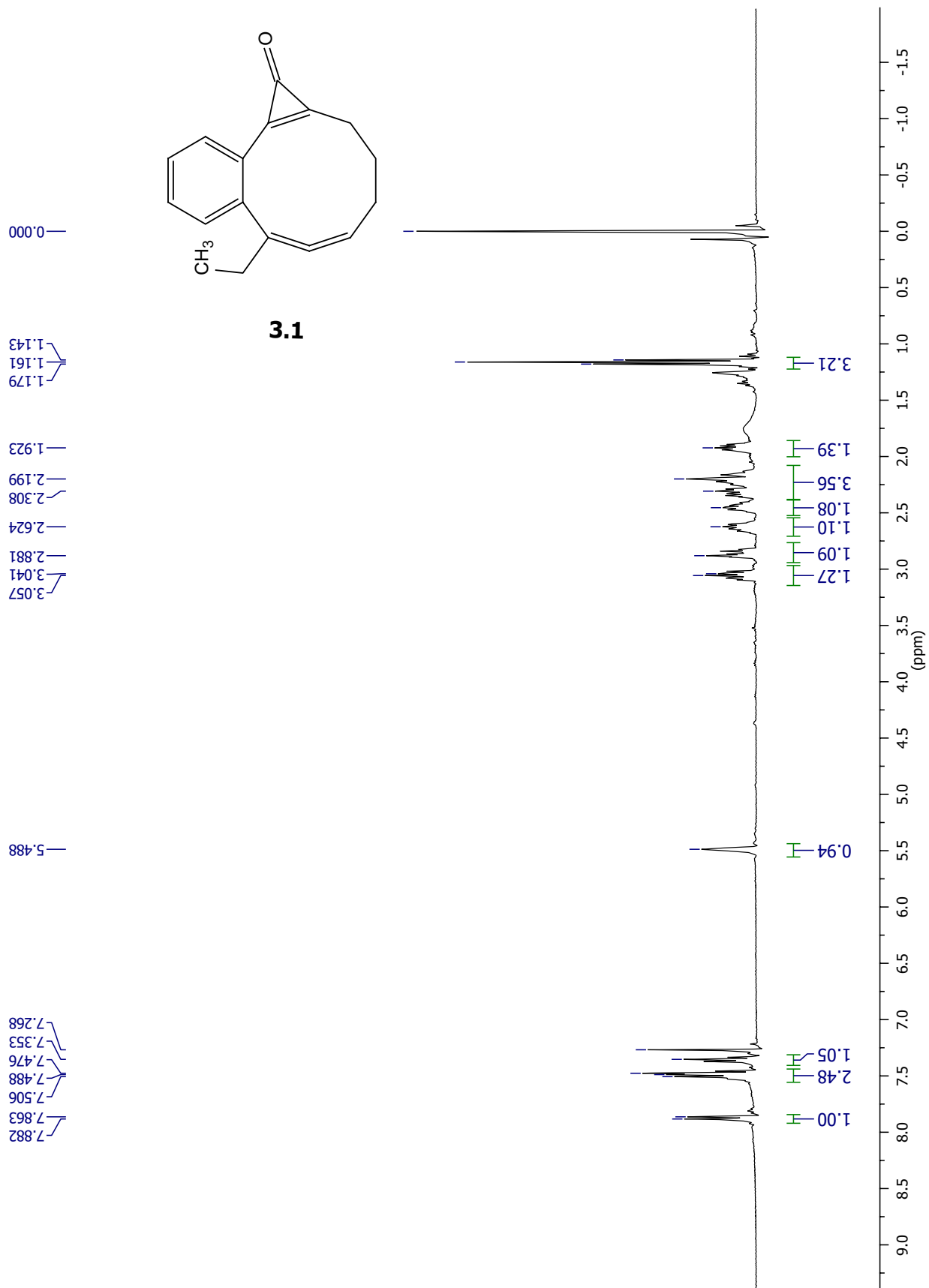


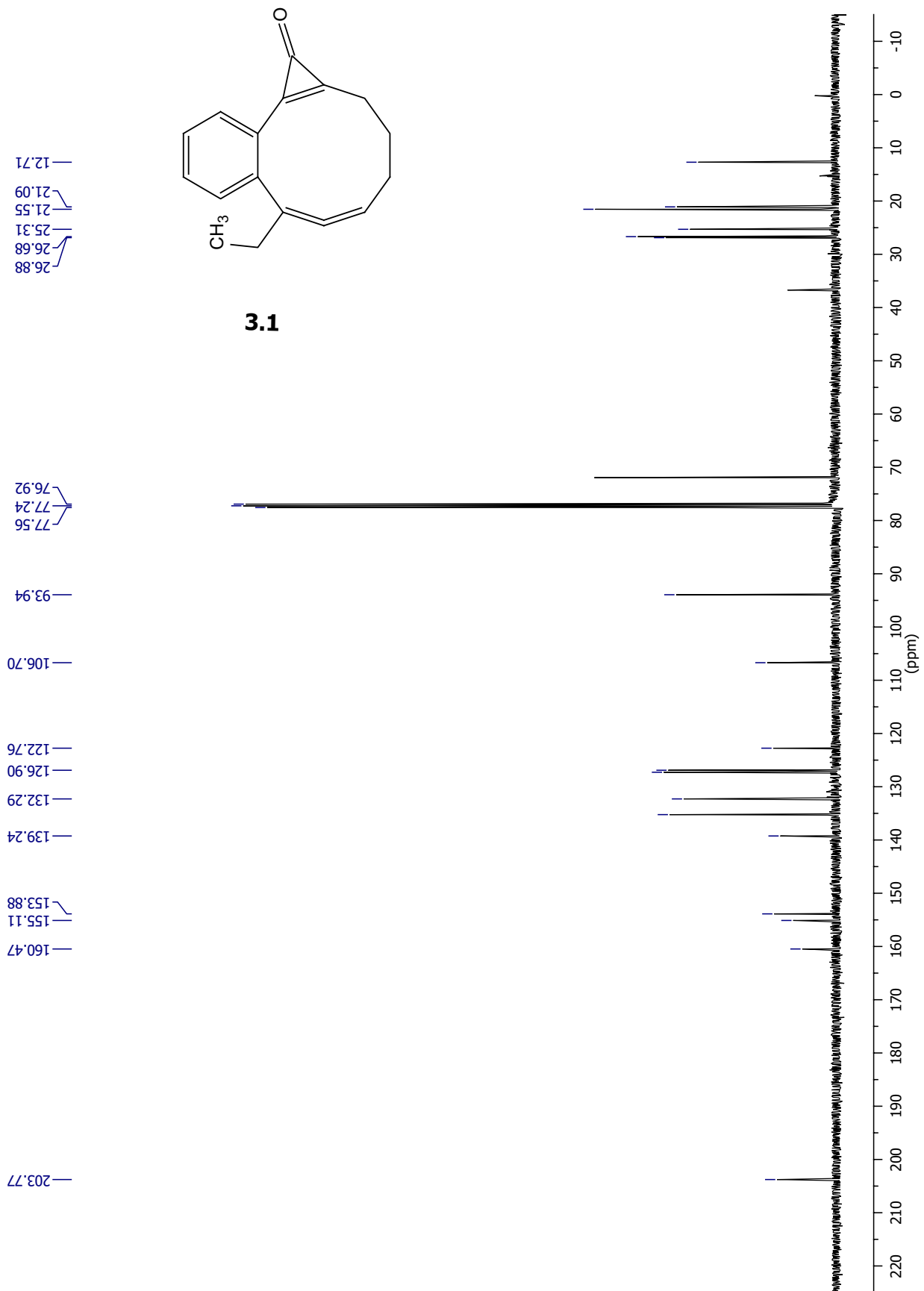


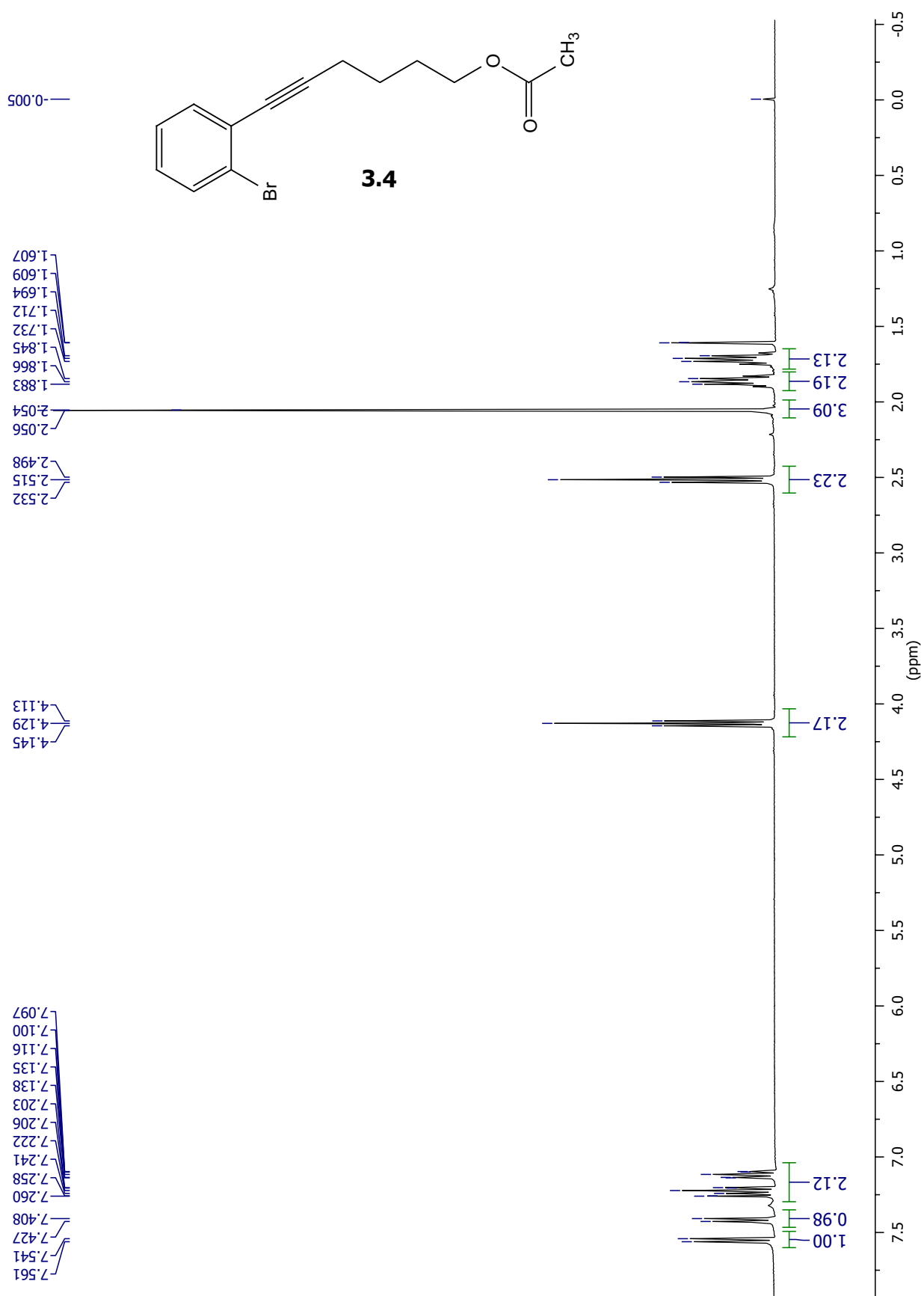


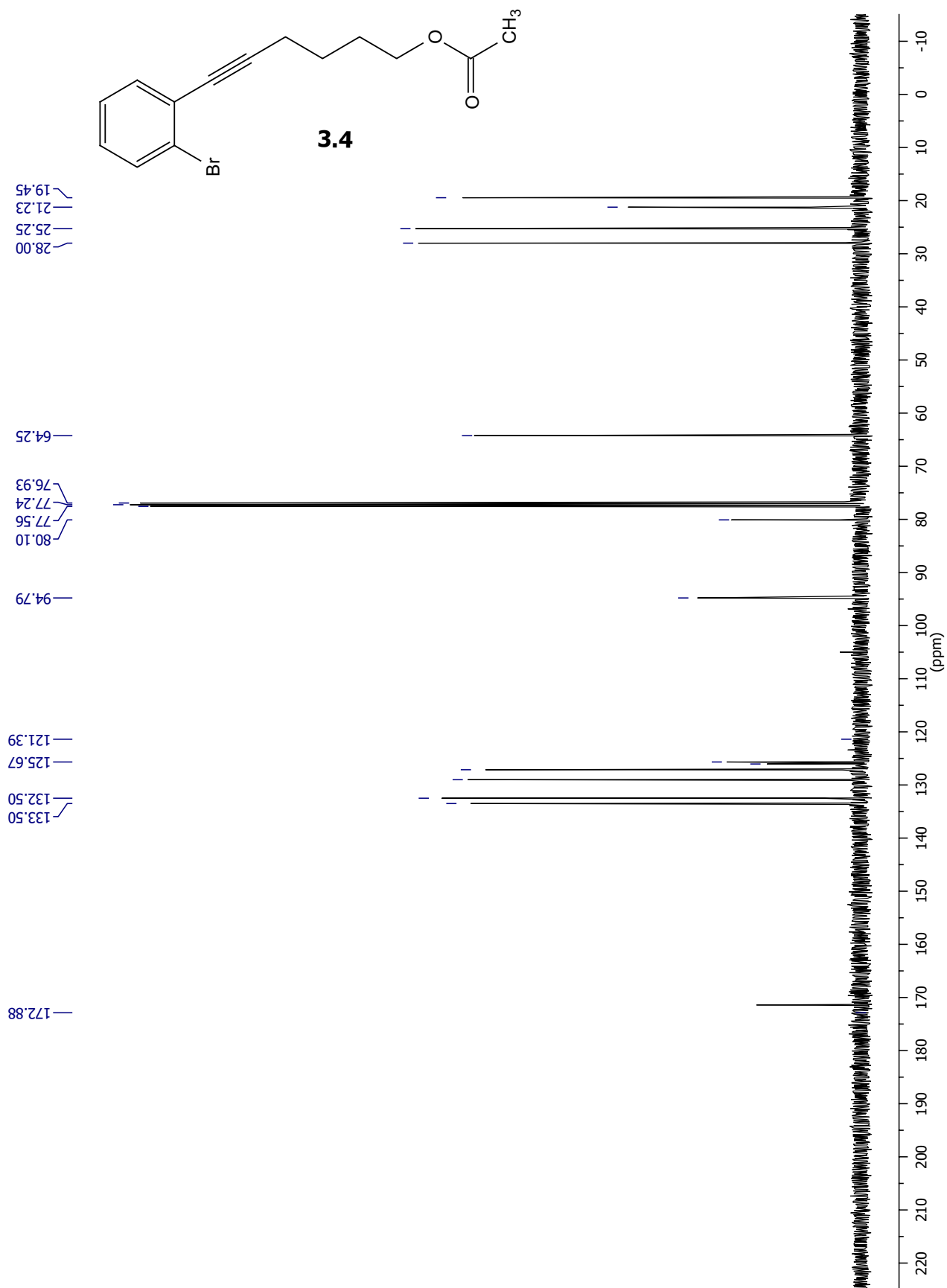


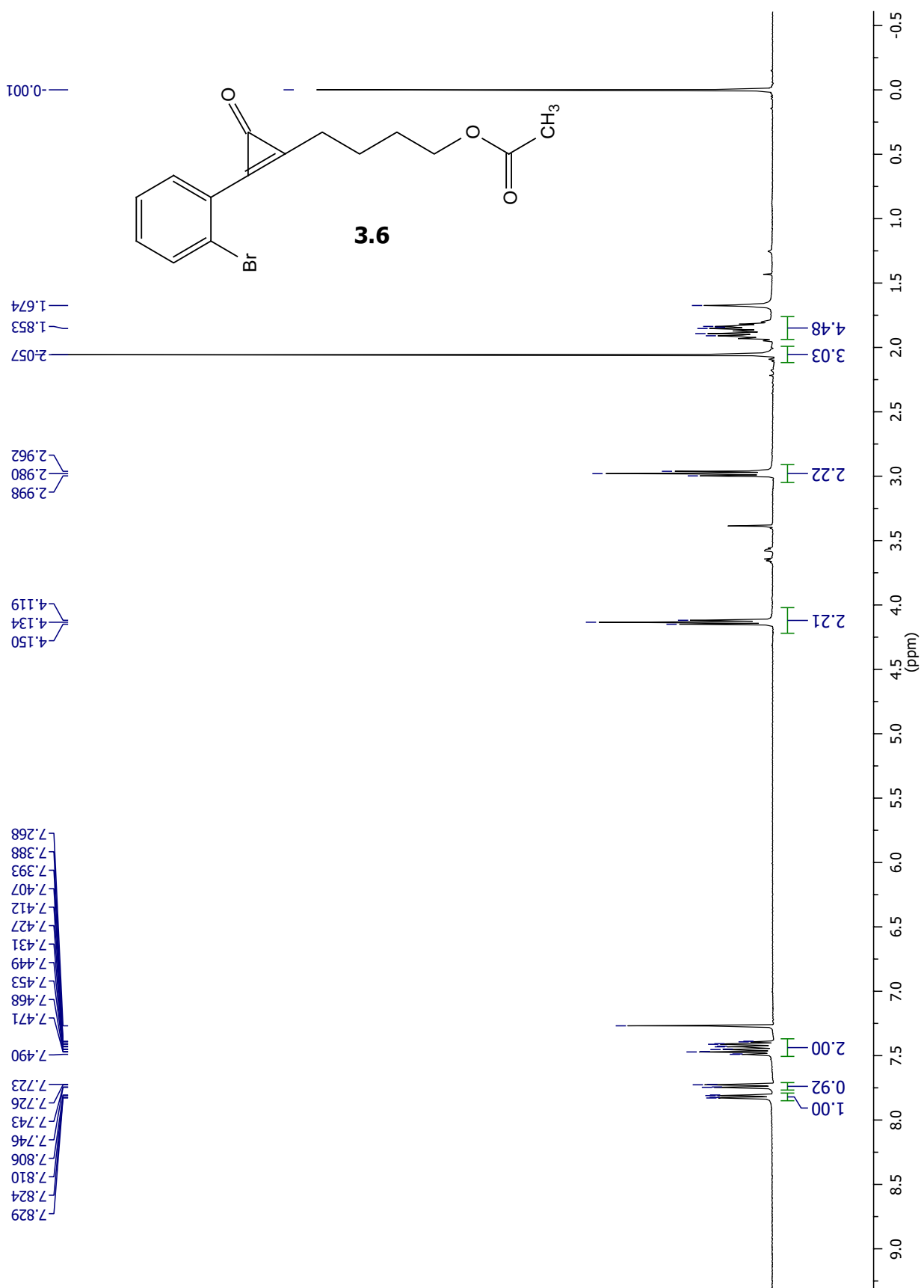


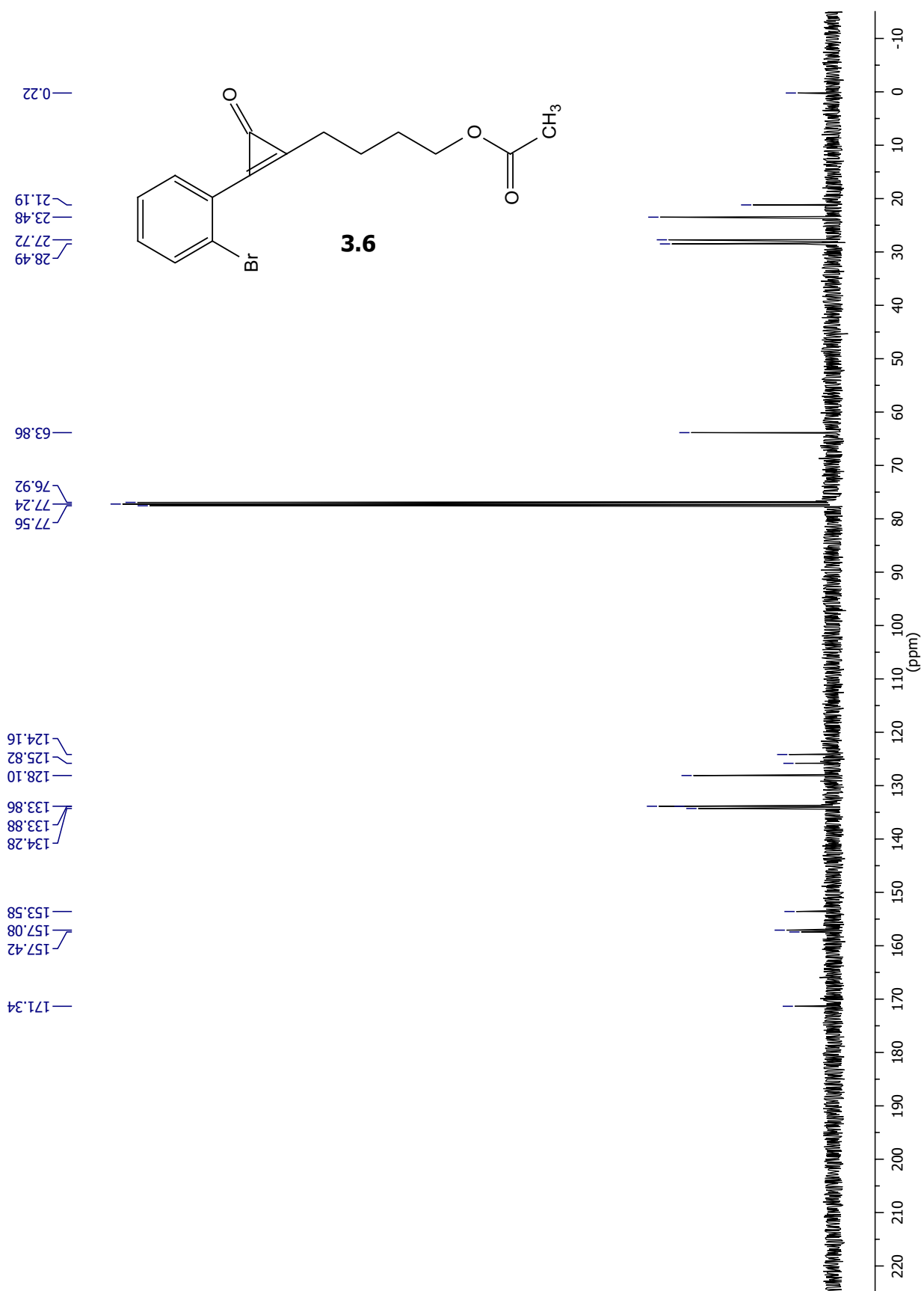


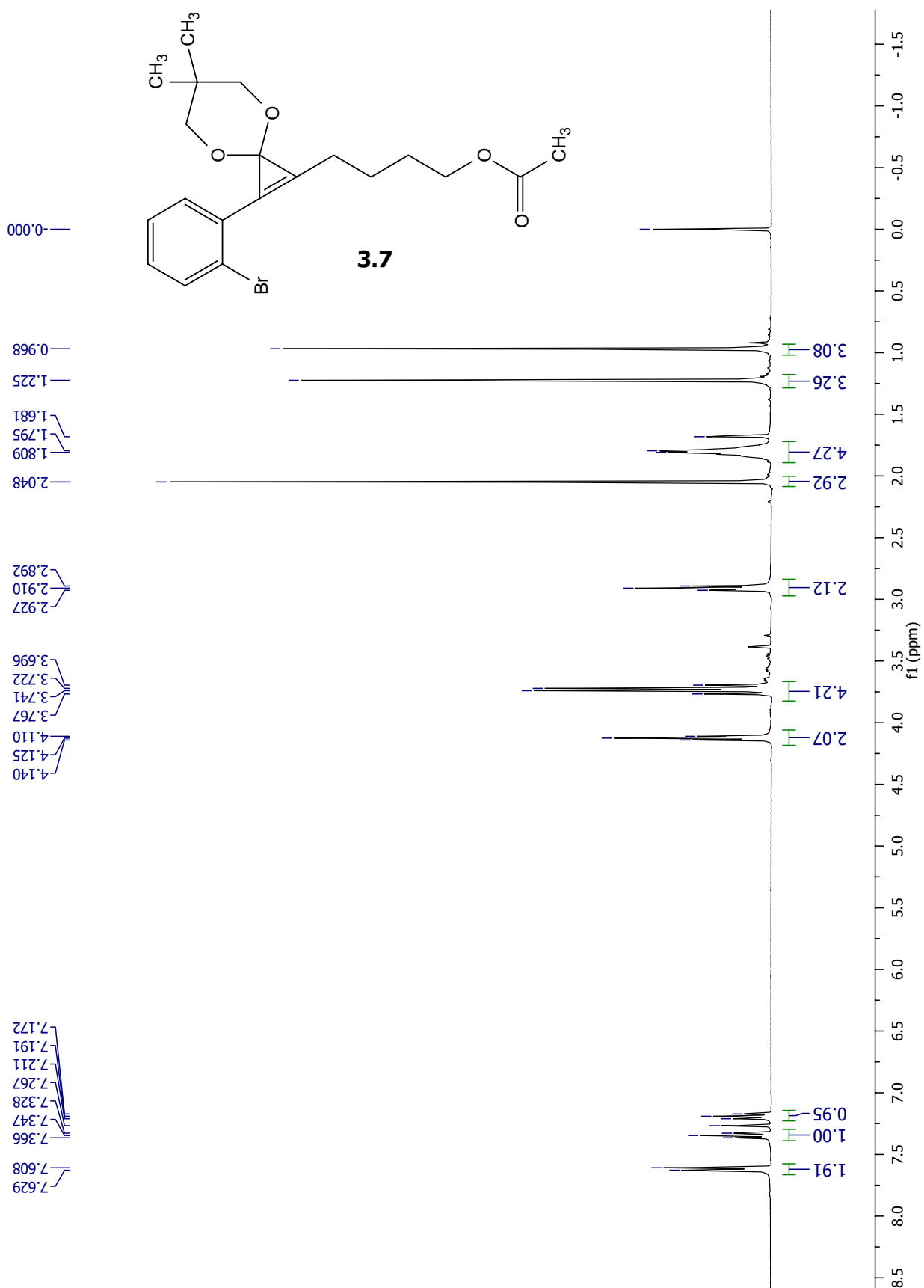


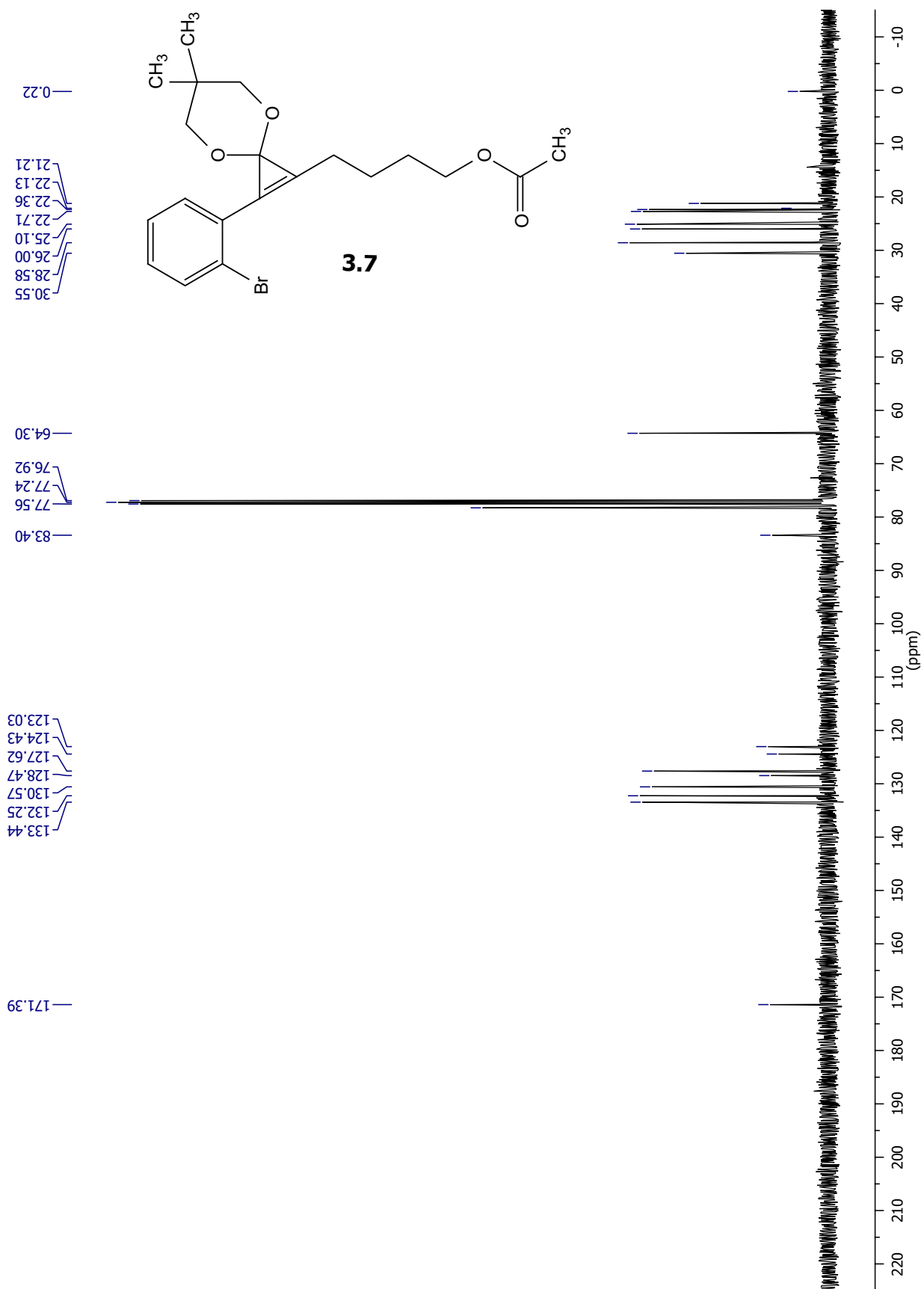


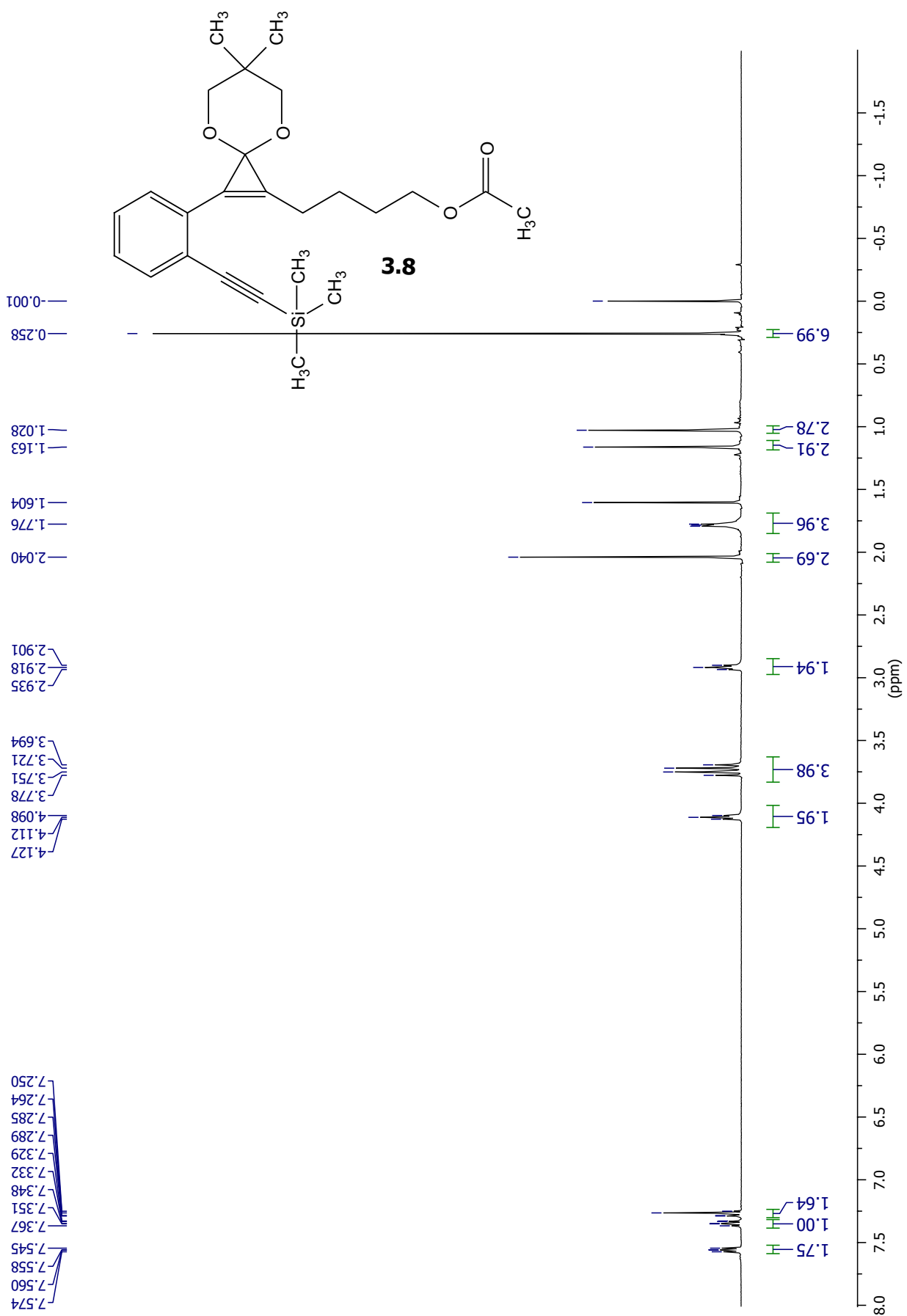


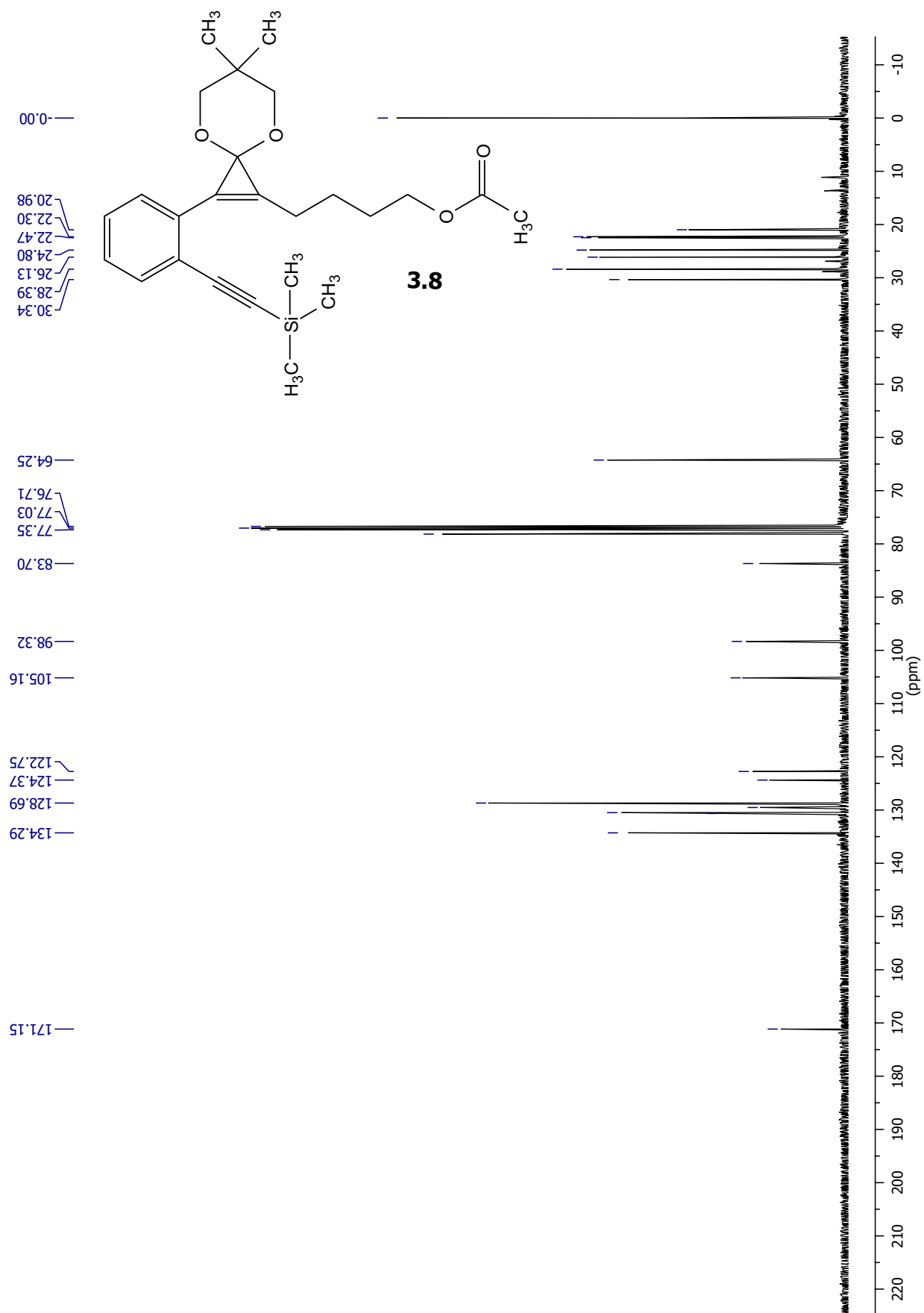


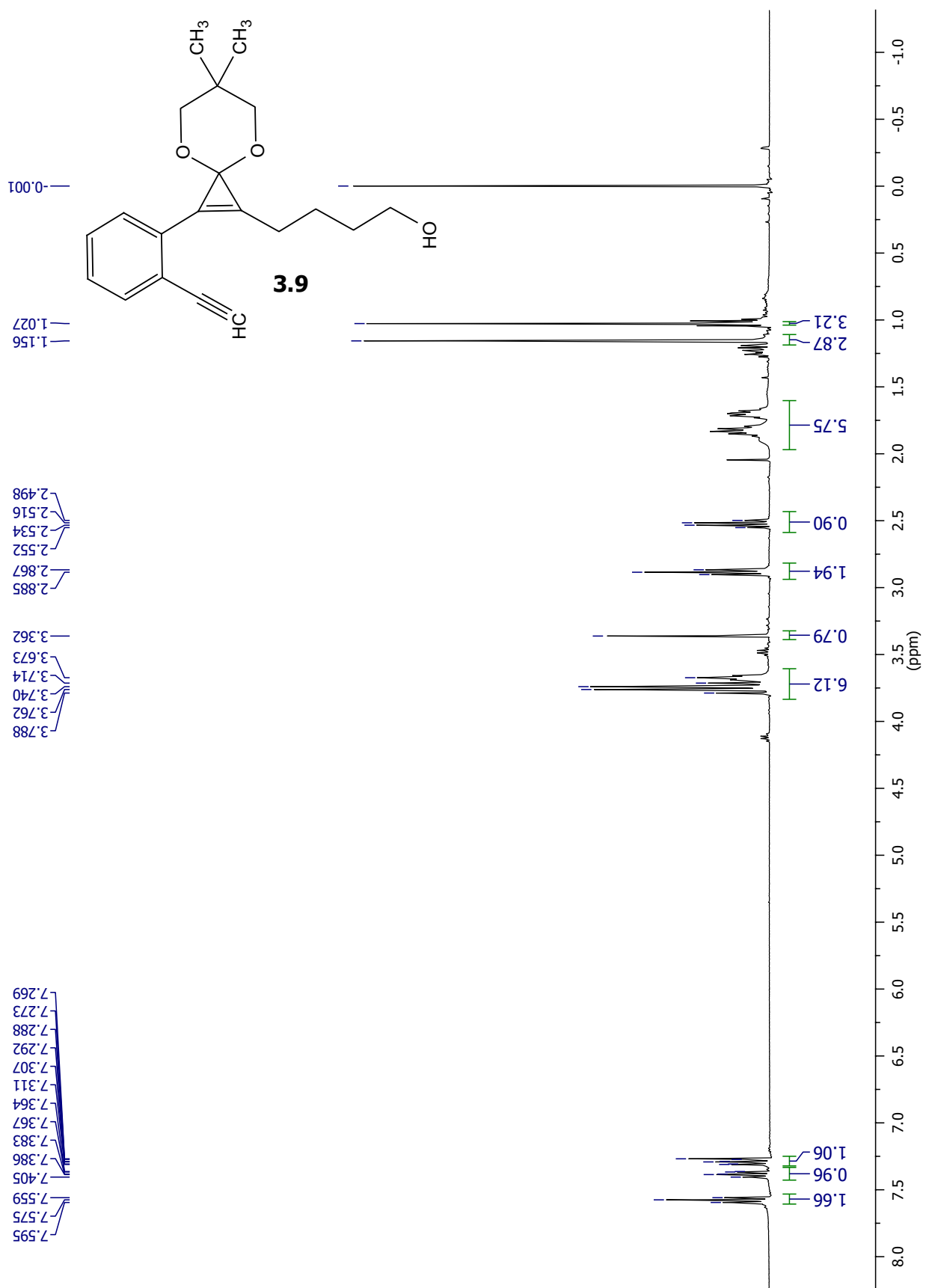


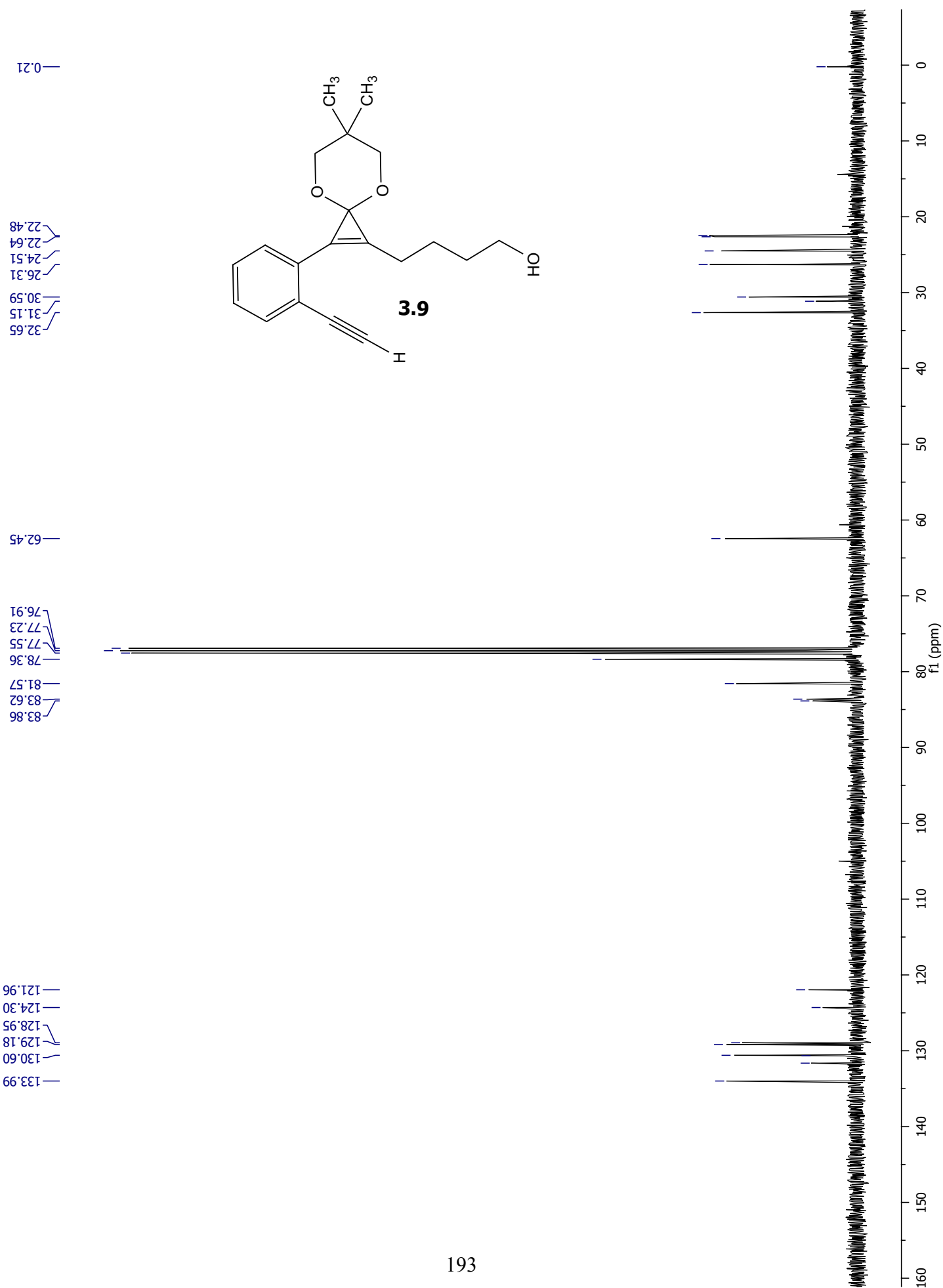


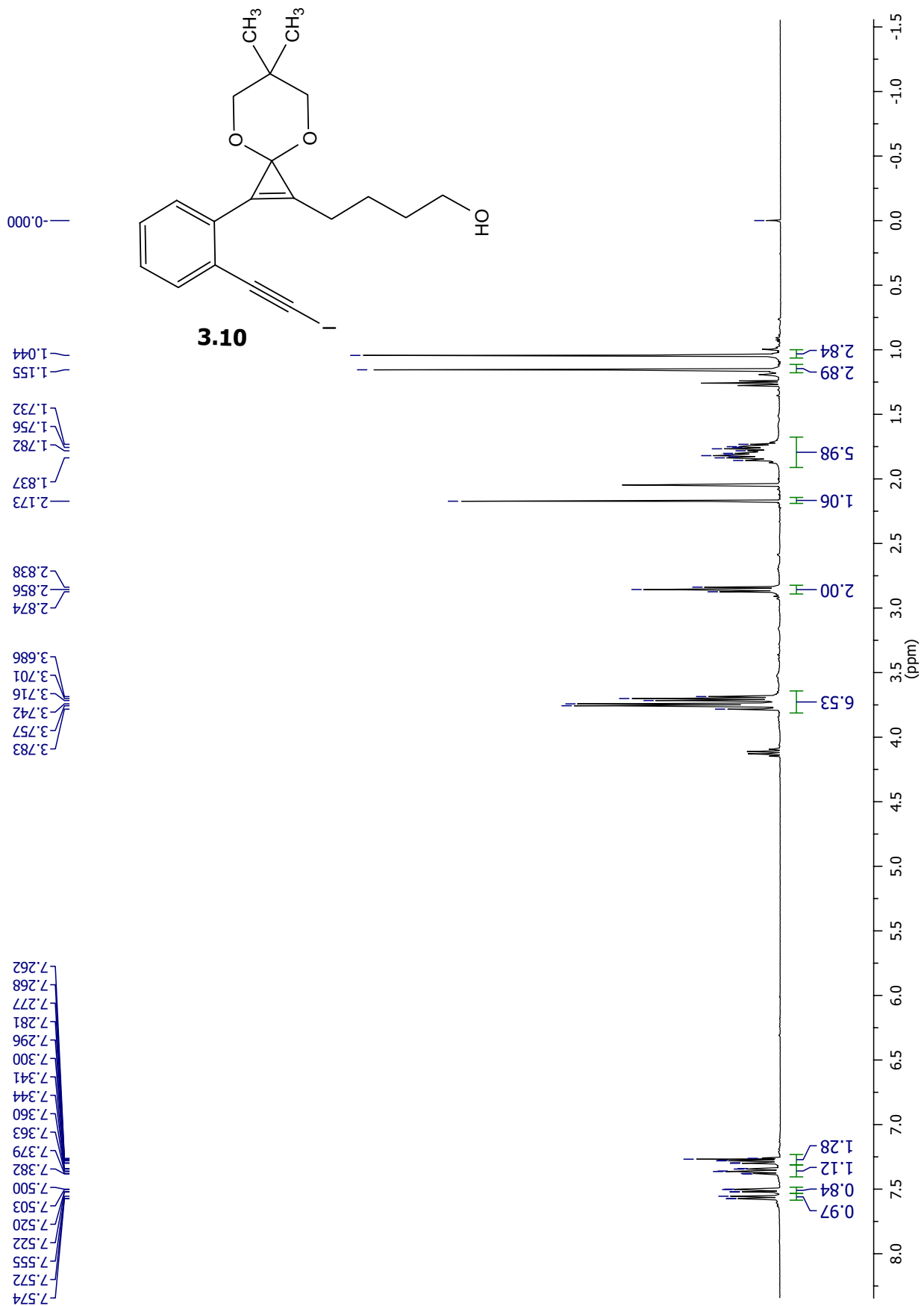


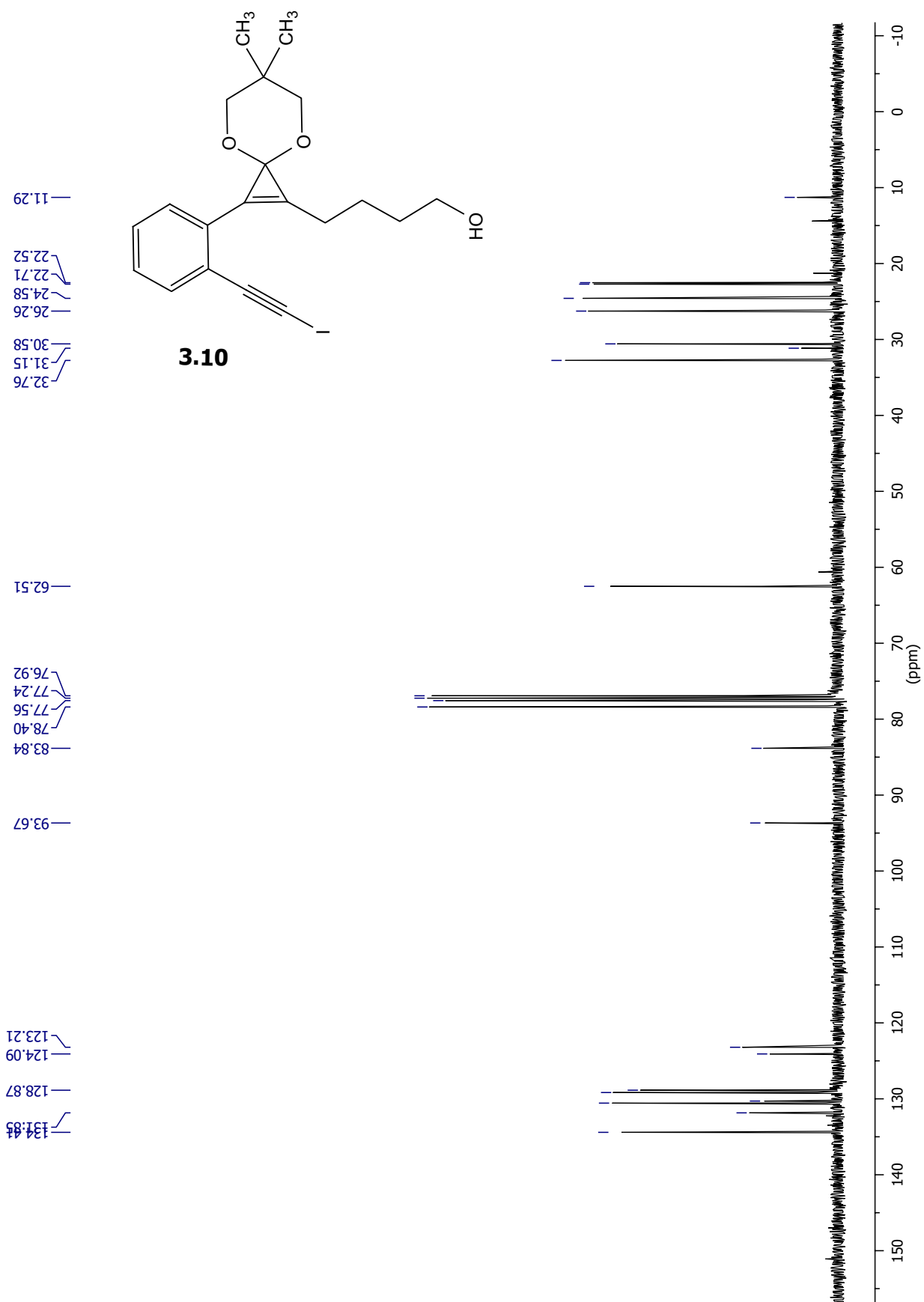


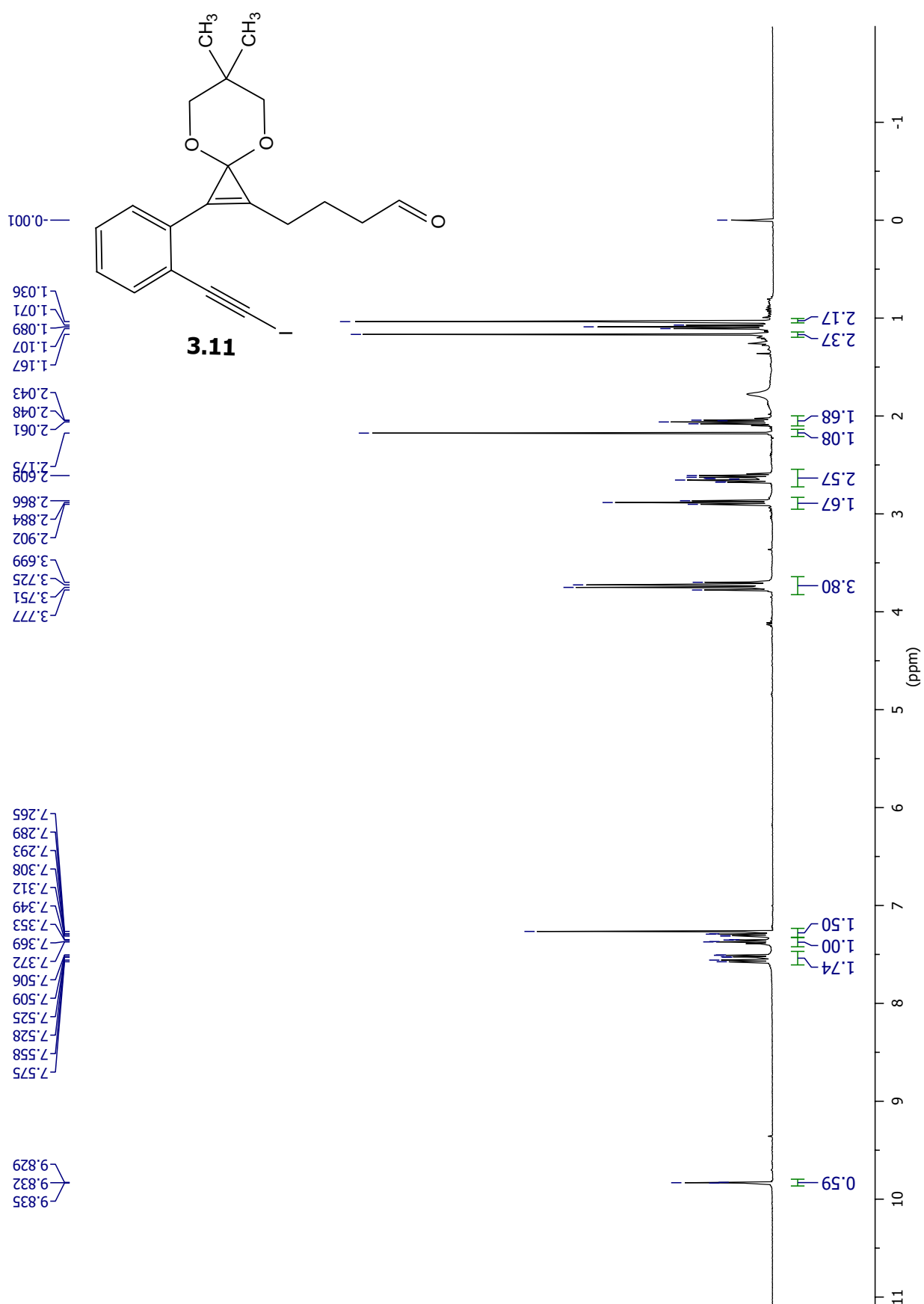


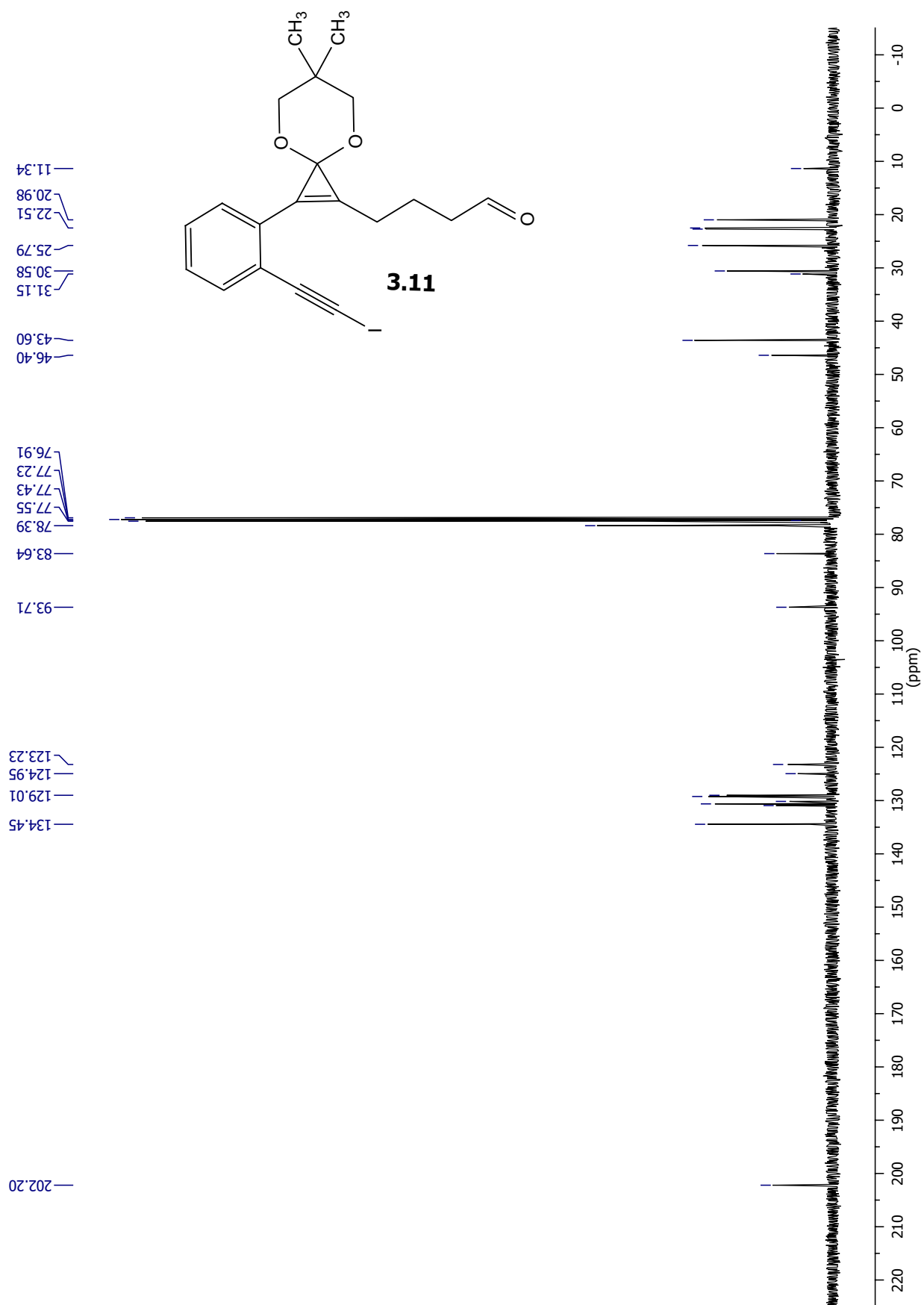


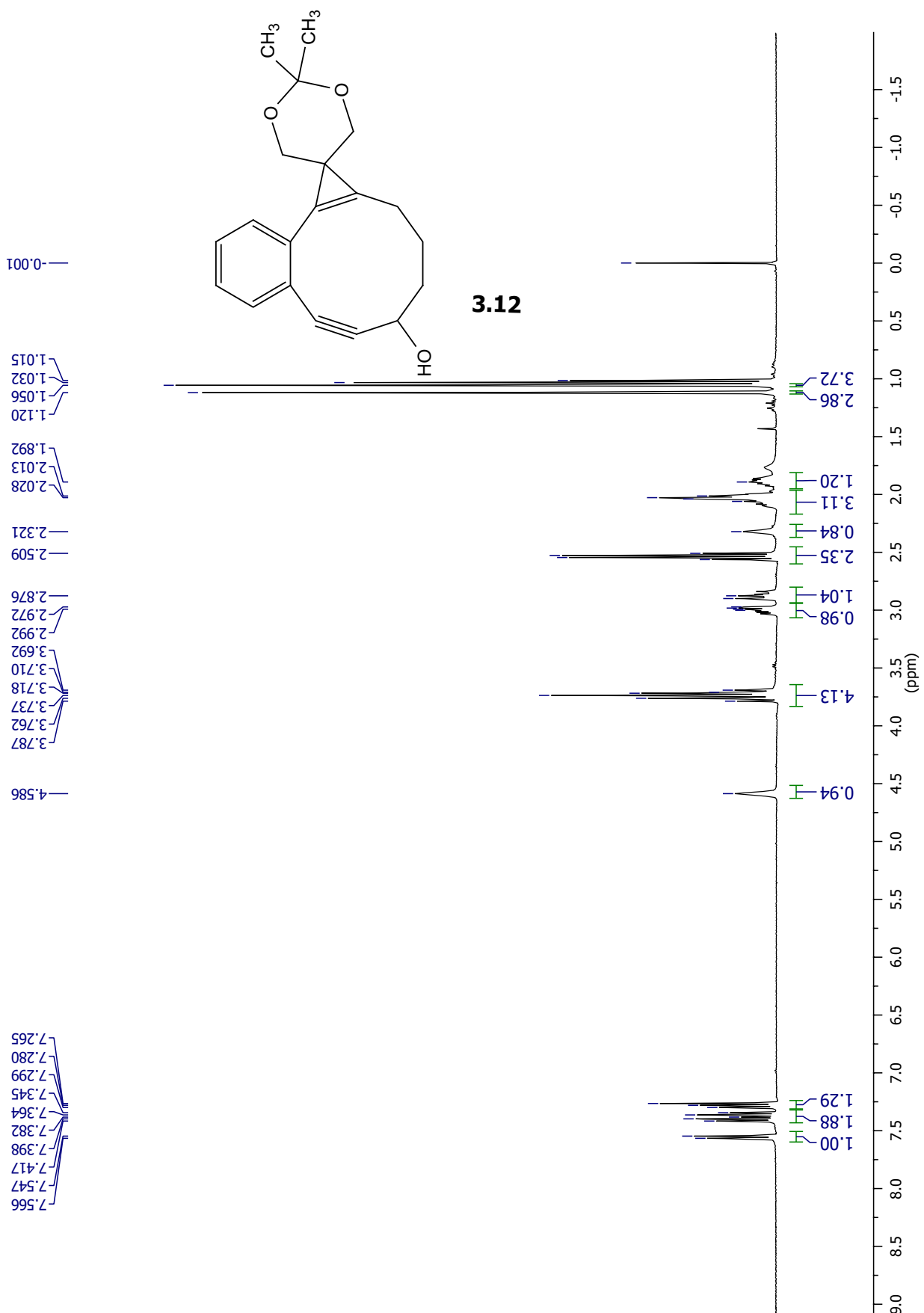


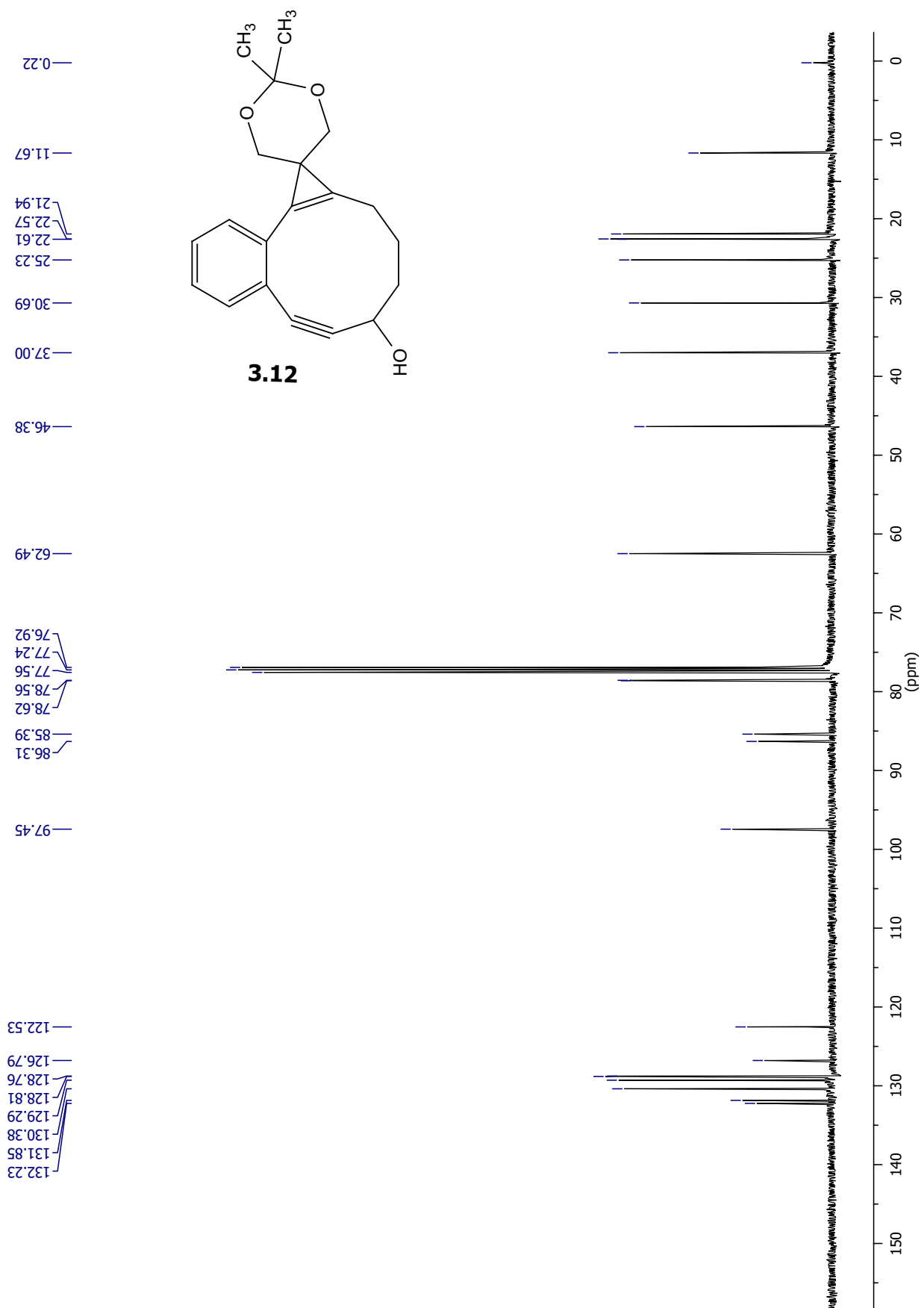


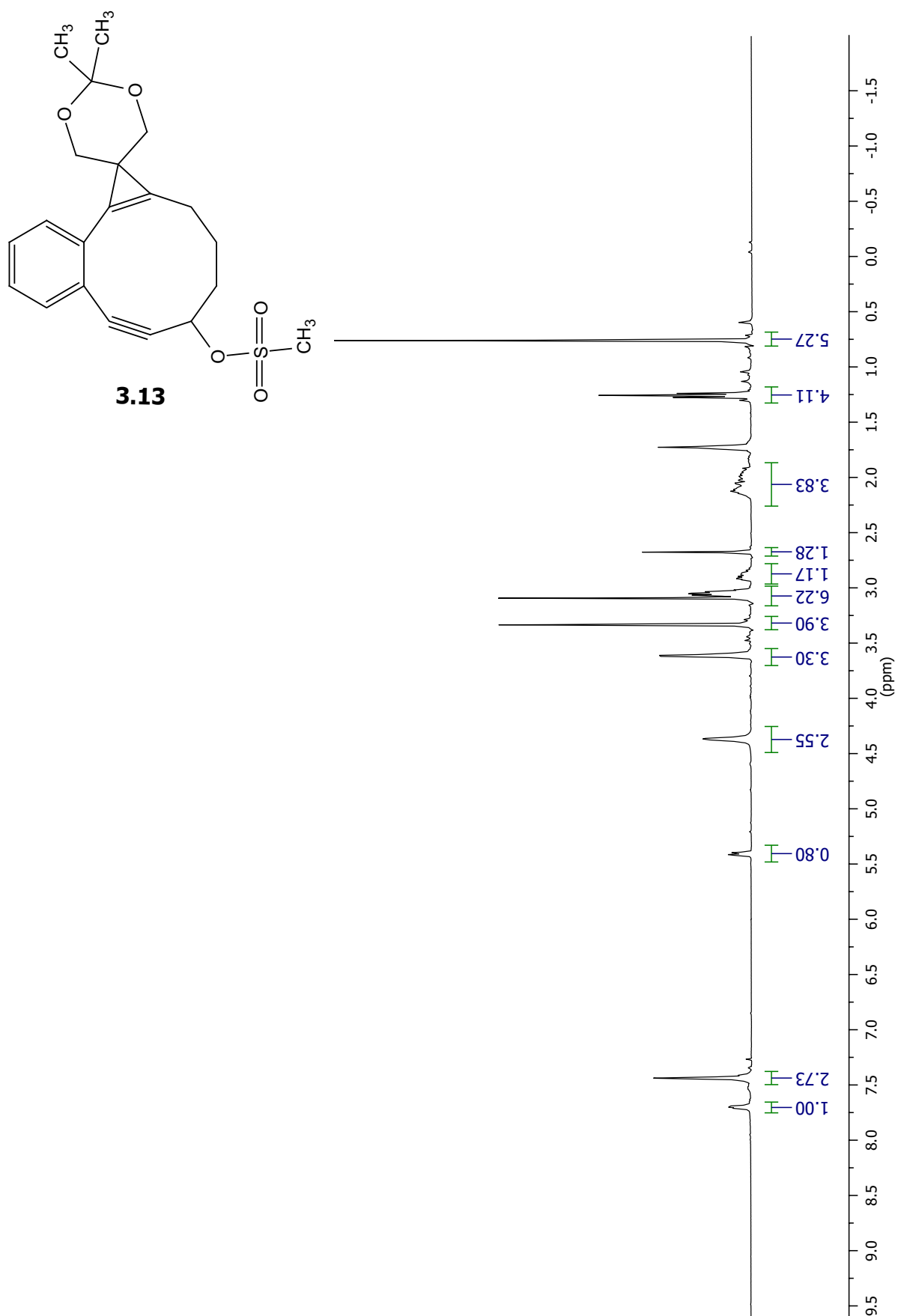


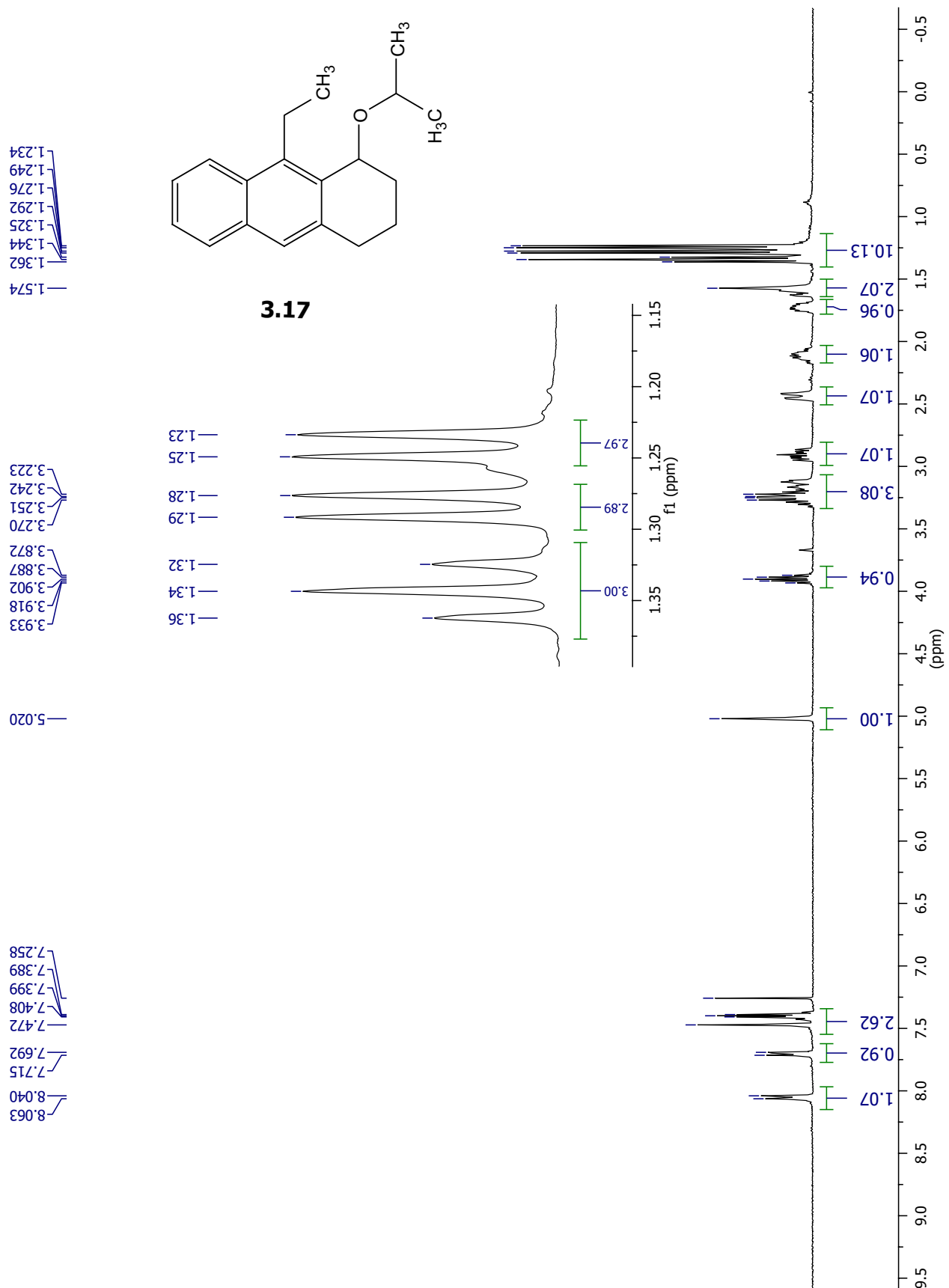


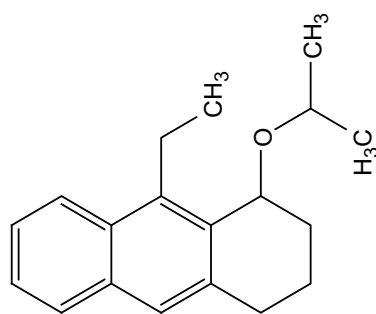










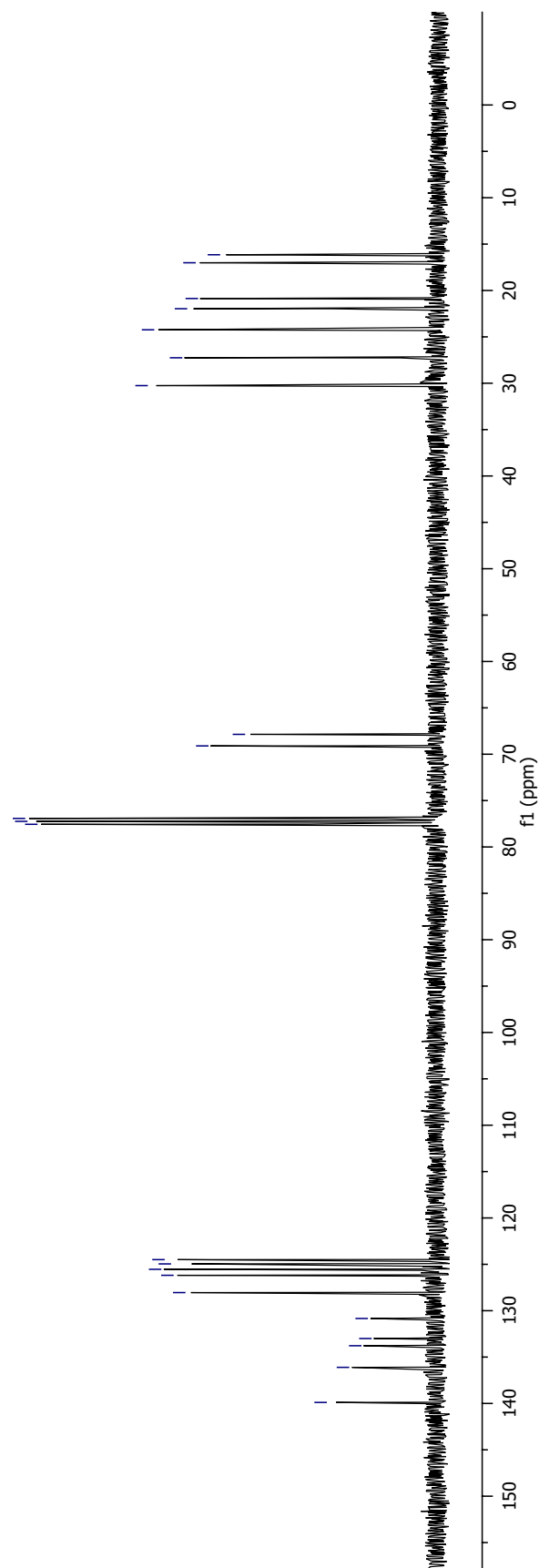


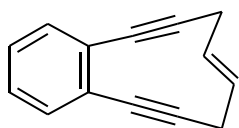
3.17

16.15
17.01
20.86
24.24
27.26
30.26

67.86
69.10
76.92
77.24
77.56

124.49
124.95
125.54
126.18
128.05
130.84
133.00
136.11
139.89

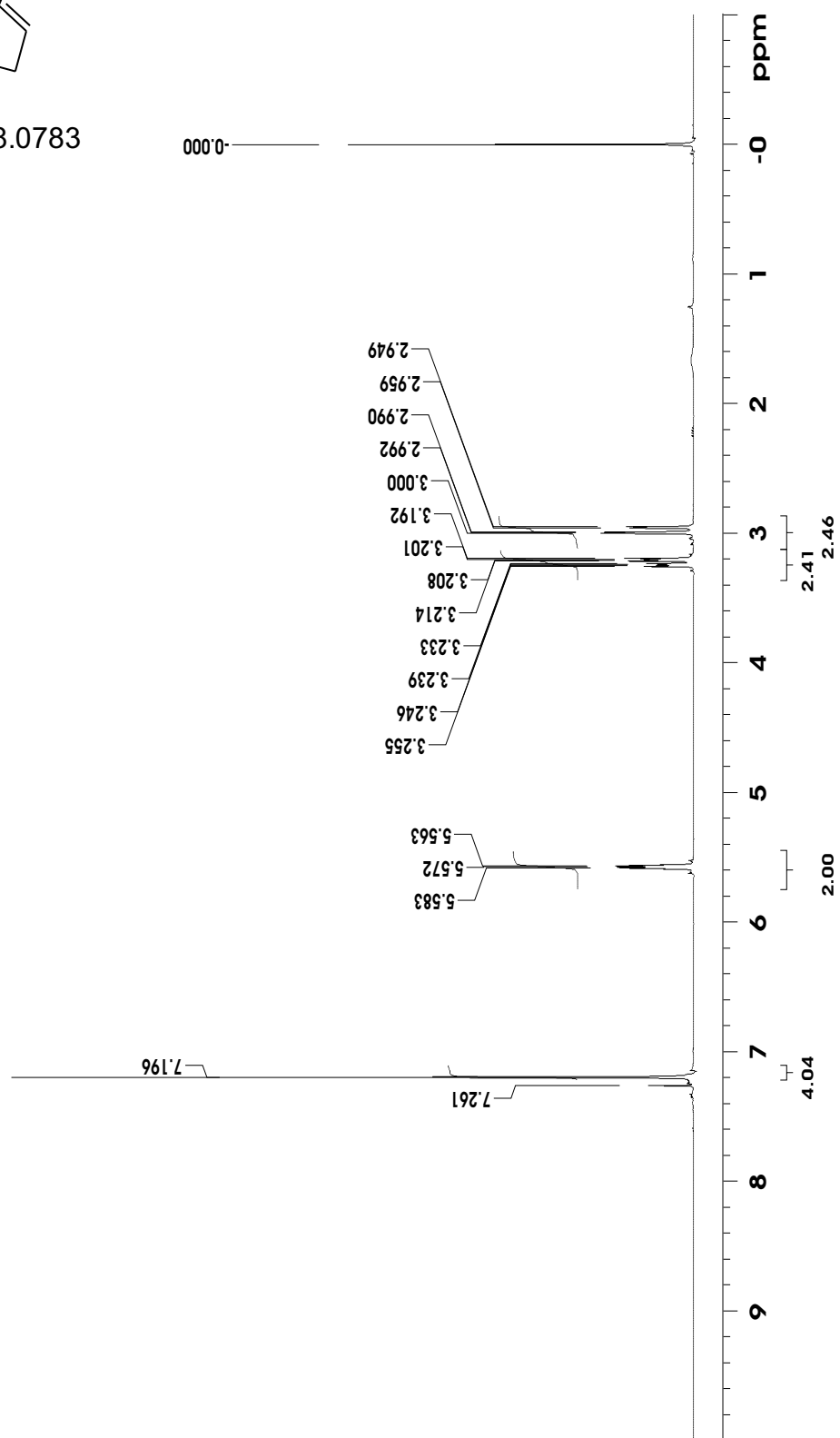


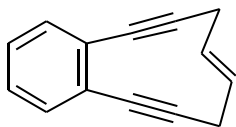


$C_{14}H_{10}$

Exact Mass: 178.0783

4.1

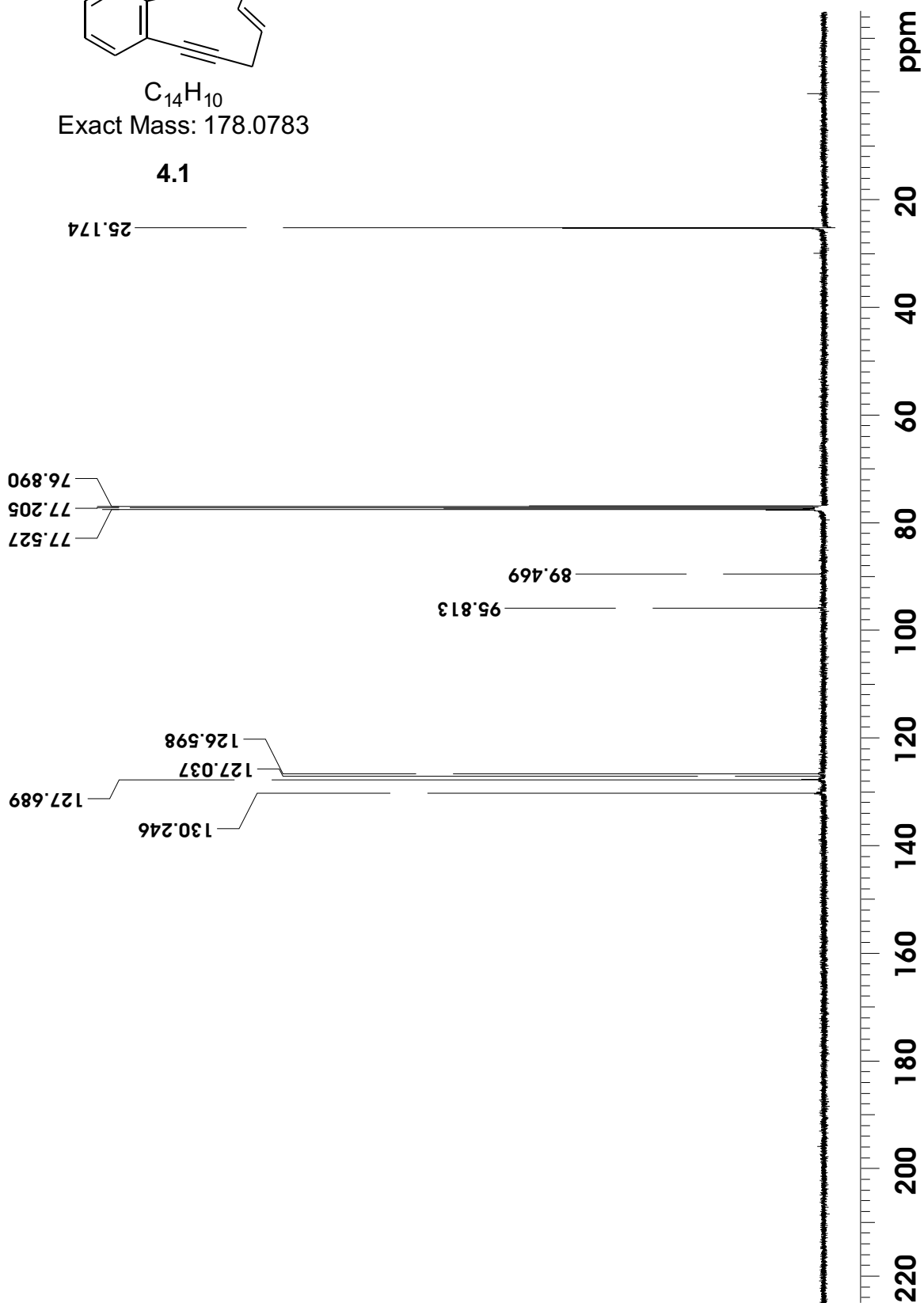


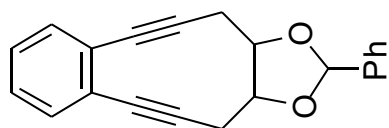


$C_{14}H_{10}$

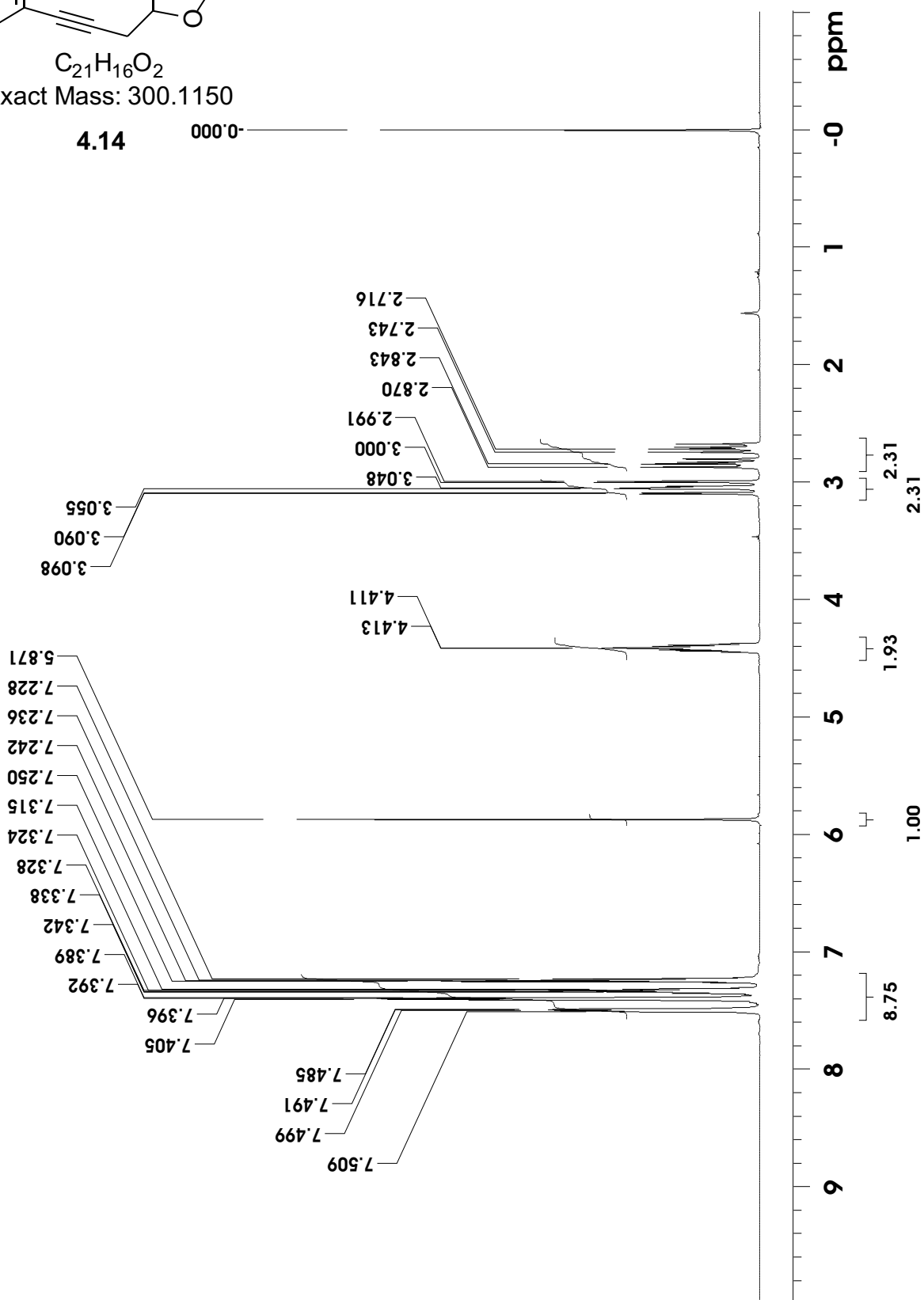
Exact Mass: 178.0783

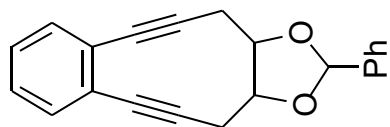
4.1





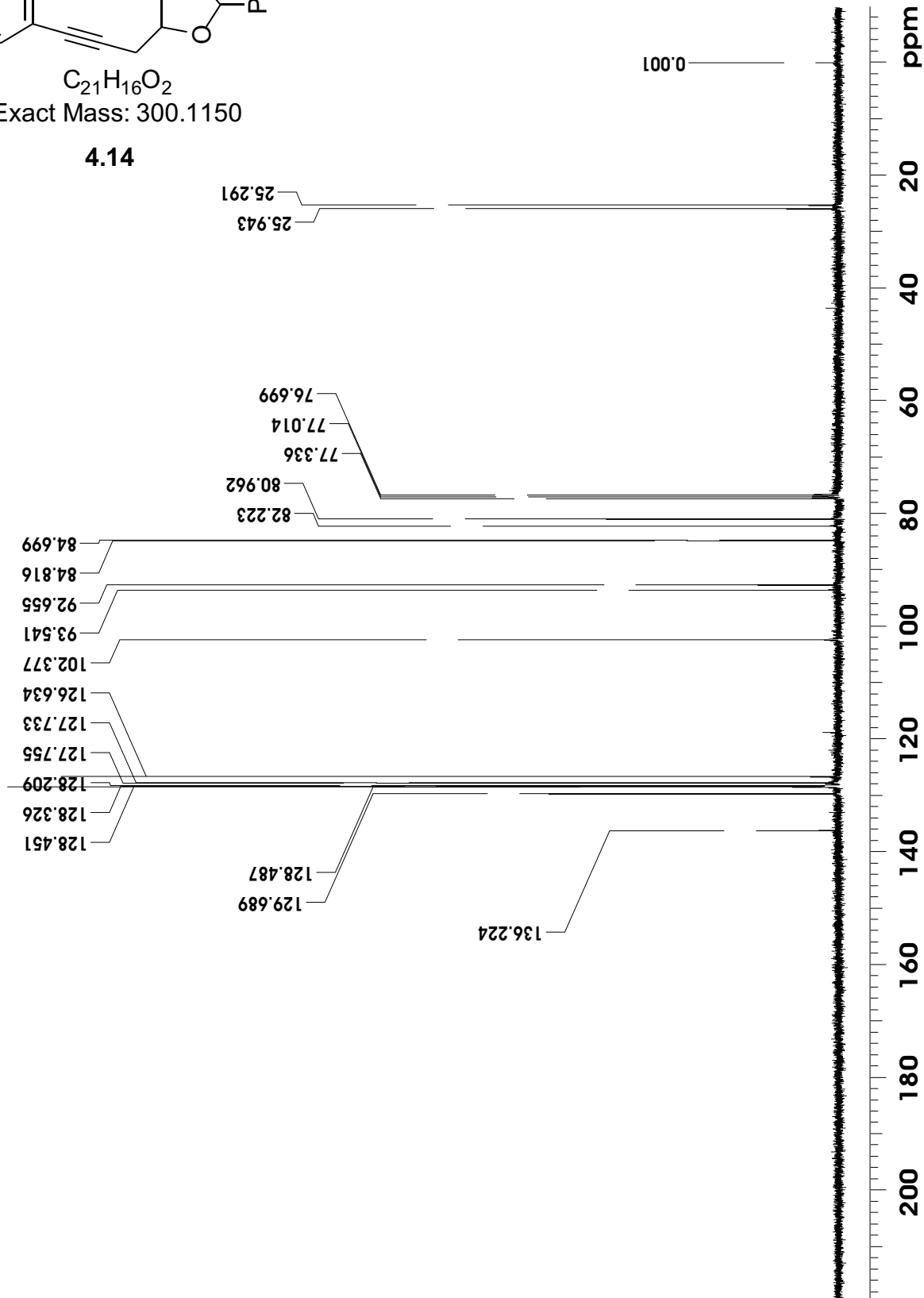
$C_{21}H_{16}O_2$
Exact Mass: 300.1150

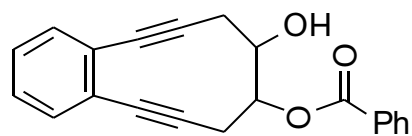




$C_{21}H_{16}O_2$
Exact Mass: 300.1150

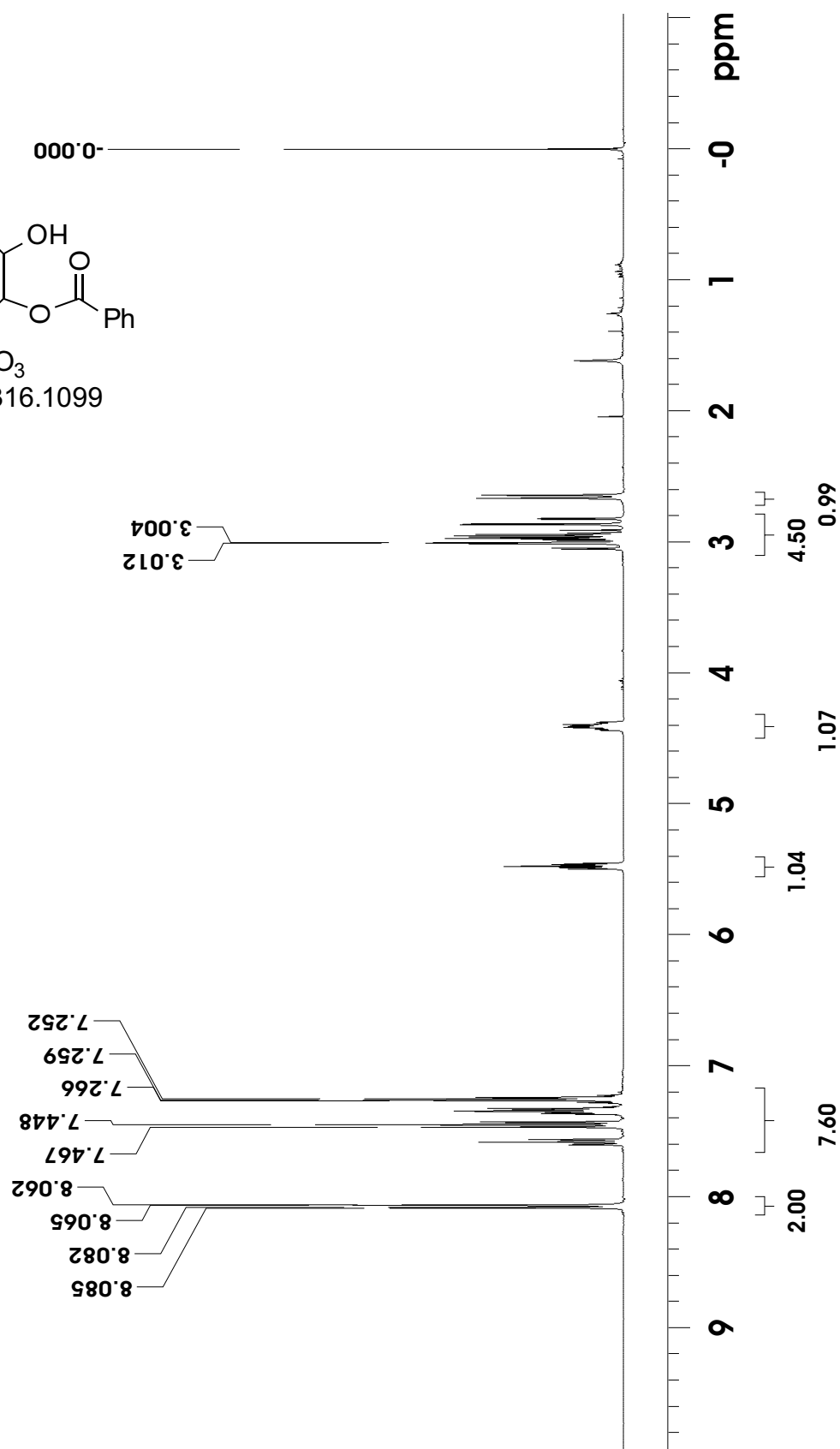
4.14

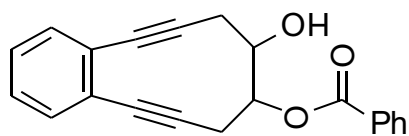




$C_{21}H_{16}O_3$
Exact Mass: 316.1099

4.15

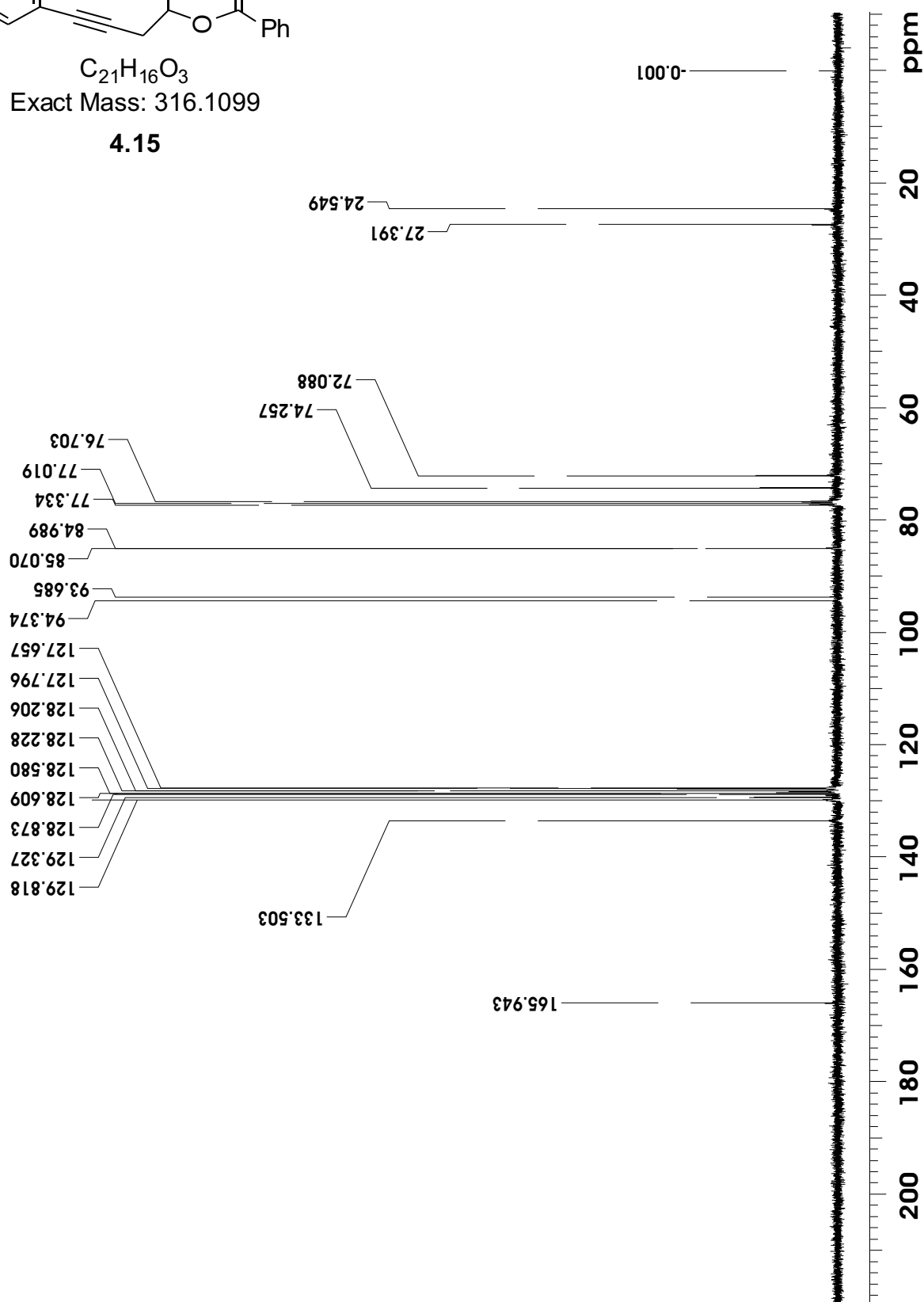




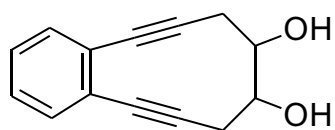
$C_{21}H_{16}O_3$

Exact Mass: 316.1099

4.15

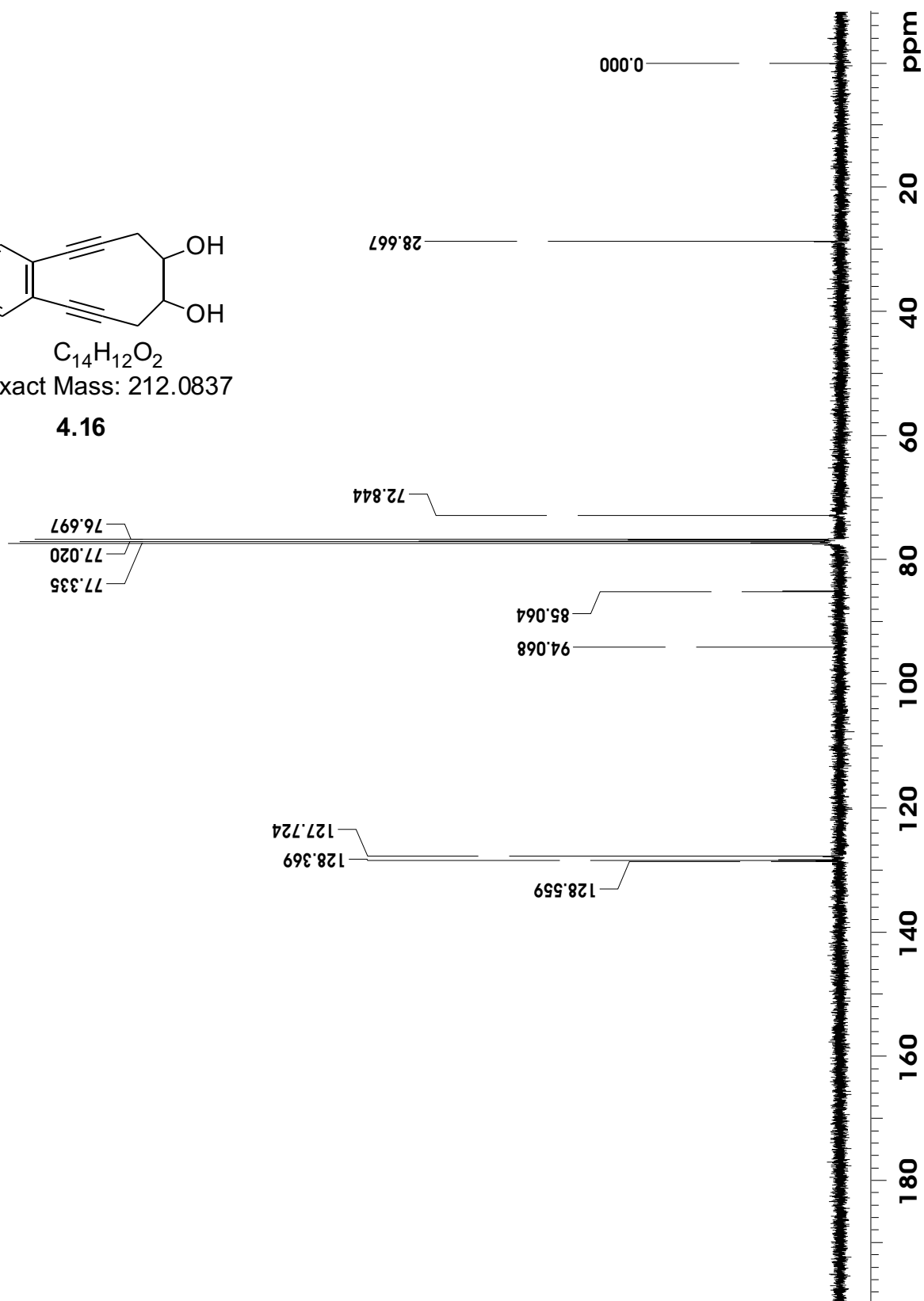


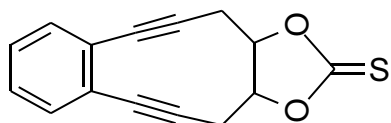




$C_{14}H_{12}O_2$
Exact Mass: 212.0837

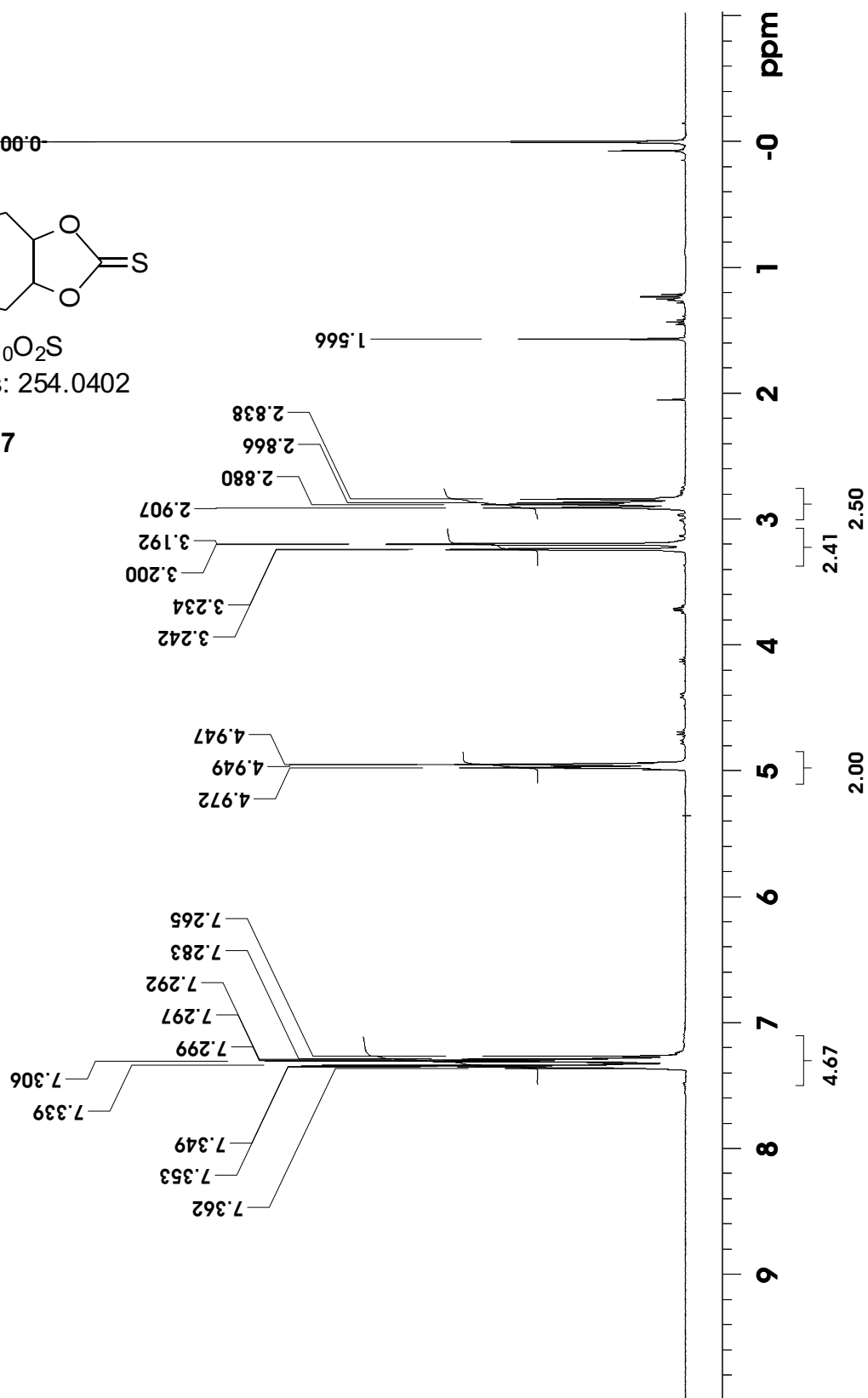
4.16

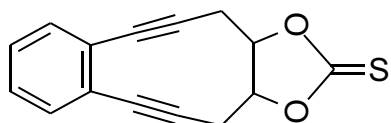




$C_{15}H_{10}O_2S$
Exact Mass: 254.0402

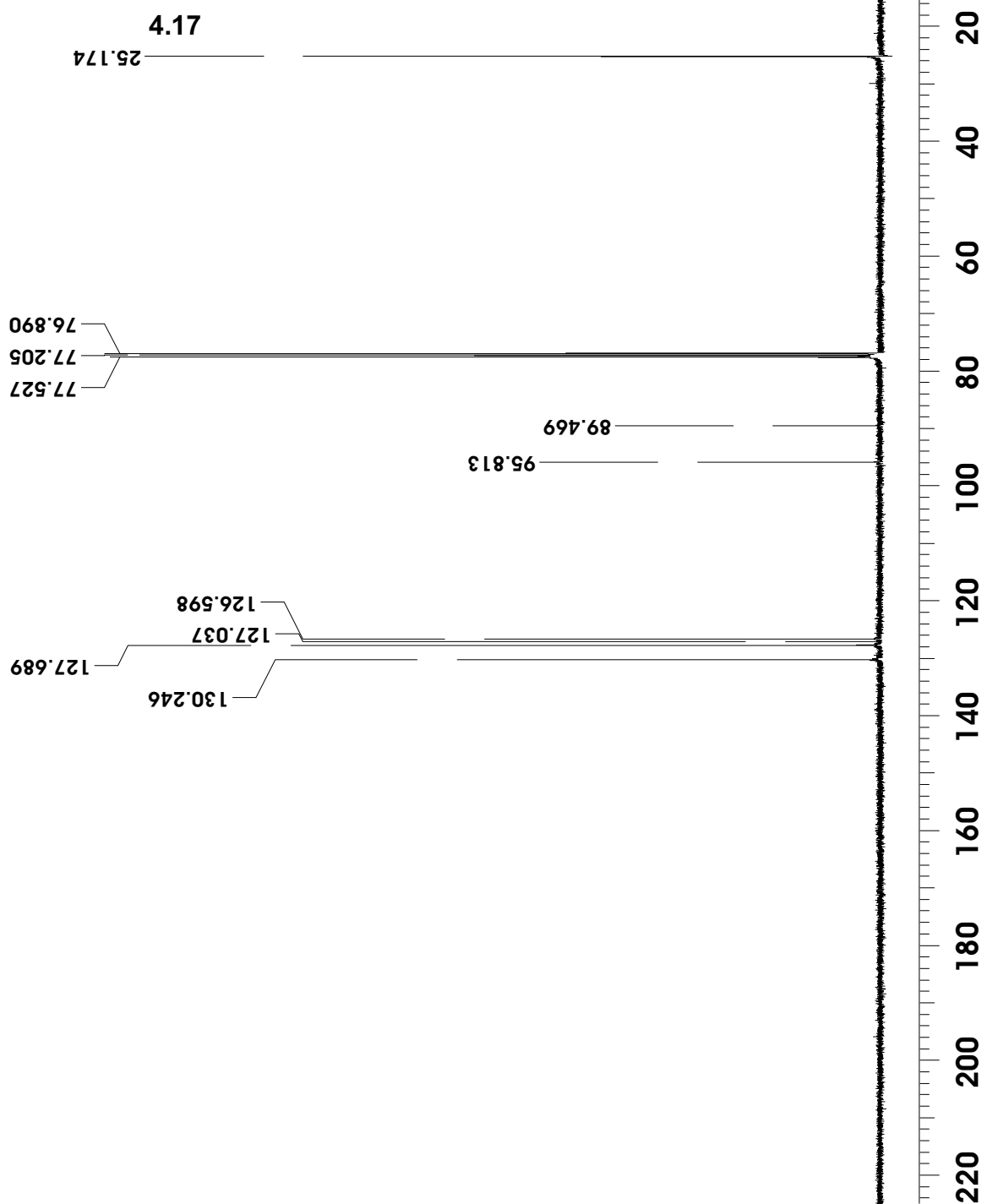
4.17

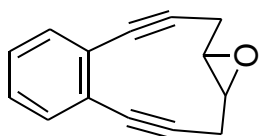




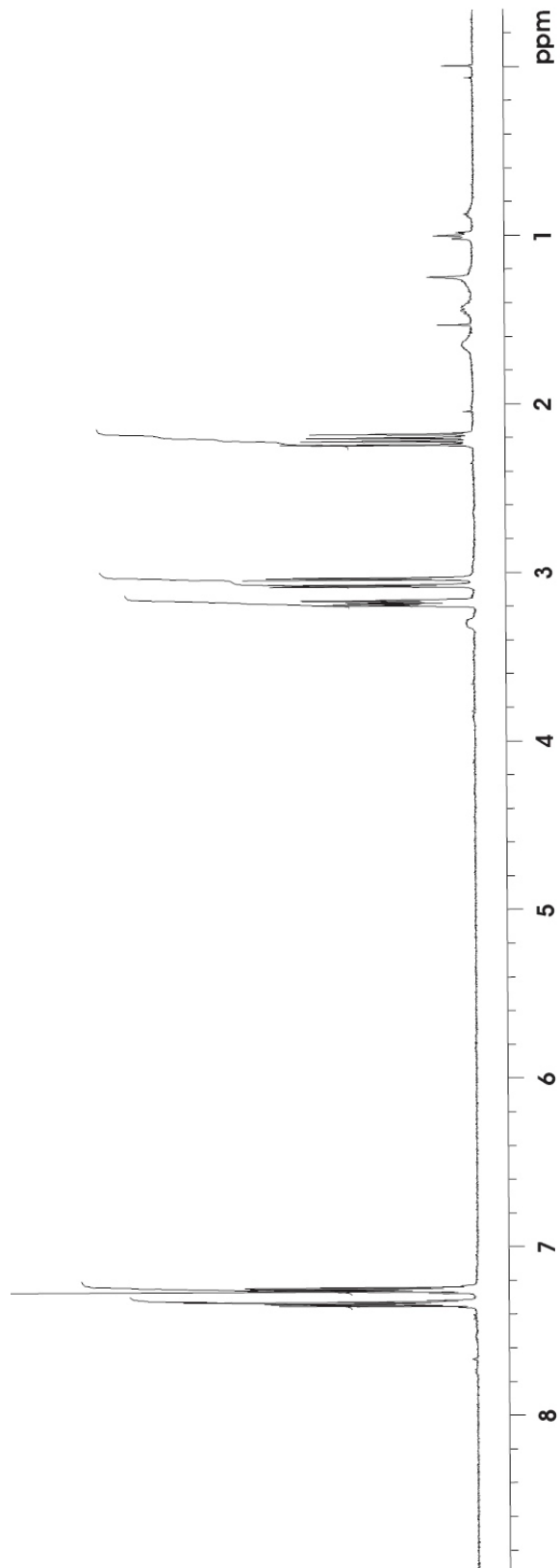
$C_{15}H_{10}O_2S$

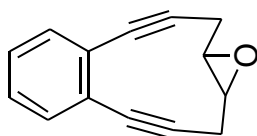
Exact Mass: 254.0402



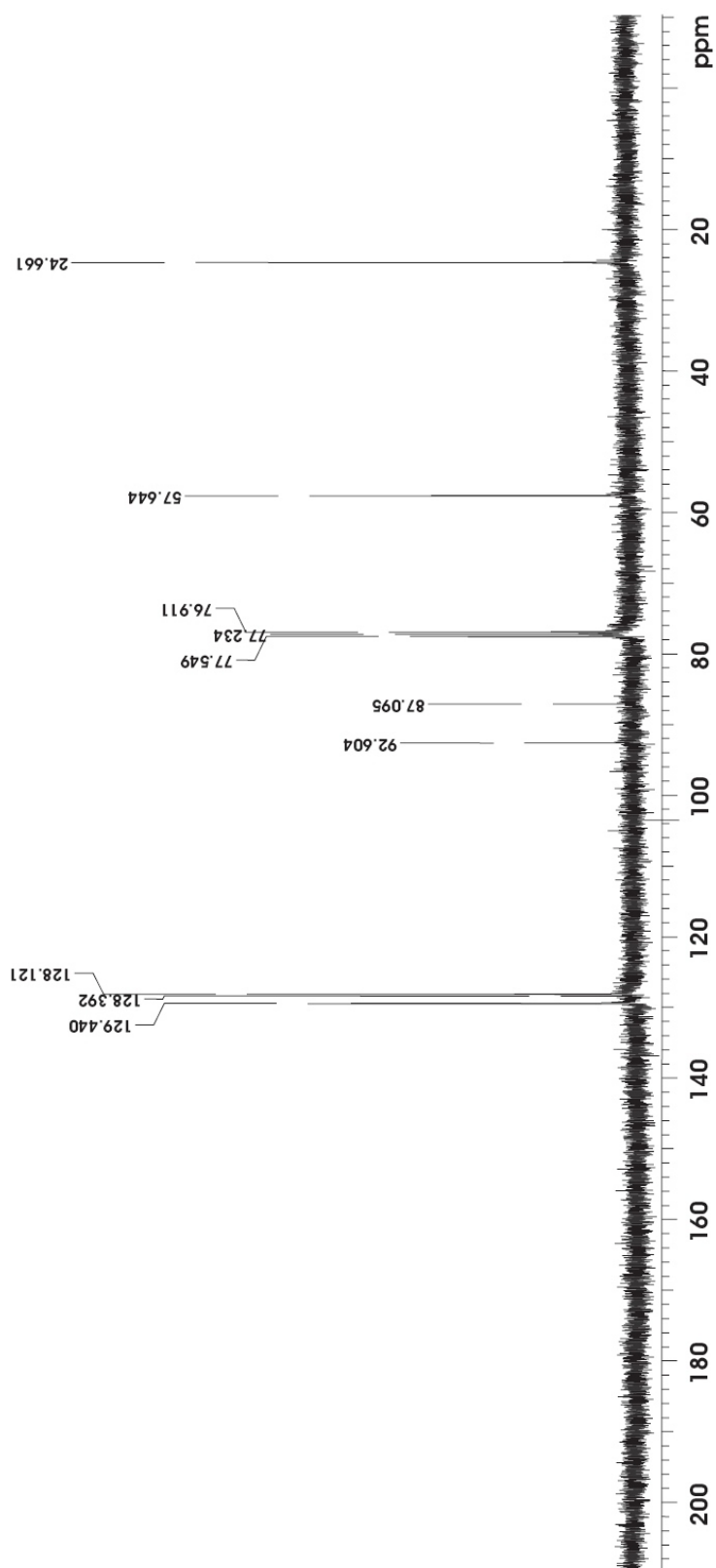


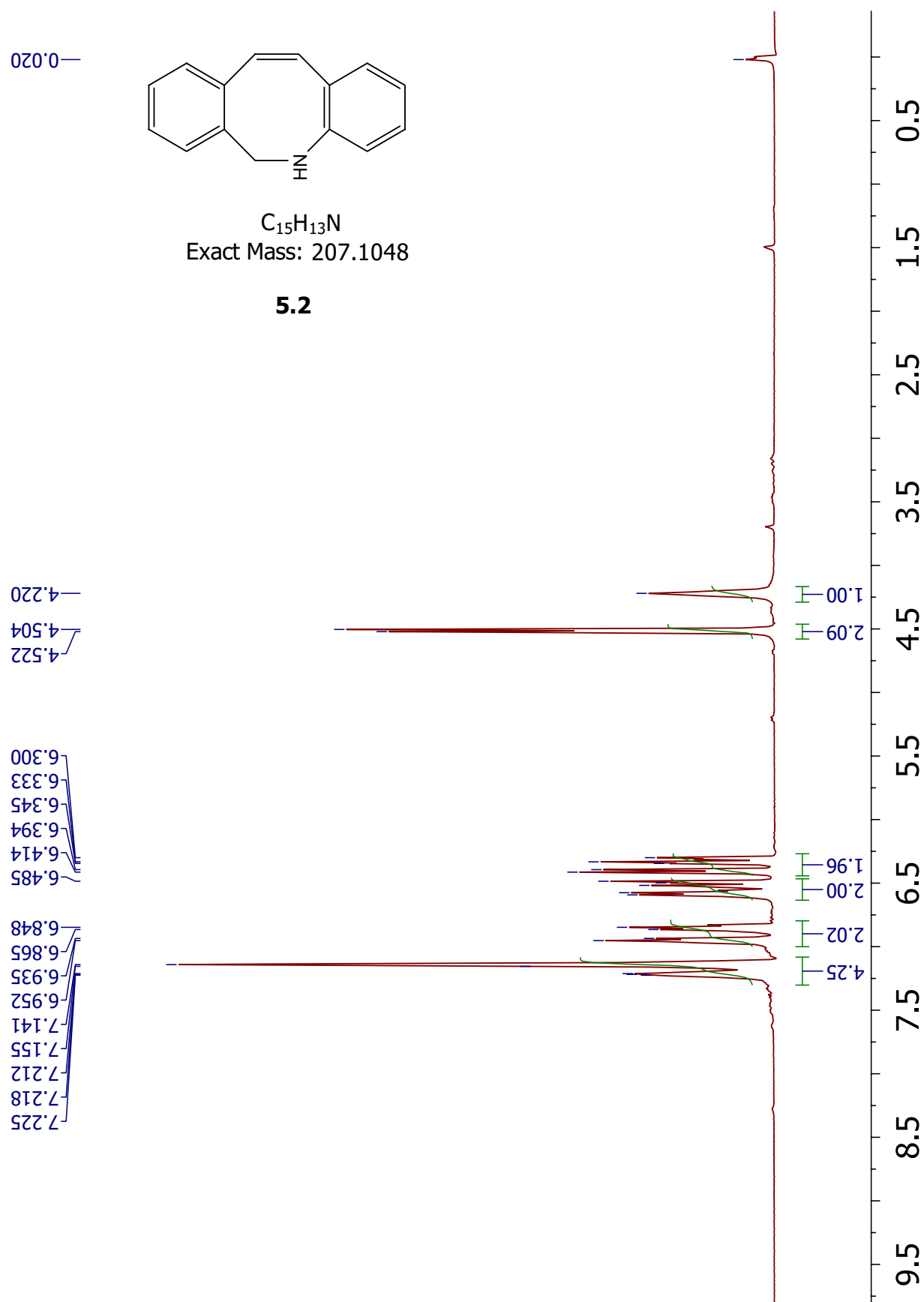
4.18

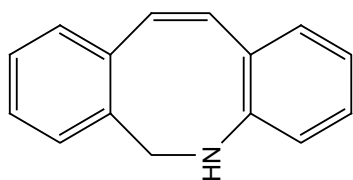




4.18

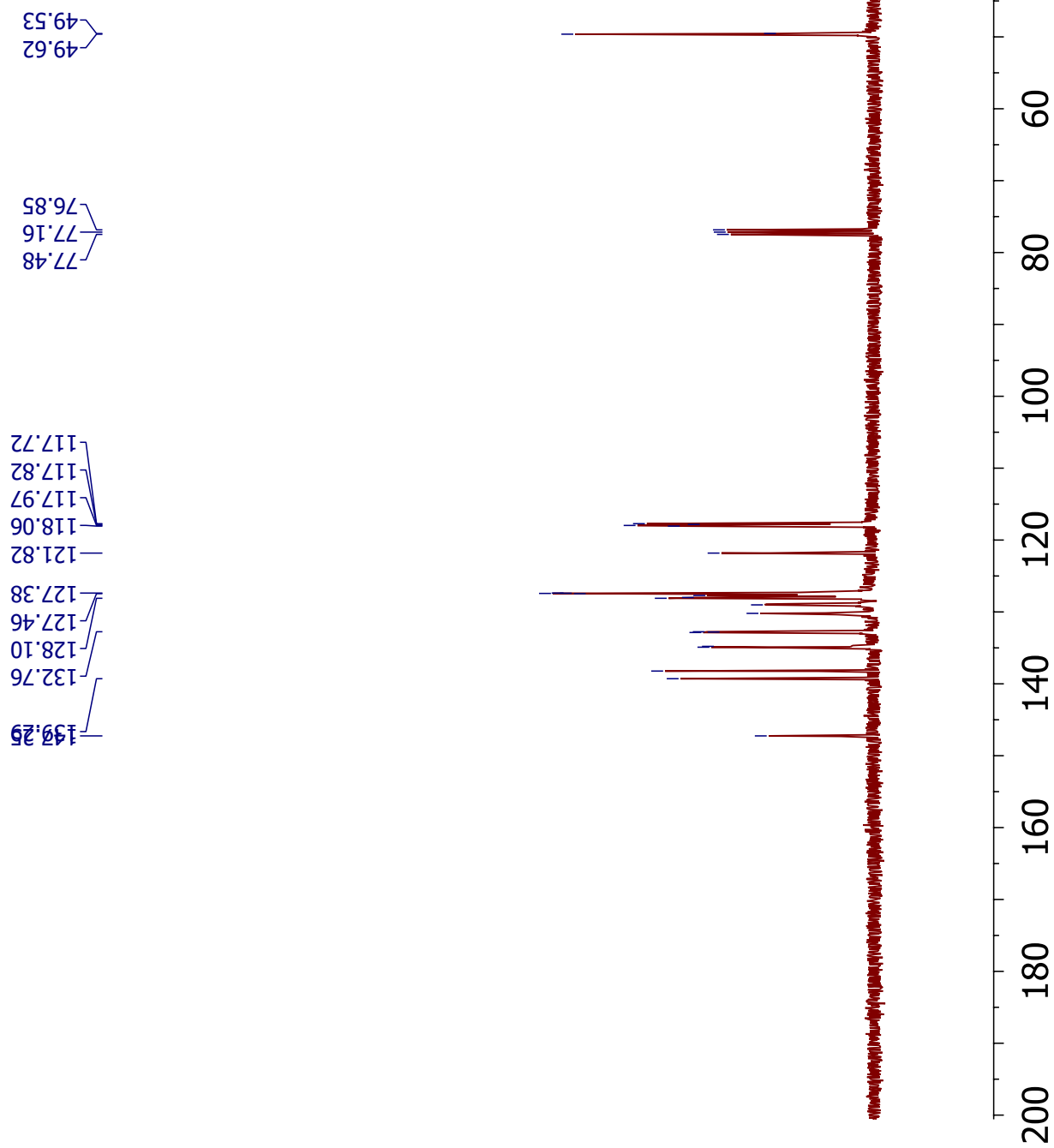


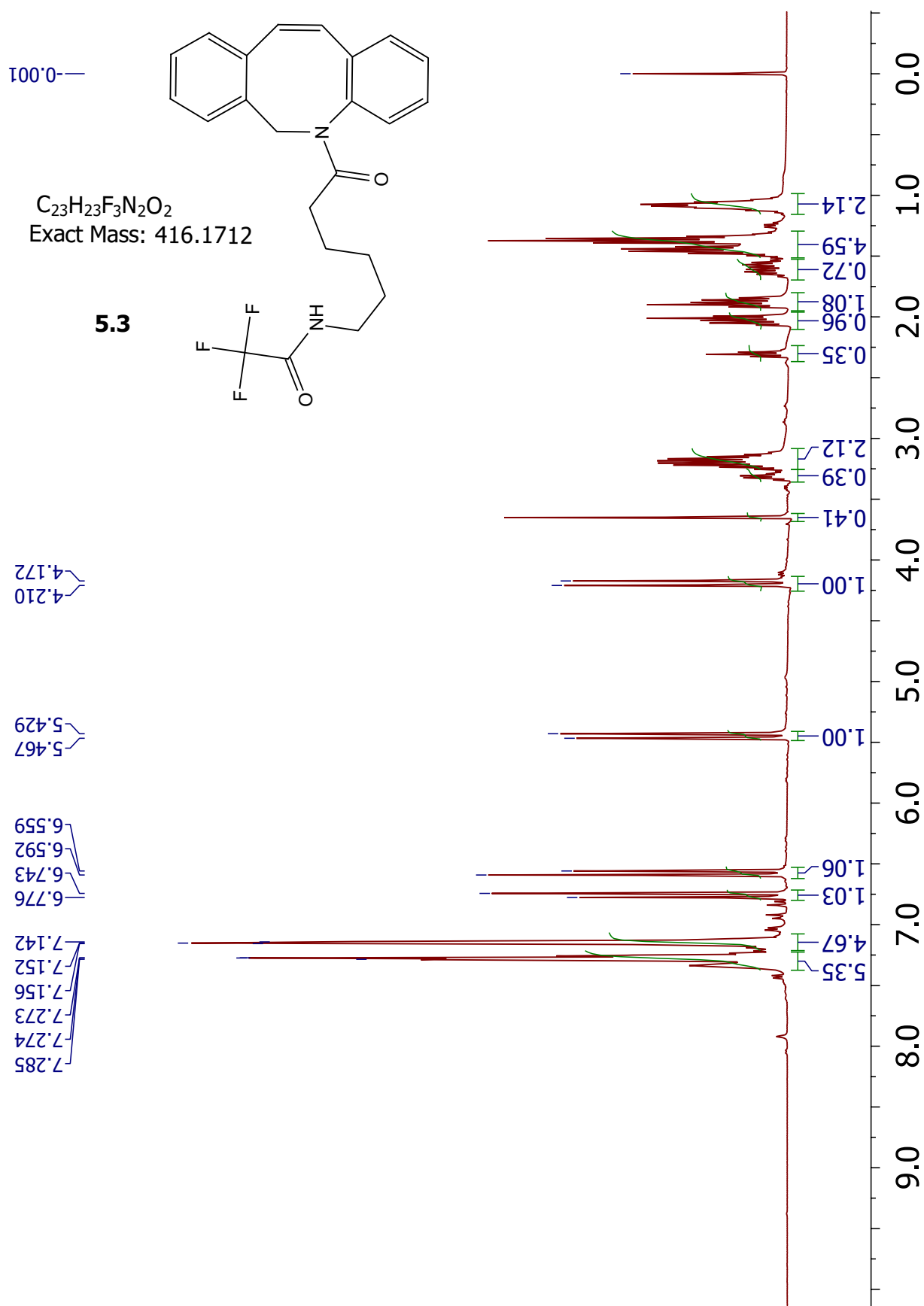


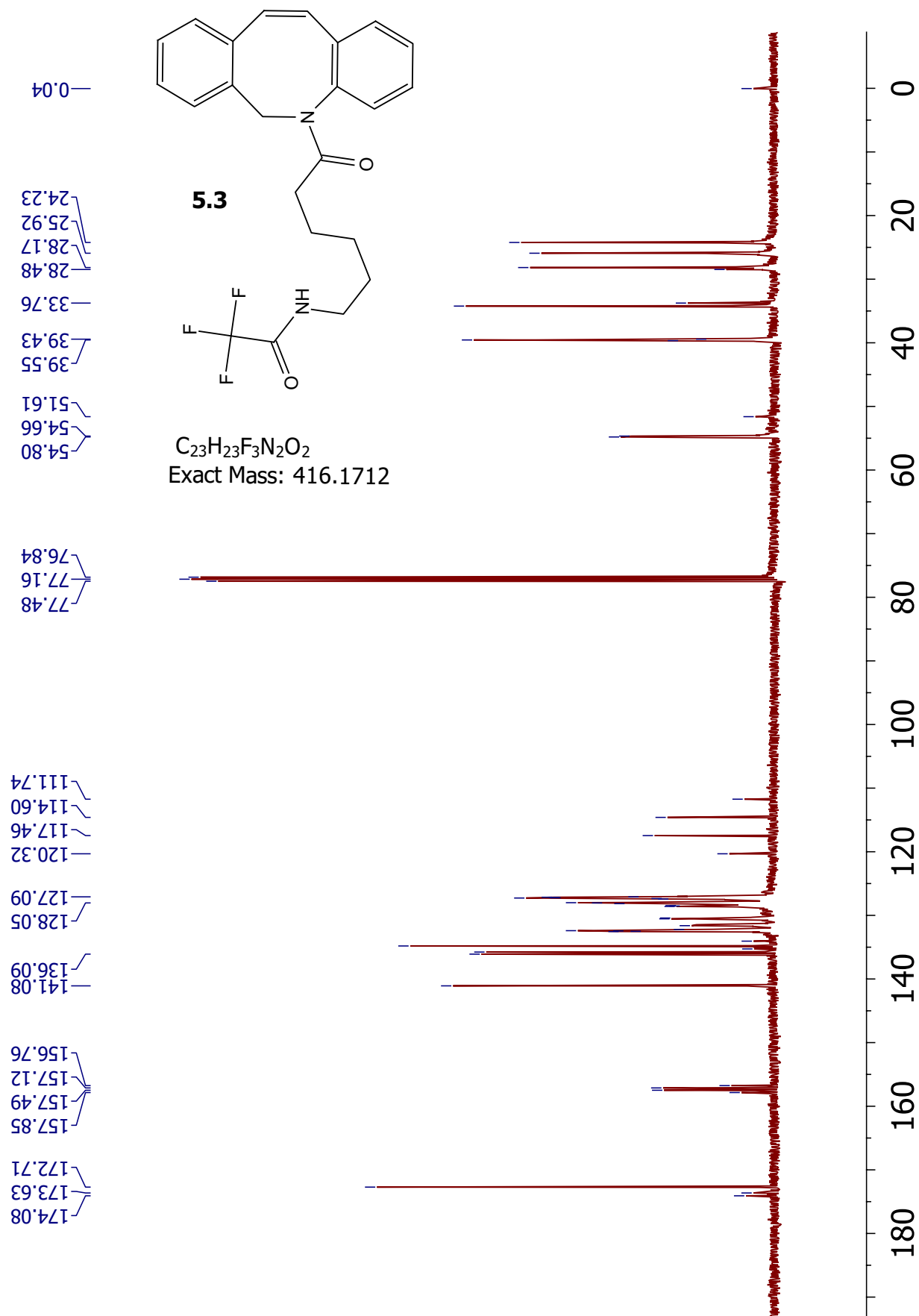


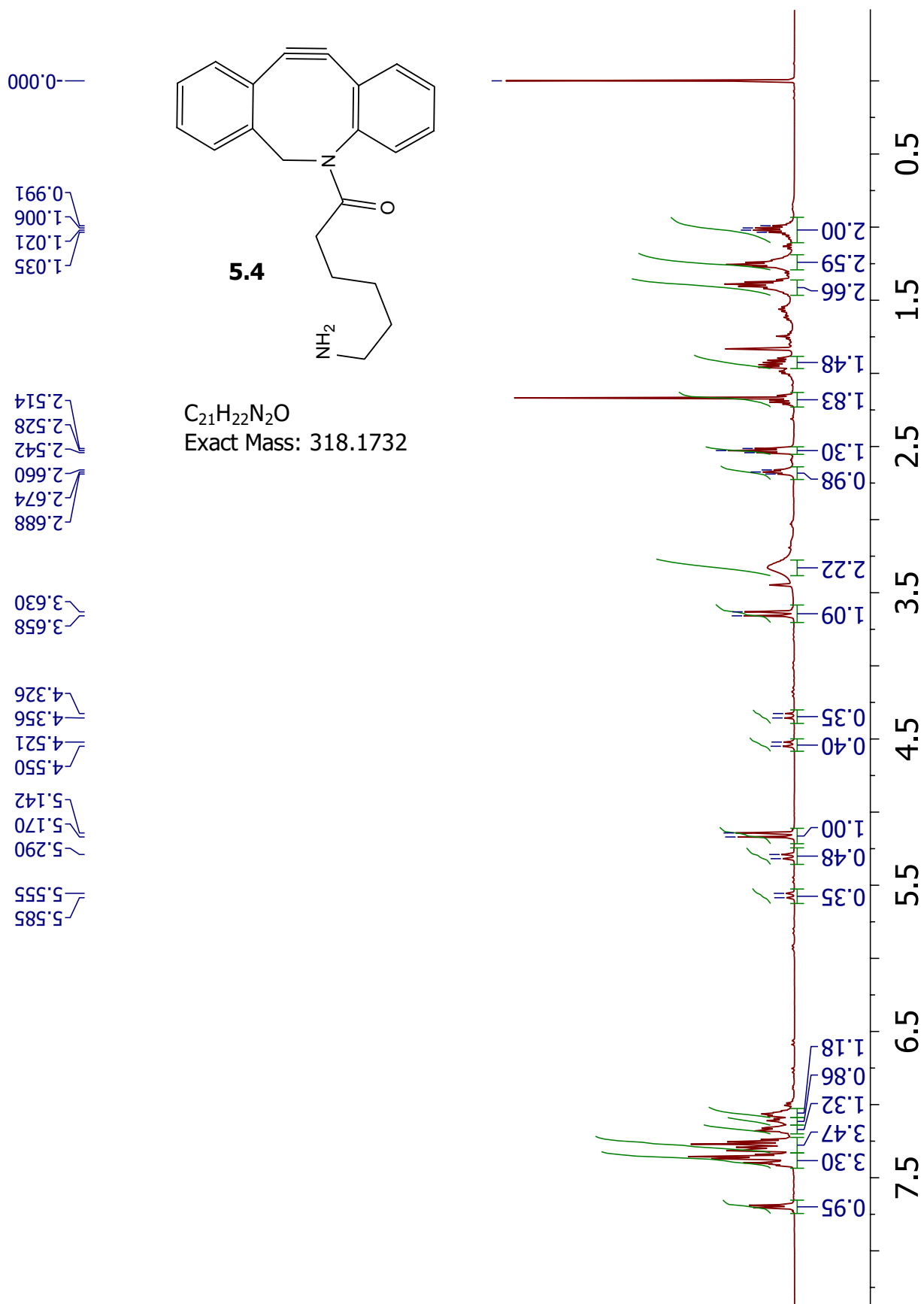
C₁₅H₁₃N
Exact Mass: 207.1048

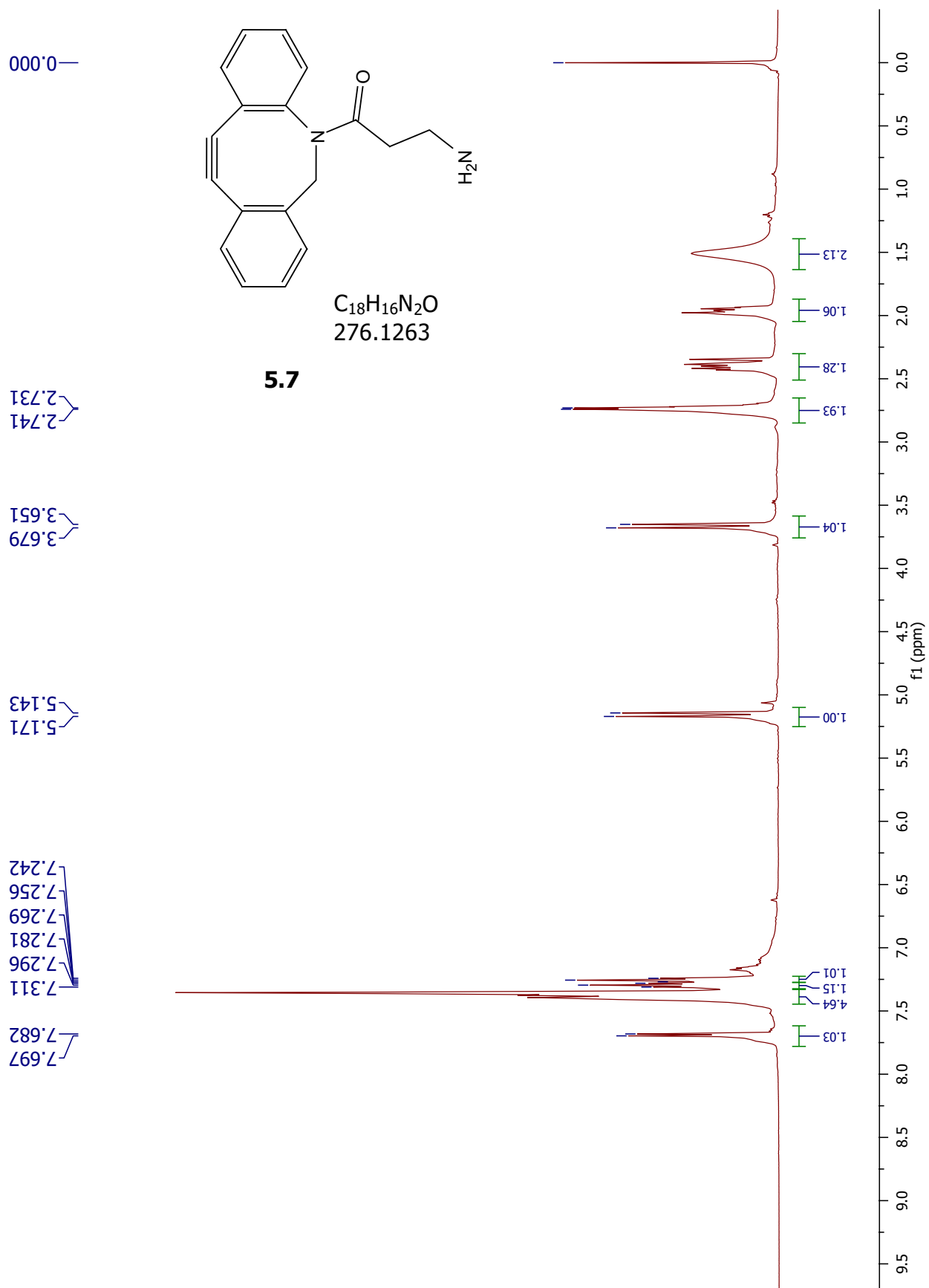
5.2

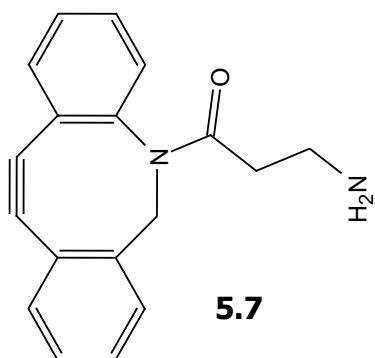












$C_{18}H_{19}N_2O$
276.1263

38.25
38.15

55.25

107.66

114.97

148.01

151.48

172.14

